SYNTHESE UND BIOLOGISCHE EVALUIERUNG ANTITUMORAKTIVER TRITERPENCARBONSÄUREDERIVATE

DISSERTATION

zur Erlangung des Doktorgrades der Naturwissenschaften
(Dr. rer. nat.)

der

Naturwissenschaftlichen Fakultät II
Chemie, Physik und Mathematik

der
Martin-Luther-Universität
Halle-Wittenberg

vorgelegt von
Herrn Oliver Kraft

Gutachter: Prof. Dr. R. Csuk (Martin-Luther-Universität Halle-Wittenberg)
Prof. Dr. F. Bracher (Ludwig-Maximilians-Universität München)

Datum der Verteidigung: 17.12.2024

Vorwort

Diese vorliegende wissenschaftliche Arbeit wurde im Zeitraum von März 2019 bis März 2023 am Institut für Chemie im Bereich für Organische Chemie der Martin-Luther-Universität Halle-Wittenberg in der Arbeitsgruppe von Prof. Dr. René Csuk angefertigt. Die Arbeit wurde kumulativ angefertigt und basiert auf wissenschaftlichen Artikeln in internationalen „peer-reviewed“ Fachzeitschriften, in denen die Forschungsergebnisse publiziert wurden.

Danksagung

An erster Stelle möchte ich mich ganz besonders bei meinem Doktorvater Herrn Prof. Dr. René Csuk für die Überlassung des überaus interessanten Themas aussprechen und für die gute Zusammenarbeit, die zahlreichen Ratschläge und den gewährten Freiraum bedanken. Ihr Blick für neue Strukturen und Reaktionswege, sowie der richtigen Strategie bei Problemen haben mich immer sehr fasziniert. Vielen Dank!

Weiterhin möchte ich mich bei der gesamten Arbeitsgruppe für die schöne gemeinsame Zeit, das angenehme Arbeitsklima und die stetige Unterstützung bedanken.

Dabei möchte ich einen besonderen Dank an Frau Dr. Sophie Hoenke richten, ohne ihren Beitrag für die biologischen Assays diese Arbeit nicht möglich gewesen wäre. Auch Herrn Dr. Niels Heise, Herrn M.Sc. Toni Denner, Frau Dipl.-Lebensmittelchem. Theresa Schmidt, Frau Dr. Marie Kozubek und Frau Dipl.-Lebensmittelchem. Julia Heisig möchte ich für die zahlreichen Gespräche jeglicher Art und die gemeinsamen Kaffeepausen danken.

Darüber hinaus möchte ich mich auch bei ehemaligen Mitgliedern der Arbeitsgruppe bedanken. So bei Frau Dr. Anne Loesche, Dr. Immo Serbian und Dr. Michael Kahnt bedanken – vielen Dank für die schöne Zeit.

Ein großes Dankeschön geht auch an alle Studierenden, durch deren direkte oder indirekte Hilfe ein Beitrag zum Gelingen dieser Arbeit geleistet wurde. Hier möchte ich mich zunächst bei Frau Dipl.-Lebensmittelchem. Anne-Kathrin Hartmann, Herrn M.Sc. Julian Zacharias und Herrn M.Sc. Gregor Mittag bedanken, einerseits für die synthesechemische Unterstützung aber vor allem für die sehr angenehme Zusammenarbeit.

Für die Aufnahme der zahlreichen NMR-Spektren danke ich Herrn Dr. Dieter. Ströhl, Frau Yvonne Schiller und Frau B.Sc. Senta Ludwig. Ein besonderer Dank geht an Frau Dipl.-Lebensmittelchem. Theresa Schmidt für die Anfertigung der ESI-MS-Spektren, die vielen hilfreichen Gespräche sowie für die angenehme gemeinsame Zeit im Praktikum. Bei Herrn Maximilian Schneider bedanke ich mich für die UV/Vis-, IR- und Drehwertmessungen.

Bei meinen Eltern und meiner Familie möchte ich mich für die zahlreiche Unterstützung während meines Studiums und meiner Promotion bedanken.

Inhaltsverzeichnis

1 Einleitung 1

1.1 Krebs – „Die zweithäufigste Todesursache“ 1

1.1.1 Entstehung, Inzidenz und Mortalität 2

1.1.2 Diagnostik 4

1.1.3 Therapie 4

1.1.4 Krebsmedikation auf Naturstoffbasis 6

1.1.5 Aktuelle Forschung 7

1.2 Terpenoide Naturstoffe als Leitstrukturen 9

1.2.1 Grundlagen und Entstehung 9

1.2.2 Asiasäure und Derivate 11

1.2.3 Weitere Triterpenoide und Derivate (Ursol-, Corosol,- und Madecassinsäure) 12

1.3 Kationische Fluoreszenzfarbstoff-Analoga als hochaktive und selektive Verbindungen 14

1.3.1 Safirinium-Konjugate 14

1.3.2 Rhodamin B-Konjugate 16

2 Zielstellung 19

3 Diskussion und Einordnung der Ergebnisse 20

3.1 Safirinium-Konjugate 20

3.1.1 Zytotoxische Triterpencarbonsäure-Safirinium-Derivat 20

3.2 Rhodamin B-Konjugate 23

3.2.1 Euscaph- und Tormentillsäure – Einfluss des E-Rings auf die zytotoxische Wirkung 23

3.2.1 Madecassinsäure als neue Leitstruktur 25

3.2.2 Asiasäure als Leitstruktur für Derivate mit submolarer Zytotoxizität 27

4 Zusammenfassung und Ausblick 30

5 Literaturverzeichnis 32

6 Abbildungsverzeichnis 51

7 Tabellenverzeichnis 53

8 Anhang 54

8.1 *„Cytotoxic triterpenoid–safirinium conjugates target the endoplasmic reticulum”* . 55

8.2 *„A tormentic acid-homopiperazine-rhodamine B conjugate of single-digit nanomolar cytotoxicity and high selectivity for several human tumor cell lines”* 56

8.3 *„Madecassic Acid—A New Scaffold for Highly Cytotoxic Agents”* 57

8.4 *„Asiatic acid as a leading structure for derivatives combining sub-nanomolar cytotoxicity, high selectivity, and the ability to overcome drug resistance in human preclinical tumor models”* 59

10 Publikationsliste 63

11 Posterbeitrag 65

12 Erklärung über Autorenanteil 66

13 Selbstständigkeitserklärung 68

14 Publikationen 69

Abkürzungsverzeichnis

$[\alpha]_{20}^{D}$	spezifische optische Drehung
AA	Asiasäure
Ac	Acetyl
APT	Engl. Attached Proton Test
BA	Betulinsäure
c	Konzentration
$CDCl_3$	Chloroform (deuteriert)
$CHCl_3$	Chloroform
δ	chemische Verschiebung
d. Th.	der Theorie
DMAP	4-(Dimethylamino)-pyridin
DMF	*N,N*-Dimethylformamid
DMSO	Dimethylsulfoxid
EC_{50}	mittlere effektive Konzentration
EDC	1-Ethyl-3-(3-dimethylaminopropyl)carbodiimid
EE	Ethylacetat
ESI	Elektrospray-Ionisation
et al.	lat. und andere
gHMBC	engl. Gradient Hetero Multibond Correlation
gHSQC	Engl. Gradient Hetero Single Quantum Coherence
HCOOH	Ameisensäure
HMPA	Hexamethylphosphorsäuretriamid
HOBt	1-Hydroxybenzotriazol
IR	Infrarot
IUPAC	International Union of Pure and Applied Chemistry
J	Kopplungskonstante

KBr	Kaliumbromid
K_i	Inhibitionskonstante
λ_{max}	maximale Wellenlänge
Lit.	Literatur
log ε	logarithmischer Extinktionskoeffizient
M	Molar (mol/L)
MA	Maslinsäure
Me	Methyl
MeOH	Methanol
M.p.	Schmelzpunkt (engl. melting point)
MS	Massenspektrometrie
m/z	Masse-Ladungs-Verhältnis
n.d.	nicht definiert
NMR	Kernmagnetische Resonanz (engl. nuclear magnetic resonance)
OA	Oleanolsäure
PA	Pomolsäure
PCC	Pyridiniumchlorochromat
PDC	Pyridiniumdichromat
ppm	engl. Parts Per Million
R	Rest
R_f	Retentionsfaktor (engl. ratio of fronts)
RT	Raumtemperatur
SiO_2	Siliziumdioxid
SI	Selektivitätsindex
SRB	Sulforhodamine B
TEA	Triethylamin
TBDMS	tert-Butyldimethylsilyl
TEMPO	2,2,6,6-Tetramethylpiperidinyloxyl
THF	Tetrahydrofuran

UV	Ultraviolettes (Licht)
UV-Vis	Ultraviolett-Visible
VIS	sichtbares (Licht)
ν	Wellenzahl

1 Einleitung

1.1 Krebs – „Die zweithäufigste Todesursache“

Trotz umfangreicher Forschungen in den vergangenen Jahrzehnten bleiben Tumorerkrankungen, im Volksmund auch als Krebs bekannt, weiterhin eine der häufigsten Todesursachen weltweit (Abbildung 1).[1] Jährlich verlieren rund eine Viertelmillion Menschen ihr Leben an bösartigen Tumoren und Prognosen deuten darauf hin, dass sich diese Zahl in den nächsten Jahren bis 2040 verdoppeln wird.[2] Allein im Jahr 2023 wurden ca. 230 000 Todesfälle alleine in Deutschland aufgrund von Krebs verzeichnet.[3]

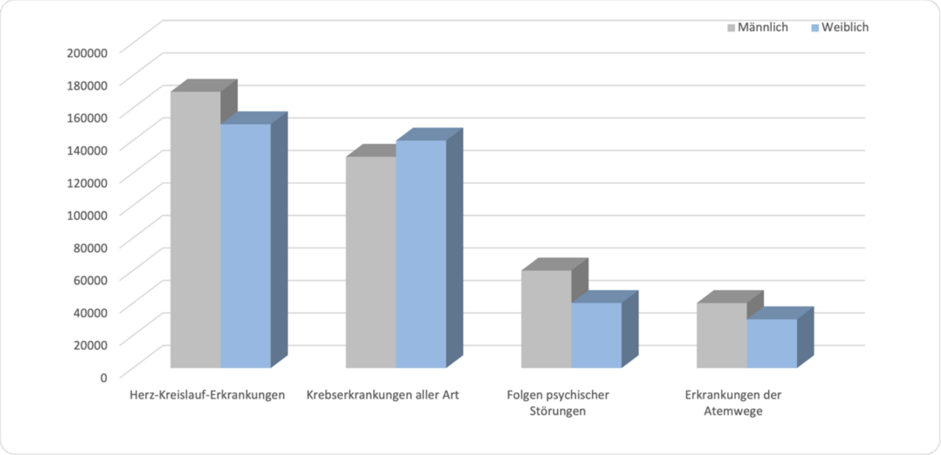

Abbildung 1: Die häufigsten Todesursachen in Deutschland in 2023. [1]

Die hierbei zum Einsatz kommenden herkömmlichen Therapieansätze umfassen die operative Entfernung des Tumorgewebes sowie die Anwendung von Strahlen- und/oder Chemotherapie.[4; 5] In Fällen von fortgeschrittenem Krebs beispielsweise mit möglicher oder bereits bestehender Metastasenbildung reichen Operation und Bestrahlung oft nicht aus und zusätzliche Chemotherapeutika sind erforderlich.[5–7] Allerdings stellt die Chemotherapie ein großes Problem dar, da sie Tumorzellen bekämpft, aber auch gesundes Gewebe schädigt.[8] Dies führt zu teilweise schweren Nebenwirkungen, zu denen Schädigungen des Herzens, des Gehirns oder des Innenohrs mit einhergehenden Hörverlust zählen.[9] Die aktuelle Forschung konzentriert sich daher darauf, Therapeutika zu entwickeln, welche selektiv Tumorzellen bekämpfen ohne dabei gesunde Zellen zu schädigen.[10] Vorbild für die moderne Wirkstoffforschung und die Entwicklung neuartiger Leitverbindungen ist hier vor allem die Natur. Die Naturstoffchemie bietet hierbei eine Vielzahl potenzieller Arzneimittel, die sich für eine gezieltere Anwendung in der Chemotherapie eignen.[11–13]

In den letzten Jahren haben bereits einige auf Naturstoffen basierende Wirkstoffmoleküle viel Aufmerksamkeit erregt, die das Krebswachstum der entarteten Zellen bekämpfen können. Bereits heute sind 40 – 50 % aller seit Beginn der klassischen Chemotherapie zur Krebsbekämpfung eingesetzten Antitumormittel Naturstoffe oder leiten sich von ihnen ab.[14–16] Diese Zahlen verdeutlichen die große Bedeutung von Naturstoffen in der modernen Medizin sowie ihr enormes Potenzial für die Zukunft. Vor allem die sogenannten "Mitocane" gewinnen hier als potenzielle Chemotherapeutika verstärkt an Aufmerksamkeit.[17] Diese lipophilen Kationen weisen eine erhöhte Löslichkeit im wässrigen Medium auf und können den Zelltod im Mitochondrium der Tumorzellen induzieren. Dadurch ist es möglich, einen programmierten Zelltod der Tumorzellen herbeizuführen und die Schädigung gesunder Zellen weitestgehend zu vermeiden.[18–20]

1.1.1 Entstehung, Inzidenz und Mortalität

Obwohl es in den letzten Jahrzehnten Fortschritte in der medizinischen Forschung gab, bleibt Krebs nach wie vor eine der tödlichsten Krankheiten weltweit.[21–23] Laut Schätzungen der Internationalen Agentur für Krebsforschung GLOBOCAN 2020-Schätzung gab es im Jahr 2020 weltweit etwa 10,0 Millionen Todesfälle und insgesamt 19,3 Millionen Neuerkrankungen an Krebs.[24] Im Vergleich zu den Schätzungen von 2010 bedeutet dies einen Anstieg der Todesfälle um etwa 32 % und einen Zuwachs von etwa 52 % bei den Neuerkrankungen.[24; 25]

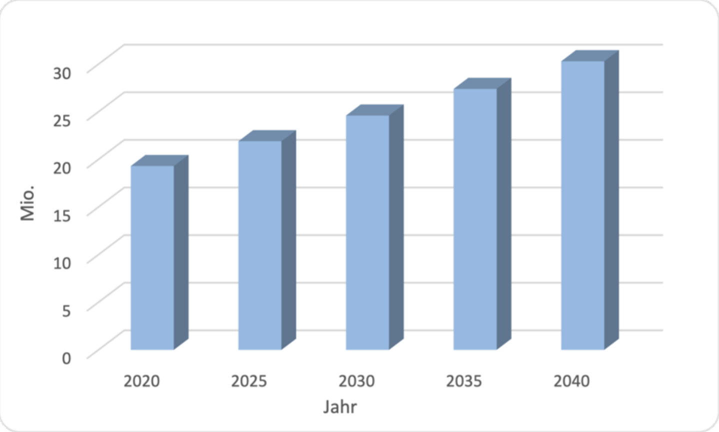

Abbildung 2: Prognostizierte neue Krebsfälle bis 2040.[26]

Abbildung 2 zeigt die weitere Entwicklung ab 2020 sowie die Prognosen für die kommenden Jahre der Neuerkrankungen. Die Prognosen deuten darauf hin, dass bis zum Jahr 2040 die Zahl der Zahl der Neuerkrankungen auf fast 30 Millionen steigen könnte.[26] Dies unterstreicht die Dringlichkeit weiterer Forschungen sowohl in der Behandlung als auch in der Diagnose von Krebs. In Deutschland wurden im Jahr 2023 schätzungsweise etwa 240.000 krebsbedingte Todesfälle verzeichnet.[27] Lungenkrebs war mit einer Mortalität von 50.560 (20 %) eine der häufigsten Todesursachen. Die meisten Neuerkrankungen in Deutschland im Jahr 2023 wurden durch Brustkrebs (69.900; 30,0%) verursacht, gefolgt von Prostatakrebs (65.200; 24,6%). [28; 29] Laut Statistischem Bundesamt Destatis war Krebs im Jahr 2023 wie auch in den Vorjahren neben Herz-Kreislauf-Erkrankungen die zweithäufigste Todesursache.[30]

Die alarmierenden Zahlen und Prognosen zur globalen Krebsbelastung mit einem besorgniserregenden Anstieg der Neuerkrankungen und Todesfälle betonen eindringlich die Notwendigkeit, unser Verständnis dieser komplexen Krankheit zu vertiefen. Der Übergang von der statistischen Betrachtung der Krebserkrankungen zu einer detaillierten Untersuchung der biologischen Grundlagen bietet einen wertvollen Einblick in die Mechanismen, die diesen Zahlen zugrunde liegen. Indem wir uns mit der Natur von Tumoren auseinandersetzen – ihrer Klassifikation in gutartige und bösartige Formen sowie den Ursachen ihrer Entstehung – eröffnen sich Wege, um die Entwicklung von Krebs besser zu verstehen und letztlich effektivere Strategien zu dessen Bekämpfung zu entwickeln. Die Beschreibung der Eigenschaften von Tumoren liefert somit eine essenzielle Grundlage, um die Dringlichkeit weiterführender Forschungen im Kontext der zuvor dargestellten epidemiologischen Entwicklungen zu verstehen.

In der medizinischen Fachsprache bezeichnet der Begriff "Tumor" eine abnorme Bildung von Gewebe, die durch Fehler in der Kontrolle des zellulären Wachstums, der Zelldifferenzierung sowie Störungen im programmierten Zelltod verursacht werden kann. Basierend auf den Wachstumseigenschaften eines Tumors wird er in gutartige (benigne) und bösartige (maligne) Formen unterteilt.[31–33] Gutartige Tumore zeichnen sich durch ein langsames und lokal begrenztes Wachstum aus. Sie sind nicht in der Lage, umliegendes Gewebe zu infiltrieren und können oft durch therapeutische Maßnahmen vollständig geheilt werden. Dagegen sind maligne Tumore durch ein schnelles und aggressives Wachstum gekennzeichnet. Sie haben die Fähigkeit, in benachbartes Gewebe zu infiltrieren und können sich über Metastasen in anderen Körperbereichen ausbreiten.[34; 35] Die Entstehung bösartiger Tumore kann durch genetische Veranlagung, Umwelteinflüsse oder Exposition gegenüber chemischen, biologischen und physikalischen Karzinogenen verursacht werden.[36; 37] Alle diese Krebsursachen können auf eine Schädigung der Erbsubstanz oder Mutationen in den Zellen zurückgeführt werden.[36; 38]

1.1.2 Diagnostik

Die Diagnose und präzise Lokalisierung von Tumoren sind ebenso bedeutend wie deren Behandlung. Je früher ein Tumor erkannt und die Krebszellen genau lokalisiert werden, desto besser kann eine effektive Therapie geplant und durchgeführt werden, was die Heilungschancen deutlich verbessert.[39] Zur Tumordiagnose stehen verschiedene bildgebende Verfahren zur Verfügung, die neben der Anamnese und klinischen Untersuchungen auch Laboranalysen und Gewebeentnahmen einbeziehen.[40–42; 31] Moderne bildgebende Technologien ermöglichen es heute, wichtige Informationen über Tumorart, Ausdehnung und Infiltration minimalinvasiv zu gewinnen. Zu den gängigen Methoden zählen die Magnetresonanztomografie (MRT), die Single Photon Emission Computed Tomography (SPECT) und die Positronen-Emissions-Tomografie (PET), bei denen verschiedene Kontrastmittel oder Tracer verwendet werden.[43–45]

1.1.3 Therapie

Grundsätzlich werden derzeit drei wesentliche Methoden zur Therapie bösartiger Tumore angewendet. Neben den lokal wirkenden Behandlungsformen wie Strahlentherapie und onkologische Chirurgie ist die systemisch wirksame zytostatische Chemotherapie eine weitere wichtige Methode zur Bekämpfung von Tumoren.[46–48] Zudem gibt es weitere relevante Therapieansätze wie die Hormontherapie oder die Immuntherapie sowie derzeit untersuchte Methoden wie Hyperthermie, Kryochirurgie oder Laserchirurgie.[49–53] Abhängig von der Art des bösartigen Gewebes und dem Fortschreiten des Tumors wird eine geeignete Methode oder Kombination zur Behandlung ausgewählt.[54; 55] Die medikamentöse Therapie kann sowohl den Primärtumor als auch lymphogene oder hämatogene Metastasen bekämpfen.

Die zytostatische Chemotherapie hat verschiedene Angriffspunkte.[48; 56] Viele Zytostatika wirken stärker auf schnell wachsendes Gewebe wie Tumore als auf Zellen mit normalem Wachstum, was jedoch eine begrenzte Spezifität für bestimmte Tumorzellen zur Folge hat. Ziel ist es, die Proliferation des malignen Gewebes weitgehend einzudämmen und gleichzeitig in den Tumorzellen den programmierten Zelltod (Apoptose) oder den traumatischen (Nekrose) auszulösen, während die Neubildung von Tumorzellen (Tumorangiogenese) oder ihre Ausbreitung (Metastase) verhindert werden sollen.[48; 38] Apoptose bezeichnet den programmierten Zelltod, der dazu dient, einzelne alte und defekte Zellen gezielt zu entfernen.

Dieser Prozess umfasst eine Reihe biochemischer Veränderungen, die letztendlich zum Tod der Zelle führen. Im Gegensatz zur Nekrose wird die Apoptose nicht von Reaktionen des Immunsystems wie Entzündung oder Schwellung des Gewebes begleitet.

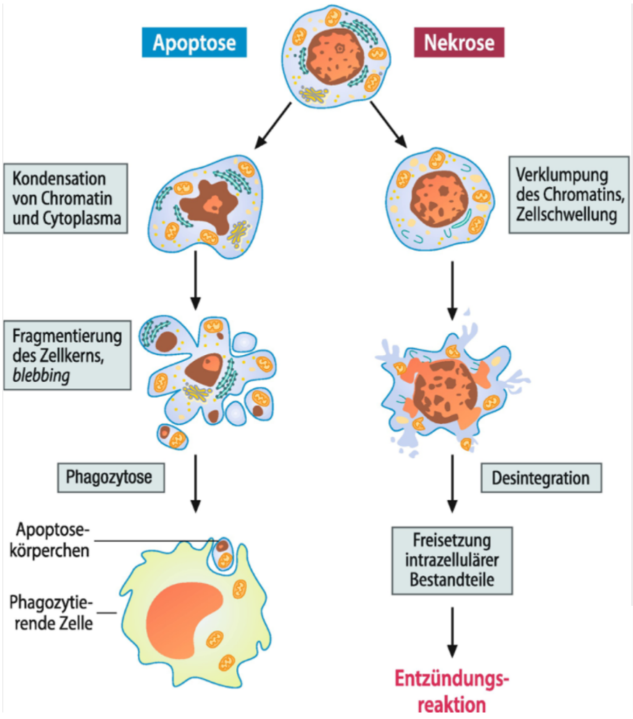
Apoptose
Nekrose
Kondensation von Chromatin und Cytoplasma
Verklumpung des Chromatins, Zellschwellung
Fragmentierung des Zellkerns, *blebbing*
Phagozytose
Desintegration
Apoptose-körperchen
Phagozytie-rende Zelle
Freisetzung intrazellulärer Bestandteile
Entzündungs-reaktion

Abbildung 3: Zelluläre Vorgänge bei Apoptose und Nekrose.[282]

Während der Apoptose durchläuft die Zelle verschiedene morphologische Veränderungen wie die Bildung von Ausbuchtungen oder Blasen (Blebs) an der Zellmembran, auch bekannt als "Blebbing" (Abbildung 3). Der Prozess der Apoptose geht außerdem mit einer Schrumpfung des Zellkerns, seiner Fragmentierung sowie dem Abbau von DNA einher und endet mit dem Zerfall der Zelle in apoptotische Partikel.[57; 58]

Mithilfe geeigneter biologischer Assays können diese Merkmale apoptotischer Zellen nachgewiesen oder beobachtet werden. Die Chemotherapie bleibt auch heute noch eine der bedeutendsten Methoden zur Behandlung bösartigen Gewebes, und eine Vielzahl von Antitumortherapeutika wird bereits klinisch eingesetzt, wobei ein Großteil davon Naturstoffe oder Naturstoffderivate sind.[59; 34]

1.1.4 Krebsmedikation auf Naturstoffbasis

Die Nutzung von pflanzlichen Naturstoffen zur Entwicklung neuer Krebsmedikamente begann in den 1950er-Jahren, als Vinblastin und Podophyllotoxin entdeckt und isoliert wurden (Abbildung 4).[60; 61] In den 1960er-Jahren wurden im Rahmen eines Forschungsprogramms, das vom United States National Cancer Institute (NCI) ins Leben gerufen wurde, eine Reihe vielversprechender Naturstoffe mit zytotoxischen Eigenschaften identifiziert. Dazu gehören unter anderem Paclitaxel und Camptothecin, die erstmals von den Chemikern Monroe E. Wall und Mansukh C. Wani isoliert und untersucht wurden und bis heute zur klinischen Behandlung von bösartigen Tumoren eingesetzt werden.[60; 62; 63]

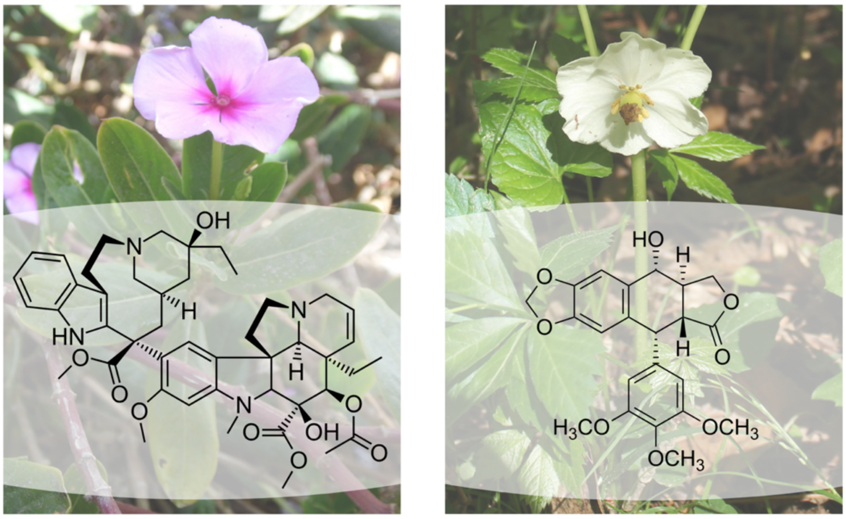

Abbildung 4: Vinblastin (aus Catharanthus roseus) und Podophyllotoxin (aus Podophyllum peltatum).[64; 65]

Seitdem wurden weiter zahlreiche antitumoraktive Wirkstoffe entwickelt, die von natürlichen Molekülen abgeleitet sind. Zwischen 1981 und 2014 wurden insgesamt 174 neue Krebsmedikamente zugelassen, wobei 85 davon Naturstoffe oder von ihnen abgeleitete Derivate waren.[66; 67; 60; 68]

1.1.5 Aktuelle Forschung

In den letzten Jahren wurden bedeutende Fortschritte in der Erforschung neuer Therapieformen zur Behandlung von Krebs erzielt. Im August 2017 erhielten die ersten adaptiven Immuntherapien, bekannt als CAR-T-Zell-Therapien, die Zulassung von der U.S. Food and Drug Administration (FDA).[69] Etwa ein Jahr später wurde diese Therapie auch von der Europäischen Kommission für den Einsatz in Europa zugelassen.[70] Diese innovativen Methoden werden als Gentherapien eingestuft und basieren auf der Modifizierung körpereigener Abwehrzellen. Dabei werden T-Lymphozyten (T-Zellen) vom Patienten entnommen und genetisch verändert, indem sie mit einem Chimären Antigen-Rezeptor (CAR) ausgestattet werden. Dieser CAR ermöglicht es den modifizierten T-Zellen, spezifische Moleküle auf der Oberfläche von Krebszellen zu erkennen und somit Tumore zu identifizieren. Nach einer Vermehrung und gründlichen Qualitätskontrolle werden die modifizierten T-Zellen dem Patienten injiziert. Dort binden sie an die entsprechenden Tumorzellen und lösen deren programmierten Zelltod aus (Abbildung 5).[71; 72]

Beispiele hierfür sind das von Novartis entwickelte Medikament Tisagenlecleucel, auch bekannt als Kymriah® und das Axicabtagenciloleucel von Kite Pharma, welches unter dem Namen Yescarta® vertrieben wird.[73][74]

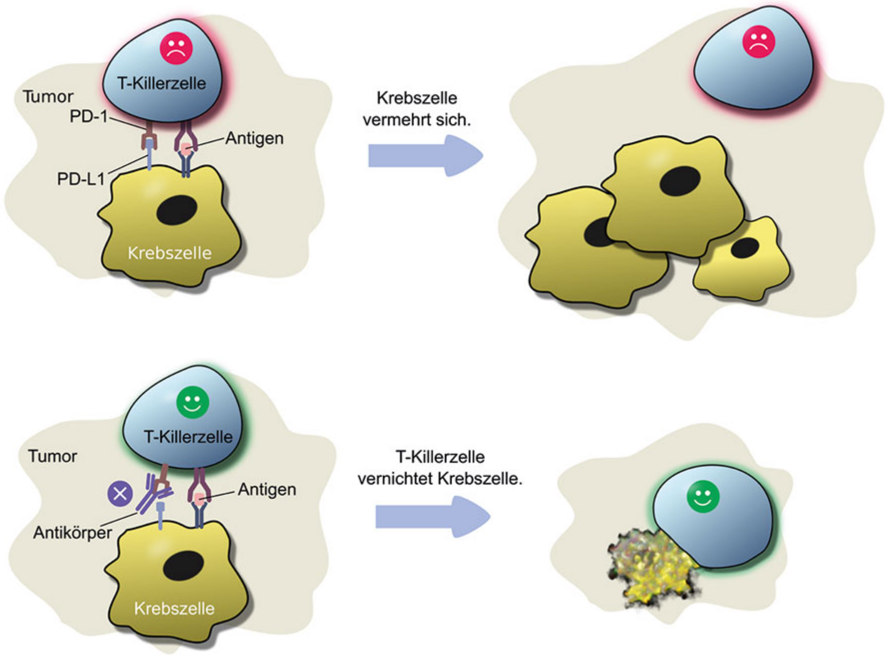
Tumor
T-Killerzelle
PD-1
Antigen
PD-L1
Krebszelle
Krebszelle vermehrt sich.
Tumor
T-Killerzelle
Antigen
Antikörper
Krebszelle
T-Killerzelle vernichtet Krebszelle.

Abbildung 5: Funktion der Immuntherapie.[75]

Obwohl das Konzept der Behandlung von Krebs durch Stimulation des körpereigenen Immunsystems keine Neuheit der letzten Jahre ist, haben frühere Beobachtungen, bei denen Krebsrückgang nach Infektionen festgestellt wurde, die Grundlage für diese Ansätze geschaffen. Bereits 1891 versuchte der New Yorker Chirurg WILLIAM COLEY, durch Injektion von Bakterien in Tumore eine Immunreaktion auszulösen, die den Tumor bekämpfen sollte.[76] Seitdem wurden viele therapeutische Ansätze verfolgt, um Tumore durch das Immunsystem des Körpers zu bekämpfen. Erstmalig berichtete die Forschungsgruppe um MITCHISON im Jahr 1955 über ein spezifisches Targeting von Tumorzellen durch den adaptiven Transfer von Lymphozyten in Mausmodellen.[77] Obwohl einige dieser Untersuchungen vielversprechend schienen, zum Beispiel spezielle Impfstoffe zur Stimulation des Immunsystems, scheiterten viele von ihnen oder führten nicht zu den gewünschten Ergebnissen. Dies lag zum Teil an den Abwehrmechanismen, die Tumore gegen die zur Immunabwehr ausgesandten T-Zellen entwickelt haben. Diese Mechanismen ermöglichten es den Tumoren, vor den T-Zellen unerkannt zu bleiben oder deren Wirkung durch die Expression bestimmter Enzyme zu hemmen.[78; 79]

Ein Durchbruch in der Immuntherapie wurde bereits im Jahr 2011 mit der Zulassung von Ipilimumab - auch bekannt als Yervoy® - zur Behandlung von Melanomen erzielt.[80]

Dieser Wirkstoff agiert als Inhibitor des Checkpoint-Enzyms CTLA-4, das normalerweise die Aktivierung der körpereigenen T-Zellen verhindert oder reguliert. Durch die Hemmung dieses Enzyms können die T-Zellen das Tumorgewebe ungehindert angreifen und bekämpfen.[81; 78] Diese Entdeckung rückte daraufhin weitere Inhibitoren, wie zum Beispiel PD-1, in den Fokus weiterer Forschungen und beschleunigte die Entwicklung neuer immunbasierter Therapieformen gegen Krebs.[82; 83] Für ihre bahnbrechenden Forschungen auf dem Gebiet der Immuntherapie von Tumoren wurden im Jahr 2018 die beiden Wissenschaftler JAMES P. ALLISON und TASUKU HONJO mit dem Nobelpreis für Physiologie oder Medizin ausgezeichnet.[84]

1.2 Terpenoide Naturstoffe als Leitstrukturen

1.2.1 Grundlagen und Entstehung

Häufig dienen bereits pharmakologisch aktive Substanzen als Ausgangspunkt für die Entwicklung neuer Wirkstoffe. Diese Substanzen, auch als Leitstrukturen bezeichnet, weisen bereits eine gewisse pharmakologische Aktivität für spezifische therapeutische Anwendungen auf. Durch gezielte chemische Modifizierungen werden diese Leitstrukturen derivatisiert, um ihre pharmakologischen Eigenschaften zu optimieren und sie somit als potenzielle Therapeutika einzusetzen.[85; 86] Die Optimierung konzentriert sich dabei auf Aspekte wie Aktivität und Selektivität, während gleichzeitig die Toxizität und Nebenwirkungen minimiert werden. Die meisten dieser Leitstrukturen sind oder basieren auf Naturstoffen, die als Grundlage für die Entwicklung neuer Wirkstoffe dienen.[87] Die Entdeckung neuer Wirkstoffe zwischen 1980 und 2020 zeigt eine signifikante Beteiligung sowohl synthetischer als auch von Naturstoffen abgeleiteter Verbindungen. Ungefähr die Hälfte aller neu zugelassenen Wirkstoffe lässt sich strukturell auf Naturprodukte zurückführen.[15]

Somit bleiben Naturstoffe ein wichtiger Bestandteil in der Wirkstoffforschung. Nicht nur aufgrund ihrer von Natur aus bestehenden Bioaktivität, sondern vor allem auch wegen ihrer einzigartigen Struktur. Naturstoffe weisen oft eine komplexe Struktur, welche so besser an die entsprechenden Rezeptoren binden können.[15; 88; 89]

Eine bedeutende Gruppe von Naturstoffen, vorwiegend pflanzlichen Ursprungs, sind die Terpene, welche eine vielversprechende Gruppe von Verbindungen dar, die zur Behandlung von Tumorerkrankungen eingesetzt werden können.[90–92] Diese setzen sich aus Isopren-Untereinheiten zusammen und werden in Abhängigkeit von der Anzahl der Isopreneinheiten bzw. Kohlenstoffatome können in Hemi- (C5), Mono- (C10), Sesqui- (C15), Di- (C20), Sester- (C25), Tri- (C30), Tetra- (C40) oder Polyterpene (>C40) eingeteilt.[93]

Wesentliche Forschungsarbeiten auf dem Gebiet der Terpene wurden von den Chemikern OTTO WALLACH und LEOPOLD RUŽIČKA geleistet. Ihre Forschungen legten die Grundlagen für zahlreiche weitere Untersuchungen terpenoider Strukturen. Neben der Strukturaufklärung gewannen hierbei auch Untersuchungen zu pharmakologischen Eigenschaften zunehmend an Bedeutung.[94; 95]

Eine wichtige Gruppe der Terpene, die bereits großes Potenzial hinsichtlich ihrer pharmakologischen Eigenschaften zeigt, sind die pentazyklischen Triterpene. Etwa 4000 der bekannten Triterpene leiten sich dabei vom Squalan oder dem strukturverwandten Squalen ab. Wichtige Grundgerüste der pentazyklischen Triterpene sind zum Beispiel Lupan, Oleanan und Ursan (Abbildung 6).[96]

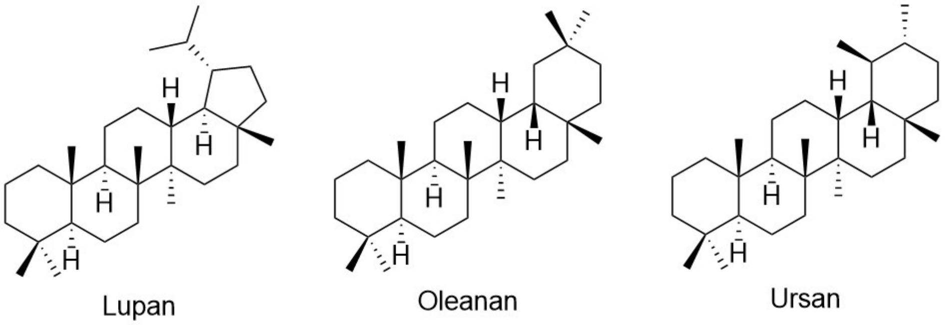

Abbildung 6: Häufige Grundgerüste der Triterpene.

Sie zeigen hierbei ein breites Spektrum an biologischem Potenzial. Unter anderem werden ihnen antitumorale und antiinflammatorisch sowie wie bakterizide, fungizide, antivirale, zytotoxische, analgetische, spermizide, kardiovaskuläre und anti-allergene Eigenschaften zugeschrieben.[97–101]

Viele dieser Verbindungen wurden zudem bezüglich ihrer pharmakologischen Wirkmechanismen umfänglich untersucht. (Tabelle 1).

Tabelle 1: Apoptotische Wirkmechanismen verschiedener Triterpencarbonsäuren.

Verbindung	**Wirkmechanismus**
Oleanolsäure [102–106]	↑Caspase 3, Caspase 8 und Caspase 9 ↓ NF-κB,Cdk, Bcl-2
Ursolsäure [107–109]	↑Caspase 3, Caspase 8 und Caspase 9 ↓ NF-κB, Bcl-2
Betulinsäure [110; 111]	↑Caspase 3, Caspase 8 und Caspase 9, Störung des mitochondrialen Membranpotentials ↓ NF-κB, Bcl-2
Asiasäure [112–114]	↑Caspase3 und Caspase 9, intrazellulären Ca^{2+}-Konzentration, Bax ↓Bcl-2

1.2.2 Asiasäure und Derivate

Die Asiasäure ist eine bislang nur begrenzt erforschte pentazyklische Triterpencarbonsäure, und wurde erstmals 1950 von Paris in *Centella asiatica* nachgewiesen (Abb. 7).[115] Sie basiert auf dem Ursan-Grundgerüst (Abb. 6). Es gibt jedoch einige Quellen, die die inhärenten pharmakologischen Eigenschaften der Asiasäure beleuchten.[116] Shukla *et al.*, Gray *et al.* und Babu *et al.* isolierten asiasäurehaltige Pflanzenextrakte, die freie Asiasäure sowie die glykosidisch gebundene Form aus *Centella asiatica*. Sowohl der Extrakt als auch die freie, aber auch glykosidisch gebundene Form zeigten bei pharmakologischen Untersuchungen einen positiven Effekt auf die Wundheilungsförderung, eine neuroprotektive Wirkung sowie auch antiproliferative Effekte.[117–119]

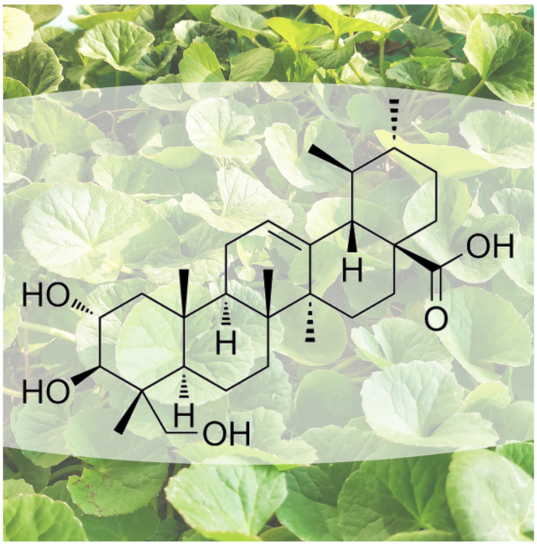

Abbildung 7: Asiasäure aus Centella asiatica.[120]

Darüber hinaus wurde festgestellt, dass Asiasäure die Fähigkeit besitzt, die Bildung neuer Blutgefäße zu hemmen, was besonders im Kontext der Krebsbehandlung von Interesse ist, da Tumore für ihr Wachstum und ihre Metastasierung auf die Bildung neuer Blutgefäße angewiesen sind (Angiogenese).[114] Infolge Untersuchung an Tiermodellen konnte der hepatoprotektive Effekte der Asiasäure gezeigt werden, was auf eine mögliche Anwendung bei der Behandlung von Lebererkrankungen hinweist.[121] KAHNT *et al.* konnten durch die Modifikation von Asiasäure und weiterer Triterpencarbonsäuren eine verbesserte Antitumoraktivität sowie Selektivität nachweisen.[122]

1.2.3 Weitere Triterpenoide und Derivate (Ursol-, Corosol,- und Madecassinsäure)

Eine Vielzahl von Vertretern aus der Gruppe der pentazyklischen Triterpene wurde bereits ausführlich hinsichtlich ihrer biologischen Aktivitäten erforscht. Insbesondere die Ursolsäure (Abb. 8) wurde in der Vergangenheit bereits umfassend untersucht.[123–125] In der Literatur gibt es zahlreiche Nachweise für ihre zytotoxischen und apoptose-induzierenden Eigenschaften.[126; 127] Verschiedene Forschungsarbeiten haben sich darauf konzentriert, den Wirkmechanismus zu untersuchen, jedoch konnte bislang keine vollständige Aufklärung erreicht werden.

Weitere wichtige pentazyklische Triterpencarbonsäuren wie Oleanolsäure und Maslinsäure (Abb. 8), die vom Oleanan-Grundgerüst abgeleitet sind, wurden ebenfalls eingehend auf ihre biologische Aktivität untersucht. Dabei wurden interessante pharmakologische Eigenschaften wie antioxidative, antivirale und antitumorale Effekte beobachtet.[128–131] Ähnlich wie bei der Ursolsäure wurden auch für Oleanolsäure und Maslinsäure apoptoseinduzierende Eigenschaften gegenüber verschiedenen Tumorzellen festgestellt.

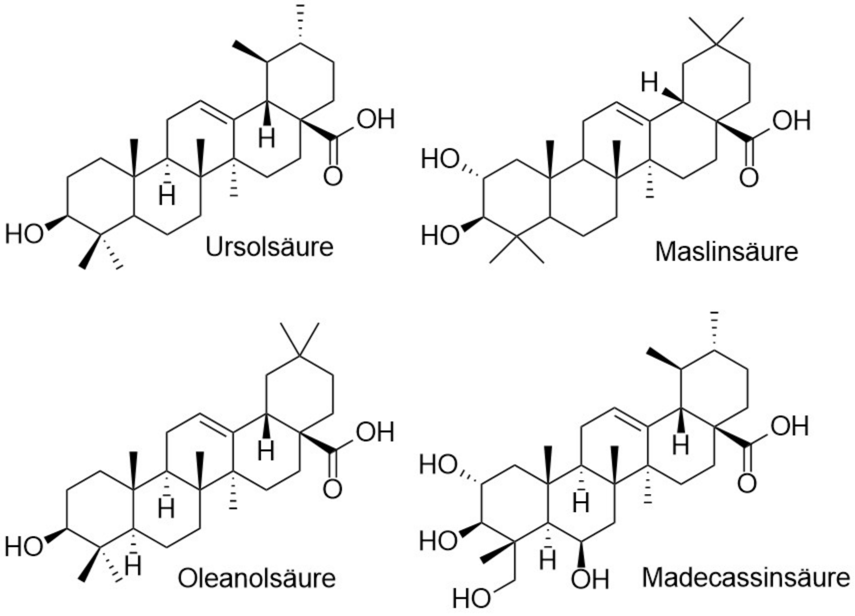

Abbildung 8: Pentazyklische Triterpencarbonsäuren.

Weitere wichtige pentazyklische Triterpencarbonsäuren wie Oleanolsäure und Maslinsäure (Abb. 8), die vom Oleanan-Grundgerüst abgeleitet sind, wurden ebenfalls eingehend auf ihre biologische Aktivität untersucht. Dabei wurden interessante pharmakologische Eigenschaften wie antioxidative, antivirale und antitumorale Effekte beobachtet.[128–131] Ähnlich wie bei der Ursolsäure wurden auch für Oleanolsäure und Maslinsäure apoptoseinduzierende Eigenschaften gegenüber verschiedenen Tumorzellen festgestellt.

Ein hingegen bisher weniger erforschtes pentazyklisches Triterpen ist die Madecassinsäure (Abb. 8), die beispielsweise in *Centella asiatica* vorkommt.[116; 132]

Es existieren verschiedene Ansätze zur Isolierung der Madecassinsäure aus dem entsprechenden Pflanzenmaterial, wobei Methoden mithilfe der Mikrowelle als mögliche Alternativen zur herkömmlichen Extraktion mittels Soxhlet oder gegenüber dem Digerieren zunehmend an Bedeutung gewinnen.[133] Hierbei gibt es jedoch eine Limitierung bezüglich der Menge des eingesetzten Pflanzenmaterials pro Extraktion.

Madecassinsäure weist ebenfalls wie die vorherigen genannten Triterpencarbonsäuren eine Vielzahl von inhärenten pharmakologischen Eigenschaften auf, einschließlich antitumoraler, antioxidativer, anti-inflammatorischer, cardio- und neuroprotektiver Aktivitäten.[134–138]

1.3 Kationische Fluoreszenzfarbstoff-Analoga als hochaktive und selektive Verbindungen

1.3.1 Safirinium-Konjugate

Krebs ist, wie bereits ausführlich erläutert, nach wie vor die zweithäufigste Todesursache. Insbesondere einige Krebsarten weisen aggressivere Phänotypen auf als andere wie Prostata- und Brustkrebs.[139; 140] Darüber hinaus führen hypoxische Tumore zu einer Versauerung der Tumorumgebung, was die Resistenz, Invasion und Proliferation des Tumors weiter erhöht.[141–143] In jüngster Zeit haben Antikrebsmedikamente, die das Mitochondrium als Wirkort haben – auch bekannt als Mitocane - immer mehr Aufmerksamkeit erlangt, da diese Verbindungen Todesignale von den Mitochondrien auslösen, wodurch Tumorzellen, die aufgrund von DNA-Schäden nicht mehr auf externe Todesignale reagieren, Apoptose auslösen.[144; 145] Dies wurde bereits für Analogverbindungen von Vitamin E sowie für Triterpenoide und Steroide gezeigt.[146–148]

Bei letzteren Verbindungen wurde dies durch die Anbindung lipophiler Kationen (wie Rhodamin B, einer BODIPY-Einheit, einer Triphenylphosphonium-Einheit, einem Ammoniumsalz oder Derivaten von Malachitgrün) an das Triterpenoid- oder Steroidgerüst erreicht (Abb. 9).[149–156] Allerdings ist die bloße Anwesenheit eines Kations nicht ausreichend, um eine gute Zytotoxizität in Tumorzellen zu erreichen. Zum Beispiel sind distale *N*-Oxide und quartäre Ammoniumsalze von Triterpenoiden deutlich weniger zytotoxisch als z. B. Benzylamide.[157; 158; 130]

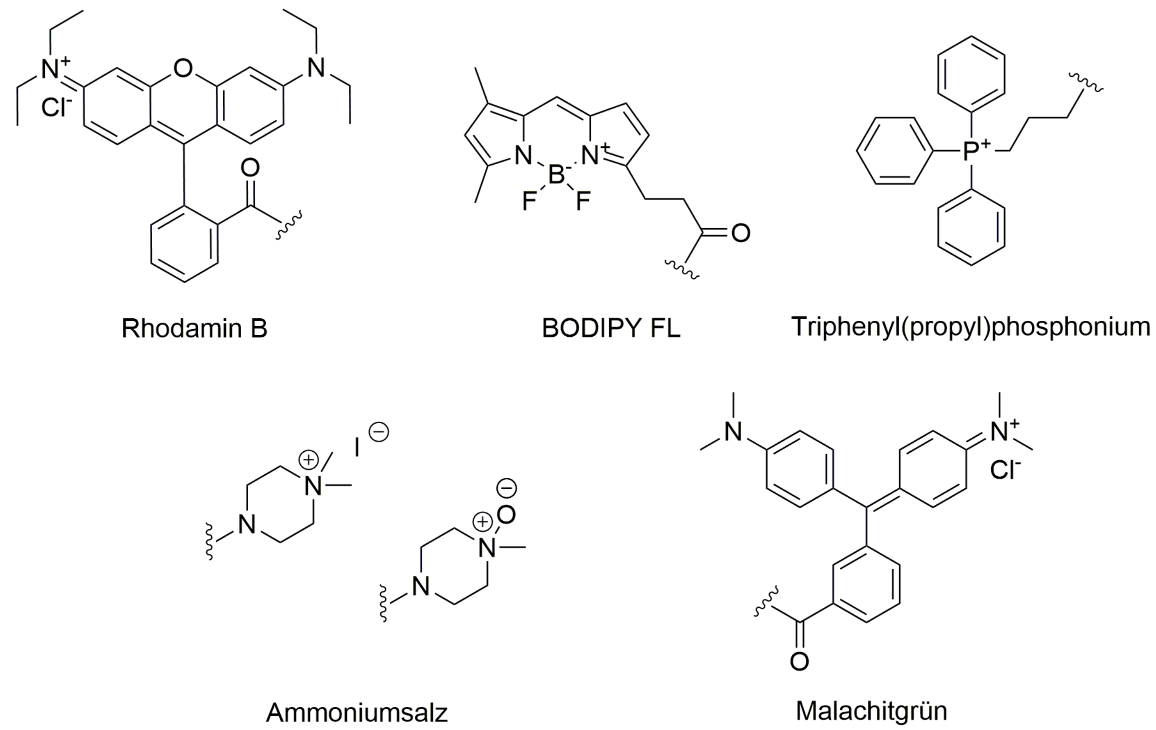

Abbildung 9: Auswahl lipohiler Kationen für die Kupplung an Triterpene und Steroide.

Vor einiger Zeit ist es SACZEWSKI *et al.* gelungen, sogenannte "Safirinium-Hybride" durch Tandem-Mannich-elektrophile Aminierungsreaktionen aus profluorogenen Isoxazolinonen und sekundären Aminen wie Chinolonen oder kurzen Peptiden zu synthetisieren.[159] Die früheren Hybride zeigten eine höhere Lipophilie, und die letzteren waren in der Lage, Sporen von *Bacillus subtilis* zu färben.[160] Hierbei wurde beobachtet, dass Safirinium-Hybride gut in Zellen transportiert werden können, was sie für die Untersuchung bezüglich des zytotoxischen Potenzials besonders interessant macht.. Die Hybridisierung ist oft mit der Fähigkeit verbunden, das bekannte Problem (Wirksamkeit, Affinität, Löslichkeit, unerwünschte Nebenwirkungen usw.) mit dem anderen Hybridteil auszugleichen. Mangelnde Löslichkeit in biologischen Systemen ist ein bekanntes Problem, das häufig mit Triterpenen in Verbindung gebracht wird.[161; 162] Dieses Problem könnte jedoch durch die Bindung an eine kationische Restgruppe wie eine Safirinium-Einheit gelöst werden. Das Interesse liegt daher darauf festzustellen, ob triterpenoide Safirinium-Hybride effizient den Zelltod auszulösen.

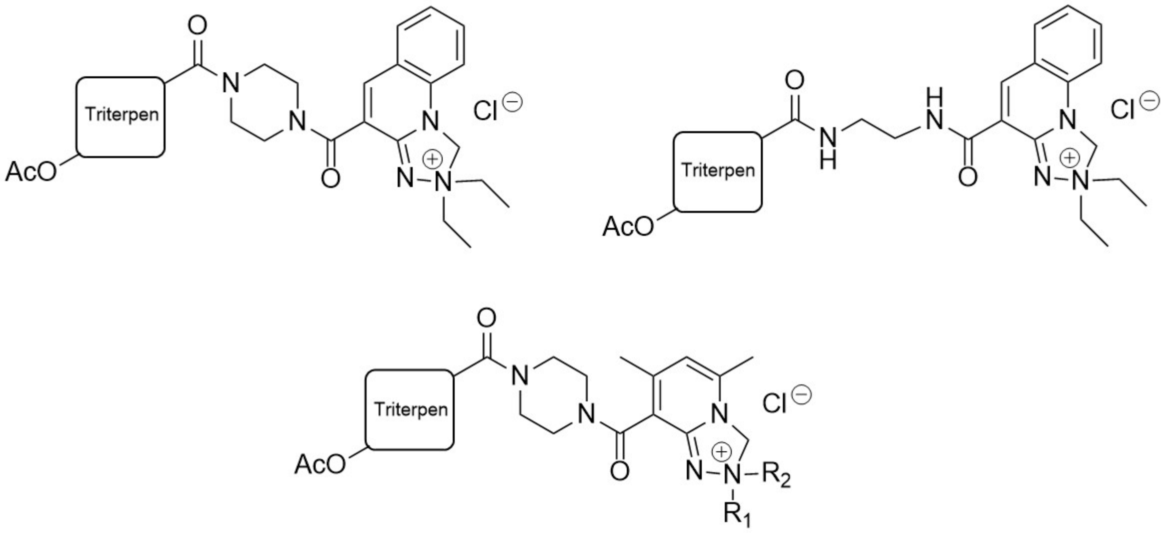

Abbildung 10: Triterpen-Safirinium P & Q-Hybride.

Betulinsäure (BA) ist zum Beispiel ein Triterpen, das vielversprechende *in-vitro-* und *in-vivo*-Antitumor-Aktivität in Melanom-, neuroektodermalen Tumor- und Gliomzelllinien zeigt.[163–166] Es zielt auf die mitochondrialen Permeabilitätsübergangsporen ab.[167–169] Es reguliert auch Bcl-2 herunter, was die Apoptose fördert, sowie VEGFR und NF-κB, die beide eng mit der Angiogenese und der Tumorproliferation verbunden sind.[170–172] Basierend auf dieser Strategie liegt der Fokus darauf, verschiedene Triterpen-Safirinium-Konjugate zu synthetisieren (Abb. 10) und ihre Zytotoxizität und Selektivität für verschiedene menschliche Tumorzelllinien zu untersuchen.

1.3.2 Rhodamin B-Konjugate

Rhodamin und seine Derivate werden häufig verwendet, um das Mitochondrium zu färben.[173–176] Frühere Forschungen haben gezeigt, dass terpenoide Rhodamin-Konjugate spezifisch auf das Mitochondrium abzielen und eine hohe Zytotoxizität gegen Tumorzellen aufweisen. Dies wurde auch für einige Rhodamin-Steroid-Konjugate festgestellt. [149; 177] Die Herausforderung bei Triterpenen besteht darin, dass sie in wässrigem Milieu von Tumorzellen nur schwer löslich sind, aber durch die Rhodamin-Konjugation wird dieses Problem verbessert.[178; 179]

Besonders einfache Rhodamin B Derivate können kostengünstig und in großen Mengen hergestellt werden, wodurch sie vielversprechende Kandidaten für die antitumorale Therapie sind.[180; 181] Zudem erfüllen sie die Lipinski-Regeln, was sie zu vielversprechenden "Lead"-Verbindungen macht. [182–184]

Die Herstellung von Verbindungen aus Ethyl-, Hexyl- und Eicosylestern sowie Amiden von Piperidin abgeleiteten Verbindungen gelang in guten bis sehr guten Ausbeuten von 48 bis 92 % aus dem Rhodaminacylchlorid. Insbesondere der Ethylester zeigte mit einer Zytotoxizität von 0,15 ± 0,02 µM sehr gute EC_{50}-Werte. Unerwarteterweise wiesen die EC_{50}-Werte des Eicosylesters hohe Werte von >20 µM auf, obwohl man aufgrund der Ähnlichkeit des Eicosylrestes zu den Triterpenen eine höhere Wirksamkeit erwartet hätte.[185] Es ist bekannt, dass hydrophobe Reste sogar schneller die Membran passieren als hydrophile.[186; 187] Es ist auch auffällig, dass die Rhodamin B Ester keine Selektivität gegenüber den Tumorzellen zeigen.

Die Rhodamin B Amide zeigen gute EC_{50}-Werte zwischen 0,27 ± 0,01 µM und 17,34 ± 0,8 µM. Allerdings fällt auf, dass das Rhodamin B Piperazinamid mit EC_{50}-Werten >30 µM deutlich weniger aktiv ist als die anderen Derivate. Weiterhin zeigen die Rhodamin B Amide eine gute Selektivität gegenüber MCF-7 (Brustkrebs) und A2780 (Eierstockkrebs) Zellen. Besonders das Morpholinderivat sticht mit guten Selektivitätswerten von S = 19,5 gegen MCF-7 und S = 18,1 gegen A2780 Zellen hervor.

Ergebnisse des SRB-Assays von KAHNT *et al.* zeigen eine hohe zytotoxische Wirksamkeit der synthetisierten Asiasäure Rhodamin B-Konjugate mit Piperazin-Spacer (Tab. 2).[122]

Tabelle 2: EC50-Werte ausgewählter Derivate nach KAHNT.[122]

#	A375	HT29	MCF7	A2780	NIH 3T3
AA	>30	>30	>30	28.2 ± 0.3	26.2 ± 2.5
8	1.3 ± 0.2	1.3 ± 0.1	2.0 ± 0.1	0.8 ± 0.09	1.8 ± 0.04
11	n.d.	0.017 ± 0.013	0.012 ± 0.002	0.008 ± 0.002	0.178 ± 0.027
Dox	n.d.	0.9 ± 0.2	1.1 ± 0.3	0.02 ± 0.01	1.7 ± 0.3

Diese Ergebnisse bestätigt abermals das allgemeine hohe pharmakologische Potenzial von terpenoiden Rhodamin B-Konjugaten, wie bereits in den Untersuchungen von SOMMERWERK *et al.* und WOLFRAM *et al.* gezeigt wurde.[178; 150]

Die Variation des Amid-Spacers führt zu einer signifikanten Veränderung hinsichtlich der Zytotoxizität des Rhodamin B-Konjugates. Im Rahmen dieser Studien wurde ebenfalls festgestellt, dass je nach verwendetem „Spacer“ die Rhodamin B-Triterpen-Derivate offensichtlich nur dann zytotoxisch, wenn eine "offene" (fluoreszierende) Form vorliegt (Abb. 11). Wenn Rhodamin B hingegen in einer geschlossenen/nicht fluoreszierenden Lacton- oder Lactam-Form vorliegt, sind die entsprechenden Konjugate praktisch nicht zytotoxisch.[178; 149]

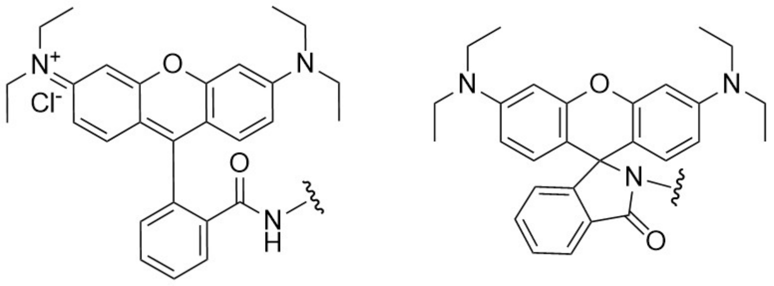

Rhodamin B-Einheit
(offene Form)

Rhodamin B-Einheit
(geschlossene Form)

Abbildung 11:Offene und geschlossene Rhodamin B-Einheit.

Konjugate, bei denen die Rhodamin B-Einheit direkt an das Grundgerüst des Triterpens angebunden ist (z. B. als Ester), sind zwar zytotoxisch, aber in der Regel nicht sehr selektiv.[150; 185] Dies verdeutlicht, dass nicht nur der Rhodamin B-Rest alleine zu einer erhöhten Zytotoxizität führt, sondern auch die Verknüpfung mit dem Triterpen-Grundgerüst über den Amin-Spacer entscheidend ist.

Basierend auf der zytotoxischen Aktivität der bereits untersuchten Triterpen-Rhodamin B-Konjugate liegt der Fokus darauf, eine zusätzliche Substanzbibliothek über die Schotten-Baumann-Methode aus Asia- und Madecassinsäure zu synthetisieren.[188] und eine systematische Variation der Amin-Spacer zu erzielen. Zudem gilt es, zytotoxische Triterpencarbonsäure-Konjugate zu entwickeln, die eine dauerhaft positiv geladene Einheit tragen; diese Verbindungen sollten auch als fluoreszierende molekulare Sonden wirken können. Diese letztere Eigenschaft ist auch mit der Fähigkeit verbunden, die Aufnahme und intrazelluläre Verteilung der Moleküle auf direktem Weg zu beobachten. Auf diese Weise können wertvolle Informationen über molekulare Mechanismen recht einfach gewonnen werden.

2 Zielstellung

Die mannigfaltige Naturstoffklasse der Terpene hat aufgrund ihrer bereits natürlichen pharmakologischen Eigenschaften schon lange das Interesse der Naturstoff- und Wirkstoffforschung geweckt. Die Forschung ist hier jedoch unterschiedlich weit fortgeschritten. Während einige Vertreter wie Betulin-, Ursol- oder Oleanolsäure umfangreich untersucht und durch zahlreiche Quellen belegt wurden, sind andere Triterpene wie Asia- oder Madacassinsäure in der Literatur bisher weniger präsent.

In dieser Arbeit steht die Synthese neuartiger Triterpencarbonsäure-Derivate im Vordergrund, mit dem Hauptziel, deren zytotoxische und selektive Wirkung gegenüber menschlichen malignen Tumorzelllinien *in vitro* zu erhöhen. Als Ausgangspunkt für die Derivatisierung zu entsprechenden Konjugaten dienen weitverbreitete pentazyklische Triterpene wie Betulin-, Oleanol-, Ursol- oder Platansäure, aber auch die selteneren Triterpencarbonsäuren Asia- und Madecassinsäure. Die Carboxylgruppe der entsprechenden Verbindungen sollen dabei als Angriffspunkte dienen, um zunächst zum entsprechenden Amid und fortsetzend zum Farbstoffkonjugat derivatisiert werden zu können.

Ein besonderer Fokus liegt dabei auf den bisher wenig erforschten Rhodamin B- und Safirinium-Konjugaten, von denen beide potenziell für eine zielgerichtete Tumortherapie in Betracht gezogen werden können. Das Potenzial von Safirinum-Derivaten als potenzielle Mitocane ist bisher noch unbekannt, da diesbezüglich bisher noch keine Untersuchungen durchgeführt wurden. Das Augenmerk liegt hierbei darauf, selektive Verbindungen zu erhalten, aber auch auf der Steigerung der Aktivität.

Des Weiteren werden am Beispiel der Asia- und Madecassinsäure zwei Vertreter der pentazyklischen Triterpencarbonsäuren verwendet, welche strukturell starken Ähnlichkeiten mit der bereits bekannten und hinreichend untersuchten Maslinsäure haben. Dadurch können Rückschlüsse auf die Wirkungsweise gezogen werden und neue Ansatzpunkte für mitocane Verbindungen zur Tumortherapie entstehen.

Zusätzlich wird beabsichtig zu untersuchen, wie sich eine hinreichend aktive und selektive Verbindung im Tumor-Sphäroid und *in vivo* verhält.

3 Diskussion und Einordnung der Ergebnisse

3.1 Safirinium-Konjugate

3.1.1 Zytotoxische Triterpencarbonsäure-Safirinium-Derivat

Krebs bleibt die zweithäufigste Todesursache, wobei bestimmte aggressive Arten wie Prostata- und Brustkrebs besonders hervorstechen. Hypoxische Tumore verschärfen diese Problematik, indem sie die Resistenz und Ausbreitung der Tumorzellen fördern.[189] In diesem Kontext erlangen mitochondriale Antikrebsmittel, auch bekannt als "Mitocane", zunehmende Aufmerksamkeit, da sie auch in resistenten Tumorzellen wirksam sind.[190–196; 185; 178; 197; 150; 198; 152; 199–201; 158; 202; 203; 190]

Besonders vielversprechend erweist sich die Kombination von lipophilen Kationen mit Triterpenoiden oder Steroiden, die bemerkenswerte zytotoxische Eigenschaften zeigt.[192; 203] Es muss jedoch beachtet werden, dass nicht alle Verbindungen gleichermaßen wirksam sind.[158; 202–205] Unser Fokus liegt daher auf zytotoxischen Triterpenkonjugaten mit dauerhaft positiv geladenen Gruppen, die zusätzlich als fluoreszierende Sonden dienen können.[206; 160]

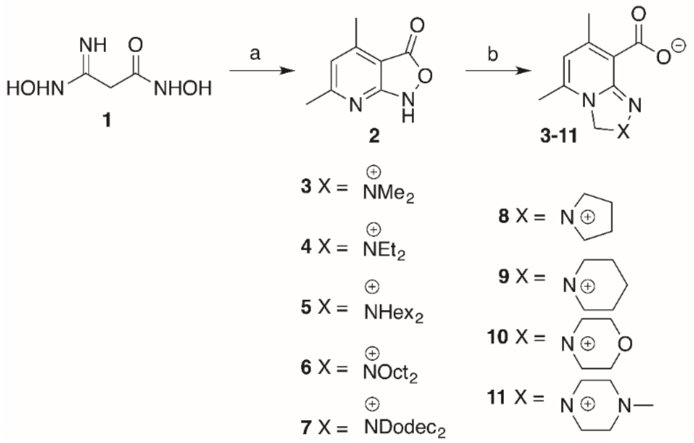

Abbildung 12: Synthese von Safirinium P.

Die bisherigen Erkenntnisse zu "Safirinium-Hybriden" inspirierten uns, das Potenzial von Safirinium-Triterpen-Hybriden hinsichtlich ihrer Zytotoxizität zu erforschen. Diese könnten bekannte Probleme wie die geringe Löslichkeit von Triterpenen in biologischen Systemen adressieren. Insbesondere Betulinsäure zeigt vielversprechende antitumorale Aktivitäten und reguliert die Tumorentwicklung.[207–209; 154; 145; 210]

Auf dieser Basis synthetisieren wir verschiedene Triterpen-Safirinium-Konjugate, um deren Wirkung auf Tumorzelllinien zu untersuchen. Die Synthese der Safirinium P-Derivate (Abb. 12) verlief erfolgreich, ebenso wie die Aktivierung der Safirinium Q-Derivate (Abb. 13).[211; 212] Die Acetylierung von Triterpensäuren führte zu vielversprechenden Verbindungen.[185; 198]

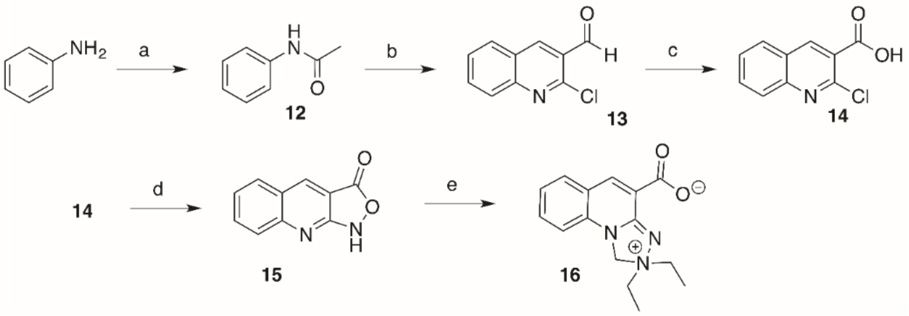

Abbildung 13: Synthese von Safirinium Q.

Die UV/Vis-Spektren der Safirinium-Betulinsäure-Hybride wiesen ähnliche Werte wie veröffentlichte Daten für Analoga auf.

Einige der synthetisierten Derivate zeigten keine Zytotoxizität (**29**, **31**, **32**, **34** und **39**), während andere eine moderate Aktivität aufwiesen (**33**, **35-38**). Ein Derivat (**30**) zeigte eine vielversprechende Zytotoxizität, war jedoch unselektiv gegenüber nicht-malignen Fibroblasten (Tab. 3). Überraschenderweise lokalisierten sich die Verbindungen im endoplasmatischen Retikulum und nicht in den Mitochondrien, was dem erwarteten Verhalten von Mitocanen widerspricht.

Tabelle 3:EC50-Werte ausgewählter Derivate.

	A375	HT29	MCF–7	A2780	FaDu	NiH3T3
Rho	> 30	> 30	> 30	> 30	> 30	> 30
3–11	> 30	> 30	> 30	> 30	> 30	> 30
29	26.2 ± 1.3	> 30	26.3 ± 2.1	21.6 ± 2.4	> 30	22.4 ± 2.2
30	5.4 ± 0.1	7.5 ± 0.3	4.9 ± 0.3	4.6 ± 0.3	6.0 ± 0.3	6.6 ± 0.3
31	16.8 ± 1.0	24.9 ± 1.7	15.7 ± 1.2	11.0 ± 1.2	10.7 ± 1.0	> 30
32	20.8 ± 1.7	27.0 ± 2.0	18.1 ± 1.0	14.1 ± 2.0	28.2 ± 2.3	> 30
33	21.4 ± 0.7	26.2 ± 0.7	19.8 ± 1.2	21.4 ± 1.9	18.1 ± 1.8	18.4 ± 2.0
34	21.4 ± 1.4	> 30	10.2 ± 1.1	9.0 ± 1.2	18.3 ± 1.1	> 30
35	15.0 ± 1.2	22.2 ± 0.9	13.2 ± 0.7	10.9 ± 1.8	13.3 ± 0.9	3.0 ± 0.6
36	18.6 ± 2.1	26.8 ± 0.6	17.6 ± 1.5	18.3 ± 2.8	12.3 ± 1.3	17.4 ± 1.7
37	19.0 ± 2.0	25.0 ± 1.0	21.8 ± 1.7	24.2 ± 2.6	27.1 ± 2.0	28.5 ± 1.1
38	13.8 ± 0.8	22.1 ± 0.8	11.7 ± 0.7	11.2 ± 1.4	10.2 ± 0.1	3.6 ± 1.0
39	16.6 ± 2.1	> 30	15.7 ± 1.4	20.8 ± 1.9	16.1 ± 1.3	21.3 ± 1.3
DX	n.d.	0.9 ± 0.01	1.1 ± 0.3	0.01 ± 0.01	n.d.	0.4 ± 0.07
ST	n.d.	0.2 ± 0.02	0.1 ± 0.01	0.1 ± 0.01	0.1 ± 0.05	0.008 ± 0.001

Die Synthesen der Safirinium-Fluoreszenzmarkierungen verliefen erfolgreich in Ausbeuten von 39 bis 57 %. Die Safirinium-Verbindungen zeigten keine Zytotoxizität, während viele Triterpenoid-Safirinium-Konjugate nur mäßige Wirkung aufwies. Ihre Lokalisierung im endoplasmatischen Retikulum könnte die geringere Zytotoxizität im Vergleich zu den Mitocanen Rhodamin B-Analoga erklären (Abb. 14).

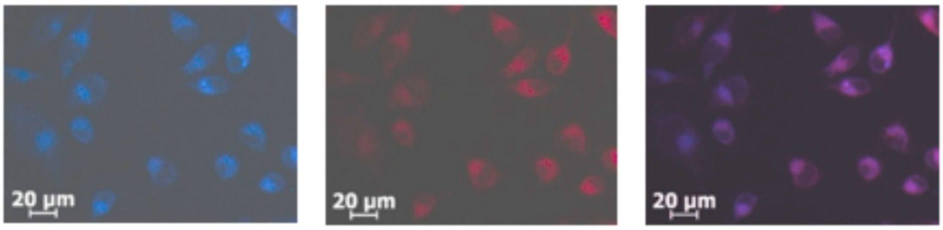

Abbildung 14: Fluoreszenzbildgebung von A375-Epithelkarzinomzellen, inkubiert mit: Verbindung 30 (links), ER-Tracker (Mitte) und zusammengeführte Bilder (rechts).

3.2 Rhodamin B-Konjugate

3.2.1 Euscaph- und Tormentillsäure – Einfluss des E-Rings auf die zytotoxische Wirkung

Der Extrakt der Blutwurzwurzeln enthält entzündungshemmende Tannine und wurde traditionell in der Volksmedizin für die Wundheilung und zur Behandlung von Durchfall eingesetzt. [213–219] Bereits seit dem Mittelalter besteht Interesse an den potenziellen krebsbekämpfenden Eigenschaften der Blutwurzwurzeln, insbesondere durch pentazyklische Triterpene wie Euscaphsäure (EA) und Tormentillsäure (TA). [220–227; 225; 228; 229] Ein verbessertes Extraktionsverfahren hat die Verfügbarkeit von EA und TA erheblich erhöht.[230–232] Während EA eine antikanzeröse Aktivität bei Leukämiezellen zeigt, weist TA nur eine schwache Aktivität gegen Tumorzelllinien auf. Aufgrund der vielversprechenden Ergebnisse werden derzeit Derivate untersucht, um ihre zytotoxische Aktivität genauer zu verstehen.[221; 226; 227; 230]

Die Extraktion der Blutwurzwurzeln ergab EA und TA.[230–232] Durch verschiedene chemische Reaktionen wurden Amide und Verbindungen synthetisiert, die mit Rhodamin B gekoppelt wurden (Abb. 15).[233–240]

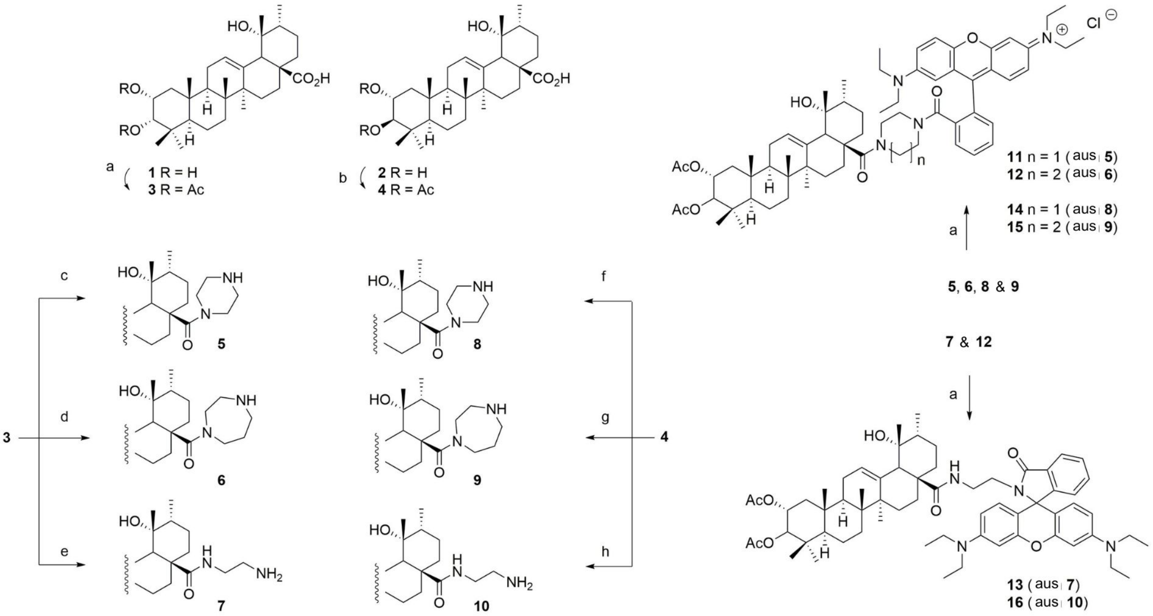

Abbildung 15: Syntheseschema zur Darstellung der Rhodamin B-Konjugate aus Tormentill- und Euscaphsäure.

Unterschiede in den Aminen spiegeln sich in ihren strukturellen und optischen Eigenschaften wider: Primäre Aminverbindungen sind farblos, während sekundäre Aminverbindungen tiefrosa erscheinen mit einem λmax von 560 ± 15 nm, typisch für kationische Rhodamin B-Derivate.[149] Diese Unterschiede deuten auf Strukturvariationen hin, wobei farblose Verbindungen mit einem Lacton- (oder Lactam-)Farbstoff in Rhodamin B-Derivaten verbunden sind.[241; 242]

Die synthetisierten Verbindungen wurden mittels des Sulforhodamin B-Assays auf ihre Zytotoxizität getestet. Während einige Verbindungen keine zytotoxische Wirkung zeigten, wiesen die Amide eine erhöhte Zytotoxizität auf. Alle Amide zeigten EC_{50}-Werte im niedrigen mikromolaren Bereich, wobei eine Verbindung (**6**) die höchste Aktivität aufwies. Kationische Rhodamin B-Konjugate wiesen im Allgemeinen die höchste Zytotoxizität auf. Besonders bemerkenswert war eine Verbindung (**15**), die eine bemerkenswerte Selektivität von 190 zwischen Tumor- und Nicht-Tumor-Zellen zeigte und eine gezielte Wirkung auf Mitochondrien hatte, die mittels Fluoreszenzmikroskopie festgestellt wurde (Tab. 4).

Tabelle 4: EC50-Werte der synthetisierten Derivate.

#	A375	HT29	MCF-7	A2780	FaDu	NIH 3T3
1	>30	>30	>30	>30	>30	>30
2	>30	>30	>30	>30	>30	>30
3	>30	>30	25.0 ± 3.5	24.2 ± 0.9	>30	>30
4	>30	>30	>30	>30	>30	>30
5	1.19 ± 0.1	2.05 ± 0.2	2.26 ± 0.3	1.77 ± 0.1	1.43 ± 0.1	2.51 ± 0.1
6	1.22 ± 0.1	2.25 ± 0.1	2.50 ± 0.1	1.78 ± 0.1	1.55 ± 0.3	2.61 ± 0.2
7	2.15 ± 0.1	3.28 ± 0.4	3.36 ± 0.3	2.57 ± 0.1	2.97 ± 0.3	4.37 ± 0.6
8	3.0 ± 0.1	4.9 ± 0.4	4.5 ± 0.6	4.0 ± 0.4	3.9 ± 0.4	6.4 ± 0.4
9	2.29 ± 0.5	3.12 ± 0.7	2.71 ± 1.3	2.98 ± 0.7	2.86 ± 06	2.83 ± 0.5
10	3.8 ± 0.1	5.9 ± 0.4	5.6 ± 0.4	5.7 ± 0.3	5.3 ± 0.3	7.3 ± 0.8
11	0.190 ± 0.004	0.191 ± 0.011	0.094 ± 0.008	0.066 ± 0.005	0.074 ± 0.006	0.210 ± 0.010
12	0.012 ± 0.001	0.012 ± 0.002	0.022 ± 0.005	0.004 ± 0.001	0.005 ± 0.001	0.164 ± 0.076
13	13.65 ± 0.4	>30	>30	>30	>30	>30
14	0.141 ± 0.031	0.162 ± 0.024	0.0084 ± 0.014	0.037 ± 0.011	0.041 ± 0.018	0.252 ± 0.017
15	0.006 ± 0.001	0.005 ± 0.001	0.008 ± 0.001	0.001 ± 0.000	0.001 ± 0.000	0.190 ± 0.026
16	12.03 ± 1.5	>30	>30	>30	>30	>30
BA	14.4 ± 1.3	12.7 ± 1.8	18.4 ± 2.0	12.0 ± 1.7	16.4 ± 1.9	16.1 ± 1.4
DX	1.0 ± 0.8	0.01 ± 0.01	0.9 ± 0.2	1.1 ± 0.3	1.7 ± 0.3	0.008 ± 0.001

Eine Gruppe von (Homo)piperazinamiden, abgeleitet von Tormentillsäure und Euscaphsäure und zusätzlich mit Rhodamin B-Farbstoff gekoppelt, wurde entwickelt und auf zytotoxische Aktivität getestet. Verbindungen mit einer Homopiperazinamid-Struktur zeigten hierbei eine hohe Zytotoxizität und Selektivität gegenüber Tumorzellen. [149]

3.2.2 Madecassinsäure als neue Leitstruktur

Trotz signifikanter Fortschritte in der Krebsforschung und -therapie bleibt die globale Krebsbelastung beträchtlich, mit 10 Millionen Todesfällen und 19,3 Millionen neuen Krebsfällen im Jahr 2020.[21; 243] Viele etablierte Chemotherapeutika haben ihren Ursprung in natürlichen Quellen oder daraus abgeleiteten Verbindungen. Dazu gehören hochzytotoxische Verbindungen wie Betulinsäure, Ursolsäure und Oleanolsäure [244–251; 117; 252–255] Weniger erforschte Substanzen wie Gypsogenin, Hederagenin und Madecassinäure zeichnen sich durch eine verbesserte Verfügbarkeit aus und könnten als potenzielle Krebsbekämpfungsmittel von Interesse sein [256–258; 138; 259–263]

Unsere aktuelle Forschung konzentrierte sich auf hochzytotoxische acetylierte pentazyklische Triterpenoidamide, insbesondere Rhodamin B-Konjugate, die bei nanomolaren Konzentrationen eine starke Wirksamkeit und eine geringere Toxizität gegenüber nicht-malignen Zellen zeigten [264; 197; 122; 149; 17; 130] Im Rahmen dieser Untersuchung wurden Gypsogenin, Hederagenin und Madecassinäure sowie deren abgeleitete Verbindungen auf ihre Zytotoxizität mittels Sulforhodamin B-Assays analysiert.

Die Synthese neuer Triterpenamide und ihrer Rhodamin B-Konjugate erfolgte über mehrere Reaktionsschritte, einschließlich der Hydrolyse von Gypsophila-Saponin, der Reduktion zu Hederagenin, der Acetylierung und der anschließenden Amidbildung (Abb. 16)[262; 263; 122] Dieser methodische Ansatz ermöglichte die Herstellung von Verbindungen mit spezifischen strukturellen Merkmalen, die für ihre biologische Aktivität von Bedeutung sind.

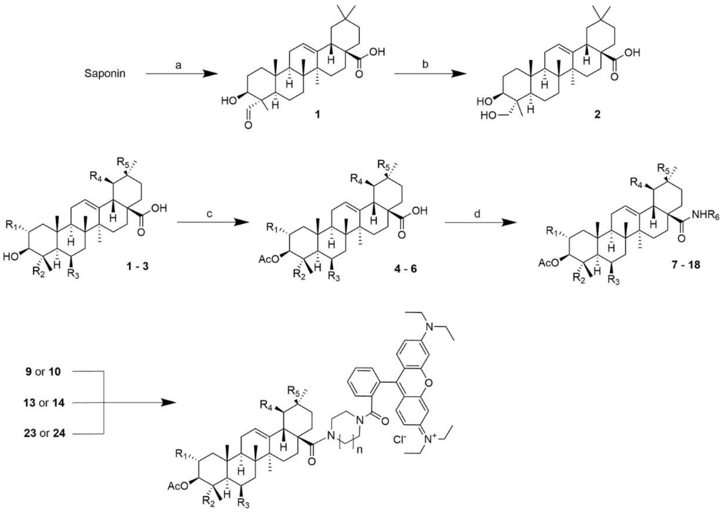

1 R_1 = H; R_2 = CHO; R_3 = H; R_4 = H; R_5 = CH_3
2 R_1 = H; R_2 = CH_2OH; R_3 = H; R_4 = H; R_5 = CH_3
3 R_1 = OH; R_2 = CH_2OH; R_3 = OH; R_4 = CH_3; R_5 = H

4 R_1 = H; R_2 = CHO; R_3 = H; R_4 = H; R_5 = CH_3
5 R_1 = H; R_2 = CH_2OAc; R_3 = H; R_4 = H; R_5 = CH_3
6 R_1 = AcO; R_2 = CH_2OAc; R_3 = OH; R_4 = CH_3; R_5 = H
7 R_1 = H; R_2 = CHO; R_3 = H; R_4 = H; R_5 = CH_3; R_6 = Bn
8 R_1 = H; R_2 = CHO; R_3 = H; R_4 = H; R_5 = CH_3; R_6 = Ph
9 R_1 = H; R_2 = CHO; R_3 = H; R_4 = H; R_5 = CH_3; R_6 = Pip
10 R_1 = H; R_2 = CHO; R_3 = H; R_4 = H; R_5 = CH_3; R_6 = HoPip

11 R_1 = H; R_2 = CH_2OAc; R_3 = H; R_4 = H; R_5 = CH_3; R_6 = Bn
12 R_1 = H; R_2 = CH_2OAc; R_3 = H; R_4 = H; R_5 = CH_3; R_6 = Ph
13 R_1 = H; R_2 = CH_2OAc; R_3 = H; R_4 = H; R_5 = CH_3; R_6 = Pip
14 R_1 = H; R_2 = CH_2OAc; R_3 = H; R_4 = H; R_5 = CH_3; R_6 = HoPip

15 R_1 = AcO; R_2 = CH_2OAc; R_3 = OH; R_4 = CH_3; R_5 = H; R_6 = Bn
16 R_1 = AcO; R_2 = CH_2OAc; R_3 = OH; R_4 = CH_3; R_5 = H; R_6 = Ph
17 R_1 = AcO; R_2 = CH_2OAc; R_3 = OH; R_4 = CH_3; R_5 = H; R_6 =Pip
18 R_1 = AcO; R_2 = CH_2OAc; R_3 = OH; R_4 = CH_3; R_5 = H; R_6 = HoPip

19 R_1 = H; R_2 = CHO; R_3 = H; R_4 = H; R_5 = CH_3; n = 1
20 R_1 = H; R_2 = CHO; R_3 = H; R_4 = H; R_5 = CH_3; n = 2

21 R_1 = H; R_2 = CH_2OAc; R_3 = H; R_4 = H; R_5 = CH_3; n = 1
22 R_1 = H; R_2 = CH_2OAc; R_3 = H; R_4 = H; R_5 = CH_3; n = 2

23 R_1 = AcO; R_2 = CH_2OAc; R_3 = OH; R_4 = CH_3; R_5 = H; n = 1
24 R_1 = AcO; R_2 = CH_2OAc; R_3 = OH; R_4 = CH_3; R_5 = H; n = 2

Abbildung 16: Syntheseschema zur Darstellung der Rhodamin B-Konjugate der Triterpencarbonsäuren aus Saponin.

Die zytotoxische Wirkung der synthetisierten Verbindungen wurde an verschiedenen Tumorzelllinien und nicht-malignen Fibroblasten getestet. Hierbei wurden freie Triterpencarbonsäuren, deren Acetate, Amide und ihre Rhodamin B-Konjugate untersucht. Die Ergebnisse zeigten, dass bestimmte modifizierte Verbindungen und Rhodamin B-Konjugate (Abb. 17) eine deutlich erhöhte Zytotoxizität und verbesserte Selektivität aufwiesen, mit Selektivitätsindizes von bis zu 20.

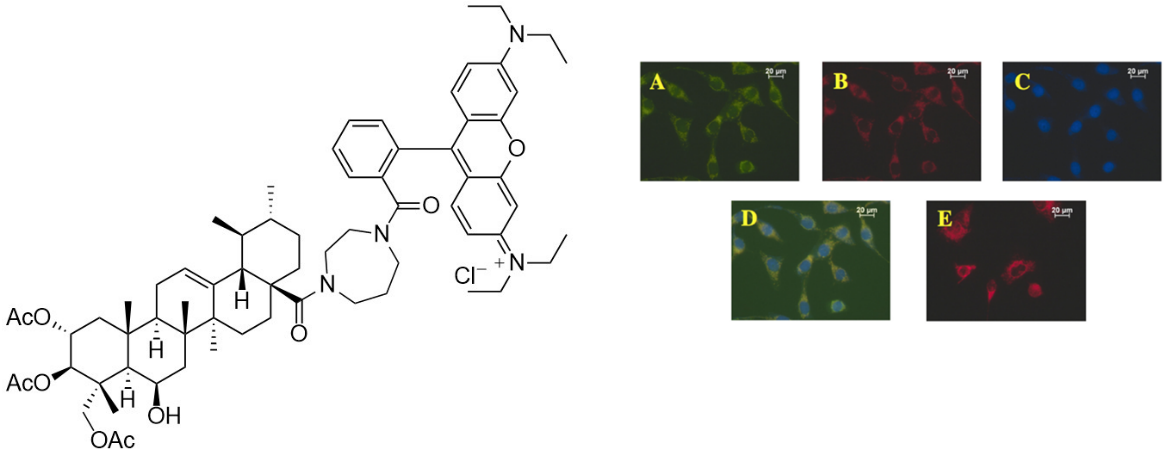

Abbildung 17: Aktivste Madecassinsäure-Derivat mit Homopiperazin-Spacer und Rhodamin B(links)und Färbeversuche: A375-Zellen, 48 Stunden; (A): Kontrolle; (B): in Gegenwart von ***24****; (C): Hoechst 33.342-Färbung; (D): zusammengeführt (Hoechst 33.342, Kontrolle); und (E): in Gegenwart von Rhodamin 123 (rechts).*

Diese Erkenntnisse bestätigen, dass Verbindungen mit spezifischen strukturellen Modifikationen hohe zytotoxische Wirkungen entfalten können. Insbesondere Triterpene, die zusätzliche Hydroxyl- oder Acetylgruppen tragen, könnten vielversprechende Kandidaten für die Weiterentwicklung von Krebsmedikamenten darstellen (Tab. 5).

Tabelle 5: EC50-Werte ausgewählter Derivate

#	A375	HT29	MCF7	A2780	HeLa	NIH 3T3
20	0.0319 ±0.0036	0.0566 ±0.0123	0.0558 ± 0.0072	0.0131 ± 0.0007	0.1021 ± 0.0263	0.1600 ± 0.0226
21	0.055 ± 0.01	0.086 ± 0.01	0.066 ± 0.008	0.025 ± 0.002	-	0.305 ± 0.06
22	0.031 ± 0.007	0.083 ± 0.02	0.086 ± 0.01	0.018 ± 0.001	-	0.441 ± 0.12
23	0.055 ± 0.01	0.108 ± 0.02	0.054 ± 0.01	0.015 ± 0.001	-	0.277 ± 0.03
24	0.0095 ± 0.0015	0.0127 ± 0.0038	0.0162 ± 0.0045	0.0029 ± 0.0005	0.0526 ± 0.0151	0.1013 ± 0.0231
DX	n.d.	0.9 ± 0.2	1.1 ± 0.3	0.02 ± 0.01	n.d.	1.7 ± 0.3

3.2.3 Asiasäure als Leitstruktur für Derivate mit submolarer Zytotoxizität

Der Einsatz natürlicher Substanzen zur Krankheitsheilung ist umfangreich dokumentiert.[265–269] Pflanzliche Inhaltsstoffe, insbesondere solche mit sekundären Pflanzenstoffen, zeigen vielversprechende gesundheitsfördernde Eigenschaften. Hierzu zählen insbesondere Behandlungsmöglichkeiten für Bluthochdruck, Entzündungen und Immunmodulation. [270–275] Ein vielversprechendes neues Forschungsgebiet befasst sich mit Mitocanen, welche gezielt auf Mitochondrien wirken und apoptotisch auf Zellen einwirken.[276; 277; 150; 192] Die Synthese neuer Mitocan-Derivate aus Triterpensäuren, welche Rhodamin-Einheiten enthalten (Abb. 18), hat vielversprechende Ergebnisse in Bezug auf die zytotoxische Aktivität gegenüber Tumorzellen gezeigt.[178; 204; 130; 278–280]

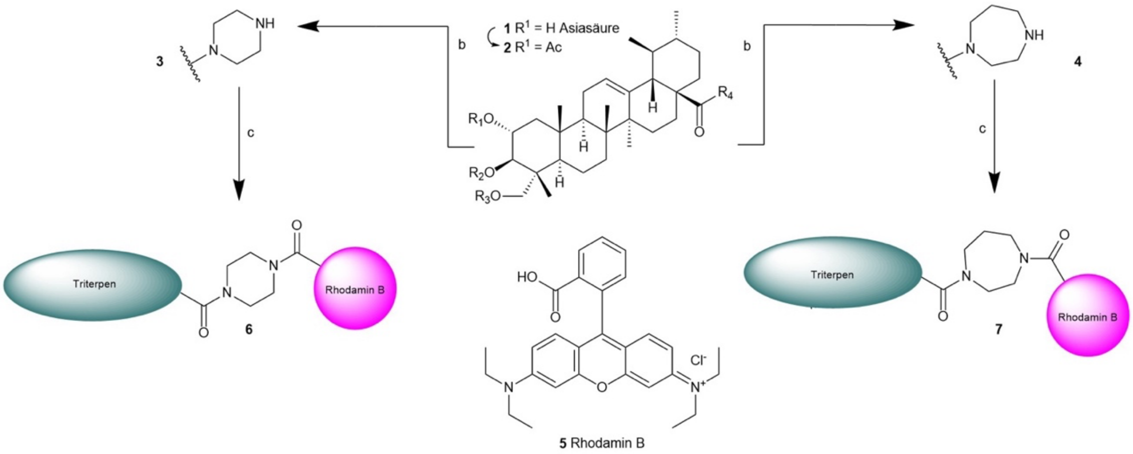
3
NH
N
b
1 R1 = H Asiasäure
2 R1 = Ac
R1O
R2O
R3O
R4
H
b
4
NH
N
c
c
Triterpen
N
N
O
O
Rhodamin B
6
HO
O
Triterpen
N
N
O
O
Rhodamin B
7
N
O
Cl-
N+
5 Rhodamin B

Abbildung 18: Syntheseschema zur Synthese der Asiasäurederivate.

Bei diesen Triterpenkonjugaten, die von Asiasäure abgeleitet sind, wurden spezifische Untersuchungen zur Zytotoxizität und Selektivität für Tumorzellen durchgeführt.

Das Hinzufügen einer Acetylgruppe zu diesen Verbindungen hat die zytotoxische Aktivität signifikant verbessert. Ein besonders wirksames Konjugat, ein Homopiperazinyl-Rhodamin B-Konjugat der Asiasäure (Abb. 19) , zeigte eine bemerkenswert niedrige EC_{50} von 0,8 nM für A2780 Ovarialkarzinomzellen.

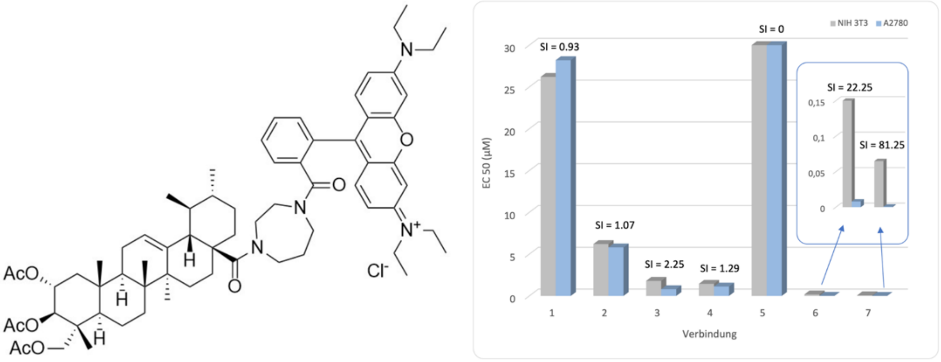

Abbildung 19: Derivat der Asiasäure (19) mit sub-nanomolarer Aktivität und hoher Selektivität.

Diese Verbindung induzierte Apoptose und zeigte eine hohe Aktivität in 3D-Sphäroidmodellen zusätzlich zur Fähigkeit, die Resistenz gegen konventionelle chemotherapeutische Medikamente zu überwinden. Im Gegensatz zu herkömmlichen chemotherapeutischen Medikamenten agiert dieses Mitocan auf eine einzigartige Weise und behält seine Aktivität auch in resistenten Tumormodellen bei (Abb. 20).

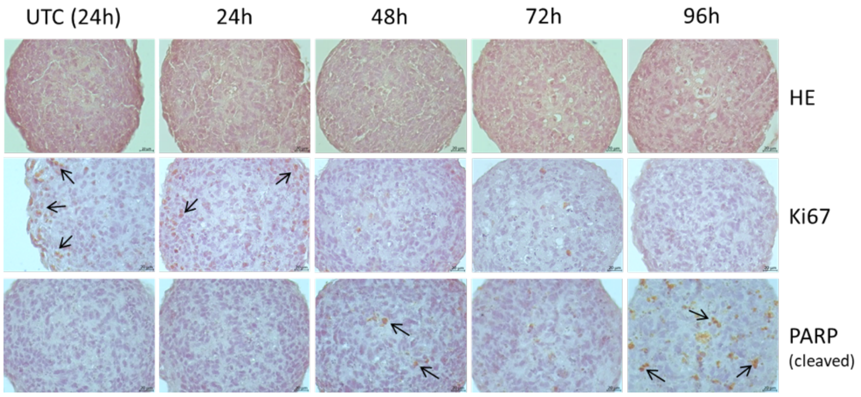
UTC (24h)
24h
48h
72h
96h
HE
Ki67
PARP
(cleaved)

Abbildung 20: Histologische und immunhistochemische Analysen von DLD1-Sphäroiden.

4 Zusammenfassung und Ausblick

Im Rahmen dieser Arbeit wurden verschiedene Triterpencarbonsäure-Konjugate synthetisiert und hinsichtlich ihrer zytotoxischen Wirkung sowie der Selektivität zwischen Tumorzellen und nicht-malignen Zellen untersucht. Die Arbeit baut auf früheren Ergebnissen und Kenntnissen ähnlicher Verbindungen auf, die aus Triterpensäuren wie Betulinsäure, Glycyrrhetinsäure, Boswelliasäure, Oleanolsäure, Ursolsäure oder Maslinsäure stammen und ebenfalls als Mitocane mit hoher Zytotoxizität bekannt sind.[208; 255; 281; 129; 279] Es stellte sich heraus, dass die zusätzliche Präsenz einer Acetylgruppe die zytotoxische Aktivität verbesserte, wobei das aktivste Konjugat, ein Homopiperazinyl-Rhodamin B-Konjugat der Asiasäure, eine EC_{50} von 0,8 nM gegen A2780 Ovarialkarzinomzellen aufwies und Apoptose induzierte. Zudem zeigte diese Verbindung eine hohe Wirksamkeit in 3D-Sphäroid-Modellen und konnte Chemotherapieresistenzen überwinden, indem sie einen völlig anderen primären Wirkmechanismus als herkömmliche Chemotherapeutika aufwies (Abb. 21). Untersuchungen der mitochondrialen Funktion und der von Glykolyse und Atmung abgeleiteten ATP-Produktion bestätigten, dass Verbindung 7 als Mitocan wirkt, zeigten aber auch eine schnelle Störung des zellulären Energiestoffwechsels als primären Wirkmechanismus, der sich von den herkömmlichen Chemotherapeutika völlig unterscheidet und somit die Fähigkeit von Verbindung 7 erklärt, die Resistenz gegen Chemotherapeutika zu überwinden.

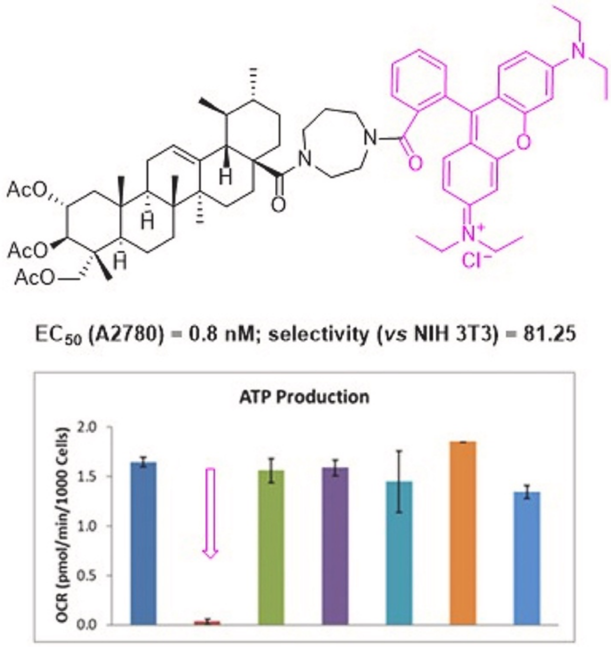

EC_{50} (A2780) = 0.8 nM; selectivity (*vs* NIH 3T3) = 81.25

Abbildung 21: Konjugat der Asiasäure mit Homopiperazin-Spacer und Rhodamin B-Einheit.

Weitere Synthesen umfassten Amide und Rhodamin B-Konjugate, die von Triterpensäuren wie Gypsogenin, Hederagenin und Madecassinsäure abgeleitet wurden. Diese Konjugate zeigten eine signifikante Zunahme der Zytotoxizität im Vergleich zu ihren Ausgangssäuren, insbesondere die Rhodamin B-Konjugate, die in nanomolarer Konzentration zytotoxisch waren und eine bemerkenswerte Tumorzellselektivität aufwiesen.

Die Synthese von Safirinium-Fluoreszenzmarkern verlief problemlos, allerdings zeigten die Safirinium-Triterpen-Konjugate nur eine moderate Zytotoxizität. Eine Ausnahme bildete ein Safirinium P abgeleitetes Konjugat, das eine niedrige EC_{50} für A375-Zellen aufwies, jedoch waren Safirinium Q-Hybride für nicht-maligne NIH 3T3-Fibroblasten zytotoxischer als für die untersuchten menschlichen Tumorzelllinien. Fluoreszenzbildgebung zeigte, dass die Safirinium-Kernstrukturen nicht in die Zellen eintreten konnten, während die Konjugate im endoplasmatischen Retikulum akkumulierte, was ihre reduzierte Zytotoxizität gegenüber menschlichen Tumorzelllinien im Vergleich zu Rhodamin B-Analoga, die in die Mitochondrien eintreten, erklären könnte.

Eine Serie von Amiden, abgeleitet von Tormentillsäure und Euscaphinsäure, die zusätzlich eine Rhodamin B-Einheit trugen, wurde ebenfalls synthetisiert und auf zytotoxische Aktivität geprüft. Hohe Zytotoxizität wurde nur beobachtet, wenn die Verbindungen als Mitocane wirken konnten. Die Kombination eines geeigneten Triterpens mit einem idealen Amid-Spacer, der an das distale Stickstoffatom ein kationisches Rhodamin-Molekül bindet, erwies sich als notwendig für die Erzielung hoher Zytotoxizität bei guter Tumorzellselektivität.

Künftige Forschungsansätze sollten sich auf erweiterte biologische Untersuchungen konzentrieren, darunter Experimente mit 3D-Tumormodellen und Tumorproben sowie Studien in lebenden Mäusen. Eine Optimierung der Mitocane könnte durch die Verbindung mit strukturell ähnlichen fluoreszierenden Farbstoffen erreicht werden. Ferner besteht die Möglichkeit, die Eigenschaften von Leukoformen, die bei der Reaktion mit primären Aminen entstehen, zu nutzen, um schaltbare Mitocane zu entwickeln

5 Literaturverzeichnis

[1] *The top 10 causes of death,* https://www.who.int/news-room/fact-sheets/detail/the-top-10-causes-of-death, **2/18/2024**.

[2] B. Redaktion, *BR24* **4/2/2020**.

[3] S. Ofer, *praktischArzt* **23.8.2023**.

[4] A. I. Holleb, *American Cancer Society textbook of clinical oncology,* American Cancer Society, Atlanta, **1991**.

[5] H.-J. Schmoll, K. Höffken und K. Possinger, *Kompendium internistische Onkologie,* 4. Aufl., Springer Medizin, Heidelberg, **2006**.

[6] Gale.robert, *Systemische Krebstherapie - Hämatologie und Onkologie - MSD Manual Profi-Ausgabe,* https://www.msdmanuals.com/de-de/profi/h%C3%A4matologie-und-onkologie/prinzipien-der-onkologischen-therapie/systemische-krebstherapie, **2/18/2024**.

[7] S. Qin, S. L. Chan, S. Gu, Y. Bai, Z. Ren, X. Lin, Z. Chen, W. Jia, Y. Jin, Y. Guo, X. Hu, Z. Meng, J. Liang, Y. Cheng, J. Xiong, H. Ren, F. Yang, W. Li, Y. Chen, Y. Zeng, A. Sultanbaev, M. Pazgan-Simon, M. Pisetska, D. Melisi, D. Ponomarenko, Y. Osypchuk, I. Sinielnikov, T.-S. Yang, X. Liang, C. Chen, L. Wang, A.-L. Cheng, A. Kaseb und A. Vogel, *Lancet (London, England)* **2023**, *402,* 1133–1146, DOI: 10.1016/S0140-6736(23)00961-3.

[8] National Cancer Institute, *Chemotherapy and You: Support for People With Cancer,* https://www.cancer.gov/publications/patient-education/chemo-and-you, **2/17/2024**.

[9] Krebsforschungszentrum, Krebsinformationsdienst, Deutsches, *Krebsinformationsdienst* **26.1.2019**.

[10] Krebsforschungszentrum, Krebsinformationsdienst, Deutsches, *Krebsinformationsdienst* **2/5/2017**.

[11] R. B. L. Internetredaktion, *Wirkstoffentwicklung - DLR Gesundheitsforschung,* https://www.gesundheitsforschung-bmbf.de/de/wirkstoffentwicklung-9466.php, **2022**.

[12] *Forschung & Entwicklung von Arzneimitteln – Roche.de,* https://www.roche.de/innovation/forschung/forschung-entwicklung-von-arzneimitteln, **3/10/2024**.

[13] Novartis – Klinische Forschung, *Entwicklung von Medikamenten | Novartis,* https://klinischeforschung.novartis.de/patienten/allgemeines-zu-klinischen-studien/entwicklung-von-medikamenten/, **9/11/2023**.

[14] *Die Chemotherapie,* https://www.krebsgesellschaft.de/onko-internetportal/basis-informationen-krebs/therapieformen/chemotherapie.html, **3/10/2024**.

[15] D. J. Newman und G. M. Cragg, *Journal of natural products* **2020**, *83,* 770–803, DOI: 10.1021/acs.jnatprod.9b01285.

[16] E. Patridge, P. Gareiss, M. S. Kinch und D. Hoyer, *Drug discovery today* **2016**, *21,* 204–207, DOI: 10.1016/j.drudis.2015.01.009.

[17] M. Kozubek, I. Serbian, S. Hoenke, O. Kraft und R. Csuk, *Results Chem.* **2020**, *2,* 100057, DOI: 10.1016/j.rechem.2020.100057.

[18] J. Neuzil, J. C. Dyason, R. Freeman, L.-F. Dong, L. Prochazka, X.-F. Wang, I. Scheffler und S. J. Ralph, *Journal of bioenergetics and biomembranes* **2007**, *39,* 65–72, DOI: 10.1007/s10863-006-9060-z.

[19] R. A. J. Smith, C. M. Porteous, A. M. Gane und M. P. Murphy, *PNAS* **2003**, *100,* 5407–5412, DOI: 10.1073/pnas.0931245100.

[20] D. R. Green und F. Llambi, *Cold Spring Harbor perspectives in biology* **2015**, *7, DOI:* 10.1101/cshperspect.a006080.

[21] *Cancer,* https://www.who.int/news-room/fact-sheets/detail/cancer, **3/6/2024**.

[22] *Cancer Today,* https://gco.iarc.fr/today/en, **3/8/2024**.

[23] D. Hanahan, *Cancer discovery* **2022**, *12,* 31–46, DOI: 10.1158/2159-8290.CD-21-1059.

[24] H. Sung, J. Ferlay, R. L. Siegel, M. Laversanne, I. Soerjomataram, A. Jemal und F. Bray, *CA: a cancer journal for clinicians* **2021**, *71,* 209–249, DOI: 10.3322/caac.21660.

[25] A. Jemal, F. Bray, M. M. Center, J. Ferlay, E. Ward und D. Forman, *CA: a cancer journal for clinicians* **2011**, *61,* 69–90, DOI: 10.3322/caac.20107.

[26] *Cancer Tomorrow,* https://gco.iarc.fr/tomorrow/en/dataviz/bars?mode=population&populations=900&types=1, **2/26/2024**.

[27] M. Malvezzi, C. Santucci, P. Boffetta, G. Collatuzzo, F. Levi, C. La Vecchia und E. Negri, *Annals of oncology : official journal of the European Society for Medical Oncology* **2023**, *34,* 410–419, DOI: 10.1016/j.annonc.2023.01.010.

[28] *Krebshäufigkeit - die aktuellen Zahlen,* https://www.krebsgesellschaft.de/onko-internetportal/basis-informationen-krebs/allgemeine-informationen/krebshaeufigkeit-die-aktuellen-daten.html, **3/10/2024**.

[29] *RKI - Zentrum für Krebsregisterdaten,* https://www.rki.de/DE/Content/Gesundheitsmonitoring/Krebsregisterdaten/krebs_node.html, **3/10/2024**.

[30] Statistisches Bundesamt, *Todesursachen in Deutschland,* https://www.destatis.de/DE/Themen/Gesellschaft-Umwelt/Gesundheit/Todesursachen/_inhalt.html, **8/21/2019**.

[31] *Robbins & Cotran pathologic basis of disease* (Hrsg.: V. Kumar, A. K. Abbas, J. C. Aster und J. R. Turner), Elsevier, Philadelphia, PA, **2021**.

[32] B. Alberts, R. Heald, A. Johnson, D. Morgan, M. Raff, K. Roberts, P. Walter, J. H. Wilson und T. Hunt, *Molecular biology of the cell,* W.W. Norton & Company, New York, NY, London, **2022**.

[33] D. Hanahan und R. A. Weinberg, *Cell* **2011**, *144,* 646–674, DOI: 10.1016/j.cell.2011.02.013.

[34] V. T. DeVita, JR., *DeVita, Hellman, and Rosenberg's Cancer,* 12. Aufl., Wolters Kluwer Health, Philadelphia, **2023**.

[35] *Schwartz's principles of surgery,* 11. Aufl. (Hrsg.: F. C. Brunicardi).

[36] F. Bunz, *Principles of Cancer Genetics,* 3. Aufl., Springer International Publishing; Imprint Springer, Cham, **2022**.

[37] *Environmental Factors, Genes, and the Development of Human Cancers,* Springer New York, New York, NY, **2010**.

[38] L. Pecorino, *Molecular biology of cancer,* Oxford University Press, Oxford, United Kingdom, **2021**.

[39] Gale.robert, *Tumormetastasen bei unbekanntem Primärtumor - Hämatologie und Onkologie - MSD Manual Profi-Ausgabe,* https://www.msdmanuals.com/de/profi/h%C3%A4matologie-und-onkologie/maligne-tumoren-im-%C3%BCberblick/tumormetastasen-bei-unbekanntem-prim%C3%A4rtumor, **3/17/2024**.

[40] S. S. Taneja, *Reviews in urology* **2004**, *6,* 101–113.

[41] P. Rubin, *Clinical oncology,* 8. Aufl., W.B. Saunders Co, Philadelphia, **2001**.

[42] *Henry's clinical diagnosis and management by laboratory methods,* 24. Aufl. (Hrsg.: R. A. McPherson), Elsevier, Philadelphia, PA, **2022**.

[43] H. C. Thoeny, R. Forstner und F. de Keyzer, *Radiology* **2012**, *263,* 326–342, DOI: 10.1148/radiol.12110446.

[44] G. B. Saha, *Fundamentals of nuclear pharmacy,* Springer, Cham, **2018**.

[45] *Principles and practice of PET and PET-CT,* 2. Aufl. (Hrsg.: R. S. Beanlands und R. L. Wahl), Wolters Kluwer Health, Philadelphia [etc.], **2009**.

[46] *Perez and Bradys Principles and Practice of Radiation Oncology,* Lippincott, Williams & Wilkins, **2019**.

[47] *Bland and Copeland's the breast,* 6. Aufl., Elsevier, Philadelphia, **opyright 2024**.

[48] *Cancer chemotherapy, immunotherapy and biotherapy* (Hrsg.: B. Chabner und D. L. Longo), Wolters Kluwer, Philadelphia, PA, **2019**.

[49] C. Yarbro, D. Wujcik und B. Gobel, *Cancer nursing,* 8. Aufl., Jones and Bartlett, **2017**.

[50] S. L. Topalian, C. G. Drake und D. M. Pardoll, *Cancer cell* **2015**, *27,* 450–461, DOI: 10.1016/j.ccell.2015.03.001.

[51] J. van der Zee, *Annals of oncology : official journal of the European Society for Medical Oncology* **2002**, *13,* 1173–1184, DOI: 10.1093/annonc/mdf280.

[52] A. T. Robilotto, J. M. Baust, R. G. van Buskirk und J. G. Baust, in: *Theory and Applications of Heat Transfer in Humans,* John Wiley & Sons, Ltd, **2018,** 591–617.

[53] A. L. McKenzie, *Physics in medicine and biology* **1990**, *35,* 1175–1209, DOI: 10.1088/0031-9155/35/9/001.

[54] *Abeloff's clinical oncology,* 6. Aufl. (Hrsg.: J. E. Niederhuber, J. O. Armitage, J. H. Doroshow, J. E. Tepper und M. B. Kastan), Elsevier, Philadelphia, PA, **2020**.

[55] L. C. Lopes-Júnior und L. C. Veronez, *International journal of environmental research and public health* **2023**, *20, DOI:* 10.3390/ijerph20043023.

[56] *Devita, Hellman, and Rosenberg's cancer,* 5. Aufl. (Hrsg.: D. Morgensztern, R. Govindan, S. Devarakonda und N. A. Trikalinos), Wolters Kluwer, Philadelphia, **2022**.

[57] H. F. Lodish, A. Berk, C. Kaiser, M. Krieger, A. Bretscher, H. L. Ploegh, K. C. Martin, M. B. Yaffe, A. Amon und J. E. Darnell, *Molecular cell biology,* Macmillan learning, Austin, New York, **2021**.

[58] D. R. Green, *Cell death,* Cold Spring Harbor Laboratory Press, Cold Spring Harbor, New York, **2018**.

[59] H. J. M. Brady, *Apoptosis methods and protocols,* Humana Press, Totowa, N.J., **2004**.

[60] G. M. Cragg und D. J. Newman, *Journal of ethnopharmacology* **2005**, *100,* 72–79, DOI: 10.1016/j.jep.2005.05.011.

[61] S. Nobili, D. Lippi, E. Witort, M. Donnini, L. Bausi, E. Mini und S. Capaccioli, *Pharmacological research* **2009**, *59,* 365–378, DOI: 10.1016/j.phrs.2009.01.017.

[62] A. Kinghorn, N. Farnsworth, D. Soejarto, G. Cordell, S. Swanson, J. Pezzuto, M. Wani, M. Wall, N. Oberlies, D. Kroll, R. Kramer, W. Rose, G. Vite, C. Fairchild, R. Peterson und R. Wild, *Pharm. Biol.* **2003**, *41,* 53–67, DOI: 10.1080/1388020039051744.

[63] M. C. Wani, H. L. Taylor, M. E. Wall, P. Coggon und A. T. McPhail, *J. Am. Chem. Soc.* **1971**, *93,* 2325–2327, DOI: 10.1021/ja00738a045.

[64] *File:Catharanthus roseus kz1.JPG - Wikimedia Commons,* **4/7/2024**.

[65] *File:Mayapple flower 2.jpg - Wikimedia Commons,* **4/7/2024**.

[66] D. J. Newman und G. M. Cragg, *Journal of natural products* **2016**, *79,* 629–661, DOI: 10.1021/acs.jnatprod.5b01055.

[67] M. S. Butler, A. A. B. Robertson und M. A. Cooper, *Natural product reports* **2014**, *31,* 1612–1661, DOI: 10.1039/c4np00064a.

[68] M. Gordaliza, *Clinical & translational oncology : official publication of the Federation of Spanish Oncology Societies and of the National Cancer Institute of Mexico* **2007**, *9,* 767–776, DOI: 10.1007/s12094-007-0138-9.

[69] S. L. Maude, T. W. Laetsch, J. Buechner, S. Rives, M. Boyer, H. Bittencourt, P. Bader, M. R. Verneris, H. E. Stefanski, G. D. Myers, M. Qayed, B. de Moerloose, H. Hiramatsu, K. Schlis, K. L. Davis, P. L. Martin, E. R. Nemecek, G. A. Yanik, C. Peters, A. Baruchel, N. Boissel, F. Mechinaud, A. Balduzzi, J. Krueger, C. H. June, B. L. Levine, P. Wood, T. Taran, M. Leung, K. T. Mueller, Y. Zhang, K. Sen, D. Lebwohl, M. A. Pulsipher und S. A. Grupp, *The New England journal of medicine* **2018**, *378,* 439–448, DOI: 10.1056/NEJMoa1709866.

[70] *First two CAR-T cell medicines recommended for approval in the European Union | European Medicines Agency,* https://www.ema.europa.eu/en/news/first-two-car-t-cell-medicines-recommended-approval-european-union, **3/17/2024**.

[71] M. Sadelain, I. Rivière und S. Riddell, *Nature* **2017**, *545,* 423–431, DOI: 10.1038/nature22395.

[72] C. H. June, R. S. O'Connor, O. U. Kawalekar, S. Ghassemi und M. C. Milone, *Science (New York, N.Y.)* **2018**, *359,* 1361–1365, DOI: 10.1126/science.aar6711.

[73] *Novartis* **Wed, 08/30/2017 - 17:04**.

[74] *Kite's Yescarta™ (Axicabtagene Ciloleucel) Becomes First CAR T Therapy Approved by the FDA for the Treatment of Adult Patients With Relapsed or Refractory Large B-Cell Lymphoma After Two or More Lines of Systemic Therapy,* https://www.gilead.com/news-and-press/press-room/press-releases/2017/10/kites-yescarta-axicabtagene-ciloleucel-becomes-first-car-t-therapy-approved-by-the-fda-for-the-treatment-of-adult-patients-with-relapsed-or-refrac, **3/17/2024**.

[75] R. B. L. Internetredaktion, *Immuntherapie – kann das Immunsystem Krebs bekämpfen? - DLR Gesundheitsforschung,* https://www.gesundheitsforschung-bmbf.de/de/immuntherapie-kann-das-immunsystem-krebs-bekampfen-7033.php, **2017**.

[76] W. B. COLEY, *The American Journal of the Medical Sciences* **1893**, *105,* 487–510, DOI: 10.1097/00000441-189305000-00001.

[77] N. A. Mitchison, *Frontiers in immunology* **2014**, *5,* 377, DOI: 10.3389/fimmu.2014.00377.

[78] D. M. Pardoll, *Nature reviews. Cancer* **2012**, *12,* 252–264, DOI: 10.1038/nrc3239.

[79] R. D. Schreiber, L. J. Old und M. J. Smyth, *Science (New York, N.Y.)* **2011**, *331,* 1565–1570, DOI: 10.1126/science.1203486.

[80] W. Alexander, *Pharmacy and Therapeutics* **2016**, *41,* 185–191.

[81] F. S. Hodi, S. J. O'Day, D. F. McDermott, R. W. Weber, J. A. Sosman, J. B. Haanen, R. Gonzalez, C. Robert, D. Schadendorf, J. C. Hassel, W. Akerley, A. J. M. van den Eertwegh, J. Lutzky, P. Lorigan, J. M. Vaubel, G. P. Linette, D. Hogg, C. H. Ottensmeier, C. Lebbé, C. Peschel, I. Quirt, J. I. Clark, J. D. Wolchok, J. S. Weber, J. Tian, M. J. Yellin, G. M. Nichol, A. Hoos und W. J. Urba, *The New England journal of medicine* **2010**, *363,* 711–723, DOI: 10.1056/NEJMoa1003466.

[82] S. L. Topalian, F. S. Hodi, J. R. Brahmer, S. N. Gettinger, D. C. Smith, D. F. McDermott, J. D. Powderly, R. D. Carvajal, J. A. Sosman, M. B. Atkins, P. D. Leming, D. R. Spigel, S. J. Antonia, L. Horn, C. G. Drake, D. M. Pardoll, L. Chen, W. H. Sharfman, R. A. Anders, J. M. Taube, T. L. McMiller, H. Xu, A. J. Korman, M. Jure-Kunkel, S. Agrawal, D. McDonald, G. D. Kollia, A. Gupta, J. M. Wigginton und M. Sznol, *The New England journal of medicine* **2012**, *366,* 2443–2454, DOI: 10.1056/NEJMoa1200690.

[83] J. Brahmer, K. L. Reckamp, P. Baas, L. Crinò, W. E. E. Eberhardt, E. Poddubskaya, S. Antonia, A. Pluzanski, E. E. Vokes, E. Holgado, D. Waterhouse, N. Ready, J. Gainor, O. Arén Frontera, L. Havel, M. Steins, M. C. Garassino, J. G. Aerts, M. Domine, L. Paz-Ares, M. Reck, C. Baudelet, C. T. Harbison, B. Lestini und D. R. Spigel, *The New England journal of medicine* **2015**, *373,* 123–135, DOI: 10.1056/NEJMoa1504627.

[84] NobelPrize.org, *The Nobel Prize in Physiology or Medicine 2018,* https://www.nobelprize.org/prizes/medicine/2018/summary/, **3/17/2024**.

[85] *Burger's medicinal chemistry, drug discovery and development* (Hrsg.: D. J. Abraham und M. Myers), Wiley, Hoboken, NJ, **2021**.

[86] G. L. Patrick, *An introduction to medicinal chemistry,* Oxford University Press, Oxford, United Kingdom, **2023**.

[87] D. Lednicer, *Strategies for Organic Drug Synthesis and Design,* 2. Aufl., John Wiley & Sons, New York, NY, **2009**.

[88] A. L. Harvey, R. Edrada-Ebel und R. J. Quinn, *Nature reviews. Drug discovery* **2015**, *14,* 111–129, DOI: 10.1038/nrd4510.

[89] B. Shen, *Cell* **2015**, *163,* 1297–1300, DOI: 10.1016/j.cell.2015.11.031.

[90] R. J. Thoppil und A. Bishayee, *World journal of hepatology* **2011**, *3,* 228–249, DOI: 10.4254/wjh.v3.i9.228.

[91] W. Chen, Y. Liu, M. Li, J. Mao, L. Zhang, R. Huang, X. Jin und L. Ye, *Journal of pharmacological sciences* **2015**, *127,* 332–338, DOI: 10.1016/j.jphs.2015.01.008.

[92] R. Paduch, M. Kandefer-Szerszeń, M. Trytek und J. Fiedurek, *Archivum immunologiae et therapiae experimentalis* **2007**, *55,* 315–327, DOI: 10.1007/s00005-007-0039-1.

[93] E. Breitmaier, *Terpenes,* 1. Aufl., Wiley-VCH, Weinheim, **op. 2008**.

[94] M. Christmann, *Angewandte Chemie (International ed. in English)* **2010**, *49,* 9580–9586, DOI: 10.1002/anie.201003155.

[95] L. Ruzicka, *Helv. Chim. Acta* **1926**, *9,* 230–248, DOI: 10.1002/hlca.19260090129.

[96] J. D. Connolly und R. Hill, *Dictionary of terpenoids,* Chapman & Hall, London, **1991**.

[97] A. Petronelli, G. Pannitteri und U. Testa, *Anti-cancer drugs* **2009**, *20,* 880–892, DOI: 10.1097/CAD.0b013e328330fd90.

[98] C. Wiart, G. Kathirvalu, C. S. Raju, V. Nissapatorn, M. Rahmatullah, A. K. Paul, M. Rajagopal, J. S. Sathiya Seelan, N. A. Rusdi, S. Lanting und M. Sulaiman, *Molecules (Basel, Switzerland)* **2023**, *28, DOI:* 10.3390/molecules28093873.

[99] P. Darshani, S. Sen Sarma, A. K. Srivastava, R. Baishya und D. Kumar, *Phytochemistry reviews : proceedings of the Phytochemical Society of Europe* **2022**, *21,* 1761–1842, DOI: 10.1007/s11101-022-09808-1.

[100] T. Rodrigues, D. Reker, P. Schneider und G. Schneider, *Nature chemistry* **2016**, *8,* 531–541, DOI: 10.1038/nchem.2479.

[101] T. Y. Shin, H. J. Jeong, D. K. Kim, S. H. Kim, J. K. Lee, B. S. Chae, J. H. Kim, H. W. Kang, C. M. Lee, K. C. Lee, S. T. Park, E. J. Lee, J. P. Lim, H. M. Kim und Y. M. Lee, *Journal of ethnopharmacology* **2001**, *74,* 133–140, DOI: 10.1016/s0378-8741(00)00360-3.

[102] M.-H. Shyu, T.-C. Kao und G.-C. Yen, *Journal of agricultural and food chemistry* **2010**, *58,* 6110–6118, DOI: 10.1021/jf100574j.

[103] H. Jo, J.-H. Oh, D.-W. Park, C. Lee und C. K. Min, *Journal of ginseng research* **2020**, *44,* 96–104, DOI: 10.1016/j.jgr.2018.09.003.

[104] Ling Liu, Jian-long Zhao, Jian-gang Wang, *CJCMM* **2015**, *40 24,* 4897–4902, DOI: 10.4268/cjcmm20152429.

[105] M. R. Akl, H. E. Elsayed, H. Y. Ebrahim, E. G. Haggag, A. M. Kamal und K. A. El Sayed, *European journal of pharmacology* **2014**, *740,* 209–217, DOI: 10.1016/j.ejphar.2014.07.011.

[106] V. C. George, D. R. N. Kumar, P. K. Suresh und R. A. Kumar, *Asian Pacific journal of cancer prevention : APJCP* **2012**, *13,* 2015–2020, DOI: 10.7314/APJCP.2012.13.5.2015.

[107] S.-H. Kwon, H.-Y. Park, J.-Y. Kim, I.-Y. Jeong, M.-K. Lee und K.-I. Seo, *Bioorganic & medicinal chemistry letters* **2010**, *20,* 6435–6438, DOI: 10.1016/j.bmcl.2010.09.073.

[108] K. A. Manu und G. Kuttan, *International immunopharmacology* **2008**, *8,* 974–981, DOI: 10.1016/j.intimp.2008.02.013.

[109] Y. H. Choi, J. H. Baek, M. A. Yoo, H. Y. Chung, N. D. Kim und K. W. Kim, *Int. J. Oncol.* **2000**, *17 3,* 565–571, DOI: 10.3892/IJO.17.3.565.

[110] S. Fulda, C. Friesen, M. Los, C. Scaffidi, W. Mier, M. Benedict, G. Núñez, P. Krammer, M. Peter, K. Debatin, K. Debatin, *Cancer research* **1997**, *57 21,* 4956–4964.

[111] W. Wick, C. Grimmel, B. Wagenknecht, J. Dichgans, M. Weller, *The Journal of pharmacology and experimental therapeutics* **1999**, *289 3,* 1306–1312.

[112] X.-L. Tang, X.-Y. Yang, H.-J. Jung, S.-Y. Kim, S.-Y. Jung, D.-Y. Choi, W.-C. Park und H. Park, *Biological & pharmaceutical bulletin* **2009**, *32,* 1399–1405, DOI: 10.1248/BPB.32.1399.

[113] Y. S. Lee, D.-Q. Jin, E. J. Kwon, S. H. Park, E.-S. Lee, T. C. Jeong, D. H. Nam, K. Huh und J.-A. Kim, *Cancer letters* **2002**, *186,* 83–91, DOI: 10.1016/S0304-3835(02)00260-4.

[114] B. C. Park, K. O. Bosire, E.-S. Lee, Y. S. Lee und J.-A. Kim, *Cancer letters* **2005**, *218,* 81–90, DOI: 10.1016/j.canlet.2004.06.039.

[115] J. T. James und I. A. Dubery, *Molecules (Basel, Switzerland)* **2009**, *14,* 3922–3941, DOI: 10.3390/molecules14103922.

[116] W. Bylka, P. Znajdek-Awiżeń, E. Studzińska-Sroka und M. Brzezińska, *Postepy dermatologii i alergologii* **2013**, *30,* 46–49, DOI: 10.5114/pdia.2013.33378.

[117] T. D. Babu, G. Kuttan und J. Padikkala, *Journal of ethnopharmacology* **1995**, *48,* 53–57, DOI: 10.1016/0378-8741(95)01284-k.

[118] A. Shukla, A. M. Rasik, G. K. Jain, R. Shankar, D. K. Kulshrestha und B. N. Dhawan, *Journal of ethnopharmacology* **1999**, *65,* 1–11, DOI: 10.1016/s0378-8741(98)00141-x.

[119] N. E. Gray, A. Alcazar Magana, P. Lak, K. M. Wright, J. Quinn, J. F. Stevens, C. S. Maier und A. Soumyanath, *Phytochemistry reviews : proceedings of the Phytochemical Society of Europe* **2018**, *17,* 161–194, DOI: 10.1007/s11101-017-9528-y.

[120] *Centella_asiatica_(থানকুনি)_(3).jpg (4000×3000),* **11/20/2018**.

[121] S. MN, M. R. Sulaiman, Z. Ahmad, L. N. Samsuddin, S. N, Da Israf und M. S, *Indian Journal of Pharmacology (ISSN: 0253-7613) Vol 36 Num 6* **2004**, *36*.

[122] M. Kahnt, J. Wiemann, L. Fischer, S. Sommerwerk und R. Csuk, *Eur J Med Chem* **2018**, *159,* 143–148, DOI: 10.1016/j.ejmech.2018.09.066.

[123] M. K. Shanmugam, X. Dai, A. P. Kumar, B. K. H. Tan, G. Sethi und A. Bishayee, *Biochemical pharmacology* **2013**, *85,* 1579–1587, DOI: 10.1016/j.bcp.2013.03.006.

[124] N. Gao, S. Cheng, A. Budhraja, Z. Gao, J. Chen, E.-H. Liu, C. Huang, D. Chen, Z. Yang, Q. Liu, P. Li, X. Shi und Z. Zhang, *British journal of pharmacology* **2012**, *165,* 1813–1826, DOI: 10.1111/j.1476-5381.2011.01684.x.

[125] S. Prasad, V. R. Yadav, B. Sung, S. C. Gupta, A. K. Tyagi und B. B. Aggarwal, *Oncotarget* **2016**, *7,* 13182–13196, DOI: 10.18632/oncotarget.7537.

[126] M. Alam, S. Ali, S. Ahmed, A. M. Elasbali, M. Adnan, A. Islam, M. I. Hassan und D. K. Yadav, *International journal of molecular sciences* **2021**, *22, DOI:* 10.3390/ijms222212162.

[127] M. Wang, C. Gu, Y. Yang, L. Chen, K. Chen, J. Du, H. Wu und Y. Li, *Frontiers in neurology* **2023**, *14,* 1269862, DOI: 10.3389/fneur.2023.1269862.

[128] N. Heise, S. Hoenke, V. Simon, H.-P. Deigner, A. Al-Harrasi und R. Csuk, *Steroids* **2021**, *172,* 108876, DOI: 10.1016/j.steroids.2021.108876.

[129] J. Wiemann, L. Heller und R. Csuk, *Bioorganic & medicinal chemistry letters* **2016**, *26,* 907–909, DOI: 10.1016/j.bmcl.2015.12.064.

[130] B. Siewert, E. Pianowski, A. Obernauer und R. Csuk, *Bioorganic & medicinal chemistry* **2014**, *22,* 594–615, DOI: 10.1016/j.bmc.2013.10.047.

[131] M. Kozubek, T. C. Denner, M. Eckert, S. Hoenke und R. Csuk, *Results Chem.* **2023**, *5,* 100708, DOI: 10.1016/j.rechem.2022.100708.

[132] K. J. Gohil, J. A. Patel und A. K. Gajjar, *Indian journal of pharmaceutical sciences* **2010**, *72,* 546–556, DOI: 10.4103/0250-474X.78519.

[133] F. N. Idris und M. Mohd Nadzir, *Antibiotics (Basel, Switzerland)* **2021**, *10, DOI:* 10.3390/antibiotics10040457.

[134] B. Yang, Y. Xu, Y. Hu, Y. Luo, X. Lu, C. K. Tsui, L. Lu und X. Liang, *Biomedicine & pharmacotherapy = Biomedecine & pharmacotherapie* **2016**, *84,* 845–852, DOI: 10.1016/j.biopha.2016.10.015.

[135] J.-H. Won, J.-S. Shin, H.-J. Park, H.-J. Jung, D.-J. Koh, B.-G. Jo, J.-Y. Lee, K. Yun und K.-T. Lee, *Planta medica* **2010**, *76,* 251–257, DOI: 10.1055/s-0029-1186142.

[136] N. N. M. Razali, C. T. Ng und L. Y. Fong, *Planta medica* **2019**, *85,* 1203–1215, DOI: 10.1055/a-1008-6138.

[137] J. H. Wong, A. M. Barron und J. M. Abdullah, *Frontiers in pharmacology* **2021**, *12,* 687935, DOI: 10.3389/fphar.2021.687935.

[138] A. S. C. Valdeira, E. Darvishi, G. M. Woldemichael, J. A. Beutler, K. R. Gustafson und J. A. R. Salvador, *Journal of natural products* **2019**, *82,* 2094–2105, DOI: 10.1021/acs.jnatprod.8b00864.

[139] Krebsforschungszentrum, Krebsinformationsdienst, Deutsches, *Krebsinformationsdienst* **9/5/2023**.

[140] Krebsforschungszentrum, Krebsinformationsdienst, Deutsches, *Krebsinformationsdienst* **15.6.2023**.

[141] S. Fedotov und A. Iomin, *Physical review letters* **2007**, *98,* 118101, DOI: 10.1103/PhysRevLett.98.118101.

[142] A. J. Crawford, C. Gomez-Cruz, G. C. Russo, W. Huang, I. Bhorkar, A. Muñoz-Barrutia, D. Wirtz und D. Garcia-Gonzalez, *bioRxiv* **2022,** 2022.11.15.516548, DOI: 10.1101/2022.11.15.516548.

[143] Y.-K. Huang, R. A. Busuttil und A. Boussioutas, *Cancers* **2021**, *13, DOI:* 10.3390/cancers13235885.

[144] D. C. Wallace, *Nature reviews. Cancer* **2012**, *12,* 685–698, DOI: 10.1038/nrc3365.

[145] S. Fulda, L. Galluzzi und G. Kroemer, *Nature reviews. Drug discovery* **2010**, *9,* 447–464, DOI: 10.1038/nrd3137.

[146] K. T. Liby und M. B. Sporn, *Pharmacological reviews* **2012**, *64,* 972–1003, DOI: 10.1124/pr.111.004846.

[147] S. J. Ralph, P. Low, L. Dong, A. Lawen und J. Neuzil, *Recent patents on anti-cancer drug discovery* **2006**, *1,* 327–346, DOI: 10.2174/157489206778776952.

[148] A. Abraham, A. J. Kattoor, T. Saldeen und J. L. Mehta, *Critical reviews in food science and nutrition* **2019**, *59,* 2831–2838, DOI: 10.1080/10408398.2018.1474169.

[149] S. Hoenke, I. Serbian, H.-P. Deigner und R. Csuk, *Molecules (Basel, Switzerland)* **2020**, *25, DOI:* 10.3390/molecules25225443.

[150] R. K. Wolfram, L. Heller und R. Csuk, *Eur J Med Chem* **2018**, *152,* 21–30, DOI: 10.1016/j.ejmech.2018.04.031.

[151] B. Brandes, S. Hoenke, C. Schultz, H.-P. Deigner und R. Csuk, *Steroids* **2023**, *189,* 109148, DOI: 10.1016/j.steroids.2022.109148.

[152] B. Brandes, S. Hoenke, L. Fischer und R. Csuk, *Eur J Med Chem* **2020**, *185,* 111858, DOI: 10.1016/j.ejmech.2019.111858.

[153] S. Hoenke, B. Brandes und R. Csuk, *Eur. J. Med. Chem. Rep.* **2023**, *7,* 100099, DOI: 10.1016/j.ejmcr.2022.100099.

[154] J. Wiemann, L. Heller, V. Perl, R. Kluge, D. Ströhl und R. Csuk, *Eur J Med Chem* **2015**, *106,* 194–210, DOI: 10.1016/j.ejmech.2015.10.043.

[155] N. Heise, S. Friedrich, V. Temml, D. Schuster, B. Siewert und R. Csuk, *Eur J Med Chem* **2022**, *227,* 113947, DOI: 10.1016/j.ejmech.2021.113947.

[156] S. Friedrich, I. Serbian, S. Hoenke, R. K. Wolfram und R. Csuk, *Synthesis and cytotoxic evaluation of malachite green derived oleanolic and ursolic acid piperazineamides,* **2020**.

[157] N. V. Heise, D. Ströhl, T. Schmidt und R. Csuk, *J. Mol. Struct.* **2022**, *1249,* 131646, DOI: 10.1016/j.molstruc.2021.131646.

[158] D. Biedermann, B. Eignerova, M. Hajduch und J. Sarek, *Synthesis* **2010**, *2010,* 3839–3848, DOI: 10.1055/s-0030-1258293.

[159] J. Sączewski, J. Fedorowicz, P. Wiśniewska und M. Gdaniec, *Applied Sciences* **2021**, *11,* 5498, DOI: 10.3390/app11125498.

[160] J. Fedorowicz, J. Sączewski, Z. Drażba, P. Wiśniewska, M. Gdaniec, B. Wicher, G. Suwiński und A. Jalińska, *Dyes Pigm.* **2019**, *161,* 347–359, DOI: 10.1016/j.dyepig.2018.09.005.

[161] P. Hashim, H. Sidek, M. H. M. Helan, A. Sabery, U. D. Palanisamy und M. Ilham, *Molecules (Basel, Switzerland)* **2011**, *16,* 1310–1322, DOI: 10.3390/molecules16021310.

[162] N. A. J C Furtado, L. Pirson, H. Edelberg, L. M Miranda, C. Loira-Pastoriza, V. Preat, Y. Larondelle und C. M. André, *Molecules (Basel, Switzerland)* **2017**, *22,* 400, DOI: 10.3390/molecules22030400.

[163] Yingmeei Tan, R. Yu, J. Pezzuto, *Clinical cancer research : an official journal of the American Association for Cancer Research* **2003**, *9 7,* 2866–2875.

[164] G. Liebscher, K. Vanchangiri, T. Mueller, K. Feige, J.-M. V. Cavalleri und R. Paschke, *Chemico-biological interactions* **2016**, *246,* 20–29, DOI: 10.1016/j.cbi.2016.01.002.

[165] J. H. Kessler, F. B. Mullauer, G. M. de Roo und J. P. Medema, *Cancer letters* **2007**, *251,* 132–145, DOI: 10.1016/J.CANLET.2006.11.003.

[166] S. Fulda, C. Friesen, M. Los, C. Scaffidi, W. Mier, M. Benedict, G. Núñez, P. Krammer, M. Peter, K. Debatin, K. Debatin, *Cancer research* **1997**, *57 21,* 4956–4964.

[167] A. Schubert und S. Grimm, *Cancer research* **2004**, *64,* 85–93, DOI: 10.1158/0008-5472.CAN-03-0476.

[168] D. H. Suh, M.-K. Kim, H. S. Kim, H. H. Chung und Y. S. Song, *Frontiers in oncology* **2013**, *3,* 41, DOI: 10.3389/fonc.2013.00041.

[169] J. C. Ghosh, M. D. Siegelin, T. Dohi und D. C. Altieri, *Cancer research* **2010**, *70,* 8988–8993, DOI: 10.1158/0008-5472.CAN-10-2225.

[170] N. F. Ayuningtyas, C. Chea, T. Ando, K. E. Saninggar, K. Tanimoto, T. Inubushi, N. Maishi, K. Hida, M. Shindoh, M. Miyauchi und T. Takata, *Pharmaceutics* **2023**, *15, DOI:* 10.3390/pharmaceutics15010165.

[171] A. Sadremomtaz, K. Mansouri, G. Alemzadeh, M. Safa, A. E. Rastaghi und S. M. Asghari, *Biochimica et biophysica acta. General subjects* **2018**, *1862,* 2688–2700, DOI: 10.1016/j.bbagen.2018.08.013.

[172] G. P. Pidgeon, M. P. Barr, J. H. Harmey, D. A. Foley und D. J. Bouchier-Hayes, *British journal of cancer* **2001**, *85,* 273–278, DOI: 10.1054/bjoc.2001.1876.

[173] J. M. Collins und K. A. Foster, *The Journal of cell biology* **1983**, *96,* 94–99, DOI: 10.1083/JCB.96.1.94.

[174] S. Goldstein und L. B. Korczack, *The Journal of cell biology* **1981**, *91,* 392–398, DOI: 10.1083/JCB.91.2.392.

[175] R. K. Emaus, R. Grunwald und J. J. Lemasters, *Biochimica et biophysica acta* **1986**, *850,* 436–448, DOI: 10.1016/0005-2728(86)90112-X.

[176] L. V. Johnson, M. L. Walsh und L. B. Chen, *PNAS* **1980**, *77,* 990–994, DOI: 10.1073/PNAS.77.2.990.

[177] N. Heise, S. Becker, T. Mueller, M. Bache, R. Csuk und A. Güttler, *International journal of molecular sciences* **2023**, *24, DOI:* 10.3390/ijms241310695.

[178] S. Sommerwerk, L. Heller, C. Kerzig, A. E. Kramell und R. Csuk, *Eur J Med Chem* **2017**, *127,* 1–9, DOI: 10.1016/j.ejmech.2016.12.040.

[179] N. V. Heise, T. C. Denner, S. Becker, S. Hoenke und R. Csuk, *Molecules (Basel, Switzerland)* **2023**, *28, DOI:* 10.3390/molecules28176404.

[180] M. Kawakami, K. Koya, T. Ukai, N. Tatsuta, A. Ikegawa, K. Ogawa, T. Shishido und L. B. Chen, *Journal of medicinal chemistry* **1998**, *41,* 130–142, DOI: 10.1021/JM970590K.

[181] I. Macașoi, I. Z. Pavel, A. E. Moacă, Ș. Avram, V. L. David, D. Coricovac, A. Mioc, D. A. Spandidos, A. Tsatsakis, C. Șoica, V. Dumitrașcu und C. Dehelean, *Oncology reports* **2020**, *44,* 1169–1183, DOI: 10.3892/or.2020.7666.

[182] R. J. Quinn, A. R. Carroll, N. B. Pham, P. Baron, M. E. Palframan, L. Suraweera, G. K. Pierens und S. Muresan, *Journal of natural products* **2008**, *71,* 464–468, DOI: 10.1021/np070526y.

[183] A. Chuprina, O. Lukin, R. Demoiseaux, A. Buzko und A. Shivanyuk, *Journal of chemical information and modeling* **2010**, *50,* 470–479, DOI: 10.1021/ci900464s.

[184] P. R. Duchowicz, A. Talevi, C. Bellera, L. E. Bruno-Blanch und E. A. Castro, *Bioorganic & medicinal chemistry* **2007**, *15,* 3711–3719, DOI: 10.1016/J.BMC.2007.03.044.

[185] I. Serbian, S. Hoenke, O. Kraft und R. Csuk, *Med. Chem. Res.* **2020**, *29,* 1655–1661, DOI: 10.1007/s00044-020-02591-8.

[186] J. LeBarron und E. London, *Langmuir : the ACS journal of surfaces and colloids* **2016**, *32,* 10752–10760, DOI: 10.1021/acs.langmuir.6b02597.

[187] M. Igawa, R. Nishiura, N. Mashiyama und Y. Usuda, *Bull. Chem. Soc. Jpn.* **1992**, *65,* 1871–1877, DOI: 10.1246/BCSJ.65.1871.

[188] H. G. Becker, *Organikum,* 23. Aufl., Wiley-VCH, Weinheim, **2009**.

[189] E. H. Gort, A. J. Groot, E. van der Wall, P. J. van Diest und M. A. Vooijs, *Current molecular medicine* **2008**, *8,* 60–67, DOI: 10.2174/156652408783565568.

[190] L.-F. Dong, V. J. A. Jameson, D. Tilly, J. Cerny, E. Mahdavian, A. Marín-Hernández, L. Hernández-Esquivel, S. Rodríguez-Enríquez, J. Stursa, P. K. Witting, B. Stantic, J. Rohlena, J. Truksa, K. Kluckova, J. C. Dyason, M. Ledvina, B. A. Salvatore, R. Moreno-Sánchez, M. J. Coster, S. J. Ralph, R. A. J. Smith und J. Neuzil, *The Journal of biological chemistry* **2011**, *286,* 3717–3728, DOI: 10.1074/jbc.M110.186643.

[191] J. Neuzil, L.-F. Dong, L. Ramanathapuram, T. Hahn, M. Chladova, X.-F. Wang, R. Zobalova, L. Prochazka, M. Gold, R. Freeman, J. Turanek, E. T. Akporiaye, J. C. Dyason und S. J. Ralph, *Molecular aspects of medicine* **2007**, *28,* 607–645, DOI: 10.1016/j.mam.2007.02.003.

[192] J. Neuzil, L.-F. Dong, J. Rohlena, J. Truksa und S. J. Ralph, *Mitochondrion* **2013**, *13,* 199–208, DOI: 10.1016/j.mito.2012.07.112.

[193] J. Neuzil, M. Tomasetti, Y. Zhao, L.-F. Dong, M. Birringer, X.-F. Wang, P. Low, K. Wu, B. A. Salvatore und S. J. Ralph, *Molecular pharmacology* **2007**, *71,* 1185–1199, DOI: 10.1124/mol.106.030122.

[194] J. Truksa, L.-F. Dong, J. Rohlena, J. Stursa, M. Vondrusova, J. Goodwin, M. Nguyen, K. Kluckova, Z. Rychtarcikova, S. Lettlova, J. Spacilova, M. Stapelberg, M. Zoratti und J. Neuzil, *Antioxidants & redox signaling* **2015**, *22,* 883–900, DOI: 10.1089/ars.2013.5594.

[195] B. Yan, M. Stantic, R. Zobalova, A. Bezawork-Geleta, M. Stapelberg, J. Stursa, K. Prokopova, L. Dong und J. Neuzil, *BMC Cancer* **2015**, *15,* 1–12, DOI: 10.1186/s12885-015-1394-7.

[196] Y. Zhao, J. Neuzil und K. Wu, *Molecular nutrition & food research* **2009**, *53,* 129–139, DOI: 10.1002/mnfr.200800045.

[197] R. K. Wolfram, L. Fischer, R. Kluge, D. Ströhl, A. Al-Harrasi und R. Csuk, *Eur J Med Chem* **2018**, *155,* 869–879, DOI: 10.1016/j.ejmech.2018.06.051.

[198] I. Serbian, S. Hoenke und R. Csuk, *Eur J Med Chem* **2020**, *199,* 112425, DOI: 10.1016/j.ejmech.2020.112425.

[199] M. Grymel, M. Zawojak und J. Adamek, *Journal of natural products* **2019**, *82,* 1719–1730, DOI: 10.1021/acs.jnatprod.8b00830.

[200] A. Y. Spivak, D. A. Nedopekina, R. R. Khalitova, R. R. Gubaidullin, V. N. Odinokov, Y. P. Bel'skii, N. V. Bel'skaya und V. A. Khazanov, *Med. Chem. Res.* **2017**, *26,* 518–531, DOI: 10.1007/s00044-016-1771-z.

[201] A. Y. Spivak, D. A. Nedopekina, E. R. Shakurova, R. R. Khalitova, R. R. Gubaidullin, V. N. Odinokov, U. M. Dzhemilev, Y. P. Bel'skii, N. V. Bel'skaya, S. A. Stankevich, E. V. Korotkaya und V. A. Khazanov, *Russ. Chem. Bull.* **2013**, *62,* 188–198, DOI: 10.1007/s11172-013-0028-y.

[202] V. E. Kataev, I. Y. Strobykina und L. Y. Zakharova, *Russ. Chem. Bull.* **2014**, *63,* 1884–1900, DOI: 10.1007/s11172-014-0680-x.

[203] V. Panda, P. Khambat und S. Patil, *IJCM* **2011**, *02,* 515–529, DOI: 10.4236/ijcm.2011.24086.

[204] B. Siewert, E. Pianowski und R. Csuk, *Eur J Med Chem* **2013**, *70,* 259–272, DOI: 10.1016/j.ejmech.2013.10.016.

[205] B. Brandes, L. Koch, S. Hoenke, H.-P. Deigner und R. Csuk, *Steroids* **2020**, *163,* 108713, DOI: 10.1016/j.steroids.2020.108713.

[206] J. Fedorowicz, M. Cebrat, M. Wierzbicka, P. Wiśniewska, A. Jalińska, S. Dziomba, M. Gdaniec, M. Jaremko, Ł. Jaremko, K. Chandra, Z. Szewczuk und J. Sączewski, *J. Mol. Struct.* **2020**, *1217,* 128426, DOI: 10.1016/j.molstruc.2020.128426.

[207] S. Fulda, C. Scaffidi, S. A. Susin, P. H. Krammer, G. Kroemer, M. E. Peter und K.-M. Debatin, *J. Biol. Chem.* **1998**, *273,* 33942–33948, DOI: 10.1074/jbc.273.51.33942.

[208] R. Csuk, *Expert Opin. Ther. Pat.* **2014**, *24,* 913–923, DOI: 10.1517/13543776.2014.927441.

[209] M. Kahnt, L. Fischer, A. Al-Harrasi und R. Csuk, *Molecules* **2018**, *23,* 2558, DOI: 10.3390/molecules23102558.

[210] S. H. Safe, P. L. Prather, L. K. Brents, G. Chadalapaka und I. Jutooru, *Anti-Cancer Agents Med. Chem.* **2012**, *12,* 1211–1220, DOI: 10.2174/187152012803833099.

[211] J. Sączewski, A. Kędzia und A. Jalińska, *Heterocycl. Commun.* **2014**, *20,* 215–223, DOI: 10.1515/hc-2014-0107.

[212] J. Sączewski, K. Hinc, M. Obuchowski und M. Gdaniec, *Chemistry – A European Journal* **2013**, *19,* 11531–11535, DOI: 10.1002/chem.201302085.

[213] Daems, *Chem. Zentralbl.* **1943**, *114,* 1649.

[214] P. Dróżdż, A. Sentkowska und K. Pyrzynska, *Nat. Prod. Res.* **2018**, *33,* 2128–2131, DOI: 10.1080/14786419.2018.1488704.

[215] M. F. Melzig und S. Böttger, *Planta medica* **2020**, *86,* 1050–1057, DOI: 10.1055/a-1129-7214.

[216] D. Anheyer, J. Frawley, A. K. Koch, R. Lauche, J. Langhorst, G. Dobos und H. Cramer, *Pediatrics* **2017**, *139, DOI:* 10.1542/peds.2017-0062.

[217] S. Shushunov, L. Balashov, A. Kravtsova, I. Krasnogorsky, K. P. Latté und A. Vasiliev, *J. Med. Food* **2009**, *12,* 1173–1176, DOI: 10.1089/jmf.2008.0281.

[218] M. Tomczyk und K. P. Latté, *Journal of ethnopharmacology* **2009**, *122,* 184–204, DOI: 10.1016/j.jep.2008.12.022.

[219] U. Wölfle, J. Hoffmann, B. Haarhaus, V. Rao Mittapalli und C. M. Schempp, *Journal of ethnopharmacology* **2017**, *204,* 86–94, DOI: 10.1016/j.jep.2017.03.058.

[220] *Hildegard von Bingen-Werke,* Beuroner Kunstvlg, Beuron, **2017**.

[221] Z.-J. Lia, C.-P. Wan, Le Cai, S.-Q. Li, X. Zheng, Y. Qi, J.-W. Dong, T.-P. Yin, Z.-X. Zhou, N.-H. Tan und Z.-T. Ding, *Phytochem. Lett.* **2015**, *13,* 246–251, DOI: 10.1016/j.phytol.2015.06.015.

[222] Y. Shi, D. Zhang, S. Li, X. Xuan, L. Zhang, Y. Li und F. Guo, *Nat. Prod. Res.* **2019**, *35,* 2044–2050, DOI: 10.1080/14786419.2019.1655414.

[223] R. Wang, M. Jin, C. Jin, J. Sun, C. Ye, T. Zong, G. Chen, W. Zhou und G. Li, *Phytochem. Lett.* **2019**, *32,* 96–100, DOI: 10.1016/j.phytol.2019.05.006.

[224] Woo, *Nat. Prod. Sci.* **2014**, *20,* 71.

[225] Yang, *Mol. Med. Rep.* **2018**, *17,* 4753.

[226] M. Alfaifi, A. Alsayari, N. Gurusamy, J. Louis, S. Eldin Elbehairi, K. Venkatesan, S. Annadurai, Y. I. Asiri, A. Shati, K. Saleh, H. Alboushnak, H. Handoussa, A. Bin Muhsinah und A. Abdel Motaal, *Molecules* **2020**, *25,* 418, DOI: 10.3390/molecules25020418.

[227] L. P. Sandjo, V. Rincheval, B. T. Ngadjui und G. Kirsch, *Chem. Nat. Compd.* **2011**, *47,* 731–734, DOI: 10.1007/s10600-011-0045-8.

[228] Zhang, *PLoS One* **2017**, *12.*

[229] B. Tian Zhao, D. Hung Nguyen, B. Mi Lee, S. Hui Seong, J. Sue Choi, B. Sun Min und M. Hee Woo, *Med. Chem. Res.* **2017**, *26,* 2870–2878, DOI: 10.1007/s00044-017-1986-7.

[230] R. Csuk, B. Siewert, C. Dressel und R. Schäfer, *Eur J Med Chem* **2012**, *56,* 237–245, DOI: 10.1016/j.ejmech.2012.08.032.

[231] O. Kraft, J. Wiemann, A. Al-Harrasi und R. Csuk, *Phytochem. Lett.* **2019**, *32,* 29–32, DOI: 10.1016/j.phytol.2019.04.016.

[232] J. Wiemann, A. M. Deckelmann und R. Csuk, *Tetrahedron Lett.* **2016**, *57,* 3952–3953, DOI: 10.1016/j.tetlet.2016.07.068.

[233] Chandel, *Indian J. Chem., Sect. B* **1977**, *15B,* 914.

[234] L. Guang-Yi, A. I. Gray und P. G. Waterman, *Journal of natural products* **1989**, *52,* 162–166, DOI: 10.1021/np50061a021.

[235] T. Seto, T. Tanaka, O. Tanaka und N. Naruhashi, *Phytochemistry* **1984**, *23,* 2829–2834, DOI: 10.1016/0031-9422(84)83023-X.

[236] K. TAKAHASHI, S. KAWAGUCHI, K. NISHIMURA, K. KUBOTA, Y. TANABE und M. TAKANI, *Chem. Pharm. Bull.* **1974**, *22,* 650–653, DOI: 10.1248/cpb.22.650.

[237] Biggs, *Nat. Prod. Commun.* **2008**, *3,* 1759.

[238] Potier, *Bull. Soc. Chim. Fr.* **1966,** 3458.

[239] C. Terreaux, M. P. Maillard, M. P. Gupta und K. Hostettmann, *Phytochemistry* **1996**, *42,* 495–499, DOI: 10.1016/0031-9422(95)00945-0.

[240] T. Yamagishi, D.-C. Zhang, J.-J. Chang, D. R. McPhail, A. T. McPhail und K.-H. Lee, *Phytochemistry* **1988**, *27,* 3213–3216, DOI: 10.1016/0031-9422(88)80028-1.

[241] Z. Qin, W. Su, P. Liu, J. Ma, Y. Zhang und T. Jiao, *ACS Omega* **2021**, *6,* 25040–25048, DOI: 10.1021/acsomega.1c04206.

[242] M. Matsui, T. Yamamoto, K. Kakitani, S. Biradar, Y. Kubota und K. Funabiki, *Dyes Pigm.* **2017**, *139,* 533–540, DOI: 10.1016/j.dyepig.2016.11.013.

[243] *Latest global cancer data: Cancer burden rises to 19.3 million new cases and 10.0 million cancer deaths in 2020,* https://www.iarc.who.int/news-events/latest-global-cancer-data-cancer-burden-rises-to-19-3-million-new-cases-and-10-0-million-cancer-deaths-in-2020/, **3/30/2024**.

[244] B. S. Siddiqui, S. Begum, S. Siddiqui und W. Lichter, *Phytochemistry* **1995**, *39,* 171–174, DOI: 10.1016/0031-9422(94)00855-N.

[245] M. Chudzik, I. Korzonek-Szlacheta und W. Król, *Molecules (Basel, Switzerland)* **2015**, *20,* 1610–1625, DOI: 10.3390/molecules20011610.

[246] Bruno M. F. Gonçalves, Jorge A. R. Salvador, Silvia Marín und Marta Cascante, *RSC Adv.* **2016**, *6,* 3967–3985, DOI: 10.1039/C5RA19120C.

[247] M.-R. Kim, H.-H. Lee, K.-S. Hahm, Y.-H. Moon und E.-R. Woo, *Arch. Pharmacal Res.* **2004**, *27,* 283–286, DOI: 10.1007/BF02980060.

[248] *Eur J Med Chem* **2013**, *68,* 121–131, DOI: 10.1016/j.ejmech.2013.07.012.

[249] M. Drag, P. Surowiak, M. Drag-Zalesinska, M. Dietel, H. Lage und J. Oleksyszyn, *Molecules* **2009**, *14,* 1639–1651, DOI: 10.3390/molecules14041639.

[250] H. Kommera, G. N. Kaluderović, S. Dittrich, J. Kalbitz, B. Dräger, T. Mueller und R. Paschke, *Bioorganic & medicinal chemistry letters* **2010**, *20,* 3409–3412, DOI: 10.1016/j.bmcl.2010.04.004.

[251] J. Wiemann, L. Heller, V. Perl, R. Kluge, D. Ströhl und R. Csuk, *Eur J Med Chem* **2015**, *106,* 194–210, DOI: 10.1016/j.ejmech.2015.10.043.

[252] A. Lewinska, J. Adamczyk-Grochala, E. Kwasniewicz, A. Deregowska und M. Wnuk, *Apoptosis : an international journal on programmed cell death* **2017**, *22,* 800–815, DOI: 10.1007/s10495-017-1353-7.

[253] J. Hao, J. Liu, X. Wen und H. Sun, *Bioorganic & medicinal chemistry letters* **2013**, *23,* 2074–2077, DOI: 10.1016/j.bmcl.2013.01.129.

[254] S. Friedrich, I. Serbian, S. Hoenke, R. K. Wolfram und R. Csuk, *Med. Chem. Res.* **2020**, *29,* 926–933, DOI: 10.1007/s00044-020-02536-1.

[255] S. Schwarz und R. Csuk, *Bioorganic & medicinal chemistry* **2010**, *18,* 7458–7474, DOI: 10.1016/j.bmc.2010.08.054.

[256] D. Rodríguez-Hernández, L. C. Barbosa, A. J. Demuner, J. P. Ataide Martins, L. Fischer und R. Csuk, *Eur J Med Chem* **2019**, *168,* 436–446, DOI: 10.1016/j.ejmech.2019.02.057.

[257] X. Liu, Y. Yang, X. Wang, K. Wang, J. Liu, L. Lei, X. Luo, R. Zhai, F. Fu, H. Wang und Y. Bi, *Eur J Med Chem* **2017**, *141,* 427–439, DOI: 10.1016/j.ejmech.2017.09.016.

[258] S. Emirdağ-Öztürk, T. Karayıldırım, A. Çapcı-Karagöz, Ö. Alankuş-Çalışkan, A. Özmen und E. Poyrazoğlu-Çoban, *Eur J Med Chem* **2014**, *82,* 565–573, DOI: 10.1016/j.ejmech.2014.05.084.

[259] N. I. Pavlova, O. V. Savinova, S. N. Nikolaeva, E. I. Boreko und O. B. Flekhter, *Fitoterapia* **2003**, *74,* 489–492, DOI: 10.1016/S0367-326X(03)00123-0.

[260] H. M. Wang, C. M. Şoica und G. Wenz, *Nat. Prod. Commun.* **2012**, *7,* 1934578X1200700, DOI: 10.1177/1934578X1200700304.

[261] E. Pisha, H. Chai, I.-S. Lee, T. E. Chagwedera, N. R. Farnsworth, G. A. Cordell, C. W. Beecher, H. H. Fong, A. D. Kinghorn, D. M. Brown, M. C. Wani, M. E. Wall, T. J. Hieken, T. K. Das Gupta und J. M. Pezzuto, *Nat. Med.* **1995**, *1,* 1046–1051, DOI: 10.1038/nm1095-1046.

[262] I. Serbian, D. Ströhl und R. Csuk, *Phytochem. Lett.* **2020**, *39,* 35–38, DOI: 10.1016/j.phytol.2020.06.005.

[263] L. Heller, S. Schwarz, B. A. Weber und R. Csuk, *Arch. Pharm.* **2014**, *347,* 707–716, DOI: 10.1002/ardp.201400103.

[264] S. Sommerwerk, L. Heller, J. Kuhfs und R. Csuk, *Eur J Med Chem* **2016**, *122,* 452–464, DOI: 10.1016/j.ejmech.2016.06.053.

[265] B. Patwardhan, A. D. B. Vaidya und M. Chorghade, *Current Science* **2004**, *86,* 789–799.

[266] Y. Xiang, Z. Guo, P. Zhu, J. Chen und Y. Huang, *Cancer medicine* **2019**, *8,* 1958–1975, DOI: 10.1002/cam4.2108.

[267] P. Hao, F. Jiang, J. Cheng, L. Ma, Y. Zhang und Y. Zhao, *J. Am. Coll. Cardiol.* **2017**, *69,* 2952–2966, DOI: 10.1016/j.jacc.2017.04.041.

[268] B. B. Aggarwal, H. Ichikawa, P. Garodia, P. Weerasinghe, G. Sethi, I. D. Bhatt, M. K. Pandey, S. Shishodia und M. G. Nair, *Expert opinion on therapeutic targets* **2006**, *10,* 87–118, DOI: 10.1517/14728222.10.1.87.

[269] R. Jain, S. Kosta und A. Tiwari, *Pharmacognosy research* **2010**, *2,* 393–394, DOI: 10.4103/0974-8490.75463.

[270] B. Patwardhan und R. A. Mashelkar, *Drug discovery today* **2009**, *14,* 804–811, DOI: 10.1016/j.drudis.2009.05.009.

[271] E. S. Teoh, *Medicinal Orchids of Asia,* 59–73, DOI: 10.1007/978-3-319-24274-3_5.

[272] S. Fulda und T. Efferth, *World Journal of Traditional Chinese Medicine* **2015**, *1,* 24–28, DOI: 10.15806/j.issn.2311-8571.2014.0005.

[273] C. D. R. Nunes, M. Barreto Arantes, S. Menezes de Faria Pereira, L. Da Leandro Cruz, M. de Souza Passos, L. Pereira de Moraes, I. J. C. Vieira und D. Barros de Oliveira, *Molecules (Basel, Switzerland)* **2020**, *25, DOI:* 10.3390/molecules25163726.

[274] C. Attardo und F. Sartori, *Bollettino chimico farmaceutico* **2003**, *142,* 54–65.

[275] A. L. Souto, J. F. Tavares, M. S. Da Silva, M. d. F. F. M. Diniz, P. F. de Athayde-Filho und J. M. Barbosa Filho, *Molecules (Basel, Switzerland)* **2011**, *16,* 8515–8534, DOI: 10.3390/molecules16108515.

[276] V. Panda, P. Khambat und S. Patil, *IJCM* **2011**, *02,* 515–529, DOI: 10.4236/ijcm.2011.24086.

[277] V. Gogvadze, B. Zhivotovsky und S. Orrenius, *Molecular aspects of medicine* **2010**, *31,* 60–74, DOI: 10.1016/j.mam.2009.12.004.

[278] B. Siewert, J. Wiemann, A. Köwitsch und R. Csuk, *Eur J Med Chem* **2014**, *72,* 84–101, DOI: 10.1016/j.ejmech.2013.11.025.

[279] S. Sommerwerk, L. Heller, J. Kuhfs und R. Csuk, *Eur J Med Chem* **2016**, *119,* 1–16, DOI: 10.1016/j.ejmech.2016.04.051.

[280] I. Serbian, B. Siewert, A. Al-Harrasi und R. Csuk, *Eur J Med Chem* **2019**, *180,* 457–464, DOI: 10.1016/j.ejmech.2019.07.049.

[281] R. Csuk, A. Niesen-Barthel, R. Schäfer, A. Barthel und A. Al-Harrasi, *Eur J Med Chem* **2015**, *92,* 700–711, DOI: 10.1016/j.ejmech.2015.01.039.

[282] SpringerLink, *Löffler/Petrides Biochemie und Pathobiochemie,* https://link.springer.com/book/10.1007/978-3-662-60266-9, **4/21/2024**.

6 Abbildungsverzeichnis

ABBILDUNG 1: DIE HÄUFIGSTEN TODESURSACHEN IN DEUTSCHLAND IN 2023. [1] 1
ABBILDUNG 2: PROGNOSTIZIERTE NEUE KREBSFÄLLE BIS 2040.[26] 2
ABBILDUNG 3: ZELLULÄRE VORGÄNGE BEI APOPTOSE UND NEKROSE.[282] 5
ABBILDUNG 4:VINBLASTIN (AUS CATHARANTHUS ROSEUS) UND PODOPHYLLOTOXIN (AUS PODOPHYLLUM PELTATUM).[64; 65] 6
ABBILDUNG 5: FUNKTION DER IMMUNTHERAPIE.[75] 8
ABBILDUNG 6: HÄUFIGE GRUNDGERÜSTE DER TRITERPENE. 10
ABBILDUNG 7: ASIASÄURE AUS CENTELLA ASIATICA.[120] 12
ABBILDUNG 8: PENTAZYKLISCHE TRITERPENCARBONSÄUREN. 13
ABBILDUNG 9: AUSWAHL LIPOHILER KATIONEN FÜR DIE KUPPLUNG AN TRITERPENE UND STEROIDE. 15
ABBILDUNG 10: TRITERPEN-SAFIRINIUM P & Q-HYBRIDE. 16
ABBILDUNG 11:OFFENE UND GESCHLOSSENE RHODAMIN B-EINHEIT. 18
ABBILDUNG 12: SYNTHESE VON SAFIRINIUM P. 20
ABBILDUNG 13: SYNTHESE VON SAFIRINIUM Q 21
ABBILDUNG 14: FLUORESZENZBILDGEBUNG VON A375-EPITHELKARZINOMZELLEN, INKUBIERT MIT: VERBINDUNG 30 (LINKS), ER-TRACKER (MITTE) UND ZUSAMMENGEFÜHRTE BILDER (RECHTS). 22
ABBILDUNG 15: SYNTHESESCHEMA ZUR DARSTELLUNG DER RHODAMIN B-KONJUGATE AUS TORMENTILL- UND EUSCAPHSÄURE. 23
ABBILDUNG 16: SYNTHESESCHEMA ZUR DARSTELLUNG DER RHODAMIN B-KONJUGATE DER TRITERPENCARBONSÄUREN AUS SAPONIN. 26
ABBILDUNG 17: AKTIVSTE MADECASSINSÄURE-DERIVAT MIT HOMOPIPERAZIN-SPACER UND RHODAMIN B(LINKS)UND FÄRBEVERSUCHE: A375-ZELLEN, 48 STUNDEN; (A): KONTROLLE; (B): IN GEGENWART VON **24**; (C): HOECHST 33.342-FÄRBUNG; (D): ZUSAMMENGEFÜHRT (HOECHST 33.342, KONTROLLE); UND (E): IN GEGENWART VON RHODAMIN 123 (RECHTS). 26
ABBILDUNG 18: SYNTHESESCHEMA ZUR SYNTHESE DER ASIASÄUREDERIVATE. 28
ABBILDUNG 19: DERIVAT DER ASIASÄURE (19) MIT SUB-NANOMOLARER AKTIVITÄT UND HOHER SELEKTIVITÄT. 28

ABBILDUNG 20: HISTOLOGISCHE UND IMMUNHISTOCHEMISCHE ANALYSEN VON DLD1-SPHÄROIDEN. 29
ABBILDUNG 21: KONJUGAT DER ASIASÄURE MIT HOMOPIPERAZIN-SPACER UND RHODAMIN B-EINHEIT. 30

7 Tabellenverzeichnis

TABELLE 1: APOPTOTISCHE WIRKMECHANISMEN VERSCHIEDENER TRITERPENCARBONSÄUREN. 11
TABELLE 2: EC50-WERTE AUSGEWÄHLTER DERIVATE NACH KAHNT.[122] 17
TABELLE 3:EC50-WERTE AUSGEWÄHLTER DERIVATE.......... 22
TABELLE 4: EC50-WERTE DER SYNTHETISIERTEN DERIVATE. 24
TABELLE 5: EC50-WERTE AUSGEWÄHLTER DERIVATE 27

8 Anhang

Die für diese Arbeit relevanten Publikationen sind wie folgt gegliedert:

Publikation 1: „Cytotoxic triterpenoid–safirinium conjugates target the endoplasmic reticulum”
Kraft, O.; Kozubek, M.; Hoenke, S.; Serbian, I.; Major, D.; Csuk, R., *Eur. J. Med. Chem.* **2021**, 209, 112920

Publikation 2: „A tormentic acid-homopiperazine-rhodamine B conjugate of single-digit nanomolar cytotoxicity and high selectivity for several human tumor cell lines”
Kraft, O.; Hoenke, S.; Csuk, R., *Eur. J. Med. Chem. Rep.* **2022**, 5, 100043

Publikation 3: „Madecassic Acid—A New Scaffold for Highly Cytotoxic Agents”
Kraft, O.; Hartmann, A-K.; Hoenke, S.; Serbian, I.; Csuk, R., *Int. J. Mol. Sci.* **2022**, 23(8), 4362

Publikation 4: „Asiatic acid as a leading structure for derivatives combining sub-nanomolar cytotoxicity, high selectivity, and the ability to overcome drug resistance in human preclinical tumor models”
Kraft, O.; Hartmann, A-K.; Brandt, S.; Hoenke, S.; Heise, N.; Csuk, R.; Müller, T., *Eur. J. Med. Chem.* **2023**, 15, 115189

8.1 „Cytotoxic triterpenoid–safirinium conjugates target the endoplasmic reticulum”

Kraft, O.; Kozubek, M.; Hoenke, S.; Serbian, I.; Major, D.; Csuk, R., *Eur. J. Med. Chem.* **2021**, 209, 112920

Graphical abstract:

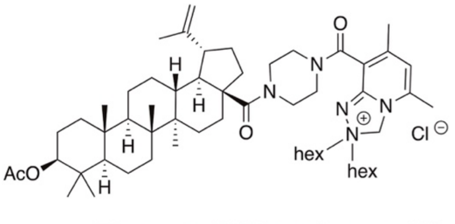

EC$_{50}$ = 5.44 µM (A375 melanoma cells)

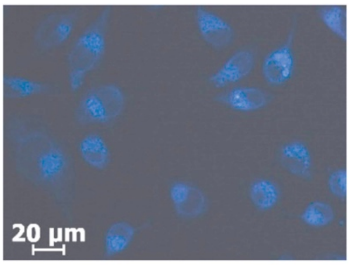

Abstract:

Safirinium P and Q fluorescence labels were synthesized and conjugated with spacered triterpenoic acids to access hybrid structures. While the parent safirinium compounds were not cytotoxic at all, many triterpenoid safirinium P and Q conjugates showed moderate cytotoxicity. An exception, however, was safirinium P derived compound **30** holding low EC$_{50}$ = 5.4 µM (for A375 cells) to EC$_{50}$ = 7.5 µM (for FaDu cells) as well as EC$_{50}$ = 6.6 µM for non-malignant fibroblasts NIH 3T3. Fluorescence imaging showed that the safirinium core structures cannot enter the cells (not even after a prolonged incubation time of 24 h), while the conjugates (as exemplified for **30**) are accumulating in the endoplasmic reticulum but not in the mitochondria. The development of safirinium-hybrids targeting the endoplasmic reticulum can be regarded as a promising strategy in the development of cytotoxic agents.

Keywords:

Betulinic acid, Safirinium, Cytotoxicity, Endoplasmatic reticulum

DOI: 10.1016/j.ejmech.2020.112920.

8.2 „A tormentic acid-homopiperazine-rhodamine B conjugate of single-digit nanomolar cytotoxicity and high selectivity for several human tumor cell lines”

Kraft, O.; Hoenke, S.; Csuk, R., *Eur. J. Med. Chem. Rep.* **2022**, 5, 100043

Graphical abstract:

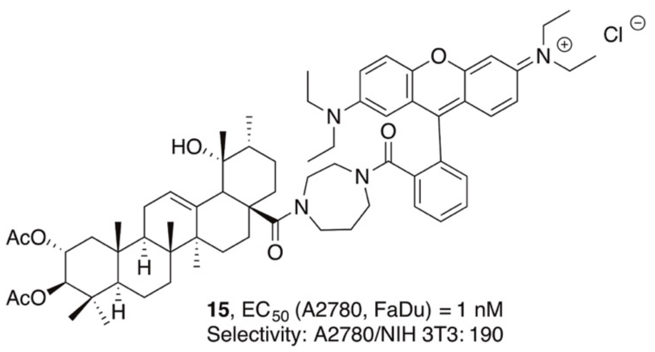

15, EC_{50} (A2780, FaDu) = 1 nM
Selectivity: A2780/NIH 3T3: 190

Abstract:

Tormentic acid and euscaphic acid were isolated from plant material and transformed into amides holding an extra rhodamine B moiety; these compounds were screened for their cytotoxic activity employing a panel of human tumor cell lines and non-malignant fibroblasts. Prerequisites for both high cytotoxicity and tumor cell selectivity seem to be the combination of an amide (from a secondary amine but not from a primary), the use of homopiperazine rather than piperazine as a spacer together with rhodamine B (as a cationic center) and – most important-a triterpene holding a (2α, 3β) configuration of the substituents in ring A of the triterpenoid skeleton. All these features are found in tormentic acid derived compound **15**; it acts as a mitocan; it is approximately 190 times more cytotoxic for ovarian carcinoma cells than for non-malignant fibroblasts, and **15** displayed an EC_{50} as low as 1 nM for several human cancer cell lines.

Keywords:

Tormentic acid, Pentacyclic triterpene, Euscaphic acid, Rhodamine B, Cytotoxicity

DOI: 10.1016/j.ejmcr.2022.100043

8.3 „Madecassic Acid—A New Scaffold for Highly Cytotoxic Agents”

Kraft, O.; Hartmann, A-K.; Hoenke, S.; Serbian, I.; Csuk, R., *Int. J. Mol. Sci.* **2022**, 23(8), 4362

Graphical abstract:

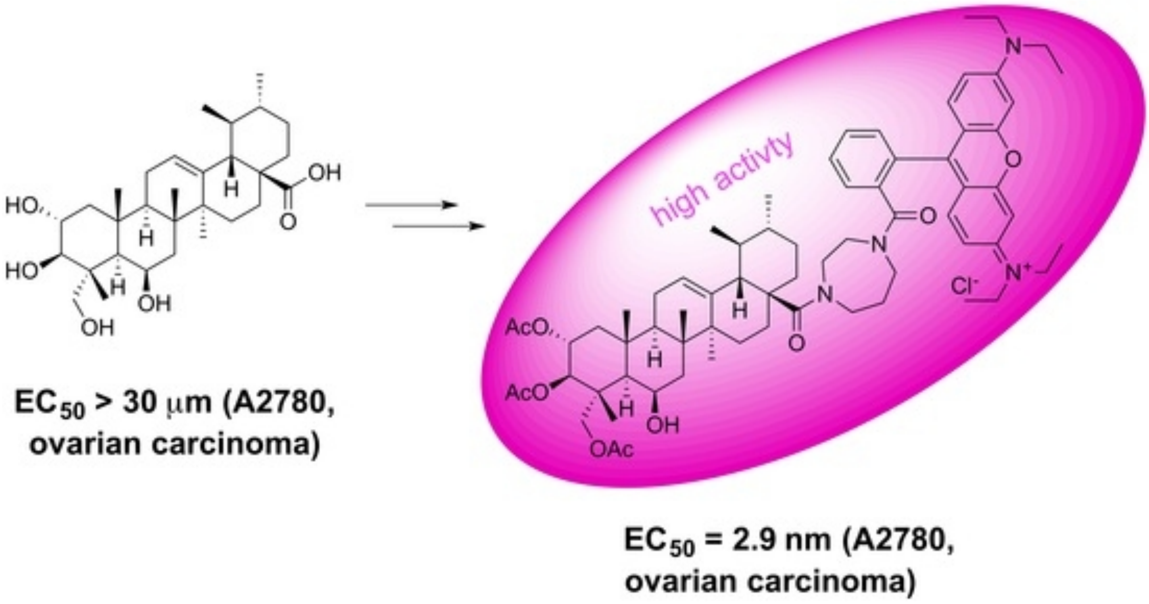
EC_{50} > 30 µm (A2780, ovarian carcinoma)
high activty
EC_{50} = 2.9 nm (A2780, ovarian carcinoma)

Abstract:

Due to their manifold biological activities, natural products such as triterpenoids have advanced to represent excellent leading structures for the development of new drugs. For this reason, we focused on the syntheses and cytotoxic evaluation of derivatives obtained from gypsogenin, hederagenin, and madecassic acid, cytotoxicity increased—by and large—from the parent compounds to their acetates. Another increase in cytotoxicity was observed for the acetylated amides (phenyl, benzyl, piperazinyl, and homopiperazinyl), but a superior cytotoxicity was observed for the corresponding rhodamine B conjugates derived from the (homo)-piperazinyl amides. In particular, a madecassic acid homopiperazinyl rhodamine B conjugate **24** held excellent cytotoxicity and selectivity for several human tumor cell lines. Thus, this compound was more than 10,000 times more cytotoxic than parent madecassic acid for A2780 ovarian cancer cells. We assume that the presence of an additional hydroxyl group at position C–6 in derivatives of madecassic, as well as the (2α, 3β) configuration of the acetates in ring A, had a beneficial effect onto the cytotoxicity of the conjugates, as well as onto tumor/non-tumor cell selectivity.

Keywords:

Madecassic acid, Gypsogenin, Hederagenin, Cytotoxicity, Mitocan

DOI: 10.3390/ijms23084362

8.4 „Asiatic acid as a leading structure for derivatives combining sub-nanomolar cytotoxicity, high selectivity, and the ability to overcome drug resistance in human preclinical tumor models"

Kraft, O.; Hartmann, A-K.; Brandt, S.; Hoenke, S.; Heise, N.; Csuk, R.; Müller, T.,
Eur. J. Med. Chem. **2023**, 15, 115189

Graphical abstract:

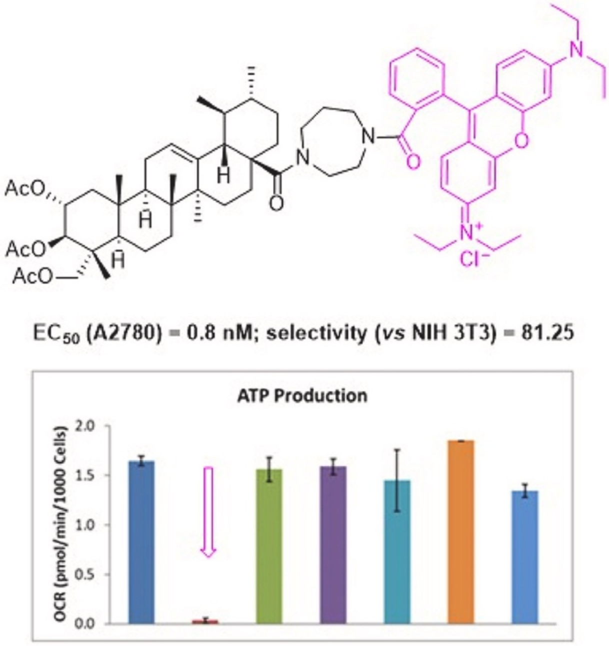
AcO
AcO
AcO
H
H
H
N
N
O
O
O
N
N⁺
Cl⁻
EC50 (A2780) = 0.8 nM; selectivity (vs NIH 3T3) = 81.25
ATP Production
OCR (pmol/min/1000 Cells)
2.0
1.5
1.0
0.5
0.0

Abstract:

Amides and rhodamine B conjugates of different pentacyclic triterpene acids have been shown outstanding cytotoxicity for human tumor cells. Starting from asiatic acid, a new rhodamine B hybrid has been synthesized, and its cytotoxic activity was investigated employing several human tumor cell lines (A375 (melanoma), HT29 (colorectal carcinoma), MCF7 (breast adenocarcinoma), A2780 (ovarian carcinoma), HeLa (cervical carcinoma), (NIH 3T3 (non-malignant murine fibroblasts). For these conjugates of this kind it has been established that the spacer attached to the carboxyl group at ring E governs the magnitude of the cytotoxicity. These asiatic acid - rhodamine B conjugates were highly cytotoxic for human tumor cell lines but also selective. For example, **7**, an acetylated homopiperazinyl spacered rhodamine B conjugate, held an EC_{50} = 0.8 nM for A2780 ovarian carcinoma cells. Additional staining experiments showed the rhodamine B conjugates to act as mitocans and to effect apoptosis. In further tests using 3D spheroid models of colorectal- and mamma carcinoma, **7** demonstrated activity in the lower nanomolar range and the ability to overcome resistance to clinically used standard chemotherapeutic drugs. Therefore **7** induces cytotoxic effects leading to an equal response in the chemotherapy of both sensitive and resistant tumor models. Analyses of mitochondrial function and glycolysis and respiration derived ATP production confirmed compound **7** to act as mitocan but also revealed a rapid perturbation of the cellular energy metabolism as the primary mechanism of action, which is completely different to conventional chemotherapeutic drugs and thereby explains the ability of compound **7** to overcome chemotherapeutic drug resistance.

Keywords:

Asiatic acid, Cytotoxicity, Drug resistance, Tumor model

DOI:10.1016/j.ejmech.2023.115189

10 Publikationsliste

„En route to anti-glioblastoma active pomolic acid"
O. Kraft, J. Wiemann, A. Al-Harrasi, R. Csuk, *Phytochem. Lett.* **2019**, *32*, 29–32.

„Synthesis and cytotoxic evaluation of hydroxycinnamaic acid rhodamine B conjugates"
M. Kozubek, I. Serbian, S. Hoenke, **O. Kraft**, R. Csuk, *Results Chem.* **2020**, *2*, 100057.

„Ester and amide derivates of rhodamin B exert cytotoxic effects on different human tumor cell lines"
I. Serbian, S. Hoenke, **O. Kraft**, R. Csuk, *Med Chem Res* **2020**, *29*, 1655–1661.

„A convenient and simple synthesis of sorokinol"
O. Kraft, A. Al-Harrasi, R. Csuk, *Phytochem. Lett.* **2020**, *39*, 8–11.

„Cytotoxic triterpenoid-safirinium conjugates target the endoplasmic reticulum"
O. Kraft, M. Kozubek, S. Hoenke, I. Serbian, D. Major, R. Csuk, *Eur. J. Med. Chem.* **2021**, *209*, 112920.

„A tormentic acid-homopiperazine-rhodamine B conjugate of single-digit nanomolar cytotoxicity and high selectivity for several human tumor cell lines"
O. Kraft, S. Hoenke, R. Csuk, *Eur. J. Med. Chem. Rep.* **2022**, *5*, 100043.

„Madecassic Acid – A New Scaffold for Highly Cytotoxic Agents"
O. Kraft, A.-K. Hartmann, S. Hoenke, I. Serbian, R. Csuk, *Int. J. Mol. Sci.* **2022**, *23*.

„Hydroxyethylamide substituted triterpenoic acids hold good cytotoxicity for human tumor cells"
T. C. Denner, S. Hoenke, **O. Kraft**, H.-P. Deigner, A. Al-Harrasi, R. Csuk, *Results Chem.* **2022**, *4*, 100371.

„Synthesis and characterization of steroidal, anellatedaminothiophenes by Gewald reaction"
O. Kraft, G. C. Mittag, S. Hoenke, N. Heise, A. Al-Harrasi, R. Csuk, *Mediterr.J.Chem.,* **2022**, *12*, 140.

„First partial synthesis of α-boswellic acid from oleanolic acid"
O. Kraft, I. Serbian, A. Al-Harrasi, R. Csuk, *Phytochem. Lett.* **2022**, *52*, 126–133.

„Small Structural Differences Govern the Carbonic Anhydrase II Inhibition Activity of Cytotoxic Triterpene Acetazolamide Conjugates"
T. C. Denner, N. Heise, J. Zacharias, **O. Kraft**, S. Hoenke, R. Csuk, *Molecules.* **2023**, *28 (3)*:1009

„Asiatic acid as a leading structure for derivatives combining sub-nanomolar cytotoxicity, high selectivity, and the ability to overcome drug resistance in human preclinical tumor models"
O. Kraft, A-K. Hartmann, S. Brandt, S. Hoenke, N. Heise, R. Csuk, T. Müller, *Eur. J. Med. Chem.* **2023**, 15, 115189

11 Posterbeitrag

O. Kraft, A-K. Hartmann, R. Csuk: Madecassic Acid – A New Scaffold for Highly Cytotoxic Agents, EFMC-ISMC, 04.-08.09.2022, Nizza, Frankreich.

12 Erklärung über Autorenanteil

Publikation 1: „Cytotoxic triterpenoid–safirinium conjugates target the endoplasmic reticulum“
Kraft, O.; Kozubek, M.; Hoenke, S.; Serbian, I.; Major, D.; Csuk, R., *Eur. J. Med. Chem.* **2021**, 209, 112920

Die Synthese der Verbindungen sowie die Auswertung der spektroskopischen Daten wurde von M. Kozubek und mir vorgenommen. Die Anfertigung der IR- und UV/Vis-Spektren sowie die Bestimmung des spezifischen Drehwertes wurden von M. Schneider durchgeführt. Die MS-Spektren wurden von T. Schmidt aufgenommen. Die Bestimmung der EC_{50}- Werte wurde von S. Hoenke ausgeführt. R. Csuk betreute die Arbeit in praktischen sowie theoretischen Aspekten.

Publikation 2: „A tormentic acid-homopiperazine-rhodamine B conjugate of single-digit nanomolar cytotoxicity and high selectivity for several human tumor cell lines“
Kraft, O.; Hoenke, S.; Csuk, R., *Eur. J. Med. Chem. Rep.* **2022**, 5, 100043

Die Synthese der Verbindungen sowie die Auswertung der spektroskopischen Daten wurde größtenteils von mir vorgenommen. Die Anfertigung der IR- und UV/Vis-Spektren sowie die Bestimmung des spezifischen Drehwertes wurden von M. Schneider durchgeführt. Die MS-Spektren wurden von T. Schmidt aufgenommen. Die Bestimmung der EC_{50}- Werte wurde von S. Hoenke ausgeführt. R. Csuk betreute die Arbeit in praktischen sowie theoretischen Aspekten.

Publikation 3: „Madecassic Acid—A New Scaffold for Highly Cytotoxic Agents“
Kraft, O.; Hartmann, A-K.; Hoenke, S.; Serbian, I.; Csuk, R., *Int. J. Mol. Sci.* **2022**, 23(8), 4362

Die Synthese der Verbindungen sowie die Auswertung der spektroskopischen Daten wurde größtenteils von A-K. Hartmann und mir vorgenommen. Die Anfertigung der IR- und UV/Vis-Spektren sowie die Bestimmung des spezifischen Drehwertes wurden von M. Schneider durchgeführt. Die MS-Spektren wurden von T. Schmidt aufgenommen. Die Bestimmung der EC_{50}- Werte wurde von S. Hoenke ausgeführt. R. Csuk betreute die Arbeit in praktischen sowie theoretischen Aspekten.

Publikation 4: **“**Asiatic acid as a leading structure for derivatives combining sub-nanomolar cytotoxicity, high selectivity, and the ability to overcome drug resistance in human preclinical tumor models”
Kraft, O.; Hartmann, A-K.; Brandt, S.; Hoenke, S.; Heise, N.; Csuk, R.; Müller, T., *Eur. J. Med. Chem.* **2023**, 15, 115189

Die Synthese der Verbindungen sowie die Auswertung der spektroskopischen Daten wurde größtenteils von mir vorgenommen. Die Anfertigung der IR- und UV/Vis-Spektren sowie die Bestimmung des spezifischen Drehwertes wurden von M. Schneider durchgeführt. Die MS-Spektren wurden von T. Schmidt aufgenommen. Die Bestimmung der EC_{50}- Werte wurde von S. Hoenke ausgeführt. Weiterführende Untersuchung wurden von S. Brandt und T. Müller geleistet. R. Csuk betreute die Arbeit in praktischen sowie theoretischen Aspekten.

13 Selbstständigkeitserklärung

Hiermit erkläre ich, dass ich die vorliegende Arbeit selbstständig und nur unter Zuhilfenahme der angegebenen Quellen und Hilfsmittel verfasst habe. Die aus den benutzten Werken wörtlich oder inhaltlich entnommenen Stellen wurden als solche kenntlich gemacht. Diese Arbeit wurde bisher an keiner anderen Universität oder Hochschule vorgelegt.

Halle (Saale), 02.06.2024

14 Publikationen

P1

European Journal of Medicinal Chemistry 209 (2021) 112920

Contents lists available at ScienceDirect

European Journal of Medicinal Chemistry

journal homepage: http://www.elsevier.com/locate/ejmech

Cytotoxic triterpenoid–safirinium conjugates target the endoplasmic reticulum

Oliver Kraft [1], Marie Kozubek [1], Sophie Hoenke, Immo Serbian, Daniel Major, René Csuk*

Martin–Luther–University Halle–Wittenberg, Organic Chemistry, Kurt–Mothes–Str. 2, D–06120, Halle, Saale, Germany

A R T I C L E I N F O

Article history:
Received 9 August 2020
Received in revised form
4 October 2020
Accepted 4 October 2020
Available online 8 October 2020

Keywords:
Betulinic acid
Safirinium
Cytotoxicity
Endoplasmic reticulum

A B S T R A C T

Safirinium P and Q fluorescence labels were synthesized and conjugated with spacered triterpenoic acids to access hybrid structures. While the parent safirinium compounds were not cytotoxic at all, many triterpenoid safirinium P and Q conjugates showed moderate cytotoxicity. An exception, however, was safirinium P derived compound **30** holding low $EC_{50} = 5.4$ μM (for A375 cells) to $EC_{50} = 7.5$ μM (for FaDu cells) as well as $EC_{50} = 6.6$ μM for non-malignant fibroblasts NIH 3T3. Fluorescence imaging showed that the safirinium core structures cannot enter the cells (not even after a prolonged incubation time of 24 h), while the conjugates (as exemplified for **30**) are accumulating in the endoplasmic reticulum but not in the mitochondria. The development of safirinium–hybrids targeting the endoplasmic reticulum can be regarded as a promising strategy in the development of cytotoxic agents.

© 2020 Elsevier Masson SAS. All rights reserved.

1. Introduction

Cancer is still the second most leading cause of death. Especially some types of cancer come with more aggressive phenotypes than others like prostate and breast cancer. Furthermore hypoxic tumors lead to an acidification of the tumor microenvironment, which further increases resistance, invasion and proliferation of the tumor [1]. Recently, mitochondrial targeted anti–cancer drugs („mitocans“) have gotten more and more attention as these compounds trigger cell death signals from the mitochondria, where tumor cells – even tumor cells not responding to death signals due to DNA damage – trigger apoptosis [2–9]. This has already been shown for analogs of vitamin E [2–9] as well as for triterpenoids [10–13] and steroids [14]. For the latter compounds this was mainly achieved by attaching lipophilic cations (such as rhodamine B [10–13], a BODIPY–moiety [15], a triphenylphosphonium residue [16–18], an ammonium salt [19,20]or derivatives of malachite green [15]) to the triterpenoid or steroidal skeleton [5,21].

However, the presence of a cation is not sufficient to achieve good cytotoxicity in tumor cells. For example, distal *N*–oxides and quaternary ammonium salts of triterpenoids [19,20] are significantly less cytotoxic than, e.g. benzylamides [19–23]. Depending on the spacer used, rhodamine B–triterpene derivatives are obviously only cytotoxic if an "open" (fluorescent) form is present. If rhodamine B, on the other hand, is present in a closed/non–fluorescent lactone or lactam form, the corresponding conjugates are practically non–cytotoxic [11]. Conjugates holding the rhodamine B residue directly attached to the basic skeleton of the triterpene (e.g. as an ester) are cytotoxic but usually not very selective [12,13].

We are particularly interested in the development of cytotoxic triterpene–conjugates carrying a permanent positively charged moiety; these compounds should also enable to act as fluorescence molecular probe [24,25]. This latter property is also associated with the ability to observe the uptake and intracellular distribution of the molecules in a more directly way. Thus, valuable information on molecular mechanisms can be gained quite easily.

Some time ago, Saczewski et al. succeeded in synthesizing so–called „safirinium–hybrids“ by tandem Mannich–electrophilic amination reactions starting from pro–fluorogenic isoxazolinones and secondary amines, such as quinolones or short peptides. The former hybrids showed higher lipophilicity and the latter were able to stain spores of *Bacillus subtilis* [24–31].

The latter observation, that safirinium hybrids are able to be well transported into cells, led us to investigate the cytotoxic potential of safirinium–triterpene hybrids. Hybridization is often associated with the ability to counterbalance the known problem (efficacy, affinity, solubility, unwanted side effects, ...) with the other hybrid part. Lack of solubility in biological systems is a

---

* Corresponding author.
E-mail address: rene.csuk@chemie.uni-halle.de (R. Csuk).
[1] These authors contributed equally.

https://doi.org/10.1016/j.ejmech.2020.112920
0223-5234/© 2020 Elsevier Masson SAS. All rights reserved.

notorious problem often associated with triterpenes. This problem, however, might be solved by binding to a cationic residue, such as a safirinium moiety. Hence, we became interested to deduce whether triterpene–safirinium hybrids would also be as efficient as rhodamine B conjugates in triggering cell death.

Betulinic acid (**BA**, Fig. 1), for example, is a triterpene, that holds promising in vitro and in vivo antitumor activity in melanoma, neuro–ectodermal tumors and glioma cell lines [32–35]. It targets the mitochondrial permeability transition pore [36]. It also down-regulates Bcl–2, which promotes apoptosis as well as VEGFR and NF–kB, which are both closely related to angiogenesis and the proliferation of tumors [37].

Based on this strategy, we set out to synthesize different triterpenoid–safirinium conjugates, and to examine their cytotoxicity and selectivity for different human tumor cell lines.

2. Results and discussion

2.1. Synthesis

The synthesis of the safirinium P derivatives (Scheme 1) was straightforward and followed the synthetic scheme previously outlined by Saczewski et al. [30,31] Compound **1** was obtained in an almost quantitative yield from the reaction of ethyl cyanoacetate with hydroxylamine following the procedure reported by Lee [38]. Compound **2** is a precursor for the safirinium P fluorophores and was obtained in 73% yield from the reaction of **1** with acetylacetone in the presence of piperidine followed by a precipitation of the product with hydrochloric acid. A major advantage of these reactions is that no time–consuming purifications are necessary at all.

The synthesis of the safirinium P derivatives (Scheme 1) proceeded also nicely as reported, and compounds **3**–**13** were obtained after precipitation from acetone in yields ranging between 43% and 91%, except for compound **7** (57%).

The synthesis of the safirinium Q derivatives (Scheme 2) followed the previously reported strategy.

As far as the synthesis of acetylated triterpenoic acid holding an ethylenediamine or a piperazinyl spacer is concerned, the corresponding triterpenoic acid (**BA**, **OA**, **UA**, **PA**; Fig. 1) was acetylated yielding compounds **17**–**20** (Scheme 3); these were activated with oxalyl chloride followed by the addition of the amine. Thus, compounds **21**–**28** were obtained in good yields. These spacers were chosen in analogy to our previous studies on spacered triterpenoid hybrids [10–14].

The safirinium P fluorophores were activated with oxalyl chloride followed by their reaction with piperazinyl–spacered 3–*O*–acetyl–betulinic acid (**21**) to yield derivatives **29**–**31** (Scheme 4).

Albeit all of these reactions proceeded well (as observed by TLC), the isolated yields of pure products were low. These compounds tend to "stick" to the silica gel used for chromatographic purification. Even elution with MeOH was incomplete. While upon addition of AcOH to the eluent reasonably high recovery rates were obtained, this procedure inevitably led to the formation of impurities in the product. Hence, yield was sacrificed for purity, and most of the compounds were eluted from the column with MeOH.

The synthesis of the safirinium Q derivatives proceeded in an analogous manner (Scheme 5) and yielded compounds **32**–**39**, respectively.

As exemplified for the safirinium–betulinic acid hybrids, their UV/Vis spectra are characterized by maxima at $\lambda_{\mu ax} = 253–254$ nm (with $\log \varepsilon = 3.92–4.07$) and $\lambda_{max} = 352–354$ nm (with $\log \varepsilon = 3.62–3.82$). These values are in perfect agreement with previously published data for analogs.

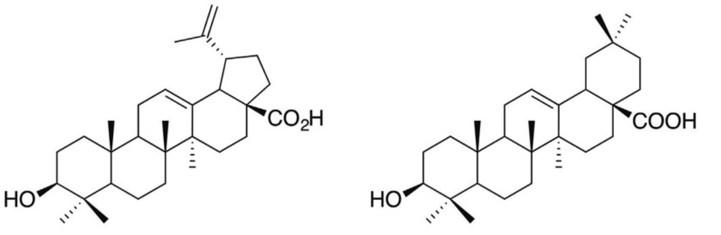

BA, Betulinic acid (BA)   **OA**, Oleanolic acid

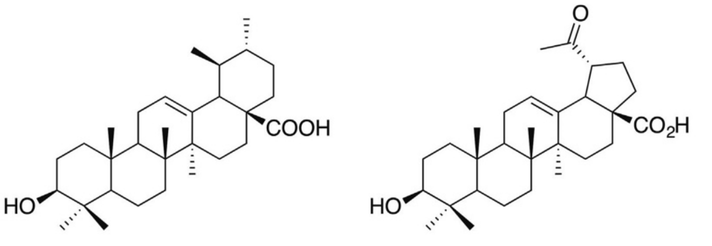

UA, Ursolic acid   **PA**, Platanic acid

Fig. 1. Structure of triterpenoic acids: **BA** (betulinic acid), **OA** (oleanolic acid), **UA** (ursolic acid), and **PA** (platanic acid).

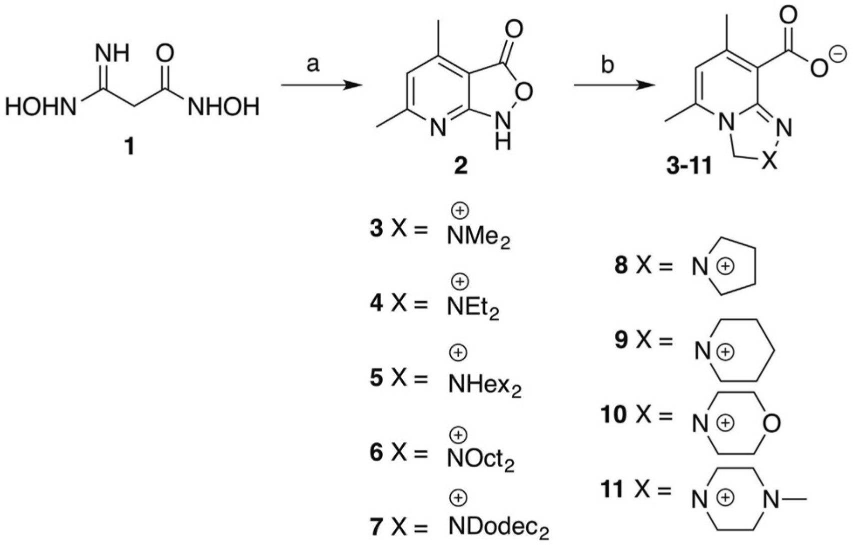

Scheme 1. Synthesis of safirinium P derivatives **3**–**11**: a) 1. acetylacetone, piperidine, H_2O, 100 °C, 15 min; 2. 4M HCl, 73%; b) formaldehyde, corresponding amine, MeOH, 4 h, 45 °C, 2 h.

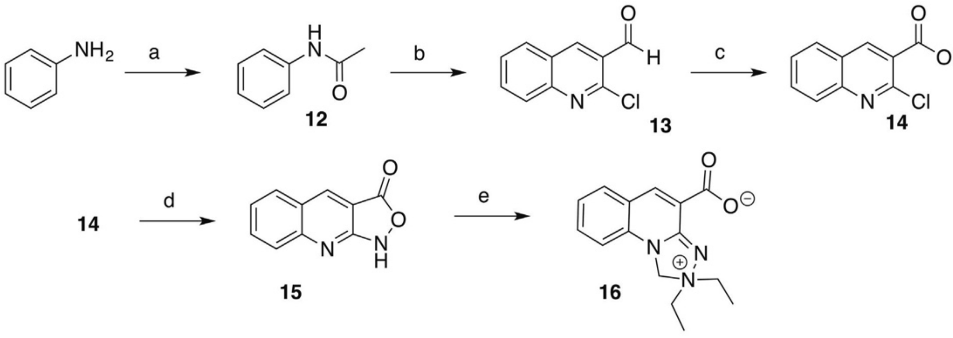

Scheme 2. Synthesis of the safirinium Q derivative **16**: a) Ac_2O, acetic acid, reflux, 1 h, 78%; b) 1. DMF, phosphoryl chloride, inert atmosphere, 0 °C → 25 °C, 4 h 2. **17**, 25 °C → reflux. 24 h, 70%; c) *n*−butanol, NaH_2PO_4, $NaClO_2$, H_2O, r.t, 2 h, 87%; d) 1. HOSA, dry DMF, 25 °C, 12 h, 2. TEA, H_2O, 25 °C, 12 h, 81%; e) diethylamine, formaldehyde (aqu., 37%), MeOH, 25 °C, 92%.

2.2. Biological evaluation

The compounds were subjected to sulforhodamine B assays to determine their cytotoxicity employing several human tumor cell lines and non−malignant fibroblasts (NIH 3T3). The results from these assays are summarized in Table 1.

The results from these assays showed safirinium P derivatives **3**–**11** as not cytotoxic up to a concentration of 30 μM, thus paralleling both previous findings as well as the also insignificant cytotoxicity of rhodamine B (Rho). Extra fluorescence imaging experiments revealed that these compounds are not taken up by the cells; this explains their non−cytotoxicity. Upon derivatization with triterpenoids, however, a slight increase in cytotoxicity was observed. Especially, betulinic acid derived **30** showed good cytotoxicity ranging between $EC_{50} = 4.6$ μM (for A2780 ovarian carcinoma cells) to $EC_{50} = 7.5$ μM (for HT29 colorectal adenocarcinoma cells). An unselective cytotoxicity, however, was also observed for this compound inasmuch as for non−malignant fibroblasts (NIH 3T3) an $EC_{50} = 6.6$ μM was noted. Most of the other safirinium hybrids were only of moderate cytotoxicity and selectivity was – by and large – missing at all. Quite on the contrary, compounds **35** and **38** were even more cytotoxic for the fibroblasts than for the tumor cells incorporated in this study. For comparison, human non−malignant HEK293 were incubated with representative compounds **30**–**32** and **36** showing these compounds also to be cytotoxic for these cells.

These results were somewhat surprising inasmuch as we expected the safirinium conjugates to act likewise the rhodamine B mitocans of previous studies. Therefore, a closer investigation of **30** was called for. Fluorescence imaging experiments showed **30** not to enter the mitochondria (within the limits of detection) but to accumulate in the endoplasmic reticulum (ER). Control

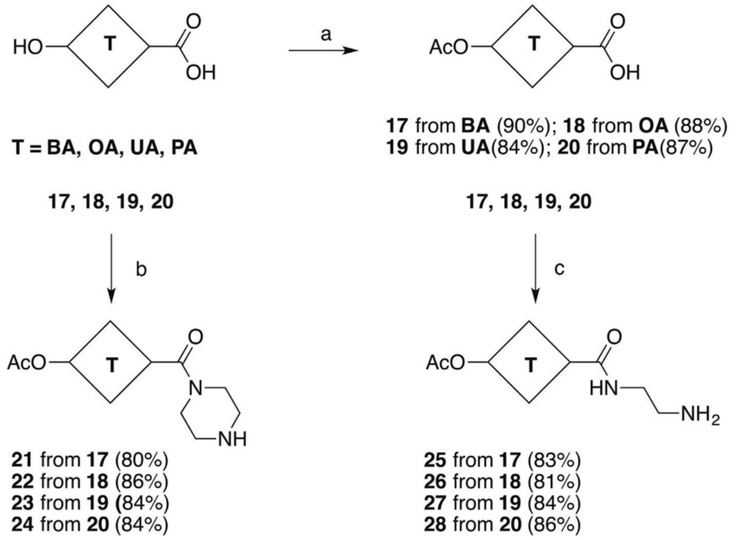
HO
T
O
OH
T = BA, OA, UA, PA
a
AcO
17 from BA (90%); 18 from OA (88%)
19 from UA(84%); 20 from PA(87%)
17, 18, 19, 20
b
17, 18, 19, 20
c
N
NH
21 from 17 (80%)
22 from 18 (86%)
23 from 19 (84%)
24 from 20 (84%)
HN
NH2
25 from 17 (83%)
26 from 18 (81%)
27 from 19 (84%)
28 from 20 (86%)

Scheme 3. Synthesis of compounds **17**–**28**: a) Ac_2O, pyridine, DMAP (cat.), 12 h, yields: **17** (90%), **18** (88%), **19** (84%), **20** (87%) b) 1. $(COCl)_2$, DCM, DMF, 0 °C → 25 °C, 4 h 2. piperazine, DCM, 0 °C → r.t. 2 h, yields: **21** (80%), **22** (86%), **23** (84%), **24** (84%); c) $(COCl)_2$, DCM, DMF, 0 °C → 25 °C, 4 h 2. ethylenediamine, DCM, 0 °C → 25 °C, 2 h, yields: **25** (83%), **26** (81%), **27** (84%), **28** (86%).

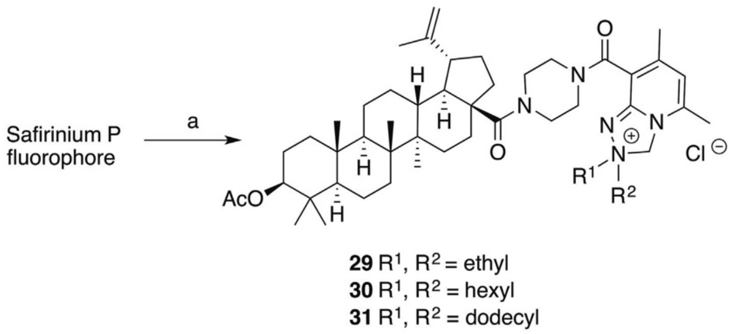
Safirinium P
fluorophore
a
H
H
H
H
AcO
O
O
N
N
N
N
N
R1
R2
Cl
29 R1, R2 = ethyl
30 R1, R2 = hexyl
31 R1, R2 = dodecyl

Scheme 4. Synthesis of betulinic acid derived safirinium hybrids **29**–**31**: a) 1. $(COCl)_2$, DCM, DMF 0 °C → 25 °C, 2 h, 2. **21**, NEt_3, 0 °C → 25 °C, yields. **29** (57%), **30** (39%), **31** (40%).

experiments were performed employing an established ER–Tracker (for the accumulation of **30** in the ER), and a Mito-Tracker (to exclude an accumulation in the mitochondria). Representative images are depicted in Fig. 2.

3. Conclusion

The syntheses of the safirinium fluorescence labels was straightforward following known procedures to allow an access to the safirinium P derivatives **3**–**11** and safirinium Q derivative **16** in good to excellent yields. The conjugation reaction with spacered triterpenoic acid derivatives **21**–**28** proceeded well applying standard coupling procedures; main obstacle of this reaction was the purification of the hybrid compounds due to their high affinity to silica gel during chromatographic purification. The safirinium compounds were not cytotoxic at all while many triterpenoid safirinium P and Q conjugates showed only moderate cytotoxicity. An exception was safirinium P derived compound **30** holding low $EC_{50} = 5.4$ μM (for A375 cells) to $EC_{50} = 7.5$ μM (for FaDu cells). However, safirinium Q hybrids **36** and **39** were even more cytotoxic for non–malignant NIH 3T3 fibroblasts than for the human tumor cell lines included in this study; the same cytotoxicity was also observed for representative compounds **30**–**32** and **36** and HEK293 cells. Fluorescence imaging showed that the safirinium core structures **3**–**11** and **16** cannot enter the cells (not even after a prolonged incubation time of 24 h), while the conjugates (as exemplified for **30**) are accumulating in the endoplasmic reticulum but not in the mitochondria. This finding might explain their diminished cytotoxic activity for human tumor cell lines as compared to rhodamine B analogs that enter the mitochondria.

While many cytostatics trigger an induced cell death via the activation of mitochondrial apoptosis, an increasing number of studies already indicated a pivotal role of drugs targeting the endoplasmic reticulum. Further development of the safirinium–triterpene hybrids can be seen as an encouraging strategy in the development of cytotoxic agents.

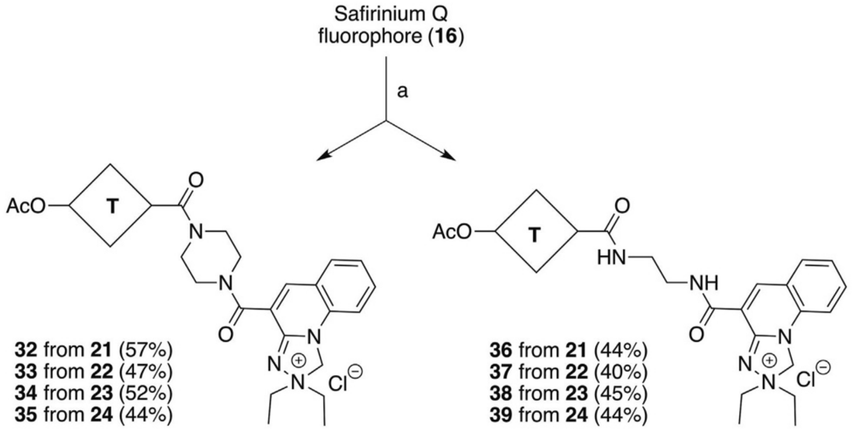

Scheme 5. a) 1. $(COCl)_2$, DCM, DMF, 0 °C → 25 °C, 2 h, 2. NEt_3, 0 °C → 25 °C, yields: **32** (57%), **33** (47%), **34** (52%), **35** (44%), **36** (44%), **37** (40%), **38** (45%), **39** (44%).

Table 1
Cytotoxicity of compounds **3–11** and rhodamine B (**Rho**) (EC50 values in μM from SRB assays after 72 h of treatment, the values are averaged from three independent experiments performed each in triplicate, confidence interval CI = 95%; mean ± standard mean error). Human cancer cell lines: A375 (epithelial melanoma), HT29 (colorectal adenocarcinoma), MCF–7 (breast adenocarcinoma), A2780 (ovarian carcinoma), FaDu (squamous cell carcinoma), non–malignant: NIH 3T3 (mouse fibroblasts), HEK293 (human embryonic kidney cells); n.d. not determined; doxorubicin (**DX**) and staurosporine (**ST**) were used as positive controls.

	A375	HT29	MCF–7	A2780	FaDu	NIH3T3	HEK293
Rho	>30	>30	>30	>30	>30	>30	>30
3–11	>30	>30	>30	>30	>30	>30	n.d.
29	26.2 ± 1.3	>30	26.3 ± 2.1	21.6 ± 2.4	>30	22.4 ± 2.2	n.d.
30	5.4 ± 0.1	7.5 ± 0.3	4.9 ± 0.3	4.6 ± 0.3	6.0 ± 0.3	6.6 ± 0.3	3.0 ± 0.3
31	16.8 ± 1.0	24.9 ± 1.7	15.7 ± 1.2	11.0 ± 1.2	10.7 ± 1.0	>30	13.3 ± 0.7
32	20.8 ± 1.7	27.0 ± 2.0	18.1 ± 1.0	14.1 ± 2.0	28.2 ± 2.3	>30	16.5 ± 0.8
33	21.4 ± 0.7	26.2 ± 0.7	19.8 ± 1.2	21.4 ± 1.9	18.1 ± 1.8	18.4 ± 2.0	n.d.
34	21.4 ± 1.4	>30	10.2 ± 1.1	9.0 ± 1.2	18.3 ± 1.1	>30	n.d.
35	15.0 ± 1.2	22.2 ± 0.9	13.2 ± 0.7	10.9 ± 1.8	13.3 ± 0.9	3.0 ± 0.6	n.d.
36	18.6 ± 2.1	26.8 ± 0.6	17.6 ± 1.5	18.3 ± 2.8	12.3 ± 1.3	17.4 ± 1.7	13.6 ± 1.0
37	19.0 ± 2.0	25.0 ± 1.0	21.8 ± 1.7	24.2 ± 2.6	27.1 ± 2.0	28.5 ± 1.1	n.d.
38	13.8 ± 0.8	22.1 ± 0.8	11.7 ± 0.7	11.2 ± 1.4	10.2 ± 0.1	3.6 ± 1.0	n.d.
39	16.6 ± 2.1	>30	15.7 ± 1.4	20.8 ± 1.9	16.1 ± 1.3	21.3 ± 1.3	n.d.
DX	n.d.	0.9 ± 0.01	1.1 ± 0.3	0.01 ± 0.01	n.d.	0.4 ± 0.07	n.d.
ST	n.d.	0.2 ± 0.02	0.1 ± 0.01	0.1 ± 0.01	0.1 ± 0.05	0.008 ± 0.001	n.d.

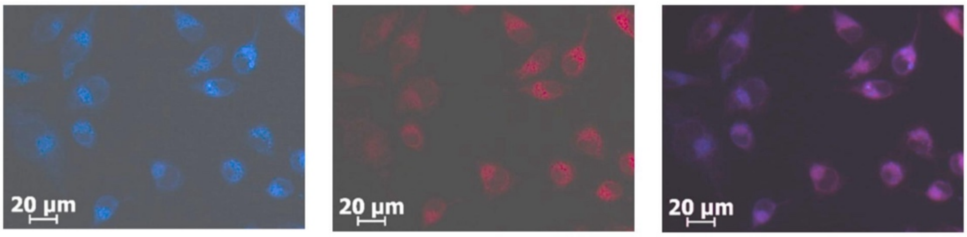

Fig. 2. Fluorescence imaging of living A375 epithelial carcinoma cells incubated with: compound **30** (left, 12 h, 5.4 μM), ER–Tracker (center) and merged pictures (right).

4. Experimental

4.1. General

Equipment and general methods have been used as previously described [10–15]. All reactions were performed under an argon; solvents were dried according to usual procedures. The triterpenoic acid were obtained from “Betulinines” (Stříbrná Skalice, Czech Republic) and used as received. The ^1H and ^{13}C NMR of all new compounds have been depicted in the Supplementary Materials file as well as a description of the SRB assay and the staining experiments.

4.2. Syntheses

*4.2.1. 3–Amino–N–hydroxy–3–(hydroxyimino)propanamide (**1**)*

Following the procedure as described by Lee [38], a mixture of ethyl cyanoacetate (10.0 g, 88.4 mmol) and hydroxylamine (50% in water, 12.9 g, 194 mmol, 2.2 eq) in EtOH (10 ml) was stirred at room temperature for 30 min. External cooling was necessary to keep the temperature constant. Upon cooling to 10 °C, crystals formed and were collected by filtration, washed with ice cold ethanol and dried in high vacuum to afford **1** as a colorless solid being used without further purification.

*4.2.2. 4,6–Dimethylisoxazolo[3,4–b]pyridin–3(1H)–one (**2**)*

A solution of **1** (20.0 g, 0.15 mol), acetylacetone (15.5 mL, 0.15 mol) and piperidine (14.8 mL, 0.15 mol) in water (250 mL) was heated under reflux for 30 min [15]. After cooling to room temperature, the reaction mixture was acidified with 2M HCl, and the resultant yellow precipitate was filtered off and washed with water (2 × 50 mL); yield 17.97 g (73%); m.p. 203 °C (lit [31].: m.p. 204–207 °C);

*4.2.3. General procedure (GPA) for the preparation of safirinium P derivatives **3–11***

A solution of **2** (2.0 g, 12.2 mmol), the corresponding amine (13.4 mmol) and 37% aqueous formaldehyde (1.0 mL, 13.4 mmol) in MeOH (40 mL) was heated at 40 °C for 3 h. The resulting reaction mixture was concentrated under reduced pressure, and the solid residue was precipitated from acetone.

*4.2.4. 2,2,5,7–Tetramethyl–2,3–dihydro–1h–imidazol[1,2–a]pyridin–4–ium–8–carboxylate (**3**)*

Following GPA; yield: 89%; m.p. 227–230 °C (lit [29].: 228–230 °C); IR (ATR): ν = 3031w, 2964w, 2882w, 1635s, 1594vs, 1549vs, 1519vs, 1499m, 1459m, 1401w, 1382s, 1371m, 1344s, 1288w, 1241w, 1228w, 1213w, 1181m, 1119w, 1068w, 1047w, 1034w, 798s, 706m, 611s, 604 s cm^{-1}; ^{1}H NMR (500 MHz, CD$_3$OD): δ = 6.02 (d, *J* = 1.2 Hz, 1H, 6–H), 5.76 (s, 2H, 3–H), 3.43 (s, 6H, 13–H + 13′–H), 2.30 (d, *J* = 1.0 Hz, 3H, 11–H), 2.21 (s, 3H, 10–H) ppm; ^{13}C NMR (125 MHz, CD$_3$OD): δ = 170.0 (C-12), 155.5 (C-5), 146.7 (C-7), 139.5 (C-9), 118.0 (C-8), 110.4 (C-6), 77.3 (C-3), 55.6 (C-13 + C-13‘), 18.5 (C-10), 16.9 (C-11) ppm; MS (ESI, MeOH): *m*/*z* (%) = 222.1 ([M+H]$^+$, 100%), 244.1 ([M+Na]$^+$, 18%); analysis calcd for $C_{11}H_{15}N_3O_2$ (221.26): C 59.21, H 6.83, N 18.99; found: C 58.97, H 7.01, N 18.77.

*4.2.5. 2,2–Diethyl–5,7–dimethyl–2,3–1h–imidazol[1,2–a]pyridin–4–ium–8–carboxylate (**4**)*

Following GPA; yield: 91%; m.p. 189–191 °C (lit [30].: 200–203 °C); IR (ATR): ν = 3367w, 3201w, 2973w, 1632s, 1586vs, 1555vs, 1528s, 1456m, 1438m, 1431m, 1407m, 1398m, 1383s, 1373s, 1353s, 1305m, 1247w, 1225m, 1193m, 1185m, 1166m, 1144w, 1121w, 1113w, 1073w, 1043w, 1031m, 802s, 784m, 752m, 687s, 669m, 618vs, 606vs, 577s, 561s, 530m, 510 s cm^{-1}; ^{1}H NMR (400 MHz, CD$_3$OD): δ = 5.99 (d, *J* = 1.1 Hz, 1H, 6–H), 5.70 (s, 2H, 3–H), 3.62 (qq, *J* = 12.8, 7.1 Hz, 4H, 13–H + 13‘–H), 2.31 (d, *J* = 1.0 Hz, 3H, 11–H), 2.20 (s, 3H, 10–H), 1.38 (t, *J* = 7.1 Hz, 6H, 14–H + 14‘–H) ppm; ^{13}C NMR (101 MHz, CD$_3$OD): δ = 170.2 (C-12), 155.9 (C-5), 146.2 (C-7), 139.1 (C-9), 118.2 (C-8), 110.1 (C-6), 71.9 (C-3), 61.2 (C-13 + C-13‘), 18.4 (C-10), 16.8 (C-11), 7.0 (C-14 + C-14‘) ppm; MS (ESI, MeOH): *m*/*z* (%) = 250.1 ([M+H]$^+$, 100%), 272.0 ([M+Na]$^+$, 4%); analysis calcd for $C_{13}H_{19}N_3O_2$ (249.31): C 62.63, H 7.68, N 16.85; found: C 62.47, H 7.90, N 16.52.

*4.2.6. 2,2–Dihexyl–5,7–dimethyl–2,3–dihydro–1h–imidazol[1,2–a]pyridin–4–ium–8–carboxylate (**5**)*

Following GPA; yield: 82%; m.p. 134–135 °C; IR (ATR): ν = 3376w, 3004w, 2947m, 2927m, 2867w, 1667m, 1635s, 1587vs, 1560s, 1531s, 1485w, 1468m, 1439w, 1433w, 1398m, 1373m, 1356m, 1302w, 1225w, 1211w, 1187m, 1143m, 1055w, 1042w, 1032w, 802m, 729m, 616m, 605 s cm^{-1}; ^{1}H NMR (500 MHz, CD$_3$OD): δ = 5.99 (d, *J* = 1.3 Hz, 1H, 6–H), 5.71 (s, 2H, 3–H), 3.53 (dddd, *J* = 31.0, 12.6, 10.7, 5.9 Hz, 4H, 13–H + 13–H’), 2.30 (d, *J* = 1.0 Hz, 3H, 11–H), 2.20 (s, 3H, 10–H), 1.86–1.75 (m, 4H, 14–H + 14‘–H), 1.41–1.30 (m, 12H, 15–17–H + 15‘–17‘–H), 0.91 (t, *J* = 6.9 Hz, 6H, 18–H + 18‘–H) ppm; ^{13}C NMR (125 MHz, CD$_3$OD): δ = 170.1 (C-12), 155.7 (C-5), 146.3 (C-7), 139.1 (C-9), 118.1 (C-8), 110.1 (C-6), 72.9 (C-3), 66.3 (C-13 + C-13‘), 31.1 (C-16 + C-16‘), 25.6 (C-15 + C-15‘), 22.2 (C-17 + C-17‘), 22.1 (C-14 + C-14‘), 18.4 (C-10), 16.8 (C-11), 12.9 (C-18 + C-18‘) ppm; MS (ESI, MeOH): *m*/*z* (%) = 362.3 ([M+H]$^+$, 100%), 384.2 ([M+Na]$^+$, 8%); analysis calcd for $C_{21}H_{35}N_3O_2$ (361.53): C 69.77, H 9.76, N 11.62; found: C 69.50, H 9.96, N 11.57.

*4.2.7. 5,7–Dimethyl–2,2–dioctyl–2,3–dihydro–1h–imidazol[1,2–a]pyridin–4–ium–8–carboxylate (**6**)*

Following GPA; yield: 83%; m.p. 131 °C; IR (ATR): ν = 3386w, 3002w, 2952m, 2926m, 2854m, 1664m, 1635s, 1587vs, 1560s, 1530s, 1484m, 1468m, 1432w, 1398m, 1375m, 1354m, 1306w, 1218w, 1184m, 1043w, 1032w, 802m, 725m, 614m, 605 m cm^{-1}; ^{1}H NMR (500 MHz, CD$_3$OD): δ = 5.99 (d, *J* = 1.1 Hz, 1H, 6–H), 5.70 (s, 2H, 3–H), 3.61–3.43 (m, 4H, 13–H + 13‘–H), 2.30 (d, *J* = 1.0 Hz, 3H, 11–H), 2.20 (s, 3H, 10–H), 1.84–1.76 (m, 4H, 14–H + 14‘–H), 1.40–1.25 (m, 21H, 15–H + 15‘–H + 16–H + 16‘–H + 17–H + 17‘–H + 18–H + 18‘–H + 19–H + 19‘–H), 0.93–0.87 (m, 6H, 20–H + 20‘–H) ppm; ^{13}C NMR (125 MHz, CD$_3$OD) δ = 170.1 (C-12), 155.7 (C-5), 146.3 (–7), 139.1 (C-9), 118.1 (C-8), 110.1 (C-6), 72.9 (C-3), 66.3 (C-13 + C-13‘), 31.5 (C-16 + C-16‘), 28.9 (C-18 + C-18‘ + C-15 + C-15‘), 26.0 (C-17 + C-17‘), 22.2 (C-19 + C-19‘ + C-14 + C-14‘), 18.4 (C-10), 16.8 (C-11), 13.0 (C-20 + C-20‘) ppm; MS (ESI, MeOH): *m*/*z* (%) = 418.4 ([M+H]$^+$, 100%), 440.2 ([M+Na]$^+$, 6%); analysis calcd for $C_{25}H_{43}N_3O_2$ (417.64): C 71.90, H 10.38, N 10.06; found: C 71.64, H 10.60, N 9.84.

*4.2.8. 2,2–Didodecyl–5,7–dimethyl–2,3–dihydro–1h–imidazol[1,2–a]pyridin–4–ium–8–carboxylate (**7**)*

Following GPA but precipitation from diethyl ether; yield: 57%; m.p. 142–145 °C; IR (ATR): ν = 3362w, 2956m, 2917vs, 2874w, 2849s, 1635s, 1583vs, 1485w, 1466m, 1446m, 1435w, 1403m, 1375s, 1347m, 1235w, 1192m, 809m, 720m, 631m, 601 s cm^{-1}; ^{1}H NMR (400 MHz, CD$_3$OD): δ = 5.98 (d, *J* = 1.2 Hz, 1H, 6–H), 5.70 (s, 2H, 3–H), 3.63–3.42 (m, 4H, 13–H + 13‘–H), 2.29 (d, *J* = 1.0 Hz, 3H, 11–H), 2.20 (s, 3H, 10–H), 1.85–1.74 (m, 4H, 14–H + 14‘–H), 1.40–1.25 (m, 36H, 15–23–H + 15‘–23‘–H), 0.88 (t, J = 7.0z Hz, 6H, 24–H + 24‘–H) ppm; ^{13}C NMR (101 MHz, CD$_3$OD): δ = 170.1 (C-12), 155.6 (C-5), 146.3 (C-7), 139.1 (C-9), 118.1 (C-8), 110.1 (C-6), 73.0 (C-3), 66.2 (C-13 + C-13‘), 31.7 (C-22 + C-22‘), 29.4–28.9 (C-16–C–21 + C-16‘– C-21‘), 26.0 (C-15 + C-15‘), 22.3 (C-23 + C-23‘), 22.2 (C-14 + C-14‘), 18.4 (C-10), 16.9 (C-11), 13.0 (C-24 + C-24‘) ppm; MS (ESI, MeOH): *m*/*z* (%) = 530.4 ([M+H]$^+$, 100%), 552.3 ([M+Na]$^+$, 2%); analysis calcd for $C_{33}H_{59}N_3O_2$ (529.85): C 74.81, H 11.22, N 7.93; found: C 74.73, H 11.02, N 7.68.

*4.2.9. 5’,7’–Dimethyl–3’H–spiro[pyrrolidine–1,2’–[1,2,4]triazolo[4,3–a]pyridin]–1–ium–8′–carboxylate (**8**)*

Following GPA; yield: 76%; m.p. 141–144 °C; IR (ATR): ν = 3386w, 3024w, 2963w, 1634m, 1591vs, 1558s, 1520m, 1478w, 1457w, 1434m, 1376s, 1345m, 1228w, 1188w, 1051w, 798m, 779m, 605m, 595 m cm^{-1}; ^{1}H NMR (500 MHz, CD$_3$OD): δ = 5.99 (d, *J* = 1.2 Hz, 1H, 6–H), 5.83 (s, 2H, 3–H), 3.88–3.75 (m, 4H, 13–H + 13‘–H), 2.40–2.32 (m, 2H, 14–H), 2.30 (d, *J* = 1.0 Hz, 3H, 11–H), 2.24–2.20 (m, 2H, 14‘–H), 2.20 (s, 3H, 10–H) ppm; ^{13}C NMR (125 MHz, CD$_3$OD): δ = 170.2 (C-12), 155.5 (C-5), 146.3 (C-7), 139.4

(C-9), 118.0 (C-8), 110.1 (C-6), 74.6 (C-3), 68.2 (C-13 + C-13’), 21.4 (C-14 + C-14‘), 18.4 (C-10), 16.9 (C-11) ppm; MS (ESI, MeOH): *m*/*z* (%) = 248.2 ($[M+H]^+$, 100%), 270.1 ($[M+Na]^+$, 4%); analysis calcd for $C_{13}H_{17}N_3O_2$ (247.30): C 63.14, H 6.93, N 16.99; found: C 62.85, H 7.14, N 16.73.

*4.2.10. 5’,7’–Dimethyl–3’H–spiro[piperidine–1,2’–[1,2,4]triazolo[4,3–a]pyridin]–1–ium–8′–carboxylate (**9**)*

Following GPA; yield: 82%; m.p. 167–171 °C; IR (ATR): ν = 3383m, 3003w, 2957w, 2858w, 1634s, 1580s, 1564vs, 1558vs, 1525s, 1482w, 1450m, 1436m, 1381m, 1372s, 1350m, 1305w, 1277w, 1266w, 1232w, 1193m, 1170w, 1029w, 805m, 697m, 667m, 622m, 595s, 478 m cm^{-1}; ^{1}H NMR (500 MHz, CD_3OD): δ = 5.98 (d, J = 1.2 Hz, 1H, 6–H), 5.71 (s, 2H, 3–H), 3.63 (dddd, J = 35.4, 12.2, 7.8, 3.7 Hz, 4H, 13–H + 13‘–H), 2.30 (d, J = 1.0 Hz, 3H, 11–H), 2.20 (s, 3H, 10–H), 2.19–2.14 (m, 2H, H-14), 1.91–1.83 (m, 2H, H-14‘), 1.73–1.67 (m, 2H, H-15) ppm; ^{13}C NMR (125 MHz, CD_3OD): δ = 170.2 (C-12), 155.3 (C-5), 146.3 (C-7), 139.5 (C-9), 118.3 (C-8), 110.1 (C-6), 75.0 (C-3), 65.2 (C-13), 20.8 (C-14), 20.4 (C-15), 18.4 (C-10), 16.8 (C-11) ppm; MS (ESI, MeOH): *m*/*z* (%) = 262.2 ($[M+H]^+$, 100%), 284.1 ($[M+Na]^+$, 4%); analysis calcd for $C_{14}H_{19}N_3O_2$ (261.33): C 64.35, H 7.33, N 16.08; found: C 64.17, H 7.51, N 15.88.

*4.2.11. 5’,7’–Dimethyl–3’H–spiro[morpholine–4,2’–[1,2,4]triazolo[4,3–a]pyridin]–4–ium–8’–carboxylate (**10**)*

Following GPA; yield: 71%; m.p. 166–168 °C; IR (ATR): ν = 3350w, 3267w, 2982w, 1632m, 1587vs, 1556s, 1514s, 1476m, 1452m, 1437m, 1427m, 1418m, 1404w, 1375s, 1348s, 1320w, 1311w, 1274w, 1250w, 1233w, 1222w, 1195s, 1138w, 1120m, 1109m, 1089w, 1073m, 845m, 803m, 775m, 689m, 659m, 602s, 559m, 530m, 513 m cm^{-1}; ^{1}H NMR (500 MHz, CD_3OD): δ = 6.04 (d, J = 1.2 Hz, 1H, 6–H), 5.79 (s, 2H, 3–H), 4.30 (ddd, J = 13.1, 8.9, 2.6 Hz, 2H, 14–H), 3.93 (dt, J = 13.2, 3.7 Hz, 2H, 14‘–H), 3.78 (ddd, J = 12.3, 8.9, 3.3 Hz, 2H, 13–H), 3.69–3.61 (m, 2H, 13‘–H), 2.31 (d, J = 1.0 Hz, 3H, 11–H), 2.21 (s, 3H, 10–H) ppm; ^{13}C NMR (125 MHz, CD_3OD): δ = 170.1 (C-12), 155.6 (C-5), 146.8 (C-7), 139.5 (C-9), 118.3 (C-8), 110.5 (C-6), 64.0 (C-14 + C-14‘), 61.6 (C-13 + C-13‘), 18.4 (C-10), 16.8 (C-11) ppm; MS (ESI, MeOH): *m*/*z* (%) = 264.2 ($[M+H]^+$, 100%), 286.1 ($[M+Na]^+$, 8%); analysis calcd for $C_{13}H_{17}N_3O_3$ (263.30): C 59.30, H 6.51, N 15.96; found: C 59.12, H 6.70, N 15.73.

*4.2.12. 4,5’,7’–Trimethyl–3’H–spiro[piperazine–1,2’–[1,2,4]triazolo[4,3–a]pyridin]–1–ium–8’–carboxylate (**11**)*

Following GPA; yield: 43%; m.p. 187–191 °C; IR (ATR): ν = 3358m, 3175w, 2996w, 2954w, 2942w, 2855w, 2811w, 2785w, 1634s, 1586vs, 1561vs, 1531s, 1456m, 1449m, 1433m, 1407m, 1379s, 1355s, 1335m, 1314w, 1291m, 1260w, 1233w, 1222m, 1191s, 1171w, 1152m, 1129m, 1115w, 1098w, 1078w, 970m, 805m, 790s, 779m, 695m, 660m, 605m, 597s, 562 m cm^{-1}; ^{1}H NMR (500 MHz, CD_3OD): δ = 6.01 (d, J = 1.1 Hz, 1H, 6–H), 5.77 (s, 2H, 3–H), 3.79–3.72 (m, 2H, 13–H), 3.72–3.65 (m, 2H, 13’–H), 3.10–3.02 (m, 2H, 14–H), 2.81–2.71 (m, 2H, 14′–H), 2.39 (s, 3H, 15–H), 2.31 (d, J = 1.0 Hz, 3H, 11–H), 2.20 (s, 3H, 10–H) ppm; ^{13}C NMR (125 MHz, CD_3OD): δ = 170.1 (C-12), 155.5 (C-5), 146.5 (C-7), 139.5 (C-9), 118.3 (C-8), 110.3 (C-6), 64.0 (C-13 + C-13‘), 49.0 (C-14 + C-14‘), 43.9 (C-15), 18.4 (C-10), 16.9 (C-11) ppm; MS (ESI, MeOH): *m*/*z* (%) = 277.2 ($[M+H]^+$, 100%), 299.1 ($[M+Na]^+$, 4%); analysis calcd for $C_{14}H_{20}N_4O_2$ (276.34): C 60.85, H 7.30, N 20.28; found: C 60.61, H 7.43, N 20.11.

*4.2.13. Acetanilide (**12**)*

Acetanilide (**12**) was prepared by usual acetylation of aniline with acetic anhydride in 78% yield; m.p. 116–118 °C (lit [39].: 116–117 °C); MS (ESI, MeOH): *m*/*z* (%) 136.1 ($[M+H]^+$, 100%), 158.0 ($[M+Na]^+$, 48%).

*4.2.14. 2–Chloro–3–quinolinecarboxaldehyde (**13**)*

To a mixture of *N*, *N*–dimethylformaldehyde (9.6 mL, 0.125 mol) and phosphoryl chloride (32 mL, 0.35 mol) at 0 °C, **1** (6.8 g, 0.05 mol) was added, and the resulting mixture was heated under reflux for 24 h. Usual aqueous workup gave a pale–yellow precipitate, that was filtered off, washed with water (2 × 50 mL) and dried to afford **13** (6.7 g, 70%) as a pale yellow solid; m.p. 152–154 °C (lit [40].: 150–151 °C); R_F = 0.69 (toluene/ethyl acetate/formic acid/*n*–heptane, 80:26:5:10); IR (ATR): ν = 3044vw, 2941vw, 2873w, 1687vs, 1579m, 1046s, 761s, 487s cm–1; UV–Vis (MeOH): λ_{max} (log ε) = 234 (5.50), 319 (4.53) nm; ^{1}H NMR (400 MHz, $CDCl_3$): δ = 10.56 (s, 1H, 9‘–H), 8.75 (s, 1H, 4–H), 8.07 (d, J = 8.5 Hz, 1H, 5–H), 7.98 (d, J = 8.2 Hz, 1H, 8–H), 7.93–7.84 (m, 1H, 7–H), 7.69–7.61 (m, 1H, 6–H) ppm; ^{13}C NMR (100 MHz, $CDCl_3$): δ = 150.3 (C-2), 149.8 (C–8a), 140.4 (C-4), 133.7 (C-7), 129.9 (C-8), 128.8 (C-5), 128.3 (C-6), 126.7 (C–4a), 126.6 (C-3) ppm; MS (ESI, MeOH): *m*/*z* (%) 192.1 ($[M+H]^+$, 28%), 194.1 ($[M+H]^+$, 10%), 224.1 ($[M + H + MeOH]^+$, 100%), 226.1 ($[M + H + MeOH]^+$, 34%).

*4.2.15. Chloroquinoline–3–carboxylic acid (**14**)*

To a solution of **2** (0.9 g, 4.68 mmol) in *n*–butanol (90 mL), a solution of sodium dihydrogen orthophosphate (5.56 g, 35.61 mmol) and sodium chlorite (4.29 g, 47.47 mmol) in water (40 mL) was added, and the mixture was stirred at 25 °C for 2 h. The mixture was concentrated under reduced pressure, diluted with water (70 mL), and ethyl acetate (50 mL) and sodium carbonate (5.0 g) were added. The aqueous layer was separated, acidified with 2M HCl and **3** (0.85 g, 87%) was obtained as an off–white solid; m.p. 192–194 °C (lit [41].: 200 °C decomp.); IR (ATR): ν = 2940w, 1729m, 1566m, 1449m, 1190s, 1023m, 789s, 747vs, 572w cm–1; UV–Vis (DMSO): λ_{max} (log ε) = 258 (4.83), 287 (4.82) nm; ^{1}H NMR (400 MHz, DMSO–d_6): δ = 13.76 (s, 1H, OH), 8.93 (s, 1H, 4–H), 8.17 (d, J = 8.2 Hz, 1H, 8–H), 8.00 (d, J = 8.4 Hz, 1H, 5–H), 7.92 (ddd, J = 8.4, 6.8, 1.5 Hz, 1H, 7–H), 7.72 (ddd, J = 8.1, 6.8, 1.3 Hz, 1H, 6–H) ppm; ^{13}C NMR (100 MHz, DMSO–d_6): δ = 165.7 (C-9), 147.3 (C–8a), 146.4 (C-2), 141.2 (C-4), 132.7 (C-5), 128.9 (C-7), 128.0 (C-6), 127.6 (C-8), 125.9 (C–4a), 125.4 (C-3) ppm; MS (ESI, MeOH): *m*/*z* (%) 208.1 ($[M+H]^+$, 100%), 210.1 $[M+H]^+$, 34%).

*4.2.16. Isoxazolo[3,4–b]quinolin–3(1H)–one (**15**)*

A solution of **3** (1000 mg, 4.8 mmol) and hydroxyamine–*O*–sulfonic acid (2172 mg, 19.2 mmol) in dry DMF (5 mL) was stirred at 25 °C for 12 h. The solid was filtered off, washed with water (3 × 3 mL), and triethylamine (2.1 mL, 15.0 mmol) and water (10 mL) were added. After stirring at 25 °C for 12 h, the precipitate was filtered off and washed with water (3 × 3 mL) to yield **4** (726 mg, 81%) as a red solid; m.p. 247–250 °C (lit [30].: 261–264 °C); IR (ATR): ν = 2899w, 1725m, 1566m, 1449m, 1250m, 1190s, 1022s, 941w, 788vs, 747vs 572 m $cm^{-1;}$ UV–Vis (DMSO): λ_{max} (log ε) = 259 (4.65), 313 (4.93), 482 (4.87) nm; ^{1}H NMR (400 MHz, DMSO–d_6): δ = 12.55 (s, 1H, NH), 8.71 (s, 1H, 4–H), 7.89 (dd, J = 8.0, 1.3 Hz, 1H, 5–H), 7.70 (ddd, J = 8.6, 7.2, 1.5 Hz, 1H, 8–H), 7.39 (d, J = 8.4 Hz, 1H, 7–H), 7.28–7.20 (m, 1H, 6–H) ppm; ^{13}C NMR (100 MHz, DMSO–d_6): δ = 168.6 (C-9), 155.2 (C-2), 143.3 (C-4), 141.0 (C–8a), 135.6 (C-8), 132.2 (C-5), 122.7 (C-6), 119.7 (C–4a), 116.8 (C-7), 112.5 (C-3) ppm; MS (ESI, MeOH): *m*/*z* (%) 187.1 ($[M+H]^+$, 100%); analysis calcd for $C_{10}H_6N_2O_2$ (186.17): C 64.52, H 3.25, N 15.05; found: C 64.31, H 3.48, N 14.81.

*4.2.17. 2,2–Diethyl–1,2–dihydro–[1,2,4]triazolo[4,3–a]quinolin–2–ium 4–carboxylate (**16**)*

A solution of **4** (514 mg, 2.76 mmol), diethylamine (0.31 mL, 3.00 mmol) and formaldehyde (37%, 0.22 mL, 2.76 mmol) in MeOH (10 mL) was stirred at 25 °C for 8 h (during this timr, the color of the mixture turned from red to slightly yellow–green). The solvent was removed under reduced pressure, and the solid was washed with acetone (3 × 2 mL) to yield **16** (780 mg, 92%; m.p. 202–204 °C (lit [30].: 202–208 °C); IR (ATR): ν = 2961w, 1751m, 1663s, 1614m, 1487m, 1321s, 1052s, 778vs, 603s, 460vs cm^{-1}; UV–Vis (DMSO): λ_{max} (log ε) = 257 (5.50), 364 (4.94) nm; ^{1}H NMR (400 MHz, DMSO–d$_6$): δ = 7.90 (s, 1H, 4–H), 7.74–7.68 (m, 1H, 5–H), 7.60–7.51 (m, 1H, 7–H), 7.26–7.18 (m, 1H, 6–H), 7.09 (d, J = 8.2 Hz, 1H, 8–H), 5.77 (s, 2H, 10–H), 3.78–3.58 (m, 4H, 13–H + 13'–H), 1.27 (t, J = 7.1 Hz, 5H, 14–H + 14′–H) ppm; ^{13}C NMR (100 MHz, DMSO–d$_6$): δ = 164.0 (C-9), 155.5 (C-2), 137.4 (C-4), 134.1 (C–8a), 131.1 (C-7), 129.4 (C-5), 127.1 (C–4a), 123.2 (C-6), 121.8 (C-3), 114.0 (C-8), 71.1 (C-10), 60.7 (C-13 + C-13′), 8.3 (C-14 + C-14′) ppm; MS (ESI, MeOH): m/z (%) 272.13 ([M+H]$^+$, 100%); analysis calcd for $C_{15}H_{17}N_3O_2$ (271.32): C 66.40, H 6.32, N 15.49; found: C 66.19, H 6.50, N 15.25.

*4.2.18. (3β) 3–O–acetyl–betulinic acid (**17**)*

Acetylation of betulinic acid (**BA**) 20.0 g, 43.7 mmol) with acetic anhydride in the presence of DMAP (cat.) as previously reported [34] gave **17** (90%) as a colorless solid; m.p. 285–290 °C (lit [42].: 287–289 °C).

*4.2.19. (3β) 3–O–acetyl–oleanolic acid (**18**)*

Acetylation of oleanolic acid (**OA**), with acetic anhydride in the presence of DMAP (cat.) as previously reported [15] gave **18** (88%) as a colorless solid; m.p. 265–267 °C (lit [43].: 264–265 °C).

*4.2.20. (3β) 3–O–acetyl–ursolic acid (**19**)*

Acetylation of ursolic acid (**UA**) with acetic anhydride in the presence of DMAP (cat.) as previously reported gave **19** (84%) as a colorless solid; m.p. 280–283 °C (lit [15].: 281–283 °C).

*4.2.21. 4.2.19 (3β) 3–O–acetyl–platanic acid (**20**)*

Acetylation of platanic acid (**PA**) with acetic anhydride in the presence of DMAP (cat.) as previously reported gave **20** (87%) as a colorless solid; m.p. 280–283 °C (lit [11].: 280–283 °C).

*4.2.22. (3β) 3–O–acetyl–betulinic acid piperazinyl amide (**21**)*

Reaction of **17** (18.0 g, 36.1 mmol) in dry DCM (220 mL) with oxalyl chloride (15.2 mL, 177.2 mmol) followed by the addition of dry piperazine (15.6 g, 181.1 mmol) as previously reported gave **21** (15.6 g, 80%) as an off–white solid; m.p. 179–181 °C (lit [11].: 177–181 °C).

*4.2.23. (3β) 3–O–acetyl–oleanolic acid piperazinyl amide (**22**)*

Reaction of **18** with oxalyl chloride followed by the addition of dry piperazine as previously reported gave **22** (86%) as an off–white solid; m.p. 173–175 °C (lit [15].: 173–175 °C).

*4.2.24. (3β) 3–O–acetyl–ursolic acid piperazinyl amide (**23**)*

Reaction of **19** with oxalyl chloride followed by the addition of dry piperazine as previously reported gave **23** (84%) as an off–white solid; m.p. 186–188 °C (lit [15].: 187–188 °C).

*4.2.25. (3β) 3–O–acetyl–platanic acid piperazinyl amide (**24**)*

Reaction of **20** with oxalyl chloride followed by the addition of dry piperazine as previously reported gave **24** (84%) as an off–white solid; m.p. 118–121 °C (lit [11].: 115–125 °C).

*4.2.26. (3β) 3–O–acetyl–betulinic acid 2–aminoethylamide (**25**)*

Reaction of **17** (1.68 g, 3.4 mmol) in dry DCM (20 mL) with oxalyl chloride (1.5 mL, 17.5 mmol) followed by the addition of ethylenediamine (1.2 mL, 18.0 mmol) as previously reported gave **25** (1.4 g, 83%) as an off–white solid; m.p. 140–142 °C (lit [15].: 142 °C).

*4.2.27. (3β) 3–O–acetyl–oleanolic acid 2–aminoethylamide (**26**)*

Reaction of **18** with oxalyl chloride followed by the addition of ethylenediamine as previously reported gave **26** (81%) as an off–white solid; m.p. 190–193 °C (lit [15].: 190.5 °C).

*4.2.28. (3β) 3–O–acetyl–ursolic acid 2–aminoethylamide (**27**)*

Reaction of **19** with oxalyl chloride followed by the addition of ethylenediamine as previously reported gave **27** (84%) as an off–white solid; m.p. 196–198 °C (lit [15].: 198 °C).

*4.2.29. (3β) 3–O–acetyl–platanic acid 2–aminoethylamide (**28**)*

Reaction of **20** (1.68 g, 3.4 mmol) with oxalyl chloride followed by the addition of ethylenediamine as previously reported gave **28** (86%) as an off–white solid; m.p. 230–233 °C (lit [44].: 230–234 °C).

4.2.30. General procedure (GPB) for the synthesis of the conjugates

The safirinium dye (1.9 mmol) in dry DCM (20 mL) was activated with oxalyl chloride (0.4 mL, 4.7 mmol) followed by the addition of the corresponding acetylated triterpenoid amide (1.9 mmol) and triethylamine (0.56 mL, 4.0 mmol). After stirring at 25 °C for 12 h followed by usual aqueous workup and column chromatography (silica gel, $CHCl_3$/MeOH → MeOH) the conjugates were obtained.

*4.2.31. (3β) 3–Acetyloxy–28–{4–[(2,2–diethyl–5,7–dimethyl–2,3–dihydro[1,2,4]triazolo[4,3–a]pyridin–2–ium–8–yl)carbonyl]–1–piperazinyl}–28–oxolup–20(29)–ene chloride (**29**)*

Following GPB **29** (0.42 g, 57%) was obtained as a pale yellow solid; m.p. 212 °C; R_F = 0.3 (silica gel, $CHCl_3$/MeOH, 9:1); IR (ATR): ν = 2943m, 2867m, 1729m, 1632s, 1566m, 1535m, 1447m, 1392m, 1371m, 1315w, 1282m, 1245s, 1188m, 1107m, 1065m, 1027m, 999s; ^{1}H NMR (500 MHz, CD_3OD): δ = 6.22 (s,1H, 45–H), 5.93–5.89 (m, 2H, 42–H), 4.75 (s, 1H, 29–H$_a$), 4.64 (s, 1H, 29–H$_b$), 4.50–4.47 (m, 1H, 3–H), 3.84–3.73 (m, 5H, 49–H$_{a,b}$ + 49‘H$_{a,b}$ + 12–H$_b$) 3.01–2.89 (m, 2H, 19–H + 13–H), 2.46 (s, 3H, 48–H), 2.26–2.23 (m, 1H, 16–H$_a$), 2.22 (s, 3H, 47–H), 2.12–2.09 (m, 1H, 22–H$_a$), 2.07 (s, 3H, 32–H), 1.92–1.84 (m, 2H, 21–H), 1.81–1.77 (m, 2H, 1–H$_a$ + 12–H$_a$), 1.75 (s, 3H, 30–H) 1.73–1.66 (m, 4H, 18–H + 16–H$_a$ + 2–H), 1.61–1.53 (m, 2H, 6–H$_a$ + 22–H$_b$), 1.51–1.36 (m, 12H, 6–H$_b$ + 11–H$_a$ + 7–H + H-15–H$_a$ + 9–H + 50–H + 50‘–H), 1.34–1.25 (m, 2H, 11–H$_b$ + 15–H$_b$), 1.07 (s, 3H, 27–H), 1.07–1.03 (m, 2H, 12–H$_b$ + 1–H$_b$), 1.01 (s, 3H, 26–H), 0.95 (s, 3H, 25–H), 0.91 (s, 3H, 23–H), 0.90 (s, 3H, 24–H 0.89–0.87 (m, 1H, 5–H) ppm; ^{13}C NMR (125 MHz, CD_3OD): δ = 176.0 (C-28), 172.8 (C-31), 165.6 (C-37), 156.4 (C-44), 152.7 (C-20), 152.4 (C-46), 144.3 (C-39), 112.3 (C-38),111.7 (C-45), 110.0 (C-29), 82.5 (C-3), 74.0 (C-42), 62.6 (C-49 + C-49‘), 56.9 (C-5), 56.1 (C-17), 53.9 (C-18), 52.1 (C-9), 47.3 (C-19), 43.0 (C-14), 42.0 (C-8), 39.6 (C-1), 38.9 (C-4), 38.4 (C-13), 38.3 (C-10), 37.0 (C-22), 35.5 (C-7), 33.4 (C-16), 32.4 (C-21), 31.0 (C-15), 28.5 (C-24), 26.9 (C-12), 24.7 (C-2), 22.3 (C-11), 21.2 (C-32), 19.8 (C-30), 19.4 (C-47), 19.3 (C-6), 18.7 (C-48), 17.0 (C-23), 16.8 (C-25), 16.7 (C-26), 15.1 (C-27), 8.7 (C-50), 8.3 (C-50‘) ppm; MS (ESI, MeOH): m/z (%) = 798.6 ([M − Cl]$^+$, 100%); analysis calcd for $C_{49}H_{76}ClN_5O_4$ (834.63): C 70.52, H 9.18, N 8.39; found: C 70.37, H 9.31, N 8.21.

*4.2.32. (3β) 3–Acetyloxy–28–{4–[(2,2–dihexyl–5,7–dimethyl–2,3–dihydro[1,2,4]triazolo[4,3–a]pyridin–2–ium–8–yl)carbonyl]–1–piperazinyl}–28–oxolup–20(29)–ene chloride (**30**)*

Following GPB **30** (0.32 g, 39%) was obtained as an yellowish solid; m.p. 189 °C; R_F = 0.6 (silica gel, $CHCl_3$/MeOH, 9:1); IR (ATR): ν = 2934m, 2868m, 1731m, 1632s, 1565m, 1535m, 1459m, 1371m, 1315m, 1282m, 1245s, 1184s, 1138m, 1108m, 1064m, 1027m, 999s; 1H NMR (500 MHz, CD_3OD): δ = 6.21 (m, 1H, 45–H), 5.94–5.84 (m, 2H, 42–$H_{a,b}$), 4.76 (s, 1H, 29–H_a), 4.64 (s, 1H, 29–H_b), 4.49–4.47 (m, 1H, 3–H), 3.72–3.66 (m, 4H, 49–$H_{a,b}$ + 49‘–$H_{a,b}$), 3.03–2.89 (m, 2H, 19–H + 13–H), 2.44 (s, 3H, 48–H), 2.27–2.19 (m, 4H, 16–H_a + 47–H), 2.12–2.05 (m, 4H, 22H_a + 32–H), 1.88–1.69 (m, 9H, 21–H_a + 50–H_a + 50’–H_a + 12–H_a + 1–H_a + 18–H + 16–H_b + 2–H), 1.62–1.25 (m, 26H, 6–$H_{a,b}$ + H-22$_b$ + 11–H_a + 15–$H_{a,b}$ + 9–H + 7–H + 51–H + 51‘–H + 52–H 52‘–H + 53–H + 53‘–H + 12–Hb + 21–Hb + 50–H_b + –50’–H_b + 11–H_b) 1.09–1.05 (m, 4H, 27–H + 1–H_b), 1.02 (s, 3H, 26–H), 1.00–0.96 (m, 6H, 54–H + 54‘–H), 0.95 (s, 3H, 25–H), 0.91 (d, J = 3.5 Hz, 6H, 23–H + 24–H) ppm; ^{13}C NMR (125 MHz, CD_3OD): δ = 176.0 (C-28), 172.81 (C-31),165.6 (C-37), 156.2 (C-44), 152.7 (C-20), 152.4 (C-46), 144.2 (C-39), 112.3 (C-38), 111.7 (C-45), 110.1 (C-29), 82.4 (C-3), 75.0 (C-42), 68.0 (C-49+ C-49‘), 56.9 (C-5), 56.2 (C-17), 56.1 (C-14), 53.9 (C-18), 52.1 (C-9), 47.3 (C-19), 42.0 (C-8), 39.6 (C-1), 38.9 (C-4), 38.4 (C-13), 38.3 (C-10), 37.0 (C-22), 35.5 (C-7), 33.4 (C-16), 32.4 (C-21), 28.5 (C-24), 27.1 (C-51 + C-51‘ + C-52 + C-52‘ + C-53 + C-53‘), 26.9 (C-12), 24.7 (C-2), 23.5 (C-50), 22.3 (C-11), 21.2 (C-32), 19.8 (C-30), 19.4 (C-47), 19.3 (C-6), 18.6 (C-48), 17.0 (C-23), 16.8 (C-25), 16.7 (C-26), 15.2 (C-27), 14.4 (C-54), 14.3 (C-54‘) ppm; MS (ESI, MeOH): *m/z* (%) = 910.4 ([M − Cl]$^+$, 100%); analysis calcd for $C_{57}H_{92}ClN_5O_4$ (946.84): C 72.31, H 9.79, N 7.40; found: C 72.15, H 9.97, N 7.31.

*4.2.33. (3β) 3–Acetyloxy–28–{4–[(2,2–didodecyl–5,7–dimethyl–2,3–dihydro[1,2,4]triazolo [4,3–a] pyridin–2–ium–8–yl)carbonyl]–1–piperazinyl}–28–oxolup–20(29)–ene chloride (**31**)*

Following GPB **31** (390 mg, 40%) was obtained as a yellow solid; m.p. 158 °C; R_F = 0.2 (silica gel, $CHCl_3$/MeOH, 95:5); IR (ATR): ν = 2923s, 2853m, 1732m, 1627s, 1567m, 1530m, 1465m, 1405m, 1371m, 1283m, 1245s, 1186s, 1133w, 1107w, 1065w, 1029m, 999 s cm^{-1}; ^{1}H NMR (500 MHz, $CDCl_3$): δ = 5.89 (s, 1H, 45–H), 4.71 (s, 1H, 29–H_a), 4.58 (s, 1H, 29–H_b), 4.47–4.44 (m, 1H, 3–H), 3.99–3.86 (m, 2H, 49–$H_{a,b}$), 3.79–3.74 (m, 1H, 42–H_a), 3.66–3.61 (m, 2H, 49–H_b + 49’–H_b), 3.47–3.39 (m, 1H, 42–H_b), 2.94 (m, 1H, 19–H), 2.81 (m, 1H, 13–H), 2.51 (s, 3H, 48–H), 2.12 (s, 3H, 47–H), 2.02 (s, 4H, 16–H_a + 32–H), 1.92–1.83 (m, 2H, 22–H_a+21–H_a), 1.73–1.66 (m, 7H, 59–H_a + 59′–H_a + 12–H_a + 30–H + 1–H_a), 1.60–1.55 (m, 4H, 2–H + 16–H_b + 18–H), 1.50–1.46 (m, 1H, 6–H_a), 1.42–1.29 (m, 15H, 22–H_b + 11–H + 21–H_b + 6–H_b + 7–H + 50–H + 50–H’ + 51–H + 51‘–H), 1.27–1.21 (m, 33H, 59–H_b + 59’–H_b + 9–H + 58–H + 58‘–H + 15–H + 52–H–57–H + 52‘–H–57‘–H), 0.95–0.94 (m, 4H, 12–H_b + 27–H), 0.92–0.90 (d, J = 4.2 Hz, 3H, 26–H), 0.88–0.86 (m, 6H, 60–H + 60‘–H), 0.84–0.81 (m, 9H, 25–H + 24–H + 23–H) ppm; ^{13}C NMR (125 MHz, $CDCl_3$): δ = 174.0 (C-28), 171.1 (C-31), 163.4 (C-37), 155.1 (C-44), 151.0 (C-20), 150.7 (C-46), 142.7 (C-39), 111.6 (C-38), 110.7 (C-45), 109.6 (C-29), 81.1 (C-3), 67.5 (C-49 + C-49‘), 67.2 (C-42), 55.7 (C-5), 54.8 (C-17), 54.8 (C-14), 52.8 (C-18), 50.9 (C-9), 45.8 (C-19), 40.8 (C-8), 38.6 (C-1), 37.9 (C-4), 37.3 (C-10), 37.1 (C-13), 36.1 (C-22), 34.5 (C-7), 32.7 (C-16), 32.1 (C-58 + C-58‘), 31.4 (C-21), 30.0 (C-15), 30.0–29.3 (C-52–C–57 + C-52‘–C–57‘), 28.1 (C-24), 26.4 (C-50 + C-50‘ + C-51 + C-51‘), 25.7 (C-12), 23.8 (C-2), 22.8 (C-59 + C-59‘), 21.4 (C-32), 21.3 (C-11), 19.7 (C-30), 19.62 (C-48), 19.60 (C-47), 18.3 (C-6), 16.6 (C-23), 16.4 (C-25), 16.2 (C-26), 14.7 (C-27), 14.2 (C-60 + C-60‘) ppm; MS (ESI, MeOH): *m/z* (%) = 1079.0 ([M − Cl]$^+$, 90%); analysis calcd for $C_{69}H_{116}ClN_5O_4$ (1115.17): C 74.32, H 10.49, N 6.28; found: C 74.03, H 10.71, N 6.05.

*4.2.34. (3β) 3–Acetyloxy–28–{4–[(2,2–diethyl–1,2–dihydro [1,2,4]triazolo[4,3–a]quinolin–2–ium–4–yl)carbonyl]–1–piperazinyl}–28–oxalupa–12,20(29)–diene chloride (**32**)*

Following GPB **32** (450 mg, 57%) was obtained as a yellow solid; m.p. 215–218 °C; IR (ATR): ν = 3373br, 2941m, 2869m, 2095m, 1731s, 1624s, 1575m, 1453m, 1243s, 980s, 751m, 583 m cm^{-1}; UV–Vis (MeOH): λ_{max} (log ε) = 246 (5.54), 287 (4.93), 371 (4.84) nm; ^{1}H NMR (500 MHz, $CDCl_3$): δ = 7.76 (s, 1H, 37–H), 7.66 (t, J = 7.7 Hz, 1H, 41–H), 7.58 (d, J = 7.3 Hz, 1H, 39–H), 7.51 (d, J = 8.6 Hz, 1H, 42–H), 7.30 (t, J = 7.6 Hz, 1H, 40–H), 6.50 (s, 2H, 44–H), 4.70 (s, 1H, 29–H_a), 4.57 (s, 1H, 29–H_b), 4.48–4.40 (m, 1H, 3–H), 4.39–4.26 (m, 2H, 46–H), 3.91–3.57 (m, 6H, 46’–H + 34–H), 3.43 (s, 4H, 33–H), 2.98–2.89 (m, 1H, 19–H), 2.85–2.75 (m, 1H, 13–H), 2.08–2.00 (m, 1H, 16–H_a), 2.01 (s, 3H, 32–H), 1.95–1.76 (m, 2H, 22–H_a + 21–H_a), 1.66 (s, 3H, 30–H), 1.74–1.52 (m, 6H, 12–H_a + 1–H_a + 2–H + 16–H_b + 18–H), 1.43 (t, J = 6.9 Hz, 6H, 47–H + 47′–H), 1.51–1.28 (m, 8H, 6–H + 22–H_b + 11–H_a + 21–H_b + 7–H + 15–H), 1.28–1.12 (m, 3H, 9–H + 11–H_b + 15–H_b), 0.94 (s, 3H, 27–H), 0.91 (s, 3H, 26–H), 1.00–0.88 (m, 2H, 1–H_b + 12–H_b), 0.82 (s, 3H, 25–H), 0.81 (s, 3H, 24–H), 0.81 (s, 3H, 23–H), 0.79–0.74 (m, 1H, 5–H) ppm; ^{13}C NMR (125 MHz, $CDCl_3$): δ = 174.2 (C-28), 171.1 (C-31), 163.1 (C-35), 154.0 (C-45), 151.0 (C-20), 140.7 (C-37), 134.2 (C-36), 134.2 (C-41), 129.9 (C-39), 124.6 (C-40), 120.3 (C-43) 118.4 (C-38), 115.1 (C-42), 109.6 (C-29), 81.0 (C-3), 72.8 (C-44), 62.6 (C-46 + C-46′), 55.6 (C-5), 54.8 (C-17), 52.7 (C-18), 50.8 (C-9), 47.5 (C-33), 45.7 (C-19), 42.5 (C-34), 42.0 (C1–4), 40.8 (C-8), 38.5 (C-1), 37.9 (C-4), 37.3 (C-10), 37.0 (C-13), 36.1 (C-22), 34.5 (C-7), 32.7 (C-16), 31.4 (C-21), 30.0 (C-15), 28.0 (C-24), 25.7 (C-12), 23.8 (C-2), 21.4 (C-1), 21.2 (C-32), 19.7 (C-30), 18.3 (C-6), 16.6 (C-23), 16.4 (C-25), 16.3 (C-26), 14.8 (C-27), 8.8 (C-47 + C-47′) ppm; MS (ESI, MeOH): *m/z* (%) 820.4 ([M − Cl]$^+$, 100%); analysis calcd for $C_{51}H_{72}ClN_5O_4$ (854.62): C 71.68H 8.49, N 8.19; found: C 71.42, H 8.67, N 8.06.

*4.2.35. (3β) 3–Acetyloxy–28–{4–[(2,2–diethyl–1,2–dihydro [1,2,4]triazolo[4,3–a]quinolin–2–ium–4–yl)carbonyl]–1–piperazinyl}–28–oxo–olean–12–ene chloride (**33**)*

Following GPB **33** (389 mg, 47%) was obtained as a yellow solid; m.p. 220–224 °C; IR (ATR): ν = 3369br, 2942s, 2096m, 1731s, 1625s, 1466m, 1391m, 1243vs, 1004s, 750m, 458 m cm^{-1}; UV–Vis (MeOH): λ_{max} (log ε) = 246 (5.57), 287 (4.98), 373 (4.87) nm; ^{1}H NMR (500 MHz, $CDCl_3$): δ = 7.76 (s, 1H, 37–H), 7.65 (t, J = 7.7 Hz, 1H, 41–H), 7.58 (d, J = 7.2 Hz, 1H, 39–H), 7.50 (d, J = 8.1 Hz, 1H, 42–H), 7.30 (t, J = 7.6 Hz, 1H, 40–H), 6.49 (s, 2H, 44–H), 5.25 (dd, J = 3.3, 3.3 Hz, 1H, 12–H), 4.50–4.43 (m, 1H, 3–H), 4.39–4.27 (m, 2H, 46–H), 3.92–3.57 (m, 6H, 46′–H + 33–H + 34–H), 3.13–2.99 (m, 1H, 18–H), 2.19–2.09 (m, 1H, 16–H_a), 2.02 (s, 3H, 32–H), 1.96–1.79 (m, 2H, 11–H_a + 2–Ha), 1.75–1.46 (m, 11H, 7–H + 19–H_a + 2–H + 15–H_a + 11–H_b + 16–H_b + 1–H_a + 9–H + 6–H_a), 1.42 (t, J = 6.7 Hz, 6H, 47–H), 1.46–1.29 (m, 3H, 22–H_a + 21–H_a + 6–H_b), 1.27–1.15 (m, 3H, 22–H_b + 21–H_b + 19–H_b), 1.12 (s, 3H, 27–H), 1.10–0.95 (m, 2H, 15–H_b + 1–H_b), 0.91 (s, 3H, 29–H), 0.90 (s, 3H, 25–H), 0.89 (s, 3H, 30–H), 0.84 (s, 3H, 24–H), 0.83 (s, 3H, 23–H), 0.83–0.78 (m, 1H, 5–H), 0.69 (s, 3H, 26–H) ppm; ^{13}C NMR (125 MHz, $CDCl_3$): δ = 175.8 (C-28), 171.1 (C-31), 163.1 (C-35), 154.0 (C-45), 144.5 (C-13), 140.7 (C-37), 134.2 (C-36), 134.1 (C-41), 129.9 (C-39), 124.6 (C-40), 121.9 (C-12), 120.3 (C-43), 118.4 (C-38), 115.0 (C-42), 81.0 (C-3), 72.9 (C-44), 62.6 (C-46), 62.5 (C-46′), 55.5 (C-5), 47.7 (C-9), 47.7 (C-17), 46.4 (C-19), 45.4 (C-34), 43.7 (C-18), 42.5 (C-33), 42.0 (C-14), 39.3 (C-8), 38.2 (C-1), 37.8 (C-4), 37.1 (C-10), 34.1(C-21), 33.1 (C-30), 33.0 (C-22), 30.5 (C-20), 30.2 (C-7), 28.1 (C-23), 28.0 (C-15), 26.0 (C-27), 24.1 (C-29), 23.6 (C-11), 23.5 (C-2), 22.9 (C-16), 21.4 (C-32), 18.3 (C-6), 17.1 (C-26), 16.8 (C-24), 15.5 (C-25), 8.8 (C-47 + C-47′) ppm; MS (ESI, MeOH): *m/z* (%) 820.2 ([M − Cl]$^+$, 100%); analysis calcd for $C_{51}H_{74}ClN_5O_4$ (856.63): C 71.51, H 8.71, N 8.18; found: C 71.32, H 8.96, N 8.01.

*4.2.36. (3β) 3–Acetyloxy–28–{4–[(2,2–diethyl–1,2–dihydro [1,2,4]triazolo[4,3–a]quinolin–2–ium–4–yl)carbonyl]–1–piperazinyl}–28–oxo–urs–12–ene chloride (**34**)*

Following GPB **34** (408 mg, 52%) was obtained as a yellow solid; m.p. 230–234 °C; IR (ATR): ν = 3373br, 2941m, 2096w, 1731m, 1624s, 1576m, 1368m, 1243vs, 1045m, 950m, 751m, 582w cm^{-1}; UV–Vis (MeOH): λ_{max} (log ε) = 246 (5.37), 287 (4.79), 371 (4.67) nm; ^{1}H NMR (500 MHz, CDCl3): δ = 7.76 (s, 1H, 37–H), 7.66 (t, *J* = 7.8 Hz, 1H, 41–H), 7.58 (d, *J* = 7.2 Hz, 1H, 39–H), 7.51 (d, *J* = 8.2 Hz, 1H, 42–H), 7.30 (t, *J* = 7.6 Hz, 1H, 40–H), 6.50 (s, 2H, 44–H), 5.22–5.18 (m, 1H, 12–H), 4.51–4.44 (m, 1H, 3–H), 4.38–4.26 (m, 2H, 46–H), 3.90–3.53 (m, 4H, 46′–H + 34–H), 3.49–3.36 (m, 2H, 33–H), 2.48–2.33 (m, 1H, 18–H), 2.23–2.09 (m, 1H, 16–H$_a$), 2.02 (s, 3H, 32–H), 1.96–1.83 (m, 2H, 11–H), 1.82–1.55 (m, 9H, 22–H + 16–H$_b$ + 21–H + 1–H$_a$ + 2–H + 15–H$_a$), 1.55–1.37 (m, 4H, 9–H + 6–H$_a$ + 7–H$_a$ + 19–H), 1.42 (t, *J* = 6.7 Hz, 6H, 47–H + 47′–H), 1.38–1.15 (m, 2H, 6–H$_b$ + 7–H$_b$), 1.14–0.96 (m, 3H, 15–H$_b$ + 1–H$_b$ + 20–H), 1.06 (s, 3H, 27–H), 0.93 (d, *J* = 6.1 Hz, 3H, 30–H), 0.91 (s, 3H, 25–H), 0.88 (d, *J* = 6.4 Hz, 6H, 29–H), 0.85 (s, 3H, 24–H), 0.83 (s, 3H, 23–H), 0.83–0.79 (m, 1H, 5–H), 0.71 (s, 3H, 26–H) ppm; ^{13}C NMR (125 MHz, CDCl$_3$): δ = 176.0 (C-28), 171.1 (C-31), 163.1 (C-35), 154.0 (C-45), 138.5 (C-13), 140.7 (C-37), 134.2 (C-41), 134.1 (C-36), 129.9 (C-39), 125.5 (C-12), 124.6 (C-40), 120.3 (C-43), 118.4 (C-38), 115.1 (C-42), 81.0 (C-3), 72.9 (C-44), 62.6 (C-46 + C-46′), 55.4 (C-5), 55.3 (C-18), 47.7 (C-17), 47.6 (C-9), 47.3 (C-33), 42.4 (C-34), 42.2 (C-14), 39.6 (C-19), 39.3 (C-8), 38.8 (C-20), 38.3 (C-1), 37.8 (C-4), 37.0 (C-10), 34.6 (C-22), 33.1 (C-7), 30.5 (C-21), 28.3 (C-15), 28.2 (C-24), 23.8 (C-27), 23.6 (C-11), 23.5 (C-16), 23.4 (C-2), 21.4 (C-32), 21.3 (C-30), 18.3 (C-6), 17.5 (C-29), 17.1 (C-26), 16.8 (C-23), 15.6 (C-25), 8.8 (C-47 + C-47′) ppm; MS (ESI, MeOH): *m*/*z* (%) 820.2 ([M – Cl]$^{+}$, 100%); analysis calcd for $C_{51}H_{74}ClN_5O_4$ (856.63): C 71.51, H 8.71, N 8.18; found: C 71.26, H 8.90, N 8.03.

*4.2.37. (3β) 3–Acetyloxy–28–{4–[(2,2–diethyl–1,2–dihydro [1,2,4]triazolo[4,3–a]quinolin–2–ium–4–yl)carbonyl]–1–piperazinyl}–20,28–dioxo–30–norlupa–12–ene chloride (**35**)*

Following GPB **35** (348 mg, 44%) was obtained as a yellow solid; m.p. 236–240 °C; IR (ATR): ν = 3373br, 2941m, 2871m, 2096m, 1731s, 1624s, 1452m, 1242vs, 1170m, 1028m, 980s, 751m, 582 m cm^{-1}; UV–Vis (MeOH): λ_{max} (log ε) = 246 (5.67), 288 (5.09), 374 (4.93) nm; ^{1}H NMR (500 MHz, CDCl$_3$): δ = 7.76 (s, 1H, 36–H), 7.69–7.62 (m, 1H, 40–H), 7.58 (d, *J* = 7.8 Hz, 1H, 38–H), 7.54–7.49 (m, 1H, 41–H), 7.30 (t, *J* = 7.5 Hz, 1H, 39–H), 6.50 (s, 2H, 43–H), 4.47–4.40 (m, 1H, 3–H), 4.40–4.21 (m, 2H, 45–H), 4.07–3.33 (m, 6H, 45′–H + 33–H + 32–H), 3.19 (dd, *J* = 11.2, 7.3 Hz, 1H, 19–H), 2.62 (dd, *J* = 12.1, 8.5 Hz, 1H, 13–H), 2.14 (s, 3H, 29–H), 2.12–2.00 (m, 2H, 18–H + 16–H$_a$), 2.01 (s, 3H, 31–H), 1.97–1.76 (m, 2H, 22–H$_a$ + 21–Ha), 1.72–1.47 (m, 7H, 1–H$_a$ + 16–H$_b$+ 2–H + 22–H$_b$ + 21–H$_b$ + 6–H$_a$), 1.43 (t, 6H, 46–H + 46′–H), 1.45–1.13 (m, 8H, 11–H + 7–H + 6–H$_b$ + 15–H + 9–H), 1.07–0.87 (m, 3H, 12–H + 1–H$_b$), 0.96 (s, 3H, 27–H), 0.89 (s, 3H, 26–H), 0.82 (s, 3H, 25–H), 0.82 (s, 3H, 24–H), 0.81 (s, 3H, 23–H), 0.80–0.73 (m, 1H, 5–H) ppm; ^{13}C NMR (125 MHz, CDCl$_3$): δ = 212.7 (C-20), 174.1 (C-28), 171.0 (C-30), 163.1 (C-34), 154.0 (C-44), 140.8 (C-36), 134.3 (C-40), 134.2 (C-35), 129.9 (C-38), 124.6 (C-39), 120.3 (C-42), 118.3 (C-37), 115.1 (C-41), 80.9 (C-3), 72.9 (C-43), 62.5 (C-45 + C-45′), 55.6 (C-5), 54.7 (C-17), 52.6 (C-18), 50.7 (C-9), 50.0 (C-19), 47.5 (C-32), 42.5 (C-33), 41.9 (C-14), 40.7 (C-8), 38.5 (C-1), 37.9 (C-4), 37.3 (C-10), 36.1 (C-13), 35.8 (C-22), 34.3 (C-7), 32.3 (C-16), 30.4 (C-29), 30.0 (C-15), 28.8 (C-21), 28.0 (C-24), 27.5 (C-12), 23.8 (C-2), 21.4 (C-31), 21.3 (C-11), 18.3 (C-6), 16.6 (C-23), 16.3 (C-25), 16.2 (C-26), 14.8 (C-27), 8.8 (C-46 + C-46′) ppm; MS (ESI, MeOH): *m*/*z* (%) 822.2 ([M – Cl]$^{+}$, 100%); analysis calcd for $C_{50}H_{70}ClN_5O_5$ (856.59): C 70.11, H 8.24, N 8.18; found: C 69.87, H 8.47, N 8.02.

*4.2.38. (3β) 3–Acetyloxy–28–[2–{[(2,2–diethyl–1,2–dihydro [1,2,4]triazolo[4,3–a]quinolin–2–ium–4–yl)carbonyl]amino} ethyl)amino]–28–oxolupa–12,20(29)–diene chloride (**36**)*

Following GPB **36** (316 mg, 44%) was obtained as a yellow solid; m.p. 200–204 °C; IR (ATR): ν = 3321br, 2942m, 2095w, 1731m, 1661m, 1474m, 1243m, 1172m, 1035s, 980m, 750w, 582 m cm^{-1}; UV–Vis (MeOH): λ_{max} (log ε) = 206 (5.26), 248 (5.13), 296 (4.66), 388 (4.36) nm; ^{1}H NMR (400 MHz, CDCl$_3$): δ = 8.75 (s, 1H, 37–H), 8.41–8.25 (m, 1H, NH), 7.81–7.71 (m, 2H, 39–H + 41–H), 7.63–7.50 (m, 1H, 42–H), 7.39 (t, *J* = 7.6 Hz, 1H, 40–H), 6.70–6.25 (m, 3H, NH + 44–H), 4.65 (s, 1H, 29–H$_a$), 4.56 (s, 1H, 29–H$_b$), 4.54–4.37 (m, 3H, 46–H + 3–H), 4.03–3.84 (m, 2H, 46′–H), 3.74–3.35 (m, 4H, 33–H + 34–H), 3.15–2.98 (m, 1H, 19–H), 2.41–2.27 (m, 1H, 13–H), 2.02 (s, 3H, 32–H), 2.06–1.94 (m, 1H, 16–H$_a$), 1.92–1.69 (m, 2H, 21–H$_a$ + 1–H$_a$), 1.64 (s, 3H, 30–H), 1.68–1.45 (m, 6H, 12–H$_a$ + 22–H$_a$ + 2–H + 16–H$_b$ + 18–H), 1.41 (t, *J* = 7.3 Hz, 3H, 47–H + 47′–H), 1.44–1.18 (m, 7H, 22–H$_b$ + 11–H$_a$ + 15–H$_a$ + 21–H$_b$ + 6–H$_a$ + 7–H$_a$ + 9–H), 1.16–1.03 (m, 4H, 7–H$_b$ + 11–H$_b$ + 6–H$_b$ + 15–H$_b$), 0.89 (s, 3H, 27–H), 1.02–0.81 (m, 2H, 12–H$_b$ + 1–H$_b$), 0.78 (s, 3H, 24–H), 0.74 (s, 3H, 23–H), 0.74 (s, 3H, 26–H), 0.72–0.58 (m, 1H, 5–H), 0.64 (s, 3H, 25–H) ppm; ^{13}C NMR (100 MHz, CDCl$_3$): δ = 177.2 (C-28), 171.0 (C-31), 161.5 (C-35), 154.5 (C-45), 150.6 (C-20), 146.1 (C-37), 135.3 (C-41), 134.4 (C-36), 131.1 (C-39), 125.1 (C-40), 120.4 (C-43), 114.9 (C-42), 114.4 (C-38), 109.6 (C-29), 80.8 (C-3), 72.3 (C-44), 63.2 (C-46 + C-46′), 55.7 (C-17), 55.3 (C-5), 50.3 (C-9), 50.0 (C-18), 46.9 (C-19), 40.6 (C-14), 40.4 (C-34), 39.7 (C-33), 38.4 (C-1), 38.3 (C-22), 37.7 (C-13), 37.7 (C-10), 37.0 (C-8), 34.2 (C-7), 33.5 (C-16), 30.8 (C-21), 29.5 (C-15), 27.9 (C-24), 25.4 (C-12), 23.6 (C-2), 21.3 (C-32), 20.9 (C-11), 19.3 (C-30), 17.9 (C-6), 16.5 (C-23), 16.2 (C-25), 16.1 (C-26), 14.5 (C-27), 8.8 (C-47), 8.6 (C-47′) ppm; MS (ESI, MeOH): *m*/*z* (%) 794.2 ([M – Cl]$^{+}$, 100%); analysis calcd for $C_{49}H_{70}ClN_5O_4$ (828.58): C 71.03, H 8.52, N 8.45; found: C 70.76, H 8.69, N 8.26.

*4.2.39. (3β) 3–Acetyloxy–28–[2–{[(2,2–diethyl–1,2–dihydro [1,2,4]triazolo[4,3–a]quinolin–2–ium–4–yl)carbonyl]amino} ethyl)amino]–28–oxo–olean–12–ene chloride (**37**)*

Following GPB **37** (314 mg, 40%) was obtained as a yellow solid; m.p. 210–214 °C; IR (ATR): ν = 3334br, 2941m, 2097w, 1731m, 1661m, 1574m,1366m, 1243m, 1027m, 750m, 583w cm–1; UV–Vis (MeOH): λ_{max} (log ε) = 213 (5.64), 248 (5.50), 296 (5.00), 387 (4.73) nm; ^{1}H NMR (400 MHz, CDCl$_3$): δ = 8.72 (s, 1H, 37–H), 8.42–8.37 (m, 1H, NH), 7.77–7.69 (m, 2H, 39–H + 41–H), 7.56 (d, *J* = 8.3 Hz, 1H, 42–H), 7.36 (t, *J* = 7.6 Hz, 1H, 40–H), 6.59–6.47 (m, 2H, 44–H), 6.44–6.37 (m, 1H, NH), 5.39 (s, 1H, 12–H), 4.53–4.37 (m, 3H, 46–H + 3–H), 4.00–3.80 (m, 1H, 46′–H), 3.73–3.42 (m, 2H, 33–H), 3.32–3.16 (m, 2H, 34–H), 2.60–2.48 (m, 1H, 18–H), 2.02 (s, 3H, 31–H), 1.97–1.83 (m, 3H, 16–H$_a$ + 11–H), 1.77–1.65 (m, 1H, 19–H$_a$), 1.62–1.50 (m, 6H, 16–H$_b$ + 22–H$_a$ + 2–H + 1–H$_a$ + 9–H), 1.50–1.37 (m, 3H, 15–H$_a$ + 6–H$_a$ + 7–H$_a$), 1.42 (t, *J* = 6.9 Hz, 6H, 47–H + 47′–H), 1.36–1.22 (m, 3H, 6–H$_b$ + 21–H$_a$ + 22–H$_b$), 1.21–1.15 (m, 2H, 7–H + 19–H$_b$), 1.12 (s, 3H), 1.11–0.94 (m, 3H, 21–H$_a$ + 1–H$_a$ + 15–H$_b$), 0.87 (s, 3H, 30–H), 0.85 (s, 3H, 25–H), 0.84 (s, 3H, 29–H), 0.82 (s, 3H, 23–H), 0.81 (s, 3H, 24–H), 0.80–0.76 (m, 1H, 5–H), 0.71 (s, 3H, 26–H) ppm; ^{13}C NMR (100 MHz, CDCl$_3$): δ = 179.2 (C-28), 171.1 (C-31), 161.5 (C-35), 154.6 (C-45), 146.0 (C-37), 144.6 (C-13), 135.3 (C-39), 134.6 (C-36), 131.1 (C-41), 125.0 (C-40), 123.0 (C-12), 120.5 (C-43), 115.1 (C-42), 114.4 (C-38), 80.9 (C-3), 72.2 (C-44), 63.3 (C-46), 63.1 (C-46‘), 55.2 (C-5), 47.5 (C-9), 46.7 (C-19), 46.4 (C-17), 42.1 (C-14), 42.0 (C-18), 40.5 (C-33), 39.8 (C-34), 39.4 (C-8), 38.2 (C-1), 37.8 (C-4), 36.9 (C-10), 34.2 (C-21), 33.0 (C-30), 32.9 (C-22), 32.4 (C-7), 30.8 (C-20), 28.1 (C-23), 27.4 (C-15), 25.8 (C-27), 23.9 (C-16), 23.7 (C-29), 23.6 (C-11), 23.6 (C-2), 21.4 (C-32), 18.2 (C-6), 17.0 (C-26), 16.8 (C-24), 15.5 (C-25), 8.9 (C-47 + C-47‘) ppm; MS (ESI, MeOH): *m*/*z* (%) 794.1 ([M – Cl]$^{+}$, 100%); analysis calcd for $C_{49}H_{72}ClN_5O_4$ (829.53): C 70.86, H 8.74, N 8.43; found: C 70.69, H 8.91, N 8.25.

*4.2.40. (3β) 3–Acetyloxy–28–[2–{[(2,2–diethyl–1,2–dihydro [1,2,4]triazolo[4,3–a]quinolin–2–ium–4–yl)carbonyl]amino} ethyl)amino]–28–oxo–urs–12–ene chloride (**38**)*

Following GPB **38** (341 mg, 45%) was obtained as a yellow solid; m.p. 198–202 °C; IR (ATR): ν = 3321br, 2940m, 2095m, 1731m, 1456m, 1367m, 1243vs, 1147w, 1027m, 982m, 750w, 582w cm^{-1}; UV–Vis (MeOH): λ_{max} (log ε) = 248 (5.54), 297 (5.04), 387 (4.79) nm; ^1H NMR (400 MHz, $CDCl_3$): δ = 8.71 (s, 1H, 37–H), 8.43–8.35 (m, 1H, NH), 7.72 (t, J = 7.0 Hz, 2H, 39–H + 41–H), 7.53 (d, J = 8.5 Hz, 1H, 42–H), 7.35 (t, J = 7.6 Hz, 1H, 40–H), 6.54 (s, 2H, 44–H), 6.40–6.31 (m, 1H, NH), 5.33–5.29 (m, 1H, 12–H), 4.52–4.40 (m, 2H, 46–H + 3–H), 3.98–3.84 (m, 2H), 3.67–3.45 (m, 2H, 33–H), 3.32–3.20 (m, 2H, 34–H), 2.01 (s, 3H, 32–H), 2.07–1.81 (m, 3H, 2–H + 18–H), 1.77–1.50 (m, 6H, 22–H_a + 11–H + 15–H_a + 1–H_a +9–H), 1.49–1.16 (m, 8H, 7–H + 6–H + 19–H + 21–H + 22–H_b), 1.44 (t, J = 6.8 Hz, 6H, 47–H + 47'–H, 1.05 (s, 3H, 27–H), 1.06–0.95 (m, 2H, 1–H_b + 15–H_b), 0.90 (s, 3H, 30–H), 0.86 (s, 3H, 25–H), 0.84 (s, 3H, 29–H), 0.82 (s, 3H, 24–H), 0.80 (s, 3H, 23–H), 0.71 (s, 3H, 26–H), 0.74–0.64 (m, 1H, 5–H) ppm; ^{13}C NMR (100 MHz, $CDCl_3$): δ = 179.0 (C-28), 170.9 (C-31), 161.2 (C-35), 154.4 (C-45), 145.8 (C-37), 139.4 (C-13), 135.2 (C-41), 134.4 (C-36), 131.0 (C-39), 125.7 (C-12), 124.9 (C-40), 120.4 (C-43), 114.9 (C-42), 114.4 (C-38), 80.7 (C-3), 72.1 (C-44), 63.1 (C-46), 63.0 (C-46′), 55.1 (C-5), 53.5 (C-18), 47.7 (C-17), 47.4 (C-9), 42.3 (C-14), 40.4 (C-33), 39.6 (C-19), 39.5 (C-8), 39.3 (C-34), 39.1 (C-20), 38.2 (C-1), 37.6 (C-4), 37.4 (C-22), 36.8 (C-10), 32.6 (C-7), 30.8 (C-21), 28.0 (C-24), 27.8 (C-15), 23.5 (C-11), 23.5 (C-16), 23.3 (C-2), 23.2 (C-27), 21.3 (C-32), 21.2 (C-30), 18.1 (C-6), 17.3 (C-29), 16.9 (C-26), 16.7 (C-23), 15.5 (C-25), 8.8 (C-47), 8.8 (C-47′) ppm; MS (ESI, MeOH): m/z (%) 794.2 ($[M - Cl]^+$, 100%); analysis calcd for $C_{49}H_{72}ClN_5O_4$ (829.53): C 70.86, H 8.74, N 8.43; found: C 70.58, H 8.93, N 8.21.

*4.2.41. (3β) 3–Acetyloxy–28–[2–{[(2,2–diethyl–1,2–dihydro [1,2,4]triazolo[4,3–a]quinolin–2–ium–4–yl)carbonyl]amino} ethyl)amino]–20,28–dioxo–30–norlupan–12–ene chloride (**39**)*

Following GPB **39** (335 mg, 44%) was obtained as a yellow solid; m.p. 196–200 °C; IR (ATR): ν = 3321br, 2941m, 2095m, 1731s, 1547m, 1243vs, 1167m, 1028m, 980m, 750w, 583 cm^{-1}; UV–Vis (MeOH): λ_{max} (log ε) = 248 (5.76), 297 (5.27), 385 (5.02) nm; ^1H NMR (500 MHz, $CDCl_3$): δ = 8.72 (s, 1H, 36–H), 8.30 (t, J = 5.3 Hz, 1H, NH), 7.77–7.70 (m, 2H, 38–H + 40–H), 7.54 (d, J = 8.1 Hz, 1H, 41–H), 7.37 (t, J = 7.6 Hz, 1H, 39–H), 6.70–6.64 (m, 1H, NH), 6.60 (d, J = 10.0 Hz, 1H, 43–H_a), 6.47 (d, J = 10.1 Hz, 1H, 43–H_b), 4.49–4.35 (m, 3H, 3–H + 45–H), 3.98–3.88 (m, 2H, 45′–H), 3.71–3.48 (m, 2H, 32–H), 3.45–3.29 (m, 3H, 33–H + 18–H), 2.19–2.08 (m, 1H, 13–H), 2.11 (s, 3H, 29–H), 2.06–2.00 (m, 2H, 16–H_a + 19–H), 2.00 (s, 3H, 31–H), 1.98–1.90 (m, 1H, 21–H_a), 1.80–1.73 (m, 1H, 22–H_a), 1.61–1.42 (m, 5H, 1–H_a + 16–H_b + 2–H + 22–H_b), 1.46 (q, J = 6.9 Hz, 6H, 46–H + 46′–H), 1.42–1.19 (m, 6H, 21–H_b + 11–H_a + 15–H_a + 6–H_a + 7–H_a + 9–H), 1.19–0.96 (m, 6H, 11–H_b + 6–H_b + 7–H_b + 15–H_b + 12–H), 0.92 (s, 3H, 27–H), 0.95–0.85 (m, 1H, 1–H_b), 0.76 (s, 3H, 24–H), 0.73 (s, 3H, 26–H), 0.72 (s, 3H, 23–H), 0.71–0.64 (m, 1H, 5–H), 0.67 (s, 3H, 25–H) ppm; ^{13}C NMR (125 MHz, $CDCl_3$): δ = 212.7 (C-20), 176.9 (C-28), 171.0 (C-30), 161.8 (C-34), 154.7 (C-44), 146.2 (C-36), 135.2 (C-40), 134.5 (C-35), 131.2 (C-38), 125.2 (C-39), 120.5 (C-42), 115.0 (C-41), 114.4 (C-37), 80.8 (C-3), 72.4 (C-43), 63.2 (C-45), 63.1 (C-45′), 55.6 (C-17), 55.4 (C-5), 51.3 (C-18), 50.3 (C-9), 50.1 (C-19), 42.3 (C-8), 40.7 (C-14), 40.1 (C-32), 40.1 (C-33), 38.4 (C-1), 38.1 (C-22), 37.8 (C-4), 37.1 (C-10), 36.9 (C-11), 34.2 (C-7), 32.8 (C-16), 30.1 (C-29), 29.6 (C-15), 28.6 (C-21), 28.0 (C-24), 27.2 (C-12), 23.7 (C-2), 21.4 (C-31), 21.0 (C-11), 18.0 (C-6), 16.6 (C-23 + C-26), 16.2 (C-25), 14.7 (C-27), 8.9 (C-46), 8.9 (C-46′) ppm; MS (ESI, MeOH): m/z (%) 796.2 ($[M - Cl]^+$, 100%); analysis calcd for $C_{48}H_{66}ClN_5O_5$ (830.55): C 69.42, H 8.25, N 8.43; found: C 69.27, H 8.41, N 8.32.

Declaration of competing interest

The authors declare that they have no known competing financial interests or personal relationships that could have appeared to influence the work reported in this paper.

Acknowledgments

We like to thank Dr. D. Ströhl, Y. Schiller and S. Ludwig for the NMR spectra and the late Dr. R. Kluge for measuring the MS spectra; some spectra were recorded by Th. Schmidt. Many thanks are also due to V. Simon and M. Schneider for taking the IR spectra. The microanalyses have been determined by S. Ludwig and M. Schneider. The cell lines have been provided by the Department of Oncology (Martin–Luther–University Halle Wittenberg).

Appendix A. Supplementary data

Supplementary data to this article can be found online at https://doi.org/10.1016/j.ejmech.2020.112920.

References

[1] E.H. Gort, A.J. Groot, E. van der Wall, P.J. van Diest, M.A. Vooijs, Hypoxic regulation of metastasis via hypoxia–inducible factors, Curr. Mol. Med. 8 (2008) 60–67.

[2] L. Dong, J. Rohlena, S. Ralph, J. Neuzil, Mitochondrial targeting of vitamin E succinate enhances its anti–cancer activity via mitochondrial complex II and presents potential benefit against tumour angiogenesis, Eur. J. Canc. 48 (2012) S221–S222.

[3] L.F. Dong, V.J.A. Jameson, D. Tilly, J. Cerny, E. Mahdavian, A. Marin–Hernandez, L. Hernandez–Esquivel, S. Rodriguez–Enriquez, J. Stursa, P.K. Witting, B. Stantic, J. Rohlena, J. Truksa, K. Kluckova, J.C. Dyason, M. Ledvina, B.A. Salvatore, R. Moreno–Sanchez, M.J. Coster, S.J. Ralph, R.A.J. Smith, J. Neuzil, Mitochondrial targeting of vitamin E succinate enhances its pro–apoptotic and anti–cancer activity via mitochondrial complex II, J. Biol. Chem. 286 (2011) 3717–3728.

[4] J. Neuzil, L.F. Dong, L. Ramanathapuram, T. Hahn, M. Chladova, X.F. Wang, R. Zobalova, L. Prochazka, M. Gold, R. Freeman, J. Turanek, E.T. Akporiaye, J.C. Dyason, S.J. Ralph, Vitamin E analogues as a novel group of mitocans: anti–cancer agents that act by targeting mitochondria, Mol. Aspect. Med. 28 (2007) 607–645.

[5] J. Neuzil, L.F. Dong, J. Rohlena, J. Truksa, S.J. Ralph, Classification of mitocans, anti–cancer drugs acting on mitochondria, Mitochondrion 13 (2013) 199–208.

[6] J. Neuzil, M. Tomasetti, Y. Zhao, L.F. Dong, M. Birringer, X.F. Wang, P. Low, K. Wu, B.A. Salvatore, S.J. Ralph, Vitamin E analogs, a novel group of "mitocans," as anticancer agents: the importance of being redox–silent, Mol. Pharmacol. 71 (2007) 1185–1199.

[7] J. Truksa, L.F. Dong, J. Rohlena, J. Stursa, M. Vondrusova, J. Goodwin, M. Nguyen, K. Kluckova, Z. Rychtarcikova, S. Lettlova, J. Spacilova, M. Stapelberg, M. Zoratti, J. Neuzil, Mitochondrially targeted vitamin E succinate modulates expression of mitochondrial DNA transcripts and mitochondrial biogenesis, Antioxidants Redox Signal. 22 (2015) 883–900.

[8] B. Yan, M. Stantic, R. Zobalova, A. Bezawork–Geleta, M. Stapelberg, J. Stursa, K. Prokopova, L.F. Dong, J. Neuzil, Mitochondrially targeted vitamin E succinate efficiently kills breast tumour–initiating cells in a complex II–dependent manner, BMC Canc. 15 (2015).

[9] Y. Zhao, J. Neuzil, K. Wu, Vitamin E analogues as mitochondria–targeting compounds: from the bench to the bedside? Mol. Nutr. Food Res. 53 (2009) 129–139.

[10] I. Serbian, S. Hoenke, O. Kraft, R. Csuk, Ester and amide derivatives of rhodamine B exert cytotoxic effects on different human tumor cell lines, Med. Chem. Res. 29 (2020) 1655–1661.

[11] S. Sommerwerk, L. Heller, C. Kerzig, A.E. Kramell, R. Csuk, Rhodamine B conjugates of triterpenoic acids are cytotoxic mitocans even at nanomolar concentrations, Eur. J. Med. Chem. 127 (2017) 1–9.

[12] R.K. Wolfram, L. Fischer, R. Kluge, D. Ströhl, A. Al–Harrasi, R. Csuk, Homopiperazine–rhodamine B adducts of triterpenoic acids are strong mitocans, Eur. J. Med. Chem. 155 (2018) 869–879.

[13] R.K. Wolfram, L. Heller, R. Csuk, Targeting mitochondria: esters of rhodamine

B with triterpenoids are mitocanic triggers of apoptosis, Eur. J. Med. Chem. 152 (2018) 21–30.
[14] I. Serbian, S. Hoenke, R. Csuk, Synthesis of some steroidal mitocans of nanomolar cytotoxicity acting by apoptosis, Eur. J. Med. Chem. 199 (2020) 112425.
[15] B. Brandes, S. Hoenke, L. Fischer, R. Csuk, Design, synthesis and cytotoxicity of BODIPY FL labelled triterpenoids, Eur. J. Med. Chem. 185 (2020) 111858.
[16] M. Grymel, M. Zawojak, J. Adamek, Triphenylphosphonium analogues of betulin and betulinic acid with biological activity: a comprehensive review, J. Nat. Prod. 82 (2019) 1719–1730.
[17] A.Y. Spivak, D.A. Nedopekina, R.R. Khalitova, R.R. Gubaidullin, V.N. Odinokov, Y.P. Bel'skii, N.V. Bel'skaya, V.A. Khazanov, Triphenylphosphonium cations of betulinic acid derivatives: synthesis and antitumor activity, Med. Chem. Res. 26 (2017) 518–531.
[18] A.Y. Spivak, D.A. Nedopekina, E.R. Shakurova, R.R. Khalitova, R.R. Gubaidullin, V.N. Odinokov, U.M. Dzhemilev, Y.P. Bel'skii, N.V. Bel'skaya, S.A. Stankevich, E.V. Korotkaya, V.A. Khazanov, Synthesis of lupane triterpenoids with triphenylphosphonium substituents and studies of their antitumor activity, Russ. Chem. Bull. 62 (2013) 188–198.
[19] D. Biedermann, B. Eignerova, M. Hajduch, J. Sarek, Synthesis and Evaluation of Biological Activity of the Quaternary Ammonium Salts of Lupane–, Oleanane–, and Ursane–Type Acids, Synthesis, 2010, pp. 3839–3848.
[20] V.E. Kataev, I.Y. Strobykina, L.Y. Zakharova, Quaternary ammonium derivatives of natural terpenoids. Synthesis and properties, Russ. Chem. Bull. 63 (2014) 1884–1900.
[21] V. Panda, P. Khambat, S. Patil, Mitocans as novel agents for anticancer therapy: an overview, Int. J. Clin. Med. 2 (2011) 515–529.
[22] B. Siewert, E. Pianowski, R. Csuk, Esters and amides of maslinic acid trigger apoptosis in human tumor cells and alter their mode of action with respect to the substitution pattern at C–28, Eur. J. Med. Chem. 70 (2013) 259–272.
[23] B. Brandes, L. Koch, S. Hoenke, H.-P. Deigner, R. Csuk, The Presence of a Cationic Center Is Not Alone Decisive for the Cytotoxicity of Triterpene Carboxylic Acid Amides, Steroids. 163 (2020), 108713, in print.
[24] J. Fedorowicz, M. Cebrat, M. Wierzbicka, P. Wisniewska, A. Jalinska, S. Dziomba, M. Gdaniec, M. Jaremko, L. Jaremko, K. Chandra, Z. Szewczuk, J. Saczewski, Synthesis and evaluation of dihydro–[1,2,4]triazolo[4,3–a]pyridin–2–ium carboxylates as fixed charge fluorescent derivatization reagents for MEKC and MS proteomic analyses, J. Mol. Struct. 1217 (2020) 128426.
[25] J. Fedorowicz, J. Saczewski, Z. Drazba, P. Wisniewska, M. Gdaniec, B. Wicher, G. Suwinski, A. Jalinska, Synthesis and fluorescence of dihydro–[1,2,4]triazolo [4,3–a]pyridin–2–ium–carboxylates: an experimental and TD–DFT comparative study, Dyes Pigments 161 (2019) 347–359.
[26] M. Cebrat, M. Wierzbicka, J. Saczewski, Z. Szewczuk, Study on the application of safirinium P derivatives as signal enhancers in mass spectrometric evaluation of peptides, J. Pept. Sci. 22 (2016) S98–S100.
[27] K. Ciura, J. Fedorowicz, F. Andric, K.E. Greber, A. Gurgielewicz, W. Sawicki, J. Saczewski, Lipophilicity determination of quaternary (Fluoro)Quinolones by chromatographic and theoretical approaches, Int. J. Mol. Sci. 20 (2019).
[28] J. Fedorowicz, J. Saczewski, Modifications of quinolones and fluoroquinolones: hybrid compounds and dual–action molecules, Monatsh. Chem. 149 (2018) 1199–1245.
[29] J. Fedorowicz, J. Saczewski, A. Konopacka, K. Waleron, D. Lejnowski, K. Ciura, T. Tomasic, Z. Skok, K. Savijoki, M. Morawska, S. Gilbert–Girard, A. Fallarero, Synthesis and biological evaluation of hybrid quinolone–based quaternary ammonium antibacterial agents, Eur. J. Med. Chem. 179 (2019) 576–590.
[30] J. Saczewski, K. Hinc, M. Obuchowski, M. Gdaniec, The tandem mannich–electrophilic amination reaction: a versatile platform for fluorescent probing and labeling, Chem. Eur J. 19 (2013) 11531–11535.
[31] J. Saczewski, A. Kedzia, A. Jalinska, New derivatives of 4,6–dimethylisoxazolo [3,4–b]pyridin–3(1H)–one: synthesis, tautomerism, electronic structure and antibacterial activity, Heterocycl. Commun. 20 (2014) 215–223.
[32] S. Fulda, C. Scaffidi, S.A. Susin, P.H. Krammer, G. Kroemer, M.E. Peter, K.M. Debatin, Activation of mitochondria and release of mitochondrial apoptogenic factors by betulinic acid, J. Biol. Chem. 273 (1998) 33942–33948.
[33] R. Csuk, Betulinic acid and its derivatives: a patent review (2008–2013), Expert Opin. Ther. Pat. 24 (2014) 913–923.
[34] M. Kahnt, L. Fischer, A. Al–Harrasi, R. Csuk, Ethylenediamine derived carboxamides of betulinic and ursolic acid as potential cytotoxic agents, Molecules 23 (2018) 1–19.
[35] J. Wiemann, L. Heller, V. Perl, R. Kluge, D. Ströhl, R. Csuk, Betulinic acid derived hydroxamates and betulin derived carbamates are interesting scaffolds for the synthesis of novel cytotoxic compounds, Eur. J. Med. Chem. 106 (2015) 194–210.
[36] S. Fulda, L. Galluzzi, G. Kroemer, Targeting mitochondria for cancer therapy, Nat. Rev. Drug Discov. 9 (2010) 447–464.
[37] S.H. Safe, P.L. Prather, L.K. Brents, G. Chadalapaka, I. Jutooru, Unifying mechanisms of action of the anticancer activities of triterpenoids and synthetic analogs, Anti–Cancer Agent Me 12 (2012) 1211–1220.
[38] W.M. Lee, H. Cui, M.A. Scialdone, A.G. Anderson, Novel Nitrile and Amidoxime Compounds and Methods of Preparation for Semiconductor Processing, 2013. US20130035272A1.
[39] H.E. French, A.F. Wirtel, α–Naphthyl isocyanate as a reagent for phenols and aliphatic amines, J. Am. Chem. Soc. 48 (1926) 1736–1739.
[40] S. Kumar, S. Bawa, S. Drabu, B.P. Panda, Design and synthesis of 2–chloroquinoline derivatives as non–azoles antimycotic agents, Med. Chem. Res. 20 (2011) 1340–1348.
[41] K. Shimizu, I. Sakamoto, S. Fukushima, Nitrogen–containing heterocyclic γ–pyrone derivatives. II, Yakugaku Zasshi 87 (1967) 672–676.
[42] C.R. Dorr, S. Yemets, O. Kolomitsyna, P. Krasutsky, L.M. Mansky, Triterpene derivatives that inhibit human immunodeficiency virus type 1 replication, Bioorg. Med. Chem. Lett 21 (2011) 542–545.
[43] L. Ruzicka, K. Hofmann, Polyterpenes and polyterpenoids. C. Transpositions in the rings A and E of oleanolic acid. Carbon skeleton of pentacyclic triterpenes, Helv. Chim. Acta 19 (1936) 114–128.
[44] M. Kahnt, L. Heller, P. Grabandt, A. Al–Harrasi, R. Csuk, Platanic acid: a new scaffold for the synthesis of cytotoxic agents, Eur. J. Med. Chem. 143 (2018) 259–265.

P2

European Journal of Medicinal Chemistry Reports 5 (2022) 100043

Contents lists available at ScienceDirect

European Journal of Medicinal Chemistry Reports

journal homepage: www.editorialmanager.com/ejmcr/default.aspx

A tormentic acid-homopiperazine-rhodamine B conjugate of single-digit nanomolar cytotoxicity and high selectivity for several human tumor cell lines

Oliver Kraft, Sophie Hoenke, René Csuk *

Martin-Luther University Halle-Wittenberg, Organic Chemistry, Kurt-Mothes-Str. 2, D-06120, Halle, (Saale), Germany

ARTICLE INFO

Keywords:
Tormentic acid
Pentacyclic tritepene
Euscaphic acid
Rhodamine B
Cytotoxicity

ABSTRACT

Tormentic acid and euscaphic acid were isolated from plant material and transformed into amides holding an extra rhodamine B moiety; these compounds were screened for their cytotoxic activity employing a panel of human tumor cell lines and non-malignant fibroblasts. Prerequisites for both high cytotoxicity and tumor cell selectivity seem to be the combination of an amide (from a secondary amine but not from a primary), the use of homopiperazine rather than piperazine as a spacer together with rhodamine B (as a cationic center) and – most important-a triterpene holding a (2α, 3β) configuration of the substituents in ring A of the triterpenoid skeleton. All these features are found in tormentic acid derived compound **15**; it acts as a mitocan; it is approximately 190 times more cytotoxic for ovarian carcinoma cells than for non-malignant fibroblasts, and **15** displayed an EC_{50} as low as 1 nM for several human cancer cell lines.

1. Introduction

Potentilla erecta (syn. Tormentilla erecta, Potentilla laeta, Potentilla tormentilla, also known as the (common) tormentil, septfoil) is a plant belonging to family of Rosaceae[1–3]. The plant is found throughout Europe, Scandinavia and East Asia and is very rich in tannins. These tannins hold anti-inflammatory, drying and contracting effects[4–7]. Thus, in folk medicine this plant was used both for the treatment of superficial wounds as well as for the therapy of diarrhea[8–11]. A very early reference to a possible application in cancer treatment can be found in medieval monastic medicine, e.g. in the writings of Hildegard von Bingen[12]. However, it is not the tannins being responsible for the cytotoxic effect, but with high probability the presence of some pentacyclic triterpenes in the plant, for example euscaphic acid (**1**, **EA**) [13–17] and tormentic acid (**2**, **TA**, Fig. 1)[18–22]. **EA** and **TA** are ursane-type pentacyclic triterpenoids holding hydroxy groups at positions 2, 3 and 19, respectively. Thereby, **EA** is a (2α, 3α) stereoisomer while **TA** is (2α, 3β) configurated. The number of publications dealing with cytotoxic effects of **EA** or **TA** remained small for many years. This is probably due to the fact that until recently the available quantities of **EA** and **TA** were rather small. However, an improved extraction process was developed some time ago which now allows these two substances to be made available in larger quantities[23–26]. Only a weak cytotoxic activity has been established for **TA** for different tumor cell lines; some anticancer activity has been found for EA for lymphocytic leukemia cells. Furthermore, **2** shows little toxicity to normal cells[13,18,19,24]. Based on the now very good accessibility of **1** and **2** as well as preliminary very promising results, we decided to make selected derivatives accessible and to investigate their cytotoxic activity in sulforhodamine B (SRB) assays.

2. Results and discussion

2.1. Chemistry

Extraction of the roots of tormentil as previously described [23–26] gave **EA** (**1**) and **TA** (**2**) whose acetylation furnished acetates **3** [27–30] and **4**[31–34], respectively (Scheme 1). Reaction of **3** with oxalyl chloride followed by the addition of piperazine, homopiperazine, or ethylenediamine, gave amides **5**–**7**, respectively. Following the same procedures from **2** compounds **8**–**10** were obtained in good yields.

Di- and triterpene derivatives holding a suitable spacer between the carboxyl group of the terpenoid skeleton and an extra rhodamine B moiety have previously been shown to be of superior cytotoxicity with EC_{50} values even in a low nano-molar range[35–41]. Therefore, **EA**

---

* Corresponding author. Martin Luther University Halle Wittenberg: Martin-Luther-Universitat Halle-Witte, Organic Chemistry, Kurt-Mothes-Str. 2, D-06120, Halle, (Saale), Germany.
E-mail address: rene.csuk@chemie.uni-halle.de (R. Csuk).

https://doi.org/10.1016/j.ejmcr.2022.100043
Received 23 February 2022; Received in revised form 25 March 2022; Accepted 29 March 2022
Available online 6 April 2022

2772-4174/© 2022 The Author(s). Published by Elsevier Masson SAS. This is an open access article under the CC BY license (http://creativecommons.org/licenses/by/4.0/).

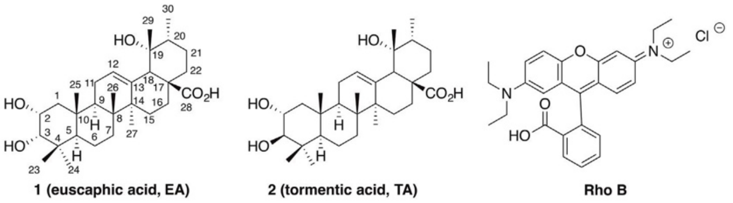

Fig. 1. Structure of euscaphic acid (**1**, **EA**) tormentic acid (**2**, **TA**), and rhodamine B (**Rho B**).

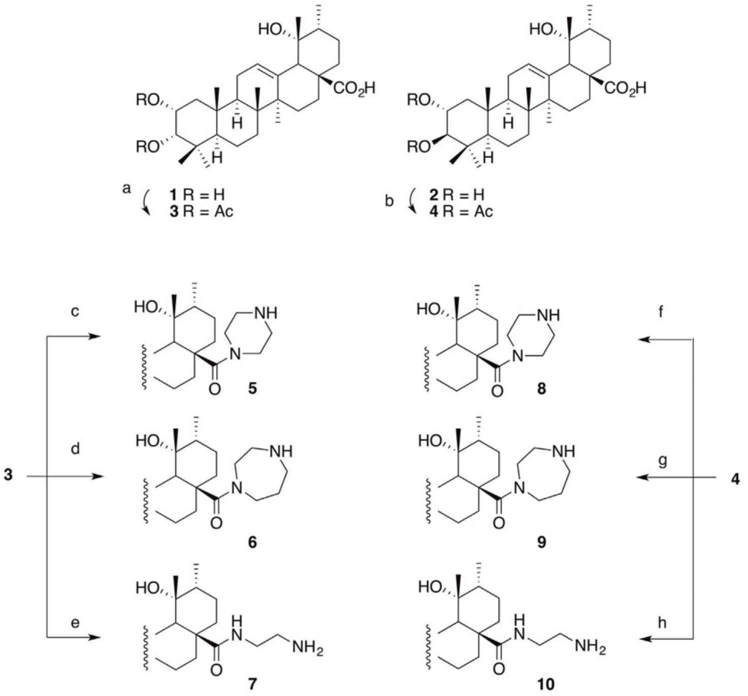

Scheme 1. Synthesis of **EA** and **TA** derivatives **3**–**10**: a) Ac_2O, NEt_3, cat. DMAP, DCM, 25 °C, 24 h, 84%; b) Ac_2O, NEt_3, cat. DMAP, DCM, 25 °C, 24 h, 86%; c) $(COCl)_2$, cat. DMF, DCM, piperazine, 25 °C, 2 h, 67%; d) $(COCl)_2$, cat. DMF, DCM, homopiperazine, 25 °C, 2 h, 89%; e) $(COCl)_2$, cat. DMF, DCM, ethylenediamine, 25 °C, 2 h, 60%; f) $(COCl)_2$, cat. DMF, DCM, piperazine, 25 °C, 2 h, 72%; g) $(COCl)_2$, cat. DMF, DCM, homopiperazine, 25 °C, 2 h, 50%; h) $(COCl)_2$, cat. DMF, DCM, ethylenediamine, 25 °C, 2 h, 71%.

derived amides **5**–**7** and **TA** derived compounds **8**–**10** were coupled with rhodamine B, and conjugates **11**–**16** obtained (Scheme 2). Due to the presence of a primary amino group in **7** and **10**, compounds **13** and **16** are different in their structure from those compounds (**11**, **12**, **14**, **15**) having been obtained from secondary amines (**5**, **6**, **8** and **9**). These two types of compounds already differ in their appearance: While the first group derived from primary amines are colorless compounds, the compounds derived from secondary amines are deep-pink; their $\lambda_{max} = 560 \pm 15$ nm. This is typical for cationic rhodamine B derivatives hence indicating an intact rhodamine B skeleton[36]. The former compounds are colorless; this has been observed for rhodamine B derivatives holding a lactone (or lactam) moiety[42,43].

2.2. Biology

Compounds **1**–**16** were subjected to sulforhodamine B assays to evaluate their cytotoxicity. The results of these assays are compiled in Table 1.

The results revealed for many compounds cytotoxic activity. While the parent compounds **1**–**4** were not cytotoxic within the borders of the assays (cut-off 30 μM), amides **5**–**10** were more cytotoxic. For all amides **5**–**10** EC_{50} values in the low μM range were found with **5** as the most active compound. The highest cytotoxicity, however, was determined for cationic rhodamine B conjugates **11, 12, 14, 15**. Due to the formation of a lactam, compounds **13** and **16** are no longer cations; as a consequence, their cytotoxicity is diminished tremendously.

Compound **15**, is not only the most cytotoxic triterpenoid reported so far, this conjugate also held the highest tumor/non-tumor cell selectivity, especially for A2780 (ovarian carcinoma) and FaDu (hypopharyngeal carcinoma) as compared to non-malignant fibroblasts NIH 3T3; a selectivity index (SI) was calculated as $EC_{50\ (NIH\ 3T3)}/EC_{50\ (A2780)} = 190$. Extra staining experiments of A2780 tumor cells with rhodamine 123 (CAS: [62669-70-9]), Hoechst 33342 (CAS: [23491-52-3]) and compound **15** showed the latter compound to target the mitochondria and to act as a mitocan.

These results seem to indicate that the presence of a homopiperazine spacer – rather than a piperazinyl moiety - results in excellent cytotoxicity when bound to a rhodamine B moiety. The presence of a cationic center is as important as the configuration in ring A. Conjugates holding a (2α, 3β) configuration are of better cytotoxicity and better selectivity

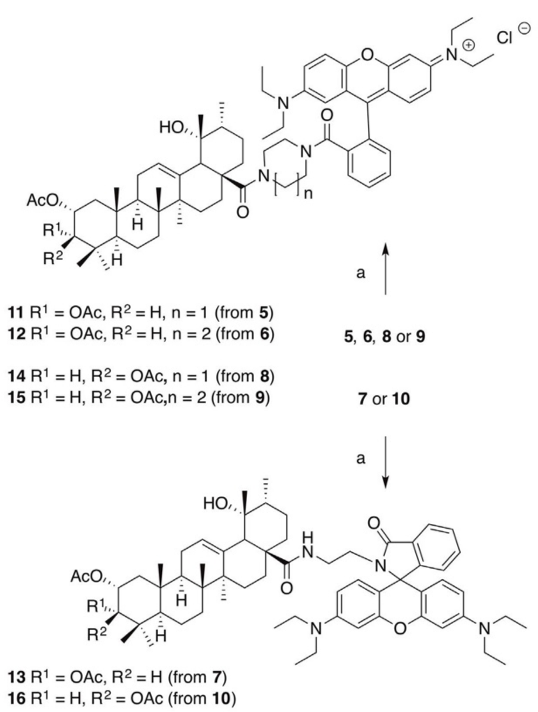
HO
AcO
R^1
R^2
H
N
O
n
$Cl^\ominus$
a
11 R^1 = OAc, R^2 = H, n = 1 (from **5**)
12 R^1 = OAc, R^2 = H, n = 2 (from **6**)
14 R^1 = H, R^2 = OAc, n = 1 (from **8**)
15 R^1 = H, R^2 = OAc,n = 2 (from **9**)
5, **6**, **8** or **9**
7 or **10**
13 R^1 = OAc, R^2 = H (from **7**)
16 R^1 = H, R^2 = OAc (from **10**)

Scheme 2. Synthesis of **EA** and **TA** derivatives **11**–**16**: a) $(COCl)_2$, rhodamine B, NEt_3, cat. DMF, DCM then compounds **5**, **6**, **7**, **10**, **11** or **12**, NEt_3, DCM, 2 h, 25 °C; yields: **11**: 68%; **12**: 46%; **13**: 66%; **14**: 51%; **15**: 54%; **16**: 64%.

than those with a (2α, 3α) configuration: $EC_{50,\ A2780}$ (**15**) = 0.001 μM vs $EC_{50,\ A2780}$ (**14**) = 0.037 μM; SI (**15**, A2780) = 190, SI (**14**, A2780) = 6.8.

3. Conclusion

A series of tormentic acid and euscaphic acid derived (homo)piperazine amides holding an extra rhodamine B moiety at the distal amino group has been devised, synthesized and screened for cytotoxic activity employing a panel of human tumor cell lines and non-malignant fibroblasts. Paralleling previous findings from our group, the presence of an arbitrary distal cation is not sufficient to obtain compounds of high cytotoxicity. High cytotoxicity was only observed when the compounds are able to act as mitocans. Furthermore, the combination of a suitable triterpene (preferentially holding a (2α, 3β) configuration of the acetates in ring A) together with an „ideal“ amide spacer (derived from a secondary amine but not from a primary, and with homopiperazine being better than piperazine) linked at the distal nitrogen to a cationic rhodamine moiety (probably not necessarily limited to rhodamine B) seems necessary for obtaining compounds of high cytotoxicity combined with good tumor cell selectivity. These prerequisites are fulfilled for compound **15**. This compound held an EC_{50} for several human tumor cells lines as low as 1 nM together with a tumor cell/non-tumor cell selectivity SI = 190.

4. Experimental part

4.1. General

Details of the instrumentation, assays and spectra (^{1}H NMR and ^{13}C APT NMR) can be found in the supplementary materials file.

Table 1

Cytotoxicity of selected compounds; SRB assay EC_{50} values [μM] after 72 h of treatment; averaged from three independent experiments performed each in triplicate; confidence interval CI = 95%. Human cancer cell lines: A375 (melanoma), HT29 (colorectal carcinoma), MCF-7 (breast adenocarcinoma), A2780 (ovarian carcinoma), FaDu (hypopharyngeal carcinoma), NIH 3T3 (non-malignant fibroblasts); cut-off 30 μM; n.d. not determined; n.s. not soluble. Betulinic acid (**BA**) and doxorubicin (**DX**) have been used as positive standards.

#	A375	HT29	MCF-7	A2780	FaDu	NIH 3T3
1	>30	>30	>30	>30	>30	>30
2	>30	>30	>30	>30	>30	>30
3	>30	>30	25.0 ± 3.5	24.2 ± 0.9	>30	>30
4	>30	>30	>30	>30	>30	>30
5	1.19 ± 0.1	2.05 ± 0.2	2.26 ± 0.3	1.77 ± 0.1	1.43 ± 0.1	2.51 ± 0.1
6	1.22 ± 0.1	2.25 ± 0.1	2.50 ± 0.1	1.78 ± 0.1	1.55 ± 0.3	2.61 ± 0.2
7	2.15 ± 0.1	3.28 ± 0.2	3.36 ± 0.3	2.57 ± 0.1	2.97 ± 0.3	4.37 ± 0.6
8	3.0 ± 0.1	4.9 ± 0.4	4.5 ± 0.6	4.0 ± 0.4	3.9 ± 0.4	6.4 ± 0.4
9	2.29 ± 0.5	3.12 ± 0.5	2.71 ± 1.3	2.98 ± 0.7	2.86 ± 06	2.83 ± 0.5
10	3.8 ± 0.1	5.9 ± 0.4	5.6 ± 0.4	5.7 ± 0.3	5.3 ± 0.3	7.3 ± 0.8
11	0.190 ± 0.004	0.191 ± 0.011	0.094 ± 0.008	0.066 ± 0.005	0.074 ± 0.006	0.210 ± 0.010
12	0.012 ± 0.001	0.012 ± 0.002	0.022 ± 0.005	0.004 ± 0.001	0.005 ± 0.001	0.164 ± 0.076
13	13.65 ± 4.3	>30	>30	>30	>30	>30
14	0.141 ± 0.031	0.162 ± 0.024	0.0084 ± 0.014	0.037 ± 0.011	0.041 ± 0.018	0.252 ± 0.017
15	0.006 ± 0.001	0.005 ± 0.001	0.008 ± 0.001	**0.001 ± 0.000**	**0.001 ± 0.000**	0.190 ± 0.026
16	12.03 ± 1.5	>30	>30	>30	>30	>30
BA	14.4 ± 1.3	12.7 ± 1.8	18.4 ± 2.0	12.0 ± 1.7	16.4 ± 1.9	16.1 ± 1.4
DX	1.0 ± 0.8	0.01 ± 0.01	0.9 ± 0.2	1.1 ± 0.3	1.7 ± 0.3	0.008 ± 0.001

4.2. Syntheses

4.2.1. General procedure GP A (acetylation)

To a solution of the triterpenoic acid (1 equiv.) in dry DCM (20 mL), triethylamine (4.5 equiv.) and a catal. amount of DMAP and acetic anhydride (4.0 equiv.) were added, and stirring was continued for 1 day at 25 °C. Usual aqueous work-up followed by chromatography gave the corresponding acetates.

4.2.2. General procedure GP B (synthesis of amides)

To a solution of the triterpenoic acid [1 equiv. in dry DCM (10 mL)] at 5 °C oxalyl chloride (4 equiv.) was added, and stirring at room temperature was continued for 4 h. Dry DMF (0.24 equiv.) and TEA (0.24 equiv.) were added, and stirring at room temperature was continued for 2 h. The solvents were removed under diminished pressure, the residue was dissolved in dry DCM (10 mL), and the corresponding amine was added. After stirring at room temperature until completion of the reaction (as checked by TLC), the solvents were removed under diminished pressure, and the residue was subjected to column chromatography.

4.2.3. General procedure GP C (synthesis of the rhodamine B derivatives)

To a solution of rhodamine B (1.5 equiv.) in dry DCM (30 mL) oxalyl chloride (6 equiv.), DMF (0.2 equiv.) and TEA (0.2 equiv.) were added, and the mixture was stirred at 25 °C for 3 h. The volatiles were removed under reduced pressure, and the residue was dissolved in dry DCM (30 mL), the corresponding amide **5**–**10** (1 equiv.), TEA (1.5 equiv.) and a catalytical amount of DMAP were added. The mixture was stirred for 2 h at 25 °C, the solvents were removed under reduced pressure, and the crude product was purified by column chromatography. Compounds **11**,

12, **14**, **15** were obtained as pink solids, and compounds **13** and **16** were obtained each as a colorless solid.

4.2.4. Euscaphic acid (1) and tormentic acid (2)

Extraction of finely powdered roots of tormentil (purchased from Dragonspice Naturwaren, Reutlingen, Germany) gave **1** and **2**. In short: The powdered roots of *Potentilla erecta* (1250 g) were suspended in ethanol (3500 mL) and extracted at room temperature for 24 h. The solution was decanted, filtered and concentrated under reduced pressure. This extraction process was repeated 4 times. The extracts were combined, the solvent was evaporated, and the residue was dissolved in 10% potassium hydroxide solution, boiled under reflux for 12 h, and the solution was neutralized at 25 °C with diluted hydrochloric acid, and the solvents were again removed under diminished pressure. After drying at 60 °C for two days, the residue was crushed, diethyl ether (1000 mL) was added, and the mixture was extracted under reflux for 1 h. The solution was decanted, filtered, and the filtrate was concentrated under reduced pressure. This process was repeated four more times. The resulting residue was suspended in *n*-hexane (250 mL), the solution was separated and discarded. After drying of the residue, the solid was dissolved in 0.5% ammonium hydroxide solution (500 mL) and stirred for 60 min at 80 °C. After cooling, the solution was extracted with diethyl ether (4 × 500 mL). Any residual diethyl ether was removed from the aqueous phase, and diluted hydrochloric acid was added. The precipitate (4205 mg) was filtered off, dried for 24 h in a desiccator followed by chromatographic purification (SiO_2, *n*-hexane/THF, 4:1) to yield **1** (2607 mg) and **2** (1123 mg) each as a colorless solid.

> Data for **1**: $R_f = 0.33$ (*n*-hexane/THF, 2:1); m.p.: 265–269 °C (lit[44].: 266–268 °C); $[\alpha]_D = +26.9°$ ($c = 0.32$, MeOH), [lit[45].: $[\alpha]_D = +20°$ ($c = 0.53$, MeOH)].
>
> Data for **2**: $R_f = 0.23$ (*n*-hexane/THF, 2:1); m.p.: 262–266 °C (lit[44].: 260–262 °C); $[\alpha]_D = +10.6°$ ($c = 0.33$, MeOH) [lit[45].: $[\alpha]_D = +11.0°$ ($c = 0.33$, MeOH)].

4.2.5. 2α,3α-Diacetyloxy-19β-hydroxyurs-12-en-28-oic acid (3)

Compound **3** (CAS: [52936-88-6]) was obtained from **1** (442 mg, 0.91 mmol) following GP A followed by column chromatography (SiO_2, *n*-hexane/ethyl acetate, 8:2) as a colorless solid (385 mg, 84%); $R_f = 0.71$ (toluene/ethyl acetate/HCOOH/heptane, 80:26:5:10); m.p. 182–184 °C (lit[28].: 185 °C); $[\alpha]_D = +4.9°$ ($c = 0.335$, MeOH) (lit[28].: $[\alpha]_D = +8°$ ($c = 0.6$, EtOH); IR (ATR): ν = 2927*br*, 1740*s*, 1368*s*, 1231*vs*, 1030 m cm^{-1}; ^1H NMR (400 MHz, $CDCl_3$): δ = 5.34 (*dd*, *J* = 3.5, 3.5 Hz, 1H, 12–H), 5.23 (*ddd*, *J* = 12.4, 4.4, 2.6 Hz, 1H, 2–H), 4.97 (d, *J* = 2.7 Hz, 1H, 3–H), 2.59–2.47 (m, 2H, 18–H + 16–H_a), 2.13–1.93 (m, 2H, 11–H_a + 11–H_b), 2.11 (s, 3H, 32–H), 1.98 (s, 3H, 34–H), 1.84–1.50 (m, 8H, 9–H + 22–H_a + 15–H_a + 21–H_a + 22–H_b + 1–H_a + 16–H_b + 7–H_a), 1.48–1.18 (m, 6H, 6–H_b + 20–H + 1–H_b + 7–H_b + 21–H_b + 5–H), 1.30 (s, 3H, 27–H), 1.20 (s, 3H, 29–H), 1.10–0.99 (m, 1H, 15–H_b), 1.03 (s, 3H, 25–H), 0.97 (s, 3H, 24–H), 0.96 (d, *J* = 7.0 Hz, 3H, 30–H), 0.87 (s, 3H, 23–H), 0.72 (s, 3H, 26–H) ppm; ^{13}C NMR (100 MHz, $CDCl_3$): δ = 184.3 (C-28), 170.8 (C-31), 170.6 (C-33), 138.1 (C-13), 129.0 (C-12), 77.1 (C-3), 73.3 (C-19), 68.4 (C-2), 52.9 (C-18), 49.7 (C-5), 47.9 (C-17), 47.2 (C-9), 41.3 (C-20), 41.2 (C-14), 40.3 (C-8), 38.9 (C-1), 38.6 (C-4), 38.3 (C-10), 37.6 (C-22), 32.6 (C-7), 28.3 (C-15), 27.9 (C-23), 27.5 (C-29), 26.1 (C-21), 25.5 (C-16), 24.8 (C-27), 23.8 (C-11), 21.7 (C-24), 21.3 (C-34), 21.1 (C-32), 18.0 (C-6), 17.2 (C-26), 16.3 (C-30), 16.3 (C-25) ppm; MS (ESI, MeOH): *m/z* (%) = 571.3 ($[M-H]^-$, 66), 1143.3 ($[2M-H]^-$, 100), 1165.5 ($[2M\text{-}2H+Na]^-$, 42.

4.2.6. 2α,3β-Diacetyloxy-19α-hydroxyurs-12-en-28-oic acid (4)

Compound **4** [CAS: 13850-14-1] was obtained from **2** (1012 mg, 2.07 mmol) following GP A followed by column chromatography (SiO_2, *n*-hexane/ethyl acetate, 8:2) as a colorless solid (1022 mg, 86%); $R_f = 0.66$ (toluene/ethyl acetate/HCOOH/heptane, 80:26:5:10); m.p. 177–179 °C (lit[32].: 186–189 °C); $[\alpha]_D = +11.5°$ ($c = 0.35$, $CHCl_3$) (lit[34].: +12° ($c = 0.5$, MeOH); IR (ATR): ν = 2936*br*, 1739*s*, 1368*s*, 1231*vs*, 1031 m cm^{-1}; ^1H NMR (500 MHz, $CDCl_3$): δ = 5.33 (*dd*, *J* = 3.5, 3.5 Hz, 1H, 12–H), 5.09 (*ddd*, *J* = 11.0, 10.6, 4.6 Hz, 1H, 2–H), 4.75 (d, *J* = 10.3 Hz, 1H, 3–H), 2.57–2.47 (m, 2H, 18–H + 16–H_a), 2.14–1.93 (m, 3H, 1–H_a + 11–H_a + 11–H_b), 2.05 (s, 3H, 32–H), 1.97 (s, 3H, 34–H), 1.82–1.46 (m, 8H, 6–H_a + 7–H_a + 9–H + 15–H_a + 16–H_b + 21–H_a + 22–H_a + 22–H_b), 1.44–1.17 (m, 4H, 6–H_b + 7–H_b + 20–H + 21–H_b), 1.24 (s, 3H, 27–H), 1.19 (s, 3H, 29–H), 1.15–0.87 (m, 3H, 1–H_a + 5–H + 15–H_b), 1.06 (s, 3H, 25–H), 0.94 (d, *J* = 6.6 Hz, 3H, 30–H), 0.89 (s, 6H, 23–H + 24–H), 0.71 (s, 3H, 26–H) ppm; ^{13}C NMR (125 MHz, $CDCl_3$): δ = 184.2 (C-28), 171.0 (C-31), 170.7 (C-33), 138.2 (C-13), 129.0 (C-12), 80.8 (C-3), 73.2 (C-19), 70.2 (C-2), 54.9 (C-5), 52.9 (C-18), 47.9 (C-17), 47.2 (C-9), 44.0 (C-1), 41.3 (C-14), 41.2 (C-20), 40.1 (C-8), 39.5 (C-4), 38.3 (C-10), 37.6 (C-22), 32.6 (C-7), 28.5 (C-23), 28.3 (C-15), 27.5 (C-29), 26.1 (C-21), 25.4 (C-16), 24.6 (C-27), 23.8 (C-11), 21.3 (C-34), 21.0 (C-32), 18.4 (C-6), 17.8 (C-24), 17.1 (C-26), 16.5 (C-25), 16.3 (C-30) ppm; MS (ESI, MeOH): *m/z* (%) = 571.3 ($[M-H]^-$, 46), 1143.1 ($[2M-H]^-$, 100), 1165.5 ($[2M\text{-}2H+Na]^-$, 26).

4.2.7. 2α,3α-Diacetyloxy-19α-hydroxy-N-(1′-piperazinyl)-urs-12-en-28-amide (5)

Compound **5** was obtained from **3** (286 mg, 0.50 mmol) according to GP B followed by column chromatography (SiO_2, $CHCl_3$/MeOH, 9:1) as a colorless solid (208 mg, 67%); $R_f = 0.44$ (SiO_2, $CHCl_3$/MeOH 9:1); m.p. 183–185 °C; $[\alpha]_D = -10.6°$ ($c = 0.15$, MeOH); IR (ATR): ν = 2964*w*, 2933*w*, 2872*w*, 1741 *m*, 1601 *m*, 1523*w*, 1445 *m*, 1365 *m*, 1252*s*, 1228*vs*, 1158 *m*, 1034*s*, 1021*s*, 993 *m*, 948 *m*, 804 m cm^{-1}; ^1H NMR (400 MHz, $CDCl_3$): δ = 5.24 (*dd*, *J* = 3.7, 3.7 Hz, 1H, 12–H), 5.03 (*ddd*, *J* = 11.5, 10.2, 4.6 Hz, 1H, 2–H), 4.67 (d, *J* = 10.2 Hz, 1H, 3–H), 3.69–3.47 (m, 4H, 35–H_a + 35–H_b), 2.88–2.71 (m, 6H, 36–H_a + 36–H_b +16–H_a + 18–H), 2.03–1.87 (m, 3H, 1–H_a + 11–H_a + 11–H_b), 1.99 (s, 3H, 32–H), 1.91 (s, 3H, 34–H), 1.83–1.70 (m, 1H, 22–H_a), 1.66–1.43 (m, 7H, 21–H_a + 9–H + 15–H_a + 16–H_b + 22–H_b + 6–H_a + 7–H_a), 1.42–1.29 (m, 2H, 20–H + 6–H_b), 1.27–1.18 (m, 2H, 7–H_b + 21–H_b), 1.19 (s, 3H, 27–H), 1.14 (s, 3H, 29–H), 1.07–0.95 (m, 2H, 1–H_b + 15–H_b), 0.99 (s, 3H, 25–H), 0.95–0.89 (m, 1H, 5–H), 0.87 (d, *J* = 6.6 Hz, 3H, 30–H), 0.85 (s, 3H, 24–H), 0.83 (s, 3H, 23–H), 0.63 (s, 3H, 26–H) ppm; ^{13}C NMR (100 MHz, $CDCl_3$): δ = 177.0 (C-28), 171.3 (C-33), 170.9 (C-31), 138.6 (C-13), 128.4 (C-12), 80.9 (C-3), 73.6 (C-19), 70.3 (C-2), 55.5 (C-18), 55.1 (C-17), 54.9 (C-5), 47.2 (C-9), 45.6 (C-35), 45.4 (C-36), 43.9 (C-1), 41.7 (C-14), 41.0 (C-20), 39.8 (C-8), 39.4 (C-4), 38.1 (C-10), 34.8 (C-22), 32.8 (C-7), 28.4 (C-23), 28.3 (C-15), 27.7 (C-29), 25.9 (C-21), 25.3 (C-16), 24.3 (C-27), 23.7 (C-11), 21.1 (C-34), 20.9 (C-32), 18.3 (C-6), 17.6 (C-24), 16.6 (C-26), 16.4 (C-25), 16.0 (C-30) ppm; MS (ESI, MeOH): *m/z* (%) = 641.3 ($[M+H]^+$, 100); analysis calcd for $C_{38}H_{60}N_2O_6$ (640.91): C 71.21, H 9.44, N 4.37; found: C 70.96, H 9.61, N 4.19.

4.2.8. 2α,3α-Diacetyloxy-N-(4′-homopiperazinyl)-19β-hydroxyurs-12-en-28-amide (6)

Compound **6** was obtained from **3** (220 mg, 0.38 mmol) according to GP B followed by column chromatography (SiO_2, $CHCl_3$/MeOH 9:1) as a colorless solid (220 mg, 89%); $R_f = 0.22$ (SiO_2, $CHCl_3$/MeOH 9:1); m.p. 161–163 °C; $[\alpha]_D = -31.3°$ ($c = 0.345$, MeOH); IR (ATR): ν = 2933*br*, 1740 *m*, 1615 *m*, 1456 *m*, 1366 *m*, 1232*vs*, 1156 *m*, 1033 *m*, 937*w*, 752 m cm^{-1}; ^1H NMR (500 MHz, $CDCl_3$): δ = 5.34 (*dd*, *J* = 3.7, 3.7 Hz, 1H, 12–H), 5.24 (*ddd*, *J* = 12.4, 12.4, 4.1 Hz, 1H, 2–H), 4.97 (d, *J* = 2.7 Hz, 1H, 3–H), 4.08–3.81 (m, 2H, 39–H_a + 39–H_b), 3.69–3.32 (m, 4H, 35–H_a + 35_b + 37–H_a + 37–H_b), 3.29–3.22 (m, 2H, 38–H_a + 38–H_b), 3.21–3.11 (m, 2H, 36–H_a + 36–H_b), 3.05–2.78 (m, 2H, 16–H_a + 18–H), 2.11 (s, 3H, 32–H), 2.07–1.97 (m, 2H, 11–H_a + 11–H_b), 1.95 (s, 3H, 34–H), 1.91–1.50 (m, 8H, 22–H_a + 9–H + 21–H_a + 1–H_a + 16–H_b + 22–H_b + 15–H_a + 7–H_a), 1.49–1.16 (m, 7H, 6–H_a + 20–H + 1–H_b + 6–H_b + 21–H_b + 7–H_b + 5–H), 1.31 (s, 3H, 27–H), 1.22 (s, 3H, 29–H), 1.11–1.02 (m, 1H, 15–H), 1.03 (s, 3H, 25–H), 0.99 (s, 3H, 24–H), 0.95 (d, *J* = 6.6 Hz, 3H, 30–H), 0.87 (s, 3H, 23–H), 0.68 (s, 3H, 26–H) ppm; ^{13}C NMR (125 MHz, $CDCl_3$): δ = 184.0 (C-28), 170.8 (C-31), 170.5 (C-33), 137.9

(C-13), 128.9 (C-12), 81.7 (C-39), 77.3 (C-3), 73.9 (C-19), 68.4 (C-2), 66.2 (C-35), 55.6 (C-18), 49.8 (C-5), 49.7 (C-36), 47.9 (C-17), 47.3 (C-9), 46.7 (C-37), 41.7 (C-14), 41.0 (C-20), 40.1 (C-8), 39.0 (C-1), 38.6 (C-4), 38.3 (C-10), 35.0 (C-22), 33.1 (C-7), 28.6 (C-38), 28.3 (C-15), 28.2 (C-29), 27.9 (C-23), 26.0 (C-21), 25.2 (C-16), 24.6 (C-27), 23.8 (C-11), 21.7 (C-24), 21.2 (C-34), 21.2 (C-32), 18.1 (C-6), 17.0 (C-26), 16.3 (C-25), 16.2 (C-30) ppm; MS (ESI, MeOH): m/z (%) = 655.4 ($[M+H]^+$, 98), 677.3 ($[M+Na]^+$, 38); analysis calcd for $C_{39}H_{62}N_2O_6$ (654.93): C 71.52, H 9.54, N 4.28; found: C 71.37, H 9.81, N 4.03.

4.2.9. 2α,3α-Diacetyloxy-N-(2′-aminoethyl)-19α-hydroxyurs-12-en-28-amide (7)

Compound **7** was obtained from **3** (270 mg, 0.47 mmol) according to GP B followed by column chromatography (SiO_2, $CHCl_3$/MeOH, 9:1) as a colorless solid (170 mg, 0.28 mmol, 60%); R_f = 0.28 (SiO_2, $CHCl_3$/MeOH 9:1); m.p. 242–244 °C (decomp.); $[\alpha]_D = +5.8°$ (c = 0.31, MeOH); IR (ATR): ν = 3543*w*, 3494*w*, 3354*w*, 2968*w*, 2946 *m*, 2871*w*, 1733*s*, 1723*s*, 1635*s*, 1521 *m*, 1463 *m*, 1452 *m*, 1366 *m*, 1269*vs*, 1240*s*, 1157 *m*, 1039*s*, 994 *m*, 929 *m*, 776 m cm^{-1}; ^{1}H NMR (500 MHz, $CDCl_3$): δ = 5.40 (*dd*, J = 3.7, 3.7 Hz, 1H, 12–H), 5.22 (*ddd*, J = 12.4, 4.5, 2.8 Hz, 1H, 2–H), 4.96 (d, J = 2.3 Hz, 1H, 3–H), 3.39–3.30 (m, 1H, 35–H_a), 3.13–3.05 (m, 1H, 35–H_b), 2.86–2.75 (m, 2H, 36–H_a + 36–H_b), 2.60 (*ddd*, J = 13.7, 13.7, 4.4 Hz, 1H, 16–H_a), 2.43 (s, 1H, 18–H), 2.10 (s, 3H, 32–H), 2.08–1.93 (m, 2H, 11–H_a + 11–H_b), 1.94 (s, 3H, 34–H), 1.91–1.73 (m, 2H, 9–H + 22–H_a), 1.70–1.49 (m, 5H, 21–H_a + 15–H_a + 1–H_a + 22–H_b + 7–H_b), 1.47–1.35 (m, 4H, 6–H_a + 20–H + 1–H_b + 6–H_b), 1.34–1.23 (m, 2H, 7–H_b + 21–H_b), 1.31 (s, 3H, 27–H), 1.21 (s, 3H, 29–H), 1.21–1.15 (m, 1H, 5–H), 1.02 (s, 3H, 25–H), 1.04–0.96 (m, 1H, 15–H_b), 0.98 (s, 3H, 23–H), 0.93 (d, J = 6.7 Hz, 3H, 30–H), 0.86 (s, 3H, 24–H), 0.73 (s, 3H, 26–H) ppm; ^{13}C NMR (125 MHz, $CDCl_3$): δ = 178.4 (C-28), 170.6 (C-33), 170.4 (C-31), 138.8 (C-13), 128.9 (C-12), 77.1 (C-3), 73.5 (C-19), 68.2 (C-2), 53.5 (C-5), 49.5 (C-18), 47.4 (C-17), 47.0 (C-9), 41.8 (C-35), 41.6 (C-14), 41.2 (C-20), 41.1 (C-36), 40.2 (C-8), 38.8 (C-1), 38.3 (C-4), 38.3 (C-22), 38.1 (C-10), 32.4 (C-7), 28.0 (C-15), 27.7 (C-23), 27.5 (C-29), 26.2 (C-21), 26.0 (C-16), 24.4 (C-27), 23.7 (C-11), 21.6 (C-34), 21.1 (C-32), 21.0 (C-24), 17.9 (C-6), 17.0 (C-26), 16.2 (C-25), 16.1 (C-30) ppm; MS (ESI, MeOH): m/z (%) = 615.4 ($[M+H]^+$, 100); analysis calcd for $C_{36}H_{58}N_2O_6$ (614.87): C 70.32, H 9.51, N 4.56; found: C 70.02, H 9.71, N 4.36.

4.2.10. 2α,3β-Diacetyloxy-19α-hydroxy-N-(1′-piperazinyl)-urs-12-en-28-amide (8)

Compound **8** was obtained from **4** (284 mg, 0.50 mmol) according to GP B followed by column chromatography (SiO_2, $CHCl_3$/MeOH, 9:1) as a colorless solid (223 mg, 72%); R_f = 0.38 (SiO_2, $CHCl_3$/MeOH 9:1); m.p. 199–202 °C; $[\alpha]_D = -22.5°$ (c = 0.34, MeOH); IR (ATR): ν = 3469*br*, 2972*w*, 2942*w*, 2879*w*, 1739*s*, 1624 *m*, 1455 *m*, 1393 *m*, 1369*s*, 1253*vs*, 1233*vs*, 1157 *m*, 1033*s*, 963 *m*, 934*w* cm^{-1}; ^{1}H NMR (500 MHz, $CDCl_3$): δ = 5.31 (*dd*, J = 3.7, 3.7 Hz, 1H, 12–H), 5.09 (*ddd*, J = 11.1, 10.9, 4.6 Hz, 1H, 2–H), 4.74 (d, J = 10.3 Hz, 1H, 3–H), 3.99–3.73 (m, 4H, 35–H_a + 35–H_b), 3.23–3.05 (m, 4H, 36–H_a + 36–H_b), 2.94–2.76 (m, 2H, 16–H_a + 18–H), 2.06–1.94 (m, 3H, 1–H_a + 11–H_a + 11–H_b), 2.04 (s, 3H, 32–H), 1.96 (s, 3H, 34–H), 1.85–1.77 (m, 1H, 22–H_a), 1.73–1.47 (m, 7H, 21–H_a + 9–H + 22–H_b + 15–H_a + 16–H_b + 6–H_a + 7–H_a), 1.46–1.36 (m, 2H, 20–H + 6–H_b), 1.32–1.26 (m, 2H, 7–H_b + 21–H_b), 1.24 (s, 3H, 27–H), 1.20 (s, 3H, 29–H), 1.13–0.96 (m, 3H, 1–H_b + 15–H_b+ 5–H), 1.05 (s, 3H, 25–H), 0.94 (d, J = 6.6 Hz, 3H, 30–H), 0.90 (s, 3H, 24–H), 0.89 (s, 3H, 23–H), 0.66 (s, 3H, 26–H) ppm; ^{13}C NMR (125 MHz, $CDCl_3$): δ = 177.0 (C-28), 171.0 (C-33), 170.6 (C-31), 138.4 (C-13), 128.7 (C-12), 80.8 (C-3), 73.8 (C-19), 70.2 (C-2), 55.5 (C-18), 55.0 (C-5), 51.7 (C-17), 47.3 (C-9), 44.4 (C-35), 44.1 (C-1), 43.6 (C-36), 41.8 (C-14), 41.0 (C-20), 39.9 (C-8), 39.6 (C-4), 38.4 (C-10), 35.0 (C-22), 32.9 (C-7), 28.6 (C-23), 28.4 (C-15), 28.1 (C-29), 26.0 (C-21), 25.5 (C-16), 24.4 (C-27), 23.9 (C-11), 21.3 (C-34), 21.0 (C-32), 18.4 (C-6), 17.8 (C-24), 16.8 (C-26), 16.5 (C-25), 16.2 (C-30) ppm; MS (ESI, MeOH): m/z (%) = 641.3 ($[M+H]^+$, 100); analysis calcd for $C_{38}H_{60}N_2O_6$ (640.91): C 71.21, H 9.44, N 4.37; found: C 70.11, H 9.62, N 4.23.

4.2.11. 2α,3β-Diacetyloxy-N-(4′-homopiperazinyl)-19α-hydroxyurs-12-en-28-amide (9)

Compound **9** was obtained from **4** (370 mg, 0.65 mmol) according to GP B followed by column chromatography (SiO_2, $CHCl_3$/MeOH, 9:1) as a colorless solid (210 mg, 50%); R_f = 0.19 (SiO_2, $CHCl_3$/MeOH 9:1); m.p. 166–168 °C; $[\alpha]_D = -32.7°$ (c = 0.305, MeOH); IR (ATR): ν = 3458*br*, 2934 *m*, 1739*s*, 1615 *m*, 1456 *m*, 1368 *m*, 1232*vs*, 1154 *m*, 1031*s*, 933 *m*, 747 m cm^{-1}; ^{1}H NMR (500 MHz, $CDCl_3$): δ = 5.31 (*dd*, J = 3.7, 3.7 Hz, 1H, 12–H), 5.09 (*ddd*, J = 10.7, 10.3, 4.3 Hz, 1H, 2–H), 4.74 (d, J = 10.3 Hz, 1H, 3–H), 3.94–3.69 (m, 2H, 39–H_a + 39–H_b), 3.67–3.53 (m, 4H, 35–H_a + 35_b + 37–H_a + 37–H_b), 3.26–3.00 (m, 4H, 38–H_a + 38–H_b + 36–H_a + 36–H_b), 2.88 (m, 2H, 18–H + 16–H_a), 2.14–1.86 (m, 4H, 1–H_a + 11–H_a + 11–H_b + 22–H_a), 2.05 (s, 3H, 32–H), 1.96 (s, 3H, 34–H), 1.72–1.33 (m, 9H, 21–H_a + 9–H + 16–H_b + 22–H_b + 15–H_a + 6–H_a + 7–H_a + 20–H + 6–H_b), 1.32–1.17 (m, 2H, 21–H_b + 7–H_b), 1.25 (s, 3H, 27–H), 1.21 (s, 3H, 29–H), 1.11–0.95 (m, 3H, 1–H_b + 15–H_b + 5–H), 1.05 (s, 3H, 25–H), 0.94 (d, J = 6.4 Hz, 3H, 30–H), 0.91 (s, 3H, 24–H), 0.89 (s, 3H, 23–H), 0.70 (s, 3H, 26–H) ppm; ^{13}C NMR (125 MHz, $CDCl_3$): δ = 184.4 (C-28), 171.0 (C-33), 170.6 (C-31), 138.8 (C-13), 128.6 (C-12), 82.0 (C-39), 80.8 (C-3), 73.9 (C-19), 70.2 (C-2), 66.3 (C-35), 55.6 (C-18), 55.0 (C-5), 53.4 (C-17), 49.8 (C-36), 47.4 (C-9), 47.0 (C-38), 46.7 (C-37), 44.1 (C-1), 41.8 (C-14), 41.0 (C-20), 39.9 (C-8), 39.5 (C-4), 38.3 (C-10), 35.0 (C-22), 32.6 (C-7), 28.6 (C-23), 28.4 (C-15), 28.2 (C-29), 26.1 (C-21), 25.0 (C-16), 24.4 (C-27), 23.9 (C-11), 21.3 (C-34), 21.1 (C-32), 18.4 (C-6), 17.8 (C-24), 16.9 (C-26), 16.5 (C-25), 16.2 (C-30) ppm; MS (ESI, MeOH): m/z (%) = 655.4 ($[M+H]^+$, 100); analysis calcd for $C_{39}H_{62}N_2O_6$ (654.93): C 71.52, H 9.54, N 4.28; found: C 71.33, H 9.75, N 4.14.

4.2.12. 2α,3β-Diacetyloxy-N-(2′-aminoethyl)-19α-hydroxyurs-12-en-28-amide (10)

Compound **10** was obtained from **4** (284 mg, 0.50 mmol) according to GP B followed by column chromatography (SiO_2, $CHCl_3$/MeOH, 9:1) as a colorless solid (213 mg, 71%); R_f = 0.22 (SiO_2, $CHCl_3$/MeOH, 9:1); m.p. 232–234 °C (decomp.); $[\alpha]_D = -9.2°$ (c = 0.30, MeOH); IR (ATR): ν = 3398*br*, 2970 *m*, 2934 *m*, 2877*w*, 1736*s*, 1635 *m*, 1522 *m*, 1453 *m*, 1436*w*, 1368*s*, 1248*vs*, 1233*vs*, 1167 *m*, 1157 *m*, 1031*s*, 963 *m*, 753 m cm^{-1}; ^{1}H NMR (400 MHz, $CDCl_3$): δ = 5.41 (*dd*, J = 3.7, 3.7 Hz, 1H, 12–H), 5.08 (*ddd*, J = 10.9, 10.8, 4.5 Hz, 1H, 2–H), 4.74 (d, J = 10.3 Hz, 1H, 3–H), 3.61–3.31 (m, 2H, 35–H_a + 35–H_b), 3.12–3.03 (m, 2H, 36–H_a + 36–H_b), 2.69–2.56 (m, 1H, 16–H_a), 2.53 (s, 1H, 18–H), 2.08–1.93 (m, 3H, 1–H_a + 11–H_a + 11–H_b), 2.05 (s, 3H, 32–H), 1.97 (s, 3H, 34–H), 1.81–1.64 (m, 3H, 9–H + 21–H_a + 22–H_a), 1.63–1.50 (m, 5H, 22–H_b + 6–H_a + 16–H_b + 15–H_a + 7–H_a), 1.48–1.36 (m, 2H, 20–H + 6–H_b), 1.34–1.17 (m, 2H, 7–H_b + 21–H_b), 1.25 (s, 3H, 27–H), 1.21 (s, 3H, 29–H), 1.14–0.95 (m, 3H, 1–H_b + 15–H_b + 5–H), 1.05 (s, 3H, 25–H), 0.92 (d, J = 6.8 Hz, 3H, 30–H), 0.91 (s, 3H, 24–H), 0.90 (s, 3H, 23–H), 0.69 (s, 3H, 26–H) ppm; ^{13}C NMR (100 MHz, $CDCl_3$): δ = 180.2 (C-28), 170.9 (C-33), 170.7 (C-31), 138.8 (C-13), 128.9 (C-12), 80.7 (C-3), 73.5 (C-19), 70.2 (C-2), 54.9 (C-5), 53.1 (C-18), 47.6 (C-17), 47.2 (C-9), 44.0 (C-1), 41.6 (C-14), 41.2 (C-20), 40.6 (C-36), 40.2 (C-8), 39.5 (C-4), 38.6 (C-35), 38.3 (C-22), 38.2 (C-10), 32.6 (C-7), 28.6 (C-23), 28.1 (C-15), 27.6 (C-29), 26.4 (C-21), 25.8 (C-16), 24.4 (C-27), 24.0 (C-11), 21.3 (C-34), 21.1 (C-32), 18.5 (C-6), 17.8 (C-24), 17.0 (C-26), 16.5 (C-25), 16.3 (C-30) ppm; MS (ESI, MeOH): m/z (%) = 615.4 ($[M+H]^+$, 100); analysis calcd for $C_{36}H_{58}N_2O_6$ (614.87): C 70.32, H 9.51, N 4.56; found: C 70.13, H 9.73, N 4.26.

4.2.13. 9’-[2’-[[4’-(2α,3α-Diacetyloxy-19α-hydroxyurs-12-en-28-oyl)-1′-piperazinyl]carbonyl]phenyl]-3′,6′-bis(diethylamino)-xanthylium chloride (11)

Compound **11** was obtained from **5** (180 mg, 0.28 mmol) according to GP C followed by column chromatography (SiO_2, $CHCl_3$/MeOH, 9:1) as a pink solid (207 mg, 68%); R_f = 0.38 (SiO_2, $CHCl_3$/MeOH 9:1); m.p. 248–252 °C; IR (ATR): ν = 3364*br*, 2932 *m*, 1733 *m*, 1628 *m*, 1586*vs*, 1465 *m*, 1411 *m*, 1335*s*, 1245*s*, 1179*vs*, 1131 *m*, 1073 *m*, 1005 *m*, 823 *m*, 773*w*, 683 m cm^{-1}; UV–Vis (MeOH): λ_{max} (log ε) = 260 (4.37), 309 (3.99), 356 (3.69), 562 (4.88) nm; ^{1}H NMR (500 MHz, CDCl$_3$): δ = 7.71–7.63 (m, 2H, 41–H + 40–H), 7.55–7.49 (m, 1H, 39–H), 7.37–7.30 (m, 1H, 42–H), 7.29–7.20 (m, 2H, 47′–H + 47–H), 7.10–6.92 (m, 2H, 46′–H + 46–H), 6.84–6.74 (m, 2H, 49′–H + 49–H), 5.27 (*dd*, *J* = 3.7, 3.7 Hz, 1H, 12–H), 5.20 (*ddd*, *J* = 12.4, 4.5, 2.7 Hz, 1H, 2–H), 4.94 (d, *J* = 2.7 Hz, 1H, 3–H), 3.73–3.56 (m, 8H, 51′–H + 51–H), 3.54–3.22 (m, 8H, 35–H$_a$ + 35–H$_b$ + 36–H$_a$ + 36–H$_b$), 2.78 (s, 1H, 18–H), 2.09 (s, 3H, 32–H), 2.23–2.05 (m, 1H, 16–H$_a$), 2.00–1.87 (m, 2H, 11–H$_a$ + 11–H$_b$), 1.92 (s, 3H, 34–H), 1.84–1.70 (m, 2H, 22–H$_a$ + 9–H), 1.68–1.46 (m, 5H, 21–H$_a$ + 1–H$_a$ + 15–H$_a$ + 7–H$_a$ + 22–H$_b$), 1.39–1.12 (m, 7H, 6–H$_a$ + 20–H + 1–H$_b$ + 6–H$_b$ + 21–H$_b$ + 7–H$_b$ + 5–H), 1.30 (t, *J* = 7.1 Hz, 12H, 52′–H + 52–H), 1.26 (s, 3H, 27–H), 1.17 (s, 3H, 29–H), 1.05–0.94 (m, 1H, 15–H$_b$), 0.98 (s, 3H, 25–H), 0.96 (s, 3H, 24–H), 0.90 (d, *J* = 6.6 Hz, 3H, 30–H), 0.86 (s, 3H, 23–H), 0.61 (s, 3H, 26–H) ppm; ^{13}C NMR (125 MHz, CDCl$_3$): δ = 175.2 (C-28), 170.7 (C-33), 170.5 (C-31), 167.8 (C-37), 157.8 (C-50‘), 157.8 (C-50), 155.8 (C-48’), 155.8 (C-44), 155.7 (C-48), 138.4 (C-13), 135.2 (C-43), 132.3 (C-47′), 132.3 (C-47), 130.8 (C-38), 130.5 (C-42), 130.3 (C-41), 130.3 (C-40), 128.5 (C-12), 127.7 (C-39), 114.6 (C-46′), 114.3 (C-46), 113.9 (C-45′), 113.8 (C-45), 96.6 (C-49′), 96.5 (C-49), 77.2 (C-3), 73.7 (C-19), 68.3 (C-2), 55.9 (C-18), 49.8 (C-17), 49.7 (C-5), 47.6 (C-36), 47.1 (C-9), 46.3 (C-51′), 46.3 (C-51), 42.1 (C-35), 41.7 (C-14), 41.0 (C-20), 40.0 (C-8), 38.9 (C-1), 38.5 (C-4), 38.2 (C-10), 34.9 (C-22), 32.9 (C-7), 28.3 (C-15), 28.0 (C-29), 27.9 (C-23), 26.0 (C-21), 24.6 (C-27), 23.7 (C-11), 21.7 (C-24), 21.3 (C-16), 21.2 (C-34), 21.1 (C-32), 18.0 (C-6), 16.9 (C-26), 16.2 (C-25), 16.2 (C-30), 12.8 (C-52′), 12.8 (C-52) ppm; MS (ESI, MeOH): *m/z* (%) = 1065.7 ([M − Cl]$^+$, 100); analysis calcd for $C_{66}H_{89}ClN_4O_8$ (1101.91): C 71.94, H 8.14, N 5.08; found: C 71.73, H 8.41, N 4.96.

4.2.14. 9’-[2’-[[4’-(2α,3α-Diacetyloxy-19α-hydroxyurs-12-en-28-oyl)-4′-homopiperazinyl]carbonyl]phenyl]-3′,6′-bis(diethylamino]-xanthylium chloride (12)

Compound **12** was obtained from **6** (170 mg, 0.26 mmol) according to GP C followed by column chromatography (SiO$_2$, CHCl$_3$/MeOH 9:1) as a pink solid (124 mg, 46%); R$_f$ = 0.20 (SiO$_2$, CHCl$_3$/MeOH 9:1); m.p. 248–252 °C; IR (ATR): ν = 3490*br*, 2933*w*, 1738 *m*, 1633 *m*, 1586*vs*, 1465 *m*, 1411 *m*, 1335*s*, 1245*s*, 1179*vs*, 1134 *m*, 1073 *m*, 921 *m*, 822 *m*, 683 s cm^{-1}; UV–Vis (MeOH): λ_{max} (log ε) = 260 (4.44), 307 (4.11), 355 (3.78), 406 (3.41), 562 (4.99) nm; ^{1}H NMR (500 MHz, CDCl$_3$): δ = 7.68–7.56 (m, 2H, 44–H + 43–H), 7.49–7.38 (m, 1H, 42–H), 7.32–7.22 (m, 3H, 45–H + 50′–H + 50–H), 7.21–7.10 (m, 2H, 49′–H + 49–H), 6.87–6.72 (m, 2H, 52′–H + 52–H), 5.33–5.24 (m, 1H, 12–H), 5.06 (*ddd*, *J* = 10.9, 10.9, 4.6 Hz, 1H, 2–H), 4.71 (*d*, *J* = 10.3, 1H, 3–H), 4.29–3.82 (m, 4H, 39–H + 35–H), 3.75–3.49 (m, 8H, 54′–H + 54–H), 3.38–2.92 (m, 4H, 37–H + 36–H), 2.90–2.66 (m, 2H, 18–H + 16–H$_a$), 2.03–1.90 (m, 3H, 1–H$_a$ + 11–H$_a$ + 11–H$_b$), 2.02 (s, 3H, 32–H), 1.94 (s, 3H, 34–H), 1.74–1.42 (m, 6H, 9–H + 16–H$_b$ + 6–H$_a$ + 21–H$_a$ + 7–H$_a$ + 22–H$_a$), 1.42–1.21 (m, 18H, 20–H + 6–H$_b$ + 22–H$_b$ + 55′–H + 55–H + 15–H$_a$ + 7–H$_b$ + 21–H$_b$), 1.21 (s, 3H, 27–H), 1.17 (s, 3H, 29–H), 1.09–0.91 (m, 3H, 1–H$_b$ + 15–H$_b$ + 5–H), 1.01 (s, 3H, 25–H), 0.90 (d, *J* = 6.4 Hz, 3H, 30–H), 0.87 (s, 3H, 24–H), 0.86 (s, 3H, 23–H), 0.64 (s, 3H, 26–H) ppm; ^{13}C NMR (125 MHz, CDCl$_3$): δ = 176.6 (C-28), 170.9 (C-33), 170.6 (C-31), 168.7 (C-40), 157.9 (C-53‘), 157.8 (C-53), 155.9 (C-47), 155.8 (C-51’), 155.7 (C-51), 138.8 (C-13), 135.6 (C-46), 132.7 (C-50′), 132.6 (C-50), 131.7 (C-49′), 131.6 (C-49), 131.1 (C-41), 130.3 (C-44), 130.1 (C-45), 129.7 (C-43), 128.5 (C-12), 126.8 (C-42), 114.0 (C-48′), 114.0 (C-48), 96.5 (C-52′), 96.3 (C-52), 80.8 (C-3), 73.8 (C-19), 70.2 (C-2), 55.7 (C-18), 55.0 (C-5), 51.8 (C-37), 51.7 (C-17), 51.1 (C-39), 47.5 (C-36), 47.3 (C-9), 46.7 (C-35), 46.4 (C-54′), 46.1 (C-54), 44.0 (C-1), 41.7 (C-14), 41.1 (C-20), 39.8 (C-8), 39.4 (C-4), 38.9 (C-22), 38.2 (C-10), 32.8 (C-7), 31.0 (C-38), 28.5 (C-23), 28.3 (C-15), 28.1 (C-29), 26.1 (C-21), 24.6 (C-16), 24.5 (C-27), 23.8 (C-11), 21.2 (C-34), 21.0 (C-32), 18.4 (C-6), 17.7 (C-24), 16.7 (C-26), 16.5 (C-25), 16.2 (C-30), 12.8 (C-55′), 12.8 (C-55) ppm; MS (ESI, MeOH): *m/z* (%) = 1079.7 ([M − Cl]$^+$, 100); analysis calcd for $C_{67}H_{91}ClN_4O_8$ (1115.94): C 72.11, H 8.22, N 5.02; found: C 71.96, H 8.41, N 4.88.

4.2.15. 9’-[2’-[[4’-(2α,3α-Diacetyloxy-19α-hydroxyurs-12-en-28-oyl)-2′-aminoethyl]carbonyl]phenyl]-3′,6′-bis(diethylamino)-xanthene (13)

Compound **13** (CAS: [2089122-03-0]) was obtained from **7** (145 mg, 0.24 mmol) according to GP C followed by column chromatography (SiO$_2$, *n*-hexane/ethyl acetate, 7:3) as a colorless solid (170 mg, 66%); R$_f$ = 0.27 (SiO$_2$, *n*-hexane/ethyl acetate, 7:3); m.p. 192–194 °C; IR (ATR): ν = 2970 *m*, 1740 *m*, 1615 *m*, 1513*s*, 1368 *m*, 1219*vs*, 1117*s*, 1031 *m*, 821 *m*, 784 *m*, 757 *m*, 703 m cm^{-1}; ^{1}H NMR (500 MHz, DMSO-*d*$_6$): δ = 7.81–7.75 (m, 1H, 39–H), 7.52–7.43 (m, 2H, 41–H + 40–H), 7.00–6.94 (m, 1H, 42–H), 6.37 (s, 2H, 47′–H + 47–H), 6.33 (s, 2H, 46′–H + 46–H), 6.39–6.29 (m, 2H, 49′–H + 49–H), 5.17–5.07 (m, 2H, 12–H + 2–H), 4.85 (d, *J* = 2.8 Hz, 1H, 3–H), 3.39–3.24 (m, 8H, 51′–H + 51–H), 3.15–3.04 (m, 2H, 36–H$_a$ + 36–H$_b$), 2.81–2.63 (m, 2H, 35′–H + 35–H), 2.53–2.42 (m, 1H, 16–H$_a$), 2.32 (s, 1H, 18–H), 2.06 (s, 3H, 32–H), 1.94–1.61 (m, 3H, 11–H$_a$ + 11–H$_b$ + 9–H), 1.88 (s, 3H, 34–H), 1.60–1.14 (m, 11H, 21–H$_a$ + 1–H$_a$ + 15–H$_a$ + 22–H$_a$ + 7–H$_a$ + 6–H$_a$ + 16–H$_b$ + 22–H$_b$ + 1–H$_b$ + 6–H$_b$ + 20–H), 1.26 (s, 3H, 27–H), 1.14–1.00 (m, 18H, 7–H$_b$ + 5–H + 52′–H + 52–H + 29–H + 21–H$_b$), 0.94 (s, 3H, 24–H), 0.92 (s, 3H, 25–H), 1.08 (d, *J* = 6.7 Hz, 3H, 30–H), 0.81 (s, 3H, 23–H), 0.78–0.72 (m, 1H, 15–H$_b$), 0.42 (s, 3H, 26–H) ppm; ^{13}C NMR (125 MHz, DMSO-*d*$_6$): δ = 176.5 (C-28), 170.1 (C-33), 169.6 (C-31), 167.6 (C-37), 153.9 (C-43), 152.5 (C-50′), 152.5 (C-50), 148.3 (C-48′), 148.3 (C-48), 138.7 (C-13), 132.7 (C-41), 129.7 (C-38), 128.2 (C-40), 128.0 (C-46′), 127.9 (C-46), 126.4 (C-12), 123.5 (C-42), 122.3 (C-39), 108.1 (C-49′), 108.0 (C-49), 104.7 (C-45′), 104.7 (C-45), 97.4 (C-47′), 97.4 (C-47), 76.1 (C-3), 71.9 (C-19), 67.5 (C-2), 64.2 (C-44), 52.6 (C-18), 49.1 (C-5), 46.5 (C-9), 46.3 (C-17), 43.7 (C-51′), 43.7 (C-51), 41.3 (C-20), 40.9 (C-8), 39.7 (C-14), 39.3 (C-10), 39.1 (C-36), 38.3 (C-35), 37.9 (C-1), 37.8 (C-22), 37.6 (C-4), 32.3 (C-7), 27.7 (C-15), 27.5 (C-23), 26.4 (C-29), 26.0 (C-21), 24.5 (C-16), 24.1 (C-27), 22.9 (C-11), 21.3 (C-24), 20.7 (C-34), 20.6 (C-32), 17.5 (C-6), 16.3 (C-30), 16.2 (C-26), 15.7 (C-25), 12.4 (C-52′), 12.4 (C-52) ppm; MS (ESI, MeOH): *m/z* (%) = 1039.7 ([M − Cl]$^+$, 100); analysis calcd for $C_{64}H_{86}N_4O_8$ (1039.41): C 73.96, H 8.34, N 5.39; found: C 73.77, H 8.56, N 5.17.

4.2.16. 9’-[2’-[[4’-(2α,3β-Diacetyloxy-19α-hydroxyurs-12-en-28-oyl)-1′-piperazinyl]carbonyl]phenyl]-3′,6′-bis(diethylamino)-xanthylium chloride (14)

Compound **14** was obtained from **8** (237 mg, 0.37 mmol) according to GP C followed by column chromatography (SiO$_2$, CHCl$_3$/MeOH 9:1) as a pink solid (209 mg, 51%); R$_f$ = 0.35 (SiO$_2$, CHCl$_3$/MeOH 9:1); m.p. 254–258 °C; IR (ATR): ν = 3490*br*, 2929*w*, 1737 *m*, 1633 *m*, 1586*vs*, 1466 *m*, 1411 *m*, 1334*s*, 1244*s*, 1179*vs*, 1131 *m*, 1072 *m*, 1004 *m*, 921 *m*, 823*w*, 772 m cm^{-1}; UV–Vis (MeOH): λ_{max} (log ε) = 259 (4.37), 308 (4.07), 356 (3.74), 562 (4.87) nm; ^{1}H NMR (500 MHz, CDCl$_3$): δ = 7.69–7.59 (m, 2H, 41–H + 40–H), 7.54–7.47 (m, 1H, 39–H), 7.34–7.29 (m, 1H, 42–H), 7.25–7.18 (m, 2H, 47′–H + 47–H), 7.06–6.86 (m, 2H, 46′–H + 46–H), 6.81–6.73 (m, 2H, 49′–H + 49–H), 5.22 (*dd*, *J* = 3.6, 3.6 Hz, 1H, 12–H), 5.03 (*ddd*, *J* = 10.1, 9.4, 4.6 Hz, 1H, 2–H), 4.59 (d, *J* = 10.7 Hz, 1H, 3–H), 3.61 (m, 8H, 51′–H + 51–H), 3.54–3.15 (m, 8H, 35–H$_a$ + 35–H$_b$ + 36–H$_a$ + 36–H$_b$), 2.74 (s, 1H, 18–H), 2.41–2.18 (m, 1H, 16–H$_a$), 2.00 (s, 3H, 32–H), 2.06–1.86 (m, 3H, 1–H$_a$ + 11–H$_a$ + 11–H$_b$), 1.92 (s, 3H, 34–H), 1.86–1.65 (m, 1H, 22–H$_a$), 1.64–1.40 (m, 6H, 21–H$_a$ + 9–H + 16–H$_b$ + 6–H$_a$ + 7–H$_a$ + 22–H$_b$), 1.38–1.23 (m, 3H, 6–H$_b$ + 20–H + 15–H$_a$), 1.28 (t, *J* = 7.1 Hz, 12H, 52′–H + 52–H), 1.23–1.16 (m, 2H, 7–H$_b$ + 21–H$_b$), 1.18 (s, 3H, 27–H), 1.13 (s, 3H, 29–H), 1.06–0.89 (m, 3H, 1–H$_b$ + 15–H$_b$ + 5–H), 0.98 (s, 3H, 25–H), 0.86 (d, *J* = 6.7 Hz, 3H, 30–H), 0.86 (s, 6H, 23–H + 24–H), 0.57 (s, 3H, 26–H), ppm; ^{13}C NMR (125 MHz, CDCl$_3$): δ = 175.0 (C-28), 170.8 (C-33), 170.5 (C-31), 167.7 (C-37), 157.8 (C-50‘), 157.8 (C-50), 155.8 (C-44), 155.7 (C-48’), 155.6 (C-48), 139.0 (C-13), 135.1 (C-43), 132.2 (C-47′), 132.2 (C-47), 130.7 (C-38), 130.4 (C-42), 130.3 (C-40), 130.2 (C-41), 128.3 (C-12), 127.7 (C-39), 114.5 (C-46′), 114.2 (C-46), 113.9 (C-45′), 113.8 (C-45), 96.5 (C-49′), 96.4 (C-49), 80.6 (C-3), 73.6 (C-19), 70.1 (C-2), 55.3 (C-18), 54.9 (C-5), 50.7 (C-17), 47.5 (C-36), 47.2 (C-9), 46.3 (C-51′), 46.2 (C-51), 43.9 (C-1), 42.1 (C-35), 41.7 (C-14), 40.9 (C-20), 39.8 (C-8), 39.4 (C-4), 38.1 (C-10), 34.8 (C-22), 32.8 (C-7), 28.5 (C-23), 28.2 (C-15), 27.9 (C-29), 25.9 (C-21), 25.1 (C-16), 24.6 (C-27), 23.7 (C-11), 21.1 (C-34), 20.9 (C-32), 18.3 (C-6), 17.7 (C-24), 16.7 (C-26), 16.4 (C-25), 16.1 (C-30), 12.7 (C-52′), 12.7 (C-50) ppm; MS (ESI, MeOH): *m/z* (%) = 1065.8 ($[M - Cl]^+$, 100); analysis calcd for $C_{66}H_{89}ClN_4O_8$ (1101.91): C 71.94, H 8.14, N 5.08; found: C 71.77, H 8.33, N 4.81.

4.2.17. 9’-[2’-[[4’-(2α,3β-Diacetyloxy-19α-hydroxyurs-12-en-28-oyl)-4′-homopiperazinyl]carbonyl]phenyl]-3′,6′-bis(diethylamino)-xanthylium chloride (15)

Compound **15** was obtained from **9** (170 mg, 0.26 mmol) according to GP C followed by column chromatography (SiO$_2$, CHCl$_3$/MeOH 9:1) as a pink solid (152 mg, 54%); R$_f$ = 0.17 (SiO$_2$, CHCl$_3$/MeOH 9:1); m.p. 256–260 °C; IR (ATR): ν = 2934*w*, 1736 *m*, 1628 *m*, 1586*vs*, 1466 *m*, 1411 *m*, 1334*s*, 1244*s*, 1178*vs*, 1131*s*, 1072*s*, 1009 *m*, 921 *m*, 823 *m*, 683 m cm^{-1}; UV–Vis (MeOH): λ_{max} (log ε) = 260 (4.31), 309 (4.05), 356 (3.71), 562 (4.87) nm; ^{1}H NMR (500 MHz, CDCl$_3$): δ = 7.68–7.58 (m, 2H, 44–H + 43–H), 7.41 (m, 1H, 42–H), 7.33–7.21 (m, 3H, 45–H + 50′–H + 50–H), 7.17 (m, 2H, 49–H + 49′-H), 6.86–6.71 (m, 2H, 52′–H + 52–H), 5.33–5.23 (m, 1H, 12–H), 5.07 (*ddd*, *J* = 10.9, 10.8, 4.5 Hz, 1H, 3–H), 4.72 (d, *J* = 10.3 Hz, 1H, 2–H), 4.25–3.82 (m, 4H, 39–H + 35–H), 3.76–3.49 (m, 8H, 54′–H + 54–H), 3.33–2.94 (m, 6H, 38–H + 37–H + 36–H), 2.88–2.66 (m, 2H, 18–H + 16–H$_a$), 2.05–1.91 (m, 3H, 1–H$_a$ + 11–H$_a$ + 11–H$_b$), 2.02 (s, 3H, 32–H), 1.94 (s, 3H, 34–H), 1.69–1.42 (m, 6H, 9–H + 16–H$_b$ + 21–H$_a$ + 6–H$_a$ + 7–H$_a$ + 22–H$_a$), 1.40–1.28 (m, 18H, 20–H + 6–H$_b$ + 55′–H + 55–H + 15–H$_a$ + 21–H$_b$ + 7–H$_b$ + 22–H$_b$), 1.20 (s, 3H, 27–H), 1.18 (s, 3H, 29–H), 1.09–0.91 (m, 3H, 1–H$_b$ + 15–H$_b$ + 5–H), 1.00 (s, 3H, 25–H), 0.92 (d, *J* = 6.5 Hz, 3H, 30–H), 0.88 (s, 3H, 24–H), 0.86 (s, 3H, 23–H), 0.65 (s, 3H, 26–H) ppm; ^{13}C NMR (125 MHz, CDCl$_3$): δ = 175.4 (C-28), 170.9 (C-33), 170.6 (C-31), 169.6 (C-40), 157.9 (C-53‘), 157.8 (C-53), 155.9 (C-47), 155.8 (C-51’), 155.7 (C-51), 138.8 (C-13), 135.2 (C-46), 132.8 (C-50′), 132.6 (C-50), 131.9 (C-49′), 131.7 (C-49), 130.9 (C-41), 130.3 (C-45), 130.1 (C-44), 129.7 (C-43), 128.3 (C-12), 126.8 (C-42), 114.0 (C-48′), 113.9 (C-48), 96.6 (C-52′), 96.3 (C-52), 80.8 (C-3), 73.8 (C-19), 70.2 (C-2), 55.7 (C-18), 55.0 (C-5), 52.6 (C-17), 51.8 (C-37), 51.1 (C-39), 47.4 (C-36), 47.3 (C-9), 46.5 (C-35), 46.4 (C-54′), 46.1 (C-54), 44.1 (C-1), 41.8 (C-14), 41.1 (C-20), 39.8 (C-8), 39.5 (C-4), 38.9 (C-22), 38.2 (C-10), 32.8 (C-7), 31.0 (C-38), 28.5 (C-23), 28.3 (C-15), 28.2 (C-29), 26.1 (C-21), 25.6 (C-16), 24.4 (C-27), 23.8 (C-11), 21.2 (C-34), 21.0 (C-32), 18.4 (C-6), 17.7 (C-24), 16.9 (C-26), 16.5 (C-25), 16.2 (C-30), 12.8 (C-55′), 12.8 (C-55) ppm; MS (ESI, MeOH): *m/z* (%) = 1079.7 ($[M - Cl]^+$, 100); analysis calcd for $C_{67}H_{91}ClN_4O_8$ (1115.94): C 72.11, H 8.22, N 5.02; found: C 71.85, H 8.38, N 4.91.

4.2.18. 9’-[2’-[[4’-(2α,3β-Diacetyloxy-19α-hydroxyurs-12-en-28-oyl)-2′-aminoethyl]carbonyl]phenyl]-3′,6′-bis(diethylamino)-xanthene (16)

Compound **16** was obtained from **10** (117 mg, 0.19 mmol) according to GP C followed by column chromatography (SiO$_2$, *n*-hexane/ethyl acetate, 7:3) as a colorless solid (120 mg, 64%); R$_f$ = 0.24 (SiO$_2$, *n*-hexane/ethyl acetate, 7:3); m.p. 195–198 °C; IR (ATR): ν = 2968*w*, 1743 *m*, 1614 *m*, 1512*s*, 1374 *m*, 1230*vs*, 1117*s*, 1035 *m*, 821 *m*, 784 *m*, 757 *m*, 703 m cm^{-1}; ^{1}H NMR (500 MHz, CDCl$_3$): δ = 7.93–7.87 (m, 1H, 39–H), 7.50–7.43 (m, 2H, 41–H + 40–H), 7.10–7.04 (m, 1H, 42–H), 6.45–6.32 (m, 4H, 46–H + 46‘–H + 47–H + 47‘–H), 6.31–6.20 (m, 2H, 49–H + 49‘–H), 5.45 (*dd*, *J* = 4.2, 4.2 Hz, 1H, 12–H), 5.07 (*ddd*, *J* = 11.5, 10.9, 4.5 Hz, 1H, 2–H), 4.74 (d, *J* = 10.3 Hz, 1H, 3–H), 3.39–3.25 (m, 10H, 51–H + 51‘–H + 36–H$_a$ + 36–H$_b$), 3.03–2.94 (m, 1H, 35–H$_a$), 2.84–2.75 (m, 1H, 35–H$_b$), 2.61–2.52 (m, 2H, 18–H + 16–H$_a$), 2.04 (s, 3H, 32–H), 1.97 (s, 3H, 34–H), 2.01–1.85 (m, 3H, 1–H$_a$ + 11–H$_a$ + 11–H$_b$), 1.73–1.60 (m, 4H, 22–H$_a$ + 21–H$_a$ + 9–H + 15–H$_a$), 1.58–1.29 (m, 6H, 16–H$_b$ + 22–H$_b$ + 6–H$_a$ + 7–H$_a$ + 20–H + 6–H$_b$), 1.26 (s, 3H, 29–H), 1.29–1.12 (m, 2H, 7–H$_b$ + 21–H$_b$), 1.24 (s, 3H, 27–H), 1.17 (t, *J* = 7.0 Hz, 12H, 52–H + 52‘–H), 1.07 (t, *J* = 12.2 Hz, 1H, 1–H$_b$), 1.02–0.92 (m, 2H, 5–H + 15–H$_b$), 0.98 (s, 3H, 25–H), 0.94 (d, *J* = 6.7 Hz, 3H, 30–H), 0.88 (s, 3H, 23–H), 0.88 (s, 3H, 24–H), 0.62 (s, 3H, 26–H) ppm; ^{13}C NMR (125 MHz, CDCl$_3$): δ = 177.8 (C-28), 170.9 (C-33), 170.7 (C-31), 170.0 (C-37), 153.9 (C-43), 153.4 (C-50‘), 153.3 (C-50), 149.9 (C-48‘), 149.9 (C-48), 138.6 (C-13), 133.0 (C-41), 130.4 (C-38), 128.8 (C-12), 128.5 (C-46‘), 128.5 (C-46), 128.4 (C-40), 124.0 (C-42), 122.9 (C-39), 108.4 (C-49‘), 108.4 (C-49), 97.9 (C-47‘) 97.8 (C-47), 96.3 (C-45‘), 96.3 (C-45), 80.8 (C-3), 73.7 (C-19), 70.2 (C-2), 65.8 (C-44), 54.9 (C-5), 53.0 (C-18), 47.3 (C-9), 47.1 (C-17), 44.5 (C-51‘), 44.5 (C-51), 44.0 (C-1), 41.5 (C-35), 41.3 (C-14), 41.3 (C-20), 40.1 (C-8), 40.0 (C-36), 39.5 (C-10), 38.5 (C-22), 38.2 (C-4), 32.6 (C-7), 28.6 (C-23), 28.0 (C-15), 27.7 (C-29), 26.4 (C-21), 25.6 (C-16), 24.7 (C-27), 23.9 (C-11), 21.3 (C-34), 21.0 (C-32), 18.5 (C-6), 17.7 (C-24), 17.1 (C-26), 16.4 (C-25), 16.4 (C-30), 12.8 (C-52‘), 12.7 (C-52) ppm; MS (ESI, MeOH): *m/z* (%) = 1039.7 ($[M - Cl]^+$, 100); analysis calcd for $C_{64}H_{86}N_4O_8$ (1039.41): C 73.96, H 8.34, N 5.39; found: C 73.71, H 8.51, N 5.12.

Acknowledgment

We like to thank Dr. D. Ströhl and his team for recording the NMR spectra and the late Dr. R. Kluge for numerous MS measurements; additional MS spectra were recorded by Ms. Th. Schmidt. UV–Vis and IR spectra as well as optical rotations and micro-analyses were performed by Ms. V. Simon, Mr. M. Schneider and S. Ludwig; the cell lines were provided by Dr. T. Müller (Dep. of Oncology, Martin-Luther-University Halle Wittenberg). We also like to thank Mr. J. Radicke for experimental help in the lab especially for preparing several of the starting materials.

Appendix A. Supplementary data

Supplementary data to this article can be found online at https://doi.org/10.1016/j.ejmcr.2022.100043.

References

[1] W.P. Daems, Tormentil potentilla erecta (L.) Baeusch, Chem. Zentralbl. 114 (2) (1943) 1649.

[2] P. Drozdz, A. Sentkowska, K. Pyrzynska, Potentilla erecta (L.) rhizomes as a source of phenolic acids, Nat. Prod. Res. 33 (2019) 2128–2131.

[3] M.F. Melzig, S. Boettger, Tormentillae rhizoma - review for an underestimated European herbal drug, Planta Med. 86 (2020) 1050–1057.

[4] V.N. Bubenchikova, S.A. Prokhorova, Y.A. Sukhomlinov, Study of the composition of phenolic compounds of Tragopogon and Potentilla plants by HPLC, Sorbtsionnye Khromatogr. Protsessy 12 (2012) 85–88.

[5] Y. He, Q. Wu, S.H. Hansen, C. Cornett, C. Moller, P. Lai, Differentiation of tannin-containing herbal drugs by HPLC fingerprints, Pharmazie 68 (2013) 155–159.

[6] C. Moeller, S.H. Hansen, C. Cornett, Characterisation of tannin-containing herbal drugs by HPLC, Phytochem. Anal. 20 (2009) 231–239.

[7] J. Moilanen, J. Sinkkonen, J.-P. Salminen, Characterization of bioactive plant ellagitannins by chromatographic, spectroscopic and mass spectrometric methods, Chemoecology 23 (2013) 165–179.

[8] D. Anheyer, A.K. Koch, R. Lauche, J. Langhorst, G. Dobos, H. Cramer, J. Frawley, R. Lauche, H. Cramer, A.K. Koch, J. Langhorst, Herbal medicines for gastrointestinal disorders in children and adolescents: a systematic review, Pediatrics 139 (2017), e20170062.

[9] S. Shushunov, L. Balashov, A. Kravtsova, I. Krasnogorsky, K.P. Latte, A. Vasiliev, Determination of acute toxicity of the aqueous extract of potentilla erecta (tormentil) rhizomes in rats and mice, J. Med. Food 12 (2009) 1173–1176.

[10] M. Tomczyk, K.P. Latte, Potentilla-A review of its phytochemical and pharmacological profile, J. Ethnopharmacol. 122 (2009) 184–204.

[11] U. Wolfle, J. Hoffmann, B. Haarhaus, C.M. Schempp, M.V. Rao, Anti-inflammatory and vasoconstrictive properties of Potentilla erecta - a traditional medicinal plant from the northern hemisphere, J. Ethnopharmacol. 204 (2017) 86–94.

[12] H. von Bingen, Hildegard von Bingen - Komplette Werkausgabe, Beuroner Kunstverlag, Eibingen-Abtei St. Hildegard, 2017.

[13] Z.-J. Lia, C.-P. Wan, L. Cai, S.-Q. Li, X. Zheng, Y. Qi, J.-W. Dong, T.-P. Yin, Z.-X. Zhou, N.-H. Tan, Z.-T. Ding, Terpenoids with cytotoxic activity from the branches and leaves of Pyrus pashia, Phytochem. Lett. 13 (2015) 246–251.

[14] Y. Shi, D. Zhang, S. Li, X. Xuan, L. Zhang, Y. Li, F. Guo, Inhibitors of BRD4 protein from the roots of Astilbe grandis Stapf ex E.H. Wilson, Nat. Prod. Res. 35 (2019) 2044–2050.

[15] R. Wang, M. Jin, C. Jin, J. Sun, C. Ye, T. Zong, G. Chen, W. Zhou, G. Li, Three new ursane-type triterpenoids from the roots of Sanguisorba officinalis L. and their cytotoxic activity, Phytochem. Lett. 32 (2019) 96–100.

[16] K.W. Woo, J.Y. Han, S.U. Choi, K.H. Kim, K.R. Lee, Triterpenes from Perilla frutescens var. acuta and their cytotoxic activity, Nat. Prod. Sci. 20 (2014) 71–75.

[17] Y. Yang, H. Jia, B. Li, D. Xing, Y. Wang, M. Zhao, Tormentic acid inhibits IL-1β-induced chondrocyte apoptosis by activating the PI3K/Akt signaling pathway, Mol. Med. Rep. 17 (2018) 4753–4758.

[18] M. Alfaifi, A. Alsayari, N. Gurusamy, J. Louis, S.E. Elbehairi, K. Venkatesan, S. Annadurai, Y.I. Asiri, A. Shati, K. Saleh, H. Alboushnak, H. Handoussa, A. Bin Muhsinah, A. Abdel Motaal, Analgesic, anti-inflammatory, cytotoxic activity screening and UPLC-PDA-ESI-MS Metabolites determination of bioactive fractions of Kleinia pendula, Molecules 25 (2020) 418.

[19] L.P. Sandjo, V. Rincheval, B.T. Ngadjui, G. Kirsch, Cytotoxic effect of some pentacyclic triterpenes and hemisynthetic derivatives of stigmasterol, Chem. Nat. Compd. 47 (2011) 731–734.

[20] Y. Yang, Y. Wang, M. Zhao, H. Jia, B. Li, D. Xing, Tormentic acid inhibits IL-1β-induced chondrocyte apoptosis by activating the PI3K/Akt signaling pathway, Mol. Med. Rep. 17 (2018) 4753–4758.

[21] J. Zhang, C. Liu, R.-Z. Huang, H.-F. Chen, Z.-X. Liao, J.-Y. Sun, X.-K. Xia, F.-X. Wang, Three new C-27-carboxylated-lupane-triterpenoid derivatives from Potentilla discolor Bunge and their in vitro antitumor activities, PLoS One 12 (2017) e0175502/0175501-e0175502/0175518.

[22] B.T. Zhao, D.H. Nguyen, B.M. Lee, S.H. Seong, J.S. Choi, B.S. Min, M.H. Woo, PTP1B inhibitory and cytotoxic activities of triterpenoids from the aerial parts of Agrimonia pilosa, Med. Chem. Res. 26 (2017) 2870–2878.

[23] R. Csuk, R. Schäfer, C. Dressel, Process for the Extraction of Tormentic Acid from Potentilla Erecta, 2015. Ger. Offen. DE10201301079 A1 20150611.

[24] R. Csuk, B. Siewert, C. Dressel, R. Schaefer, Tormentic acid derivatives: synthesis and apoptotic activity, Eur. J. Med. Chem. 56 (2012) 237–245.

[25] O. Kraft, J. Wiemann, A. Al-Harrasi, R. Csuk, En route to anti-glioblastoma active pomolic acid, Phytochem. Lett. 32 (2019) 29–32.

[26] J. Wiemann, A.M. Deckelmann, R. Csuk, A remarkably simple and convergent partial synthesis of pomolic acid, Tetrahedron Lett. 57 (2016) 3952–3953.

[27] R.S. Chandel, R.P. Rastogi, Acuminatic acid, a new triterpene from Pygeum acuminatum Coleb, Indian J. Chem., Sect. B 15B (1977) 914–916.

[28] G.Y. Liang, A.I. Gray, P.G. Waterman, Pentacyclic triterpenes from the fruits of Rosa sterilis, J. Nat. Prod. 52 (1989) 162–166.

[29] T. Seto, T. Tanaka, O. Tanaka, N. Naruhashi, β-Glucosyl esters of 19α-hydroxyursolic acid derivatives in leaves of Rubus species, Phytochemistry 23 (1984) 2829–2834.

[30] K. Takahashi, S. Kawaguchi, K. Nishimura, K. Kubota, Y. Tanabe, M. Takani, Constituents of medicinal plants. XIII. Constituents of the pericarps of the capsules of Euscaphis japonica. 1, Chem. Pharm. Bull. 22 (1974) 650–653.

[31] D.A.C. Biggs, R.B.R. Porter, W.F. Reynolds, L.A.D. Williams, A new hyptadienic acid derivative from Hyptis verticillata (Jacq.) with insecticidal activity, Nat. Prod. Commun. 3 (2008) 1759–1762.

[32] P. Potier, B. Das, A.M. Bui, M.M. Janot, A. Pourrat, H. Pourrat, Structure of tormentic acid, a pentacyclic triterpene acid isolated from the roots of Potentilla tormentilla, Bull. Soc. Chim. Fr. (1966) 3458–3465.

[33] C. Terreaux, M.P. Maillard, M.P. Gupta, K. Hostettmann, Triterpenes and triterpene glycosides from Paradrymonia macrophylla, Phytochemistry 42 (1996) 495–499.

[34] T. Yamagishi, D.C. Zhang, J.J. Chang, D.R. McPhail, A.T. McPhail, K.H. Lee, Antitumor agents. Part 94. The cytotoxic principles of Hyptis capitata and the structures of the new triterpenes hyptatic acid A and B, Phytochemistry 27 (1988) 3213–3216.

[35] N. Heise, S. Hoenke, V. Simon, H.P. Deigner, A. Al-Harrasi, R. Csuk, Type and position of linkage govern the cytotoxicity of oleanolic acid rhodamine B hybrids, Steroids 172 (2021) 108876.

[36] S. Hoenke, I. Serbian, H.P. Deigner, R. Csuk, Mitocanic di- and triterpenoid rhodamine B conjugates, Molecules 25 (2020) 5443.

[37] M. Kahnt, J. Wiemann, L. Fischer, S. Sommerwerk, R. Csuk, Transformation of asiatic acid into a mitocanic, bimodal-acting rhodamine B conjugate of nanomolar cytotoxicity, Eur. J. Med. Chem. 159 (2018) 143–148.

[38] I. Serbian, S. Hoenke, O. Kraft, R. Csuk, Ester and amide derivatives of rhodamine B exert cytotoxic effects on different human tumor cell lines, Med. Chem. Res. 29 (2020) 1655–1661.

[39] S. Sommerwerk, L. Heller, C. Kerzig, A.E. Kramell, R. Csuk, Rhodamine B conjugates of triterpenoic acids are cytotoxic mitocans even at nanomolar concentrations, Eur. J. Med. Chem. 127 (2017) 1–9.

[40] R.K. Wolfram, L. Fischer, R. Kluge, D. Ströhl, A. Al-Harrasi, R. Csuk, Homopiperazine-rhodamine B adducts of triterpenoic acids are strong mitocans, Eur. J. Med. Chem. 155 (2018) 869–879.

[41] R.K. Wolfram, L. Heller, R. Csuk, Targeting mitochondria: esters of rhodamine B with triterpenoids are mitocanic triggers of apoptosis, Eur. J. Med. Chem. 152 (2018) 21–30.

[42] Z.H. Qin, W.W. Su, P. Liu, J.M. Ma, Y.R. Zhang, T.F. Jiao, Facile preparation of a rhodamine B derivative-based fluorescent probe for visual detection of iron ions, ACS Omega 6 (2021) 25040–25048.

[43] M. Matsui, T. Yamamoto, K. Kakitani, S. Biradar, Y. Kubota, K. Funabiki, UV-vis absorption and fluorescence spectra, solvatochromism, and application to pH sensors of novel xanthene dyes having thienyl and thieno[3,2-b]thienyl rings as auxochrome, Dyes Pigments 139 (2017) 533–540.

[44] A. Numata, P.M. Yang, C. Takahashi, R. Fujiki, M. Nabae, E. Fujita, Cytotoxic triterpenes from a Chinese-medicine, Goreishi, Chem Pharm Bull 37 (1989) 648–651.

[45] N. Hirai, M. Sugie, M. Wada, E.H. Lahlou, T. Kamo, R. Yoshida, M. Tsuda, H. Ohigashi, Triterpene phytoalexins from strawberry fruit, Biosci Biotech Bioch 64 (2000) 1707–1712.

P3

International Journal of
Molecular Sciences

MDPI

Article

Madecassic Acid—A New Scaffold for Highly Cytotoxic Agents

Oliver Kraft, Ann-Kathrin Hartmann, Sophie Hoenke, Immo Serbian and René Csuk *

Organic Chemistry, Martin-Luther-University Halle-Wittenberg, Kurt-Mothes-Str. 2,
D-06120 Halle (Saale), Germany; oliver.kraft@chemie.uni-halle.de (O.K.); ak.hartmann@gmx.de (A.-K.H.);
sophie.hoenke@chemie.uni-halle.de (S.H.); immoserbian@gmail.com (I.S.)
* Correspondence: rene.csuk@chemie.uni-halle.de

Abstract: Due to their manifold biological activities, natural products such as triterpenoids have advanced to represent excellent leading structures for the development of new drugs. For this reason, we focused on the syntheses and cytotoxic evaluation of derivatives obtained from gypsogenin, hederagenin, and madecassic acid, cytotoxicity increased—by and large—from the parent compounds to their acetates. Another increase in cytotoxicity was observed for the acetylated amides (phenyl, benzyl, piperazinyl, and homopiperazinyl), but a superior cytotoxicity was observed for the corresponding rhodamine B conjugates derived from the (homo)-piperazinyl amides. In particular, a madecassic acid homopiperazinyl rhodamine B conjugate **24** held excellent cytotoxicity and selectivity for several human tumor cell lines. Thus, this compound was more than 10,000 times more cytotoxic than parent madecassic acid for A2780 ovarian cancer cells. We assume that the presence of an additional hydroxyl group at position C–6 in derivatives of madecassic, as well as the (2α, 3β) configuration of the acetates in ring A, had a beneficial effect onto the cytotoxicity of the conjugates, as well as onto tumor/non-tumor cell selectivity.

Keywords: madecassic acid; gypsogenin; hederagenin; cytotoxicity; mitocan

check for updates

Citation: Kraft, O.; Hartmann, A.-K.; Hoenke, S.; Serbian, I.; Csuk, R. Madecassic Acid—A New Scaffold for Highly Cytotoxic Agents. *Int. J. Mol. Sci.* **2022**, *23*, 4362. https://doi.org/10.3390/ijms23084362

Academic Editor: Daniela Grimm

Received: 23 March 2022
Accepted: 13 April 2022
Published: 14 April 2022

Publisher's Note: MDPI stays neutral with regard to jurisdictional claims in published maps and institutional affiliations.

Copyright: © 2022 by the authors. Licensee MDPI, Basel, Switzerland. This article is an open access article distributed under the terms and conditions of the Creative Commons Attribution (CC BY) license (https://creativecommons.org/licenses/by/4.0/).

1. Introduction

Despite all efforts and tremendous achievements in the fight against cancer, in 2020 10 million people worldwide died as a consequence of this disease [1], and 19.3 million new cases were reported by the International Agency for Research on Cancer [2]. Many chemotherapeutic agents hitherto used for the therapy of cancer are natural products or derived from them. Several compounds derived from pentacyclic triterpenes were successfully encountered as highly cytotoxic as well as exhibiting pronounced tumor-selectivity [3–7]. A closer look into this class of compounds, however, revealed that research was mainly focused on derivatives of betulinic, ursolic, and oleanolic acid and—to a minor extent—of glycyrrhetinic acid [8–15]. The number of investigations dealing with cytotoxic agents derived from gypsogenin, hederagenin, or madecassic acid, however, remained small over many years [16–19]. This may be due to the fact that the availability of these compounds is considered to be worse than that of, for example, betulinic acid [20–22]. This has changed as gypsogenin can now be obtained in good yields from the corresponding saponin (which is available in large technical quantities). Hederagenin was previously only available from extracts from the pericarp of the soap tree [23,24]. However, it is now even more convenient, obtained by a partial synthesis from also readily available gypsogenin [23]. Furthermore, hederagenin and gypsogenin can be interconverted into each other by a short sequence and in good yields [23].

Recently, we were able to show that acetylated pentacyclic triterpenoid amides are highly cytotoxic for many human tumor cell lines [24–27], while parent triterpenoic acids possess low cytotoxicity. The cytotoxicity of these compounds, however, intensifies upon acetylation and amidation, and even more by linking them with rhodamine B [28]. Thus, the synthesis of different rhodamine B conjugates has moved into the focus of scientific interest [25–27,29]. For example, benzyl-, piperazinyl-, and homopiperazinyl-amides and their resulting rhodamine B conjugates show cytotoxic effects even in nanomolar concentration. The presence of an extra cationic moiety such as a rhodamine B scaffold enhances their cytotoxic activity tremendously. However, many of these conjugates were also less cytotoxic to non-malignant fibroblasts (NIH 3T3) [26–28,30]. As a consequence of these promising results, and to have a closer look into this class of compounds, gypsogenin and hederagenin were chosen as starting materials for further studies. For comparison, madecassic acid was also included to investigate the possible influence of the presence of extra hydroxyl groups onto cytotoxic activity and selectivity. During our work, different acetylated triterpenoic derivatives modified at their carboxylic group were accessed, such as substituted benzyl, piperazinyl, and homopiperazinyl amides which were subsequently linked at their distal amino group as an amide to a rhodamine B moiety. Previous studies showed an increase in malignant cells' membrane potential in relation to non-malignant cells. Thus, cationic compounds such as rhodamine B conjugates accumulate in these areas and cause selective cell death [31,32]. This is regarded as the main reason for the selective cell death of tumor cells upon incubation with the rhodamine B conjugates.

Our main objective was to find out whether triterpene amides, as well as spacered triterpene rhodamine conjugates, exhibit good cytotoxicity when the pentacyclic triterpene skeleton holds a vicinal hydroxyl groups in ring A, and optionally another hydroxyl group at another position. These requirements are fulfilled, for example, by the compounds gypsogenin, hederagenin, or madecassic acid. This should also allow a comparison with the conjugates of ursolic, oleanolic, and maslinic acid presented earlier.

Thus, a set of novel terpenoic amides and their rhodamine B conjugates was synthesized, and the cytotoxicity of the compounds was determined by sulforhodamine B (SRB) assays.

2. Results and Discussion

2.1. Chemistry

Hydrolysis of Gypsophila saponin provided gypsogenin as previously reported (**1**, Scheme 1), whose reduction with $NaBH_4$ gave hederagenin (**2**) in 78% isolated yield [23]; madecassic acid (**3**) was purchased from different local suppliers.

Acetylation of **1**–**3** gave acetates **4**–**6,** respectively [16,24,27]. These compounds were each treated with oxalyl chloride followed by the addition of benzylamine, aniline, piperazine, or homopiperazine to furnish amides **7**–**18**, respectively.

Coupling amides **9**, **10**, **13**, **14**, **17**, and **18** with rhodamine B (after having being activated in situ with oxalyl chloride) gave the rhodamine B conjugates **19**–**24**, respectively (Scheme 2) [33].

Thus, compounds **19**–**24** can be regarded as analogs of previously reported piperazinyl and homopiperazinyl rhodamine B conjugates [26,33], whereas **7**, **8**, **11**, **12**, **15**, and **16** are structurally similar to the benzyl- and phenylamides previously reported by Siewert et al. [30] and Kaminskyy et al. [34] However, compounds of this study differ from those previously synthesized from ursolic, oleanolic, glycyrrhetinic, betulinic, or platanic acid inasmuch as the conjugates of this study hold (an) extra hydroxyl group(s) (protected, in part, as an acetate).

2.2. Biological Evaluation

To assess their cytotoxicity parent, triterpenoic acids **1**–**3**, their acetates **4**–**6**, the amides **7**–**18,** as well as the respective rhodamine B conjugates **19**–**24** were subjected to SRB assays employing several human tumor cell lines (A375, HT29, MCF-7, A2780, and HeLa) as well as non-malignant fibroblasts (NIH 3T3). The results from these assays are compiled in Table 1. The EC_{50} values in μM from SRB assays were determined after 72 h of treatment, and the values are averaged from three independent experiments performed each in triplicate, confidence interval CI = 95%; mean ± standard mean error).

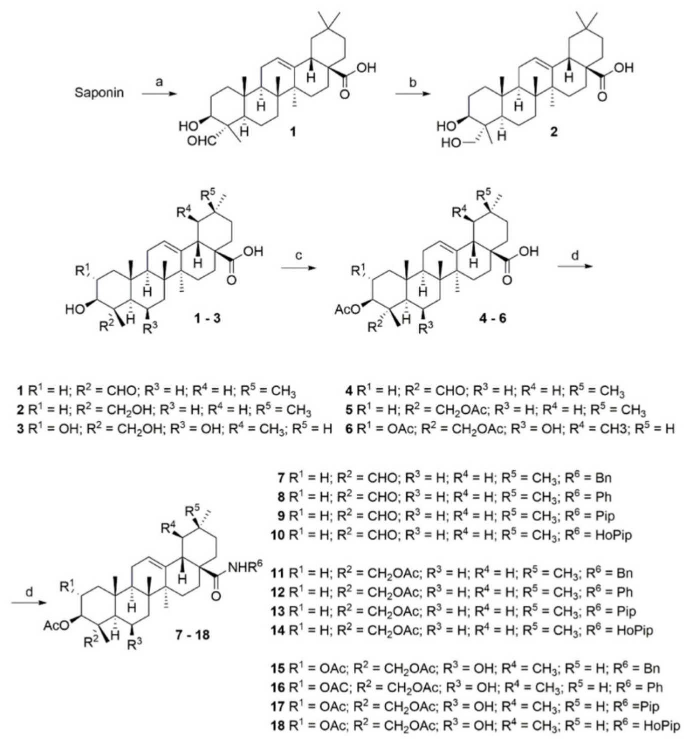
Saponin
a
b
c
d
OH
O
HO
OHC
H
1
2
1 - 3
4 - 6
7 - 18
R1
R2
R3
R4
R5
AcO
NHR6
1 R1 = H; R2 = CHO; R3 = H; R4 = H; R5 = CH3
2 R1 = H; R2 = CH2OH; R3 = H; R4 = H; R5 = CH3
3 R1 = OH; R2 = CH2OH; R3 = OH; R4 = CH3; R5 = H
4 R1 = H; R2 = CHO; R3 = H; R4 = H; R5 = CH3
5 R1 = H; R2 = CH2OAc; R3 = H; R4 = H; R5 = CH3
6 R1 = OAc; R2 = CH2OAc; R3 = OH; R4 = CH3; R5 = H
7 R1 = H; R2 = CHO; R3 = H; R4 = H; R5 = CH3; R6 = Bn
8 R1 = H; R2 = CHO; R3 = H; R4 = H; R5 = CH3; R6 = Ph
9 R1 = H; R2 = CHO; R3 = H; R4 = H; R5 = CH3; R6 = Pip
10 R1 = H; R2 = CHO; R3 = H; R4 = H; R5 = CH3; R6 = HoPip
11 R1 = H; R2 = CH2OAc; R3 = H; R4 = H; R5 = CH3; R6 = Bn
12 R1 = H; R2 = CH2OAc; R3 = H; R4 = H; R5 = CH3; R6 = Ph
13 R1 = H; R2 = CH2OAc; R3 = H; R4 = H; R5 = CH3; R6 = Pip
14 R1 = H; R2 = CH2OAc; R3 = H; R4 = H; R5 = CH3; R6 = HoPip
15 R1 = OAc; R2 = CH2OAc; R3 = OH; R4 = CH3; R5 = H; R6 = Bn
16 R1 = OAC; R2 = CH2OAc; R3 = OH; R4 = CH3; R5 = H; R6 = Ph
17 R1 = OAc; R2 = CH2OAc; R3 = OH; R4 = CH3; R5 = H; R6 =Pip
18 R1 = OAc; R2 = CH2OAc; R3 = OH; R4 = CH3; R5 = H; R6 = HoPip

Scheme 1. Reactions and conditions: (**a**) aq. HCl, 60 °C, 5 d, 2%; (**b**) $NaBH_4$, THF/MeOH, 0 °C, 2 h, 72%; (**c**) Ac2O, NEt_3, DMAP (cat.), DCM, 23 °C, 1 h, **4** (79%), **5** (94%), **6** (78%); (**d**) $(COCl)_2$, DCM, DMF (cat.), then amine, 23 °C, 1 h; → **7** (81%), **8** (65%), **9** (64%), **10** (83%), **11** (52%), **12** (98%), **13** (80%), **14** (41%), **15** (41%), **16** (60%), **17** (41%), and **18** (81%).

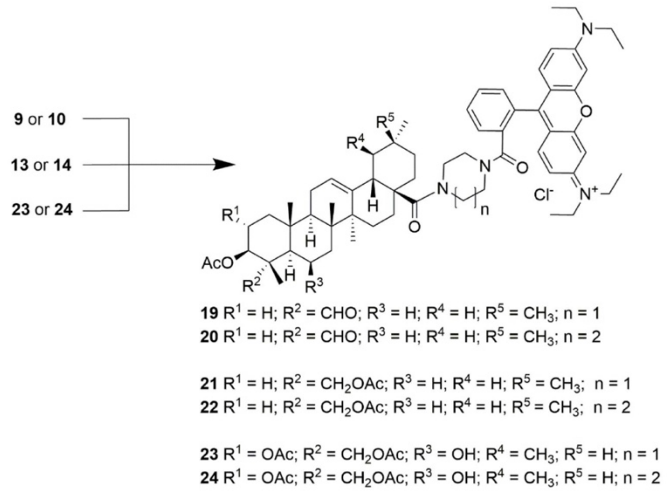
9 or 10
13 or 14
23 or 24
R1
R2
R3
R4
R5
AcO
H
O
N
n
Cl-
N+
19 R1 = H; R2 = CHO; R3 = H; R4 = H; R5 = CH3; n = 1
20 R1 = H; R2 = CHO; R3 = H; R4 = H; R5 = CH3; n = 2
21 R1 = H; R2 = CH2OAc; R3 = H; R4 = H; R5 = CH3; n = 1
22 R1 = H; R2 = CH2OAc; R3 = H; R4 = H; R5 = CH3; n = 2
23 R1 = OAc; R2 = CH2OAc; R3 = OH; R4 = CH3; R5 = H; n = 1
24 R1 = OAc; R2 = CH2OAc; R3 = OH; R4 = CH3; R5 = H; n = 2

Scheme 2. Reactions and conditions: rhodamine B, $(COCl)_2$, DCM, NEt_3 (cat.), DMF (cat.), 23 °C, 1 h, then starting material, 0 °C → 23 °C, 1 h; → **19** (64%), **20** (56%), **21** (47%), **22** (31%), **23** (56%), and **24** (48%).

Table 1. SRB assay: EC50 values (µM) after 72 h of treatment; averaged from three independent experiments performed each in triplicate; confidence interval CI = 95%. Human cancer cell lines: A375 (melanoma), HT29 (colorectal carcinoma), MCF7 (breast adenocarcinoma), A2780 (ovarian carcinoma), HeLa (cervical carcinoma), and (NIH 3T3 (non-malignant fibroblasts); cut-off 30 µM, n.d. not determined. Doxorubicin (DX) has been used as a positive standard.

#	A375	HT29	MCF7	A2780	HeLa	NIH 3T3
1	17.3 ± 1.6	>30	18.5 ± 2.2	13.0 ± 1.6	25.0 ± 4.1	16.7 ± 2.8
2	26.3 ± 1.8	>30	25.7 ± 1.9	19.6 ± 1.6	>30	>30
3	>30	>30	>30	>30	n.d.	>30
4	>30	>30	24.6 ± 4.7	18.7 ± 2,7	>30	13.0 ± 1,5
5	17.1 ± 1.1	19.0 ± 0.6	9.8 ± 1.0	11.9 ± 0.5	12.4 ± 0.7	9.6 ± 0.6
6	3.5 ± 0.5	14.5 ± 1.1	7.1 ± 0.6	8.1 ± 0.7	n.d.	7.6 ± 0.8
7	3.3 ± 0.3	10.7 ± 1.8	8.8 ± 1.6	4.4 ± 0.3	n.d.	18.5 ± 4.6
8	7.9 ± 3.3	>30	>30	19.9 ± 1.4	n.d.	>30
9	1.5 ± 0.2	1.7 ± 0.3	2.1 ± 0.3	1.6 ± 0.2	n.d.	2.3 ± 0.3
10	1.6 ± 0.6	0.7 ± 0.1	2.0 ± 0.2	1.7 ± 0.5	1.7 ± 0.3	1.4 ± 0.2
11	1.1 ± 0.6	3.8 ± 0.7	3.4 ± 0.4	1.3 ± 0.3	n.d.	>30
12	0.6 ± 0.2	1.9 ± 0.6	1.9 ± 0.1	0.8 ± 0.2	n.d.	>30
13	1.3 ± 0.4	1.9 ± 0.5	1.9 ± 0.4	1.4 ± 0.2	n.d.	2.0 ± 0.3
14	1.2 ± 0.3	1.9 ± 0.1	1.7 ± 0.2	2.0 ± 0.2	2.2 ± 0.3	1.7 ± 0.3
15	1.0 ± 0.1	2.3 ± 0.2	2.7 ± 0.4	1.4 ± 0.1	n.d.	17.9 ± 2.1
16	1.3 ± 0.1	3.7 ± 0.4	4.5 ± 0.9	2.2 ± 0.1	n.d.	21.1 ± 1.1
17	1.9 ± 0.4	2.1 ± 0.6	2.0 ± 0.4	2.1 ± 0.3	n.d.	2.4 ± 0.6
18	2.2 ± 0.3	2.4 ± 0.4	2.4 ± 0.3	2.8 ± 0.3	n.d.	2.5 ± 0.2
19	n.d.	n.d.	n.d.	n.d.	n.d.	n.d.
20	0.0319 ±0.0036	0.0566 ±0.0123	0.0558 ± 0.0072	0.0131 ± 0.0007	0.1021 ± 0.0263	0.1600 ± 0.0226
21	0.055 ± 0.01	0.086 ± 0.01	0.066 ± 0.008	0.025 ± 0.002	-	0.305 ± 0.06
22	0.031 ± 0.007	0.083 ± 0.02	0.086 ± 0.01	0.018 ± 0.001	-	0.441 ± 0.12
23	0.055 ± 0.01	0.108 ± 0.02	0.054 ± 0.01	0.015 ± 0.001	-	0.277 ± 0.03
24	0.0095 ± 0.0015	0.0127 ± 0.0038	0.0162 ± 0.0045	0.0029 ± 0.0005	0.0526 ± 0.0151	0.1013 ± 0.0231
DX	n.d.	0.9 ± 0.2	1.1 ± 0.3	0.02 ± 0.01	n.d.	1.7 ± 0.3

As a result, and as expected, the parent compounds **1**–**3** (holding unsubstituted hydroxyl groups) were—by and large—less cytotoxic than their corresponding acetates **4**–**6**. The former compounds showed some cytotoxicity for all human tumor cell lines and moderate selectivity.

The latter compounds, however, holding one or more acetyl groups at positions 2, 3, and 23, showed an increased cytotoxic activity for all cancer lines, with EC_{50} values as low as EC_{50} = 3.50 µM (for A375 and compound **6**).

Transforming the carboxyl group into an amide led to compounds of increased cytotoxic effects onto the tumor cells. Benzylamides (**7**, **11**, and **15**), phenyl amides (**8**, **12**, and **16**), piperazinyl amides (**9**, **13**, and **17**) and homopiperazinyl amides (**10**, **14**, and **18**) held high cytotoxicity and moderate selectivity. In this series of compounds, hederagenin derived phenyl amide **12** was most cytotoxic with an EC_{50} value of 0.66 µM for A375 tumor cells. Comparing the cytotoxic effects of phenyl- and benzyl amides conjugates with those measured for the corresponding piperazinyl and homopiperazinyl analogues showed the former of higher cytotoxicity but also of an improved selectivity (malignant vs. non-malignant cells).

Rhodamine B analogues **19**–**24** showed both an increased cytotoxicity but also improved selectivity. The lowest EC_{50} value was determined for **24** with EC_{50} = 0.0029 ± 0.0005 for A2780 ovarian tumor cells.

The selectivity between malignant cells and the non-malignant cells was also affected by the kind of spacer linking the triterpene with the rhodamine B moiety. Thereby, a significant difference in cytotoxicity was detected between compounds holding a homopiperazinyl (**20**, **22**, and **24**) instead of piperazinyl spacer (**19**, **21**, and **23**).

As a result, compound **24**, the most active as well as selective compound with homopiperazinyl spacer, was nearly 10,000 times more cytotoxic than parent madecassic acid.

The mode of action—as previously shown for several triterpene-rhodamine B conjugates—is to act as mitocans. To demonstrate this also for **24**—the most cytotoxic compound of this study—A375 cells were stained with acridine orange (AO), rhodamine 123, and Hoechst 33,342. Thereby, Hoechst 33,342 binds selectively to DNA while rhodamine 123 is usually applied for dying mitochondria. The results of these staining experiments are depicted in Figure 1 and prove that **24** also acts as a mitocan, as this compound is localized within the cells exactly in the same area as rhodamine 123, while a location in the nucleus can be ruled out from the staining experiments using Hoechst 33,342.

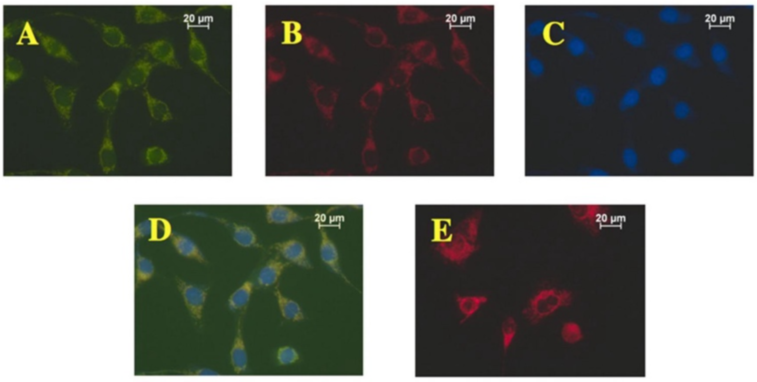

Figure 1. Staining experiments: A375 cells, 48 h; (**A**): control; (**B**): in the presence of **24**; (**C**): Hoechst 33,342 staining; (**D**): merged (Hoechst 33,342, control); and (**E**): in the presence of rhodamine 123.

The influence of an extra hydroxyl group in ring B can best be seen from the cytotoxicity of the analogs of madecassic acid. The results from the SRB assays showed compounds **3**, **6**, **15**, **16**, **17**, **18**, **23**, and **24** as cytotoxic with EC_{50} values as low as 0.015 ± 0.001 μM; for compound **24** and A2780 cells, a selectivity index $SI_{EC50,\ NIH\ 3T3/EC50,\ A2780}$ of approximately 20 can be calculated. From these results, we conclude that the presence of an additional hydroxyl group at position C-6 in the triterpenoid skeleton might be responsible for a significantly improved cytotoxicity.

As compounds holding two acetyl groups in ring A with (2α, 3β) configuration (such as **24** or the analogues prepared earlier from maslinic or tormentic acid) are clearly more cytotoxic than those bearing only one acetyl group (such as oleanolic and ursolic, but also glycyrrhetinic, betulinic, or platanic acid), this confirms our original working hypothesis. At present, triterpenes with a larger number of hydroxyl or acetyl groups are being converted to the corresponding spacered rhodamine B conjugates in our laboratories in order to verify whether the trend shown here has general validity.

3. Materials and Methods

3.1. General

A detailed description of materials and methods can be found in the Supplementary Materials File. For biological screening, the cell lines were obtained from ATCC: A375 (CRL-1619), HT29 (HTB-38), MCF7 (HTP-22), A2780 (HTP-77), HeLa (CCL-2), and NIH 3T3 (CRL-1573) ^{13}C NMR spectra (Supplementary Materials) were recorded as APT spectra showing CH and CH_3 groups as positive signals and CH_2 groups and quaternary carbons as negative signals.

3.2. General Procedure for the Acetylation of Triterpenoic Acids (GPA)

The triterpenoic acids **1**–**3** (1 eq.) were each dissolved in dry DCM (20 mL), treated with TEA (4.5 eq.), DMAP (cat.), and acetic anhydride (4.0 eq.). The mixture was stirred at room temperature for 24 h; for work-up, aq. ammonium hydroxide (7 M, 0.5 mL) was added. After 30 min, the mixture was diluted with Et_2O (250 mL), washed with HCl (0.1 M, 1 × 250 mL), water (2 × 250 mL), and brine (1 × 125 mL), dried with $MgSO_4$, and the organic phase was concentrated under reduced pressure. The crude product was subjected to column chromatography (SiO_2, *n*-hexane/ethyl acetate) to afford compounds **4**–**6**, each as a colorless solid.

3.3. General Procedure for the Synthesis of of Triterpenoic Amides 7–18 (GPB)

To a solution of **4**–**6** (1 eq.) in dry DCM (10 mL), oxalyl chloride (4 eq.), DMF (0.24 eq.), and TEA (0.24 eq.) were added. After stirring for 2 h at room temperature, the solvent was removed under reduced pressure, re-evaporated with DCM (3 × 10 mL), and the residue was dissolved in dry DCM (10 mL). A solution of the respective amine or diamine (3 eq.) in dry DCM, TEA (1 eq.), and DMAP (cat.) was added, and stirring at room temperature was continued until completion of the reaction (as indicated by TLC). The solvent was removed under reduced pressure, and the crude product was subjected to column chromatography to yield compounds **7**–**18**.

3.4. General Procedure for Synthesis of Rhodamine B Conjugates 19–24 (GPC)

A solution of rhodamine B (1.5 eq.), oxalyl chloride (6 eq.), DMF (0.2 eq.), and TEA (0.2 eq.) in dry DCM (30 mL) was stirred at ambient temperature for 3 h. The solvent was removed under reduced pressure, re-evaporated with dry DCM (3 × 30 mL), and the residue was dissolved in dry DCM (30 mL). To this solution, compounds **9**, **10**, **13**, **14**, **17**, or **18** (1 eq.), TEA (1.5 eq.), and DMAP (cat.) were added. After stirring for 1 h, the solvent was removed under reduced pressure, and the resulting solid was subjected to column chromatography (SiO_2, chloroform/methanol, 9:1 or *n*-hexane/ethyl acetate, 7:3) to yield compounds **19**–**24**, each as a purple solid.

*3.5. (3β,4α) 3-Hydroxy-23-oxoolean-12-en-28-oic Acid (**1**) [639-14-5]*

The saponin of *Gypsophila* (300 g; Dr. H. Schmittmann GmbH, Velbert, Germany) was treated with aq. hydrochloric acid (15%, 1000 mL) at 60 °C for 120 h. The solvent was removed under reduced pressure, the residue was air dried, grounded, and extracted with ethyl acetate (2 L) under reflux. The solvent was evaporated, and the dark brown residue was subjected to column chromatography (SiO_2, *n*-hexane/ethyl acetate, 7:3) to yield **1** (6.2 g) as a colorless solid; m.p.: 275–278 °C (lit.: [24] 274–276 °C); $[\alpha]_D^{20}$ = +89.5° (*c* = 0.5, EtOH), [lit.: [35] $[\alpha]_D^{20}$ = +91.4° (*c* = 1.45, EtOH)]; and MS (ESI): *m/z* (%) 491.0 ($[M + Na]^+$, 100).

*3.6. (3β,4α) 3,23-Dihydroxyolean-12-en-28-oic Acid (**2**) [465-99-6]*

To an ice-cold solution of **1** (2.0 g, 4.23 mmol) in THF/MeOH (100 mL, 1:1) $NaBH_4$ (193 mg, 5.1 mmol) was added, and the reaction was stirred for 2 h, quenched with aq. hydrochloric acid (2 M, 50 mL) and extracted with chloroform (3 × 50 mL). The combined organic phases were dried over $MgSO_4$, the solvent was removed under reduced pressure, and the crude product was subjected by column chromatography (SiO_2, *n*-hexane/ethyl acetate, 7:3) to yield **2** (1.4 g, 72%) as a colorless solid; m.p.: 331–334 °C (lit.: [23] 332–335 °C); $[\alpha]_D^{20}$ = +80.3° (*c* = 0.52, pyridine), [lit.: [36] $[\alpha]_D^{20}$ = +81.2° (pyridine)]; and MS (ESI): *m/z* (%) 471.1 ($[M-H]^-$, 100).

*3.7. Madecassic Acid (**3**)*

This compound was obtained from different local suppliers and used as received.

3.8. (3β,4α) 3-(Acetyloxy)-23-oxoolean-12-en-28-oic Acid (**4**) [27706-38-3]

Following GPA from **1** (1500 mg, 3.18 mmol) followed by column chromatography (SiO_2, *n*-hexane/ethyl acetate, 8:2), **4** (2.40 mmol, 79%) was obtained as a colorless solid; m.p.: 175–178 °C (lit.: [24] 177–178 °C); $[\alpha]_D^{20}$ = +77° (*c* = 0.6, $CHCl_3$), [lit.: [37] $[\alpha]_D^{20}$ = +78° (*c* = 0.6, $CHCl_3$)]; and MS (ESI): *m*/*z* (%) 511.6 ($[M-H]^-$, 90).

3.9. (3β,4α) 3,23-Bis(acetyloxy)olean-12-en-28-oic Acid (5) [5672-32-2]

Following GPA from **2** (2000 mg, 4.23 mmol) followed by column chromatography (SiO_2, *n*-hexane/ethyl acetate, 8:2), **5** (1880 mg, 94%) was obtained as a colorless solid; m.p.: 185–189 °C (lit.: [38] 173–175 °C); $[\alpha]_D^{20}$ = +76.8° (*c* = 0.17, $CHCl_3$) [lit.: [39] $[\alpha]_D^{20}$ = +78° ($CHCl_3$)]; R_F = 0.37 (SiO_2, *n*-hexane/ethyl acetate, 8:2); IR (ATR): ν = 2944*br*, 1738*s*, 1692*s*, 1467*w*, 1366*s*, 1239*vs*, 1040*s*, 771*w* cm^{-1}; ^{1}H NMR (500 MHz, $CDCl_3$): δ = 5.29–5.24 (*m*, 1H, 12–H), 4.79 (*dd*, *J* = 11.6, 4.8 Hz, 1H, 3–H), 3.87 (*d*, *J* = 11.6 Hz, 1H, 23–H$_a$), 3.70 (*d*, *J* = 11.6 Hz, 1H, 23–H$_b$), 2.82 (*dd*, *J* = 13.9, 4.6 Hz, 1H, 18–H), 2.06 (*s*, 3H, 15–H$_a$ + 16–H$_a$ + 22–H$_a$), 2.04 (*s*, 3H, 34–H), 2.02 (*s*, 3H, 32–H), 1.97 (d*d*, *J* = 13.4, 4.0 Hz, 2H, 11–H$_a$ + 11–H$_b$), 1.92–1.86 (*m*, 3H, 16–H$_b$ + 2–H$_a$ + 2–H$_b$), 1.79 (*d*, *J* = 4.4 Hz, 1H, 22–H$_b$), 1.77 (*d*, *J* = 4.4 Hz, 1H, 7–H$_a$), 1.65–1.56 (*m*, 5H, 7–H$_b$ + 19–H$_a$ + 9–H +1–H$_a$ + 5–H), 1.43–1.33 (*m*, 3H, 6–H$_a$ + 6 –H$_b$ + 21–H$_a$), 1.24–1.16 (*m*, 3H, 19–H$_b$ + 21–H$_b$ + 15–H$_b$), 1.12 (*s*, 1H, 1–H$_b$) 1.11 (*s*, 3H, 27–H), 0.97 (*s*, 3H, 25–H), 0.92 (*s*, 3H, 29–H), 0.90 (*s*, 3H, 30–H), 0.82 (*s*, 3H, 24–H), 0.74 (*s*, 3H, 26–H) ppm; ^{13}C NMR (125 MHz, $CDCl_3$): δ = 184.0 (C–28), 171.0 (C–31), 170.7 (C–33), 143.6 (C–13), 122.4 (C–12), 74.5 (C–3), 65.4 (C–23), 52.0 (C–5), 47.7 (C–9), 46.5 (C–17), 45.8 (C–19), 41.5 (C–4), 40.9 (C–14), 40.5 (C–18), 39.3 (C–8), 37.7 (C–1), 36.8 (C–10), 33.8 (C–21), 33.0 (C–30), 32.4 (C–7), 32.2 (C–20), 30.7 (C–15), 27.6 (C–2), 25.8 (C–27), 23.6 (C–29), 23.4 (C–11), 22.9 (C–16) 22.8 (C–22), 21.2 (C–32), 20.9 (C–34), 17.9 (C–6), 17.1 (C–26), 15.8 (C–25), 13.1 (C–24) ppm; and MS (ESI): *m*/*z* (%) 555.6 ($[M-H]^-$, 90).

3.10. (2α,3β,4α,6β) 2,3,23-Tris(acetyloxy)-6-hydroxyurs-12-en-28-oic Acid (**6**) [99598-46-6]

Following GPA from **3** (500 mg, 0.99 mmol) followed by column chromatography (SiO_2, *n*-hexane/ethyl acetate, 8:2), **6** (392 mg, 78%) was obtained as a colorless solid; m.p.: 188–194 °C (lit.: [40] 189–192 °C); $[\alpha]_D^{20}$ = +15.0° (*c* = 0.18, $CHCl_3$) [lit.: [41] $[\alpha]_D^{20}$ = +19.5° ($CHCl_3$)]; R_F = 0.19 (SiO_2, $CHCl_3$/MeOH 100:1); IR (ATR): ν = 3533*br*, 3230*br*, 2921*br*, 2875*w*, 1755*s*, 1726*s*, 1707*s* 1458*w*, 1363*w*, 1230*s*, 1031*s* cm^{-1}; ^{1}H NMR (400 MHz, $CDCl_3$): δ = 5.28 (*t*, *J* = 3.6 Hz, 1H, 12–H), 5.23 (*ddd*, *J* = 11.6, 10.3, 4.8 Hz, 1H, 2–H), 5.01 (*d*, *J* = 10.2 Hz, 1H, 3–H), 4.34 (*d*, *J* = 3.9 Hz, 1H, 6–H), 3.94 (*d*, *J* = 12.0 Hz, 1H, 23–H$_a$), 3.71 (*d*, *J* = 12.0 Hz, 1H, 23–H$_b$), 2.29–2.14 (*m*, 1H, 18–H), 2.06 (*s*, 3H, 36–H), 2.03 (*s*, 3H, 32–H), 1.98 (*s*, 3H, 34–H), 2.05–1.97 (*m*, 2H, 16–H$_a$ + 16–H$_b$), 1.95–1.78 (*m*, 2H, 11–H$_a$ + 11–H$_b$), 1.77–1.60 (*m*, 4H, 22–H$_a$ + 22–H$_b$ + 15–H$_a$ + 5–H), 1.58–1.48 (*m*, 2H, 21–H$_a$, 20–H), 1.46 (*d*, *J* = 2.6 Hz, 3H, 29–H), 1.37 (*d*, *J* = 1.8 Hz, 1H, 9–H), 1.35–1.28 (*m*, 5H, 21–H$_b$ + 1–H$_a$ + 1–H$_b$ + 7–H$_a$ + 7–H$_b$), 1.26 (*s*, 3H, 26–H), 1.22 (*s*, 1H, 19–H), 1.08 (*s*, 1H, 15–H$_b$), 1.05 (*s*, 3H, 25–H), 1.04 (*s*, 3H, 27–H), 0.95 (*d*, *J* = 6.2 Hz, 3H, 30–H), 0.86 (*s*, 3H, 24–H) ppm; ^{13}C NMR (100 MHz, $CDCl_3$): δ = 183.3 (C–28), 170.8 (C–35), 170.4 (C–31), 170.3 (C–33), 137.2 (C–13), 125.6 (C–12), 74.9 (C–3), 69.9 (C–2), 67.9 (C–6), 65.4 (C–23), 52.4 (C–18), 48.2 (C–5), 47.9 (C–17), 47.8 (C–9), 47.1 (C–10), 45.8 (C–4), 42.4 (C–1), 40.7 (C–20), 39.0 (C–19), 38.8 (C–8), 38.6 (C–7), 37.3 (C–14), 36.6 (C–22), 30.6 (C–21), 27.9 (C–15), 24.0 (C–16), 23.5 (C–11), 23.3 (C–27), 21.1 (C–30), 21.0 (C–34), 20.9 (C–32), 20.8 (C–36), 18.6 (C–29), 18.5 (C–25), 16.9 (C–26), 15.3 (C–24) ppm; and MS (ESI): *m*/*z* (%) 629.3 ($[M-H]^-$, 90); analysis calculated for $C_{36}H_{54}O_9$ (630.81): C 68.54, H 8.63; found: C 68.36, H 8.90.

3.11. (3β,4α) 3-Acetyloxy-N-(benzyl)-23-oxo-olean-12-en-28-amide (**7**)

Following GPB from **4** (300 mg, 0.58 mmol) and benzylamine (186 mg, 1.74 mmol) followed by chromatography (SiO_2, *n*-hexane/ethyl acetate, 8:2), **7** (242 mg, 81%) was obtained as a colorless solid; m.p.: 119–121 °C; $[\alpha]_D^{20}$ = +35.1° (*c* = 0.15, $CHCl_3$); R_F = 0.30 (SiO_2, *n*-hexane/ethyl acetate, 8:2); IR (ATR): ν = 3391*br*, 2944*w*, 2872*w*, 1732*s*, 1645*s*, 1513*s*, 1452*s*, 1363*s*, 1233*vs*, 1028*s*, 696*w* cm^{-1}; UV-Vis ($CHCl_3$): λ_{max} (log ε) = 245 nm (2.37); ^{1}H

NMR (400 MHz, $CDCl_3$): δ = 9.27 (*s*, 1H, 23–H), 7.38–7.17 (*m*, 6H, 35–H + 39–H + 37–H + 36–H + 38–H), 5.31 (*t*, *J* = 3.6 Hz, 1H, 12–H), 4.96 (*t*, *J* = 5.7 Hz, 1H, 3–H), 4.96 (*t*, *J* = 5.7 Hz, 1H, 33–H$_a$), 4.59 (*dd*, *J* = 14.7, 6.2 Hz, 1H, 33–H$_b$), 2.61–2.52 (*m*, 1H, 18–H), 2.03 (*s*, 1H, 32–H), 1.95 (*s*, 2H, 16–H$_a$ + 16–H$_b$), 1.92–1.84 (*m*, 2H, 11–H$_a$ + 11–H$_b$), 1.84–1.62 (*m*, 9H, 9–H + 19–H$_a$ + 1–H$_a$ + 7–H$_a$ + 7–H$_b$ + 15–H$_a$ + 15–H$_b$ + 2–H$_a$ + 2–H$_b$), 1.60–1.49 (*m*, 2H, 22–H$_a$ + 6–H$_a$), 1.43–1.37 (*m*, 1H, 21–H$_a$), 1.36–1.31 (*m*, 1H, 5–H), 1.25 (*t*, *J* = 7.1 Hz, 2H, 22–H$_b$ + 21–H$_b$), 1.21–1.17 (*m*, 1H, 19–H$_b$), 1.16 (*s*, 3H, 27–H), 1.12–1.00 (*m*, 2H, 15–H$_b$ + 1–H$_b$), 1.08 (*s*, 3H, 24–H), 0.97–0.82 (*m*, 2H, 6–H$_a$ + 6–H$_b$), 0.98 (*s*, 3H, 26–H), 0.94 (*s*, 3H, 29–H), 0.90 (*s*, 3H, 30–H), 0.66 (*s*, 3H, 25–H) ppm; ^{13}C NMR (100 MHz, $CDCl_3$): δ = 204.4 (C–23), 177.8 (C–28), 170.3 (C–31), 144.9 (C–13), 138.4 (C–34), 128.6 (C–35), 128.6 (C–39), 127.8 (C–36), 127.8 (C–38), 127.4 (C–37), 122.3 (C–12), 73.3 (C–3), 54.2 (C–4), 47.8 (C–5), 47.5 (C–9), 46.6 (C–17), 46.3 (C–19), 43.6 (C–33), 42.3 (C–14), 42.1 (C–18), 39.7 (C–80), 37.8 (C–1), 35.7 (C–10), 34.1 (C–21), 33.0 (C–29), 32.7 (C–7), 31.7 (C–22), 30.7 (C–20), 27.3 (C–15), 25.7 (C–27), 23.8 (C–30), 23.6 (C–11), 22.5 (C–2), 21.0 (C–16), 21.0 (C–32), 20.4 (C–6), 16.9 (C–25), 15.6 (C–26), 9.5 (C–24) ppm; MS (ESI): *m*/*z* (%) 602.6 ([M + H]$^+$, 20); 624.6 ([M + Na]$^+$, 60); and 640.6 ([M + K]$^+$, 30); analysis calculated for $C_{39}H_{55}NO_4$ (601.87): C 77.83, H 9.21, N 2.33; found: C 77.59, H 9.43, N 2.08.

3.12. *(3β,4α) 3-Acetyloxy-N-(phenyl)-23-oxo-olean-12-en-28-amide (**8**)*

Following GPB from **4** (300 mg, 0.58 mmol) and aniline (162 mg, 1.74 mmol) followed by chromatography (SiO_2, *n*-hexane/ethyl acetate, 9:1), **8** (194 mg, 65%) was obtained as a colorless solid; m.p.: 150–152 °C; $[\alpha]_D^{20}$ = +85.3° (*c* = 0.17, $CHCl_3$); R_F = 0.20 (SiO_2, *n*-hexane/ethyl acetate, 9:1); IR (ATR): ν = 3385*br*, 2941*br*, 2857*w*, 1735*s*, 1596*s*, 1239*vs*, 1025*s*, 751*vs*, 690*vs* cm^{-1}; UV-Vis ($CHCl_3$): λ_{max} (log ε) = 243 nm (0.4); ^{1}H NMR (500 MHz, $CDCl_3$): δ = 9.28 (*s*, 1H, 23–H), 7.50–7.44 (*m*, 2H, 34–H + 38–H), 7.35–7.29 (*m*, 2H, 35–H + 37–H), 7.17–7.15 (*m*, 1H, 36–H), 5.56 (*q*, *J* = 2.8, 1.9 Hz, 1H, 12–H), 5.03 (*d*, *J* = 4.6 Hz, 1H, 3–H), 2.73–2.65 (*m*, 1H, 18–H), 2.14–2.01 (*m*, 3H, 32–H), 1.98 (*s*, 2H, 16–H$_a$ + 16–H$_b$), 1.88–1.77 (*m*, 3H, 11–H$_a$ + 11–H$_b$ + 7–H$_a$), 1.76–1.54 (*m*, 7H, 9–H + 19–H$_a$ + 1–H$_a$ + 7–H$_b$ + 15–H$_a$ + 2–H$_a$ + 2–H$_b$), 1.53–1.46 (*m*, 2H, 22–H$_a$ + 6–H$_a$), 1.42–1.32 (*m*, 1H, 21–H$_a$), 1.30–1.24 (*m*, 1H, 5–H), 1.23–1.21 (*m*, 2H, 22–H$_b$ + 21–H$_b$ + 6–H$_b$), 1.23 (*s*, 1H, 19–H$_b$), 1.20 (*s*, 3H, 27–H), 1.10–1.04 (*m*, 2H, 15–H$_b$ + 1–H$_b$), 1.07 (*s*, 3H, 24–H) 1.02 (*s*, 3H, 26–H), 0.94 (*s*, 3H, 29–H), 0.92 (*s*, 3H, 30–H), 0.73 (*s*, 3H, 25–H) ppm; ^{13}C NMR (125 MHz, $CDCl_3$): δ = 177.0 (C–28), 171.3 (C–33), 170.9 (C–31), 138.6 (C–13), 128.4 (C–12), 80.9 (C–3), 73.6 (C–19), 70.3 (C–2), 55.5 (C–18), 55.1 (C–17), 54.9 (C–5), 47.2 (C–9), 45.6 (C–35), 45.4 (C–36), 43.9 (C–1), 41.7 (C–14), 41.0 (C–20), 39.8 (C–8), 39.4 (C–4), 38.1 (C–10), 34.8 (C–22), 32.8 (C–7), 28.4 (C–23), 28.3 (C–15), 27.7 (C–29), 25.9 (C–21), 25.3 (C–16), 24.3 (C–27), 23.7 (C–11), 21.1 (C–34), 20.9 (C–32), 18.3 (C–6), 17.6 (C–24), 16.6 (C–26), 16.4 (C–25), 16.0 (C–30) ppm; and MS (ESI): *m*/*z* (%) 586.7 ([M-H]$^-$, 90); analysis calculated for $C_{38}H_{53}NO_4$ (587.85): C 77.64, H 9.09, N 2.38; found: C 77.41, H 9.23, N 2.05.

3.13. *(3β,4α) 3-Acetyloxy-N-(piperazinyl)-23-oxo-olean-12-en-28-amide (**9**)*

Following GPB from **4** (300 mg, 0.58 mmol) and piperazine (150 mg, 1.74 mmol) followed by chromatography (SiO_2, chloroform/methanol, 9:1), **9** (243 mg, 81%) was obtained as a colorless solid; m.p.: 150–154 °C; $[\alpha]_D^{20}$ = +36.5° (*c* = 1.15, $CHCl_3$); R_F = 0.27 (SiO_2, $CHCl_3$/MeOH, 95:5); IR (ATR): ν = 3325*br*, 2947*br*, 2855*w*, 1735*s*, 1625*s*, 1239*vs*, 754s cm^{-1}; ^{1}H NMR (400 MHz, $CDCl_3$): δ = 9.26 (*s*, 1H, 23–H), 5.21 (*t*, *J* = 3.7 Hz, 1H, 12–H), 4.98 (*dd*, *J* = 11.0, 5.3 Hz, 1H, 3–H), 3.71–3.56 (*m*, 4H, 34–H$_a$ + 34–H$_b$ + 35–H$_a$ + 35–H$_b$), 3.31–3.29 (*m*, 4H, 33–H$_a$ + 33–H$_b$ + 36–H$_a$ + 36–H$_b$), 3.08–2.83 (*m*, 1H, 18–H), 2.15–2.13 (*m*, 4H, 11–H$_a$ + 11–H$_b$ + 16–H$_a$ + 16–H$_b$), 1.93 (*s*, 3H, 32–H), 1.82–1.54 (*m*, 8H, 9–H + 19–H$_a$ + 1–H$_a$ + 7–H$_a$ + 7–H$_b$ + 15–H$_a$ + 2–H$_a$ + 2–H$_b$), 1.50–1.40 (*m*, 3H, 22–H$_a$ + 6–H$_a$ + 21–H$_a$), 1.29–1.25 (*m*, 1H, 5–H), 1.25–1.20 (*m*, 2H, 22–H$_b$ + 21–H$_b$), 1.20 (*s*, 3H, 27–H), 1.18–1.16 (*m*, 1H, 19–H$_b$), 1.06 (*s*, 3H, 24–H), 1.08–1.0 (*m*, 2H, 15–H$_b$ + 1–H$_b$), 1.02 (*s*, 3H, 25–H), 0.98–0.84 (*m*, 1H, 6–H$_b$), 0.94 (*s*, 3H, 30–H), 0.91 (*s*, 3H, 29–H), 0.77 (*s*, 3H, 26–H) ppm; ^{13}C NMR (100 MHz, $CDCl_3$): δ = 204.9 (C–23), 175.8 (C–28), 170.5 (C–31), 144.6 (C–13), 121.2

(C–12), 73.4 (C–3), 54.0 (C–4), 48.2 (C–33), 48.2 (C–36), 48.0 (C–17), 47.8 (C–5), 47.6 (C–9), 46.9 (C–19), 45.0 (C-34), 45.0 (C–35), 43.7 (C–18), 41.7 (C–14), 39.4 (C–8), 37.4 (C–1), 35.6 (C–10), 33.5 (C–21), 33.0 (C–7), 32.1 (C–29), 31.9 (C–22), 29.8 (C–20), 27.7 (C–15), 25.1 (C–27), 23.0 (C–30), 22.9 (C–11), 22.6 (C–16), 22.1 (C–2), 20.2 (C–32), 19.4 (C–6), 16.2 (C–26), 14.6 (C–25), 8.5 (C–24) ppm; and MS (ESI): *m*/*z* (%) 581.6 ([M + H]$^+$, 90); analysis calculated for $C_{36}H_{56}N_2O_4$ (580.85): C 74.44, H 9.72, N 4.82; found: C 74.06, H 9.98, N 4.61.

*3.14. (3β,4α) 3-Acetyloxy-N-(homopiperazinyl)-23-oxo-olean-12-en-28-amide (**10**)*

Following GPB from **4** (300 mg, 0.58 mmol) and homopiperazine (174 mg, 1.74 mmol) followed by chromatography (SiO_2, chloroform/methanol, 9:1), **10** (286 mg, 83%) was obtained as a colorless solid; m.p.: 176–179 °C; $[\alpha]_D^{20}$ = −4.39° (*c* = 0.145 $CHCl_3$); R_F = 0.34 (SiO_2, $CHCl_3$/MeOH, 9:1); IR (ATR): ν = 2923*w*, 1741*s*, 1621*w*, 1455*w*, 1368*m*, 1230*vs*, 1156*w*, 1087*w*, 1043*m*, 1029*m*, 964*w*, 920*w*, 751*m*, 665*w*, 460*w*, 422*w* cm^{-1}; ^{1}H NMR (400 MHz, $CDCl_3$): δ = 9.26 (*s*, 1H, 23-H), 5.27–5.22 (*m*, 1H, 12–H), 5.00–4.91 (*m*, 1H, 3–H), 3.97–3.37 (*m*, 6H, 33–H + 35–H + 37–H), 3.36–2.90 (*m*, 3H, 34–H + 18–H), 2.34–2.00 (*m*, 3H, 36–H + 16–H), 1.98–1.81 (*m*, 2H, 11–H), 1.94 (*s*, 3H, 32–H), 1.79–1.58 (*m*, 8H, 2–H + 1–H_a + 16–H_b + 19–H_a + 22–H + 9–H), 1.57–1.39 (*m*, 3H, 15–H_a + 6–H_a + 7–H_a), 1.39–1.26 (*m*, 2H, 21–H_a + 5–H), 1.26–0.99 (*m*, 5H, 21–H_b + 7–H_b + 19–H_b + 1–H_b + 15–H_b), 1.14 (*s*, 3H, 27–H), 1.06 (*s*, 3H, 24–H), 0.99–0.88 (*m*, 1H, 6–H_b), 0.96 (*s*, 3H, 26–H), 0.93 (*s*, 3H, 30–H), 0.89 (*s*, 3H, 29–H), 0.73 (*s*, 3H, 25–H) ppm; ^{13}C NMR (100 MHz, $CDCl_3$): δ = 204.5 (C–23), 176.2 (C–28), 170.3 (C–31), 144.7 (C–13), 121.3 (C–12), 73.4 (C–3), 54.3 (C–4), 49.2 (C–35), 47.9 (C–5), 47.8 (C–17), 47.7 (C–9), 47.2 (C–34), 46.5 (C–33 + C–37), 46.3 (C–19), 43.6 (C–18), 42.0 (C–14), 39.4 (C–8), 37.7 (C–1), 35.9 (C–10), 33.9 (C–21), 33.0 (C–29), 32.1 (C–7), 30.4 (C–20), 30.0 (C–22), 27.8 (C–15), 26.6 (C–36), 25.9 (C–27), 24.0 (C–30), 23.3 (C–11), 22.5 (C–16), 22.5 (C–2), 21.0 (C–32), 20.4 (C–6), 16.9 (C–25), 15.6 (C–26), 9.5 (C–24) ppm; and MS (ESI): *m*/*z* (%) = 595.1 ([M + H]$^+$, 100); analysis calculated for $C_{37}H_{58}N_2O_4$ (594.87): C 74.71, H 9.82, N 4.71; found: C 74.50, H 10.02, N 4.55.

*3.15. (3β,4α) 3,23-Bis(acetyloxy)-N-(benzyl)-olean-12-en-28-amide (**11**)*

Following GPB from **5** (450 mg, 0.81 mmol) and benzylamine (260 mg, 2.43 mmol) followed by chromatography (SiO_2, *n*-hexane/ethyl acetate, 8:2), **11** (117 mg, 26%) was obtained as a colorless solid; m.p.: 210–214 °C; $[\alpha]_D^{20}$ = +39.22° (*c* = 0.159, $CHCl_3$); R_F = 0.20 (SiO_2, *n*-hexane/ethyl acetate, 8:2); IR (ATR): ν = 3432*w*, 2950*br*, 1726*vs*, 1631*s*, 1253*vs*, 1034*s*, 745*vs* cm^{-1}; UV-Vis ($CHCl_3$): λ_{max} (log ε) = 260 nm (3.28); ^{1}H NMR (400 MHz, $CDCl_3$): δ = 7.35–7.27 (*m*, 2H, 37–H + 41–H), 7.25–7.19 (*m*, 3H, 38–H + 40–H + 39–H), 5.30 (*t*, *J* = 3.6 Hz, 1H, 12–H), 4.76 (*dd*, *J* = 11.3, 4.9 Hz, 1H, 3–H), 4.63–4.57 (*m*, 1H, 35–H_a), 4.14 (*dd*, *J* = 14.7, 4.4 Hz, 1H, 35–H_b), 3.86 (*d*, *J* = 11.6 Hz, 1H, 23–H_a), 3.70 (*d*, *J* = 11.7 Hz, 1H, 23–H_b), 2.60–2.50 (*m*, 1H, 18–H), 2.05 (*s*, 3H, 15–H_a + 16–H_a + 22–H_a), 2.05 (*s*, 3H, 34–H), 2.01 (*s*, 3H, 32–H), 1.99–1.91 (*m*, 5H, 11–H_a + 11–H_b + 16–H_b), 1.87–1.77 (*m*, 1H, 22–H_b), 1.76–1.54 (*m*, 5H, 7–H_a + 7–H_b + 19–H_a + 9–H + 1–H_a), 1.52 (*d*, *J* = 4.2 Hz, 1H, 2–H_a), 1.45–1.31 (*m*, 3H, 6–H_a + 6–H_b + 21–H_a), 1.28–1.15 (*m*, 4H, 19–H_b + 21–H_b + 15–H_b + 5–H), 1.14–0.95 (*m*, 2H, 1–H_b + 2–H_b) 1.13 (*s*, 3H, 27–H), 0.93 (*s*, 3H, 25–H), 0.91 (*s*, 3H, 29–H), 0.90 (*s*, 3H, 30–H), 0.83 (*s*, 3H, 24–H), 0.66 (*s*, 3H, 26–H) ppm; ^{13}C NMR (100 MHz, $CDCl_3$): δ = 177.9 (C–28), 170.9 (C–31), 170.6 (C–33), 144.9 (C–13), 138.4 (C–36), 128.6 (C–37), 128.6 (C–41), 127.8 (C-38), 127.8 (C–40), 127.3 (C–39), 122.7 (C–12), 74.4 (C–3), 65.4 (C–23), 47.8 (C–5), 47.6 (C–9), 46.6 (C–17), 46.3 (C–19), 43.6 (C–35), 42.3 (C–4), 42.0 (C–14), 40.5 (C–18), 39.3 (C–8), 37.8 (C–1), 36.6 (C–10), 34.1 (C–21), 33.0 (C–30), 32.6 (C–7), 32.0 (C–20), 30.7 (C–15), 27.3 (C–2), 25.6 (C–27), 23.8 (C–29), 23.6 (C–11), 23.4 (C–16), 22.9 (C–22), 21.2 (C–32), 20.9 (C–34), 17.9 (C–6), 16.9 (C–26), 15.8 (C–25), 13.1 (C–24) ppm; and MS (ESI): *m*/*z* (%) 646.8 ([M + H]$^+$, (23)), 668.7 ([M + Na]$^+$, 55), 684.6 ([M + K]$^+$, 60); analysis calculated for $C_{41}H_{59}NO_5$ (645.93): C 76.24, H 9.21, N 2.17; found: C 75.98, H 9.44, N 2.02.

*3.16. (3β,4α) 3,23-Bis(acetyloxy)-N-(phenyl)-olean-12-en-28-amide (**12**)*

Following GPB from **5** (450 mg, 0.81 mmol) and aniline (226 mg, 2.43 mmol) followed by chromatography (SiO_2, *n*-hexane/ethyl acetate, 8:2), **12** (440 mg, 98%) was obtained as a colorless solid; m.p.: 210–214 °C; $[\alpha]_D^{20}$ = +39.2° (*c* = 0.16, $CHCl_3$); R_F = 0.20 (SiO_2, *n*-hexane/ethyl acetate, 8:2); IR (ATR): ν = 2947*br*, 1744*s*, 1657*s*, 1267*s*, 1028*w*, 748*s* cm^{-1}; UV-Vis ($CHCl_3$): λ_{max} (log ε) = 237 nm (0.4); ^1H NMR (400 MHz, $CDCl_3$): δ = 7.49–7.46 (*m*, 2H, 36–H + 40–H), 7.35–7.24 (*m*, 2H, 37–H + 39–H), 7.10–7.05 (*m*, 1H, 38–H), 5.55 (*t*, *J* = 3.6 Hz, 1H, 12–H), 4.78 (*dd*, *J* = 11.5, 4.9 Hz, 1H, 3–H), 3.85 (*d*, *J* = 11.6 Hz, 1H, 23–H_a), 3.70 (*d*, *J* = 11.6 Hz, 1H, 23–H_b), 2.72–2.64 (*m*, 1H, 18–H), 2.06 (*s*, 3H, 15–H_a + 16–H_a + 22–H_a), 2.05 (*s*, 3H, 34–H), 2.02 (*s*, 3H, 32–H), 1.98 (*d*, *J* = 3.6 Hz, 2H, 11–H_a + 11–H_b), 1.88–1.69 (*m*, 5H, 16–H_b + 2–H_a + 2–H_b + 22–H_b + 7–H_a), 1.64–1.59 (*m*, 5H, 7–H_b + 19–H_a + 9–H + 1–H_a + 5–H), 1.47–1.33 (*m*, 3H, 6–H_a + 6–H_b + 21–H_a), 1.31–1.22 (*m*, 3H, 19–H_b + 21–H_b + 15–H_b), 1.19 (*s*, 3H, 27–H), 1.10 (*tq*, *J* = 10.8, 3.5 Hz, 1H, 1–H_b), 0.94 (*s*, 3H, 29–H), 0.94 (*s*, 3H, 30–H), 0.94 (*s*, 3H, 25–H), 0.81 (*s*, 3H, 24–H), 0.72 (*s*, 3H, 26–H) ppm; ^{13}C NMR (100 MHz, $CDCl_3$): δ = 176.4 (C–28), 170.9 (C–31), 170.7 (C–33), 145.1 (C–13), 138.0 (C–35), 128.8 (C–37), 128.8 (C–39), 124.1 (C–38), 123.1 (C–12), 119.8 (C–36), 119.8 (C–40), 74.4 (C–3), 65.4 (C–23), 47.8 (C–5), 47.6 (C–9), 47.2 (C–17), 46.7 (C–19), 42.6 (C–4), 42.1 (C–14), 40.5 (C–18), 39.4 (C–8), 37.8 (C–1), 36.7 (C–10), 34.2 (C–21), 33.0 (C–30), 32.5 (C–7), 32.0 (C–20), 30.7 (C–15), 27.3 (C–2), 25.6 (C–27), 24.1 (C–29), 23.6 (C–11), 23.6 (C–16), 22.9 (C–22), 21.2 (C–32), 20.9 (C–34), 17.8 (C–6), 16.9 (C–26), 15.9 (C–25), 13.1 (C–24) ppm; and MS (ESI): *m*/*z* (%) 632.7 ($[M + H]^+$, 40), 654.7 ($[M + Na]^+$, 35), 670.7 ($[M + K]^+$, 25); analysis calculated for $C_{40}H_{57}NO_5$ (631.90): C 76.03, H 9.09, N 2.22; found: C 75.81, H 9.27, N 1.97.

*3.17. (3β,4α)3,23-Bis(acetyloxy)-N-(piperazinyl)-olean-12-en-28-amide (**13**)*

Following GPB from **5** (450 mg, 0.81 mmol) and piperazine (210 mg, 2.43 mmol) followed by chromatography (SiO_2, *n*-hexane/ethyl acetate, 8:2), **13** (360 mg, 80%) was obtained as a colorless solid; m.p.: 183–187 °C; $[\alpha]_D^{20}$ = +37.9° (*c* = 0.18, $CHCl_3$); R_F = 0.20 (SiO_2, *n*-hexane/ethyl acetate, 8:2); IR (ATR): ν = 3354*br*, 2947*br*, 1735*s*, 1625*s*, 1410*w*, 1242*vs*, 1002*s*, 754*w* cm^{-1}; ^1H NMR (500 MHz, $CDCl_3$): δ = 5.25 (*t*, *J* = 3.3 Hz, 1H, 12–H), 4.78 (*dd*, *J* = 11.5, 5.0 Hz, 1H, 3–H), 3.87 (*dd*, *J* = 11.6, 2.1 Hz, 1H, 23–H_a), 3.71–3.51 (*m*, 5H, 23–H_b + 35–H_a + 35–H_b + 38–H_a + 38–H_b), 3.37–2.96 (*m*, 4H, 36–H_a + 36–H_b + 37–H_a + 37–H_b), 2.96–2.75 (*m*, 1H, 18–H), 2.44 (*dd*, *J* = 17.5, 9.9 Hz, 1H, 5–H), 2.22–2.08 (*m*, 1H, 22–H_a), 2.08–2.05 (*m*, 5H, 15–H_a + 16–H_a), 2.05 (*s*, 3H, 34–H), 2.01 (*s*, 3H, 32–H), 1.88 (*td*, *J* = 17.7, 16.0, 11.8 Hz, 5H, 11–H_a + 11–H_b + 16–H_b + 2–H_a + 2–H_b), 1.76–1.54 (*m*, 6H, 22–H_b + 7–H_a + 7–H_b + 19–H_a + 9–H + 1–H_a), 1.41–1.27 (*m*, 3H, 6–H_a + 6–H_b + 21–H_a), 1.26–1.13 (*m*, 3H, 19–H_b + 21–H_b + 15–H_b), 1.11 (*s*, 3H, 27–H), 1.04 (*dd*, *J* = 13.7, 4.0 Hz, 1H, 1–H_b), 0.95 (*s*, 3H, 25–H), 0.91 (*s*, 3H, 29–H), 0.89 (*s*, 3H, 30–H), 0.82 (*s*, 3H, 24–H), 0.73 (*s*, 3H, 26–H) ppm; ^{13}C NMR (125 MHz, $CDCl_3$): δ = 174.9 (C–28) 171.0 (C–31), 170.6 (C–33), 144.9 (C–13), 121.3 (C–12), 74.6 (C–3), 65.5 (C–23), 51.6 (C–5), 47.9 (C–35), 47.9 (C–38), 47.9 (C-9), 47.3 (C–17), 46.4 (C–19), 46.2 (C–36), 46.2 (C–37), 45.0 (C–4), 41.8 (C–14), 40.5 (C–18), 39.1 (C–8), 37.7 (C–1), 36.8 (C–10), 34.0 (C–21), 33.0 (C–30), 32.5 (C–7), 32.2 (C–20), 30.4 (C–15), 29.9 (C–2), 27.9 (C–27), 25.8 (C–29), 24.1 (C–11), 23.4 (C–16), 22.9 (C–22), 21.2 (C–32), 20.9 (C–34), 17.9 (C–6), 16.9 (C–26), 15.8 (C–25), 13.1 (C–24) ppm; and MS (ESI): *m*/*z* (%) 626.0 ($[M + H]^+$, 80); analysis calculated for $C_{38}H_{60}N_2O_5$ (624.91): C 73.04, H 9.68, N 4.48; found: C 72.84, H 9.82, N 4.15.

*3.18. (3β,4α)3,23-Bis(acetyloxy)-N-(homopiperazinyl)-olean-12-en-28-amide (**14**)*

Following GPB from **5** (450 mg, 0.81 mmol) and homopiperazine (243 mg, 2.43 mmol) followed by chromatography (SiO_2, chloroform/methanol, 9:1), **14** (186 mg, 41%) was obtained as a colorless solid; m.p.: 176–180 °C; $[\alpha]_D^{20}$ = +31.2° (*c* = 0.11, $CHCl_3$); R_F = 0.36 (SiO_2, $CHCl_3$/MeOH 9:1); IR (ATR): ν = 2944*br*, 1738*s*, 1622*w*, 1467*w*, 1239*s*,1034*s*, 745*w* cm^{-1}; ^1H NMR (400 MHz, $CDCl_3$): δ = 5.27–5.22 (*m*, 1H, 12–H), 4.77 (*dd*, *J* = 11.5, 5.0 Hz, 1H, 3–H), 4.02–3.82 (*m*, 1H, 23–H_a), 3.69 (*d*, *J* = 11.7 Hz, 1H, 23–H_b), 3.44–3.14 (*m*, 2H, 39–H_a + 39–H_b), 3.06 (*d*, *J* = 13.4 Hz, 2H, 35–H_a + 35–H_b), 2.83- 2.50 (*m*, 5H, 36–H_a + 36–H_b + 37–H_a + 37–H_b

+ 18–H), 2.18–2.08 (*m*, 2H, 16–H$_a$ + 22–H$_a$), 2.05 (*s*, 3H, 34–H), 2.01 (*s*, 3H, 32–H), 2.00–1.79 (*m*, 2H, 11–H$_a$ + 11–H$_b$), 1.77–1.44 (*m*, 10H, 16–H$_b$ + 15–H$_a$ + 38–H$_a$ + 38– H$_b$ + 22–H$_b$ + 2–H$_a$ + 2–H$_b$ + 19–H$_a$ + 1–H$_a$ + 5–H), 1.40–1.33 (*m*, 5H, 7–H$_a$ + 19–H$_b$ + 6–H$_a$ + 6–H$_b$ + 21–H$_a$), 1.26–1.14 (*m*, 5H, 7–H$_b$ + 9–H + 1–H$_b$ + 21–H$_b$ + 15–H$_b$), 1.11 (*s*, 3H, 27–H), 0.94 (*s*, 3H, 25–H), 0.93 (*s*, 3H, 29–H), 0.89 (*s*, 3H, 30–H), 0.82 (*s*, 3H, 24–H), 0.71 (*s*, 3H, 26–H) ppm; ^{13}C NMR (100 MHz, $CDCl_3$): δ = 176.4 (C–28), 170.9 (C–31), 170.6 (C–33), 144.5 (C–13), 121.7 (C–12), 74.5 (C–3), 65.5 (C–23), 56.6 (C–39), 47.8 (C–5), 47.8 (C–9), 47.0 (C–36), 46.6 (C–17), 45.7 (C–19), 46.3 (C–37), 43.7 (C–35), 41.9 (C–4), 40.9 (C–14), 40.5 (C–18), 39.1 (C–8), 37.7 (C–1), 36.8 (C–10), 33.8 (C–21), 33.0 (C–30), 32.4 (C–7), 31.9 (C–20), 30.0 (C–15), 27.8 (C–2), 25.9 (C–38), 25.5 (C–27), 24.0 (C–29), 23.3 (C–11), 22.9 (C–16), 21.2 (C–32), 20.9 (C–34), 22.9 (C–22), 17.9 (C–6), 16.9 (C–26), 15.8 (C–25), 13.1 (C–24) ppm; and MS (ESI): *m*/*z* (%) 639.7 ([M + H]$^+$, 90); analysis calculated for $C_{39}H_{62}N_2O_5$ (638.93): C 73.31, H 9.78, N 4.38; found: C 73.05, H 9.93, N 4.11.

*3.19. (2α,3β,4α,6β) 2,3,23-Tris(acetyloxy)-N-(benzyl)-6-hydroxyurs-12-en-28-amide (**15**)*

Following GPB from **6** (150 mg, 0.24 mmol) and benzylamine (77 mg, 0.72 mmol) followed by chromatography (SiO_2, *n*-hexane/ethyl acetate, 8:2), **15** (186 mg, 41%) was obtained as a colorless solid; m.p.: 90–95 °C; $[\alpha]_D^{20} = -11.7°$ (*c* = 0.12, $CHCl_3$); R_F = 0.25 (SiO_2, *n*-hexane/ethyl acetate, 8:2); IR (ATR): ν = 3388*br*, 2924*br*, 1741*vs*, 1643*s*, 1371*s*, 1233*vs*, 1028*vs*, 601*w* cm^{-1}; UV-Vis ($CHCl_3$): λ_{max} (log ε) = 260 nm (0.1); ^{1}H NMR (400 MHz, $CDCl_3$): δ = 7.32 (*dd*, *J* = 8.0, 6.3 Hz, 2H, 40–H + 42–H), 7.30–7.22 (*m*, 3H, 39–H + 43–H + 41–H), 5.33–5.26 (*m*, 2H, 12–H + 2–H), 5.13–4.99 (*m*, 1H, 3–H), 4.50 (*d*, *J* = 5.7 Hz, 1H, 6–H), 4.47 (*d*, *J* = 5.6 Hz, 2H, 1–H$_a$ + 37–H$_a$), 4.26–4.19 (*m*, 3H, 23–H$_a$ + 1–H$_b$ + 37–H$_b$), 3.69 (*d*, *J* = 12.0 Hz, 1H, 23–H$_b$), 2.34 (*dd*, *J* = 19.0, 6.4 Hz, 1H, 18–H), 2.05 (*s*, 3H, 36–H), 2.00 (*s*, 3H, 32–H), 2.00 (*s*, 1H, 16–H$_a$), 1.98 (*s*, 3H, 34–H), 1.95–1.80 (*m*, 3H, 11–H$_a$ + 11–H$_b$ + 16–H$_b$), 1.70–1.56 (*m*, 4H, 22–H$_a$ + 22–H$_b$ + 15–H$_a$ + 5–H), 1.56–1.44 (*m*, 2H, 21–H$_a$ + 20–H), 1.40–1.28 (*m*, 4H, 9–H + 19–H + 21–H$_b$ + 7–H$_a$), 1.25 (*s*, 3H, 24–H), 1.20 (*s*, 3H, 26–H), 1.18–1.15 (*m*, 1H, 15–H$_b$), 0.95 (*d*, *J* = 5.9 Hz, 1H, 7–H$_b$), 0.95 (*s*, 3H, 29–H), 0.88 (*s*, 3H, 25–H), 0.84 (*s*, 3H, 27–H), 0.83 (*s*, 3H, 24–H), 0.82 (*d*, *J* = 5.7 Hz, 3H, 30–H) ppm; ^{13}C NMR (100 MHz, $CDCl_3$): δ = 177.6 (C–28), 171.0 (C–35), 170.4 (C–31), 170.2 (C–33), 141.0 (C–38), 138.3 (C–13), 128.7 (C–39), 128.7 (C–43), 128.0 (C–40), 128.0 (C–42), 127.5 (C–41), 126.2 (C–12), 73.4 (C–3), 69.1 (C–2), 67.9 (C–6), 64.9 (C–23), 54.4 (C–18), 48.1 (C–5), 47.2 (C–10), 46.0 (C–17), 45.0 (C–4), 43.9 (C–1), 43.8 (C–37), 42.3 (C–9), 39.0 (C–19), 38.9 (C–8), 38.4 (C–7), 38.2 (C–14), 37.0 (C–20), 32.3 (C–22), 30.8 (C–21), 27.1 (C–15), 24.7 (C–16), 23.4 (C–11), 22.3 (C–26), 21.9 (C–34), 21.2 (C–30), 21.1 (C–25), 21.0 (C–27), 20.9 (C–32), 20.8 (C–36), 17.3 (C–29), 14.1 (C–24) ppm; and MS (ESI): *m*/*z* (%) 702.3 ([M + H−H_2O]$^-$, 90), 724.2 ([M + H− H_2O + Na]$^+$, 85); analysis calculated for $C_{43}H_{61}NO_8$ (719.96): C 71.74, H 8.54, N 1.95; found: C 71.55, H 8.71, N 1.68.

*3.20. (2α,3β,4α,6β) 2,3,23-Tris(acetyloxy)-N-(phenyl)-6-hydroxyurs-12-en-28-amide (**16**)*

Following GPB from **6** (150 mg, 0.24 mmol) and aniline (67 mg, 0.72 mmol) followed by chromatography (SiO_2, *n*-hexane/ethyl acetate, 8:2), **16** (170 mg, 60%) was obtained as a colorless solid; m.p.: 135–139 °C; $[\alpha]_D^{20} = +10.9°$ (*c* = 0.08, $CHCl_3$); R_F = 0.15 (SiO_2, *n*-hexane/ethyl acetate, 8:2); IR (ATR): ν = 3403*br*, 2927*br*, 1741*s*, 1438*s*, 1233*vs*, 1031*s*, 757*s*, 690*s* cm^{-1}; UV-Vis ($CHCl_3$): λ_{max} (log ε) = 246 nm (0.3); ^{1}H NMR (500 MHz, $CDCl_3$): δ = 7.50–7.42 (*m*, 2H, 38–H + 42–H), 7.33–7.24 (*m*, 2H, 39–H + 41–H), 7.10–7.05 (*m*, 1H, 40–H), 5.62 (*d*, *J* = 3.7 Hz, 1H, 12–H), 5.33–5.25 (*m*, 1H, 2–H), 5.15 (*d*, *J* = 10.4 Hz, 1H, 3–H), 4.34 (*d*, J = 3.9 Hz, 1H, 6–H), 4.23 (*d*, *J* = 11.9 Hz, 1H, 23–H$_a$), 3.70 (*d*, *J* = 12.0 Hz, 1H, 23–H$_b$), 2.38 (*s*, 1H, 21–H$_a$), 2.36 (*dd*, *J* = 18.9, 6.4 Hz, 1H, 18–H), 2.07 (*s*, 3H, 36–H), 2.06 (*s*, 3H, 32–H), 2.02 (*s*, 3H, 34–H), 2.00–1.98 (*m*, 3H, 16–H$_a$ + 16–H$_b$ + 7–H$_a$), 1.91–1.79 (*m*, 4H, 11–H$_a$ + 11–H$_b$ + 5–H + 9–H), 1.72 (*td*, *J* = 13.8, 4.3 Hz, 1H, 15–H$_a$), 1.66–1.53 (*m*, 3H, 22–H$_a$ + 22–H$_b$ + 7–H$_b$), 1.50–1.42 (*m*, 2H, 21–H$_b$ + 19–H), 1.42–1.30 (*m*, 3H, 1–H$_a$ + 1–H$_b$ + 20–H), 1.26–1.22 (*m*, 1H, 15–H$_b$), 1.21 (*s*, 3H, 26–H), 1.12 (*s*, 3H, 27–H), 1.02 (*s*, 3H, 25–H), 0.99 (*d*, *J* = 2.0 Hz, 3H, 29–H), 0.92 (*d*, *J* = 6.4 Hz, 3H, 30–H), 0.87 (*s*, 3H, 24–H) ppm; ^{13}C NMR (125 MHz, $CDCl_3$): δ = 176.1 (C–28), 170.9 (C–35), 170.4 (C–31), 170.3 (C–33), 141.4

(C–13), 138.1 (C–37), 129.1 (C–39) 129.1 (C–41), 126.6 (C-12), 124.1 (C-40), 119.7 (C-38), 119.7 (C–42), 73.5 (C–3), 69.1 (C–2), 67.6 (C–6), 64.9 (C–23), 54.7 (C–18), 48.0 (C–5), 47.8 (C–17), 46.1 (C–9), 45.0 (C–4), 44.1 (C–10), 42.4 (C–1), 39.1 (C–19), 38.7 (C–8), 38.5 (C–7), 38.2 (C–20), 37.3 (C–14), 36.8 (C–22), 32.3 (C–21), 27.1 (C–15), 24.9 (C–16), 23.7 (C–11), 22.4 (C–27), 21.9 (C–30), 21.1 (C–34), 20.9 (C–32), 20.8 (C–36), 18.6 (C–29), 17.4 (C–25), 17.2 (C–26), 15.3 (C–24) ppm; and MS (ESI): *m*/*z* (%) 686.1 ($[M\text{-}H\text{-}H_2O]^-$, 90), 704.2 ($[M\text{-}H]^-$, 17); analysis calculated for $C_{42}H_{59}NO_8$ (705.93): C 71.46, H 8.42, N 1.98; found: C 71.21, H 8.57, N 1.62.

*3.21. (2α,3β,4α,6β) 2,3,23-Tris(acetyloxy)-N-(piperazinyl)-6-hydroxyurs-12-en-28-amide (**17**)*

Following GPB from **6** (500 mg, 0.79 mmol) and piperazine (204 mg, 2.37 mmol) followed by chromatography (SiO_2, chloroform/methanol, 9:1), **17** (206 mg, 41%) was obtained as a colorless solid; m.p.: 133–138 °C; $[\alpha]_D^{20}$ = +20.25° (*c* = 0.08, $CHCl_3$); R_F = 0.66 (SiO_2, $CHCl_3$/MeOH, 9:1); IR (ATR): ν = 3414*br*, 2932*br*, 1741*s*, 1631*s*, 1366*s*, 1233*vs*, 1025*s*, 748*s* cm^{-1}; ^1H NMR (500 MHz, $CDCl_3$): δ = 5.36–5.23 (*m*, 1H, 12–H), 5.13 (*d*, *J* = 10.4 Hz, 2H, 3–H + 2–H), 4.24 (*d*, *J* = 11.9 Hz, 2H, 6–H + 23–H_a), 3.73–3.57 (*m*, 1H, 23–H_b), 3.42–3.24 (*m*, 4H, 37–H_a + 37–H_b + 40–H_a + 40–H_b), 2.89–2.46 (*m*, 4H, 38–H_a + 38–H_b +39–H_a + 39–H_b), 2.44 (*d*, *J* = 11.2 Hz, 1H, 18–H), 2.33 (*dd*, *J* = 18.8, 6.2 Hz, 1H, 22–H_a), 2.03 (*s*, 3H, 36–H), 1.99 (*s*, 3H, 32–H), 1.98 (*s*, 3H, 1–H_a, 16–H_a + 16–H_b), 1.98 (*s*, 3H, 34–H), 1.93–1.79 (*m*, 2H, 11–H_a + 11–H_b), 1.75 (*dd*, *J* = 11.7, 5.3 Hz, 1H, 9–H), 1.68–1.58 (*m*, 2H, 22–H_b + 5–H), 1.52–1.46 (*m*, 1H, 21–H_a), 1.36–1.26 (*m*, 5H, 1–H_b + 21–H_b + 20–H + 19–H + 7–H_a), 1.21 (*s*, 3H, 26–H), 1.16 (*d*, *J* = 3.6 Hz, 1H, 15–H_a), 1.12 (*s*, 3H, 29–H), 1.09–0.98 (*m*, 1H, 7–H_b), 0.95 (*s*, 3H, 25–H), 0.96–0.92 (*m*, 1H, 15–H_b), 0.94 (*s*, 3H, 27–H), 0.88 (*s*, 3H, 30–H), 0.85 (*s*, 3H, 24–H) ppm; ^{13}C NMR (125 MHz, $CDCl_3$): δ = 175.3 (C–28), 171.1 (C–35), 170.4 (C–31), 170.2 (C–33), 143.9 (C–13), 126.1 (C–12), 73.6 (C–3), 69.1 (C–2), 67.9 (C–6), 65.0 (C–23), 58.8 (C–18), 48.8 (C–37), 48.8 (C–40), 46.1 (C–17), 45.9 (C–9), 45.8 (C–4), 45.5 (C–5), 45.4 (C–10), 45.0 (C–38), 45.0 (C–39), 42.3 (C–1), 40.5 (C–20), 39.5 (C–19), 38.7 (C–8), 38.3 (C–7), 38.3 (C–14), 32.3 (C–22), 30.4 (C–21), 30.3 (C–16), 27.4 (C–15), 25.4 (C–11), 23.4 (C–25), 23.3 (C–27), 22.4 (C–26), 22.3 (C–30), 21.9 (C–34), 21.2 (C–29), 20.9 (C–32), 20.6 (C–36), 17.5 (C–24) ppm; and MS (ESI): *m*/*z* (%) 681.3 ($[M + H-H_2O]^+$, 90); analysis calculated for $C_{40}H_{62}N_2O_8$ (698.94): C 68.74, H 8.94, N 4.01; found: C 68.45, H 9.13, N 3.83.

*3.22. (2α,3β,4α,6β) 2,3,23-Tris(acetyloxy)-N-(homopiperazinyl)-6-hydroxyurs-12-en-28-amide (**18**)*

Following GPB from **6** (500 mg, 0.79 mmol) with homopiperazine (254 mg, 2.37 mmol) followed by chromatography (SiO_2, chloroform/methanol, 9:1), **18** (437 mg, 81%) was obtained as a colorless solid; m.p.: 146.5–150.5 °C; $[\alpha]_D^{20}$ = +14.38 (*c* = 0.142 $CHCl_3$); R_F = 0.45 (SiO_2, $CHCl_3$/MeOH, 9:1); IR (ATR): ν = 2943*m*, 1731*s*, 1620*m*, 1464*m*, 1402*m*, 1371*m*, 1237*vs*, 1210*m*, 1180*m*, 1044*m*, 1029*s*, 976*m*, 938*m*, 749*s* cm^{-1}; ^1H NMR (500 MHz, $CDCl_3$): δ = 5.24–5.09 (m, 2H, 12–H, 2–H), 5.08–5.01 (m, 1H, 3–H), 3.83 (d, *J* = 11.8 Hz, 1H, 23–H_a), 3.55 (d, *J* = 11.8 Hz, 1H, 23–H_b), 4.02–2.87 (m, 10H, 38–H + 41–H + 40–H + 37–H + 39–H), 2.50–2.11 (m, 2H, 18–H + 16–H_a), 2.06 (s, 3H, 32–H), 1.99 (s, 3H, 36–H), 2.09–1.84 (m, 3H, 1–H + 11–H), 1.95 (s, 3H, 34–H), 1.83–1.68 (m, 1H, 22–H_a), 1.66–1.54 (m, 2H, 9–H + 22–H_b), 1.53–1.18 (m, 8H, 21–H + 7–H + 19–H + 6–H + 5–H), 1.15–0.98 (m, 3H, 1–H_b + 15–H), 1.07 (s, 3H, 25–H), 1.05 (s, 3H, 27–H), 0.93 (d, *J* = 5.9 Hz, 3H, 30–H), 0.86 (s, 3H, 24–H), 0.84 (d, *J* = 5.7 Hz, 3H, 29–H), 0.70 (s, 3H, 26–H) ppm; ^{13}C NMR (125 MHz, $CDCl_3$): δ = 176.6 (C–28), 171.0 (C–35), 170.5 (C–31), 170.5 (C–33), 138.7 (C–13), 124.9 (C–12), 75.0 (C–3), 70.0 (C–2), 65.4 (C–23), 55.2 (C–18), 49.1 (C–41), 47.8 (C–40), 47.7 (C–39), 47.7 (C–5), 47.7 (C–9), 47.7 (C–38), 46.5 (C–17), 43.8 (C–1), 43.8 (C–37), 42.4 (C–14), 42.0 (C–4), 39.5 (C–19), 38.7 (C–20), 38.0 (C–8), 37.9 (C–10), 34.4 (C–22), 32.5 (C–7), 30.5 (C–21), 28.1 (C–15), 26.1 (C–16), 23.4 (C–11), 23.4 (C–27), 21.3 (C–30), 21.2 (C–34), 21.0 (C–36), 20.9 (C–32), 18.0 (C–6), 17.4 (C–29), 17.2 (C–25), 17.1 (C–26), 14.0 (C–24) ppm; and MS (ESI): *m*/*z* (%) 701.5 ($[M + H]^+$, 100); analysis calculated for $C_{40}H_{64}N_2O_8$ (712.97): C 69.07, H 9.05, N 3.93; found: C 68.86, H 9.28, N 3.70.

*3.23. N-[9-[2-({4-(3β,4α)-3-Acetyloxy-23,28-dioxours-12-en-28-yl]-1-piperazinyl}carbonyl) phenyl]-6-diethylamino-3H-xanthen-3-ylidene]-N-ethylethanaminium Chloride (**19**)*

Following GPC from **9** (186 mg, 0.32 mmol) followed by chromatography (SiO_2, chloroform/methanol, 9:1), **19** (213 mg, 64%) was obtained as a purple solid; m.p.: 243–247 °C; R_F = 0.29 (SiO_2, $CHCl_3$/MeOH, 9:1); IR (ATR): ν = 2928*w*, 1633*m*, 1586*vs*, 1481*m*, 1411*s*, 1335*s*, 1273*m*, 1244*s*, 1179*vs*, 1132*s*, 1044*w*, 921*m*, 788*w*, 482*w*, 410*w* cm^{-1}; UV-Vis ($CHCl_3$): λ_{max} (log ε) = 260 (4.54), 307 (4.20), 356 (3.90), 561 (5.08) nm; ^1H NMR (400 MHz, $CDCl_3$): δ = 9.25 (*s*, 1H, 23–H), 7.71–7.59 (*m*, 1H, 38–H), 7.56–7.46 (*m*, 1H, 37–H), 7.37–7.20 (*m*, 1H, 39–H), 7.16–6.89 (*m*, 2H, 44–H + 44′–H), 6.82–6.70 (*m*, 2H, 47–H + 47′–H), 5.23–5.17 (*m*, 1H, 12–H), 4.99–4.90 (*m*, 1H, 3–H), 3.84–3.13 (*m*, 16H, 49–H + 49′–H + 34–H + 33–H), 3.07–2.80 (*m*, 1H, 18–H), 2.20–1.98 (*m*, 1H, 16–H_a), 1.93 (*s*, 3H, 32–H), 1.91–1.82 (*m*, 2H, 11–H), 1.78–1.51 (*m*, 6H, 2–H + 1–H_a + 19–H_a + 9–H + 22–H_a), 1.49–1.36 (*m*, 3H, 6–H_a + 15–H_a + 7–H_a), 1.29 (*t*, *J* = 7.0 Hz, 13H, 49–H + 49′–H + 5–H), 1.25–1.16 (*m*, 2H, 22–H_b), 1.09 (*s*, 3H, 27–H), 1.16–1.00 (*m*, 4H, 19–H_b + 21–H_b + 7–H_b + 1–H_b), 1.04 (*s*, 3H, 23–H), 0.92 (*s*, 3H, 25–H), 1.00–0.78 (*m*, 3H, 15–H), 0.85 (*s*, 3H, 30–H), 0.83 (*s*, 3H, 29–H), 0.63 (*s*, 3H, 26–H) ppm; ^{13}C NMR (100 MHz, $CDCl_3$): δ = 204.6 (C–24), 175.7 (C–28), 170.4 (C–31), 167.8 (C–35), 157.8 (C–48), 157.8 (C–48′),155.9 (C–46), 155.8 (C–46′), 155.7 (C–42), 144.9 (C–13), 135.1 (C–41), 132.4 (C–45), 132.4 (C–45′), 130.8 (C–36), 130.4 (C–39), 130.3 (C–40), 130.3 (C–38), 127.7 (C–37), 121.1 (C–12), 114.4 (C–44), 114.4 (C–44′), 113.9 (C–43), 113.9 (C–43′), 96.4 (C–47), 96.4 (C–47′), 73.5 (C–3), 54.4 (C–4), 47.9 (C–5), 47.9 (C–34), 47.9 (C–41), 47.7 (C–9), 47.6 (C–17), 46.3 (C–49), 46.3 (C–49′), 46.3 (C–19), 43.7 (C–18), 42.0 (C–14), 42.0 (C–33), 42.0 (C–39), 39.5 (C–8), 37.8 (C–1), 36.0 (C–10), 34.0 (C–21), 33.0 (C–29), 32.3 (C–7), 30.4 (C–20), 29.8 (C–22), 27.9 (C–15), 25.9 (C–27), 24.1 (C–30), 23.4 (C–11), 22.6 (C–2), 22.4 (C–16), 21.1 (C–32), 20.5 (C–6), 16.98 (C–26), 15.7 (C–25), 12.8 (C–50), 12.8 (C–50′), 9.5 (C–24) ppm; and MS (ESI): *m*/*z* (%) 1005.7 ($[M-Cl]^+$, 100); analysis calculated for $C_{64}H_{85}ClN_4O_6$ (1041.86): C 73.78, H 8.22, N 5.38; found: C 73.49, H 8.47, N 5.08.

*3.24. N-[9-[2-({4-(3β, 4α)-3-Acetyloxy-23,28-dioxours-12-en-28-yl]-1,4-diazepan-1-yl}carbonyl) phenyl]-6-diethylamino-3H-xanthen-3-ylidene]-N-ethylethanaminium Chloride (**20**)*

Following GPC from **10** (176 mg, 0.30 mmol) followed by chromatography (SiO_2, chloroform/methanol, 9:1), **20** (171 mg, 56%) was obtained as a purple solid; m.p.: 270–276 °C; R_F = 0.29 (SiO_2, $CHCl_3$/MeOH, 9:1); IR (ATR): ν = 2927*w*, 1739*m*, 1650*w*, 1644*w*, 1625*m*, 1587*vs*, 1529*w*, 1468*m*, 1412*s*, 1381*m*, 1336*s*, 1245*s*, 1180*vs*, 1074*m*, 975*m*, 824*w*, 748*m*, 620*w*, 472*w*, 412*w* cm^{-1}; UV-Vis ($CHCl_3$): λ_{max} (log ε) = λ_{max} (log ε) = 260 (4.19), 308 (3.89), 356 (3.59), 562 (4.75) nm; ^1H NMR (400 MHz, $CDCl_3$): δ = 9.25 (s, 1H, 24–H), 7.73–7.53 (m, 1H, 41–H), 7.49–7.37 (m, 1H, 40–H), 7.36–7.08 (m, 3H, 48–H + 42–H), 7.04–6.58 (m, 2H, 50–H + 50′–H), 5.31–5.16 (m, 1H, 12–H), 5.05–4.86 (m, 1H, 3–H), 4.22–3.47 (m, 8H, 52–H + 52′–H + 33–H + 35–H + 37–H), 3.45–2.94 (m, 1H, 34–H + 18–H), 2.41–2.17 (m, 2H, 36–H), 1.93 (s, 3H, 32–H), 2.15–1.80 (m, 2H, 11–H), 1.79–1.56 (m, 6H, 16–H + 1–H_a + 19–H_a + 22–H_a + 9–H), 1.56–1.24 (m, 4H, 7–H_a + 5–H + 2–H), 1.31 (t, *J* = 6.2 Hz, 12H, 53–H + 53′–H), 1.23–0.99 (m, 5H, 21–H + 7–H_b + 19–H_b + 1–H_a), 1.10 (s, 3H, 27–H), 1.04 (s, 3H, 23–H), 1.04–0.80 (m, 15–H + 6–H), 0.94 (s, 3H, 25–H), 0.90 (s, 3H, 30–H), 0.85 (s, 3H, 29–H), 0.67 (s, 3H, 26–H) ppm; ^{13}C NMR (100 MHz, $CDCl_3$): δ = 204.5 (C–24), 175.6 (C–28), 170.3 (C–31), 167.7 (C–38), 157.7 (C–51), 157.7 (C–51′), 155.8 (C–49), 155.7 (C-49′), 155.6 (C–45), 144.8 (C–13), 135.0 (C–44), 132.3 (C–48), 130.7 (C–39), 130.3 (C–43), 130.2 (C–42), 130.2 (C–41), 127.6 (C–40), 121.0 (C–12), 114.3 (C–47), 114.3 (C–47′), 113.8 (C–46), 113.8 (C–46′), 96.4 (C–50), 96.3 (C–50′), 73.4 (C–3), 54.3 (C–4), 49.2 (C-35), 47.8 (C–5), 47.6 (C–9), 47.4 (C–17), 47.2 (C-34), 46.5 (C-33 + C-37), 46.2 (C–19), 46.2 (C–52), 46.1 (C–52′), 43.5 (C–18), 41.9 (C–14), 39.4 (C–8), 37.7 (C–1), 35.8 (C–10), 33.9 (C–21), 32.9 (C–29), 32.2 (C–7), 30.3 (C–22), 27.7 (C–15), 26.6 (C-36), 25.8 (C-27), 24.0 (C–30), 23.2 (C–11), 22.4 (C–16), 21.9 (C–2), 21.0 (C–32), 20.4 (C–6), 16.9 (C–26), 15.5 (C–25), 12.7 (C–53), 12.7 (C–53′), 9.4 (C–23) ppm; and MS (ESI): *m*/*z* (%) 1019.1 ($[M-Cl]^+$, 100); analysis calculated for $C_{65}H_{87}ClN_4O_6$ (1055.88): C 73.94, H 8.31, N 5.31; found: C 73.76, H 8.57, N 5.05.

*3.25. N-9-[2-({4-[(3β,4α)-3,23-Bis(acetyloxy)-28-oxours-12-en-28-yl]-1-piperazinyl}carbonyl) phenyl]-6-diethylamino-3H-xanthen-3-ylidene]-N-ethylethanaminium Chloride (**21**)*

Following GPC from **13** (500 mg, 0.80 mmol) followed by chromatography (SiO_2, chloroform/methanol, 9:1), **21** (237 mg, 47%) was obtained as a purple solid; m.p.: 236–243 °C; R_F = 0.19 (SiO_2, $CHCl_3$/MeOH 95:5); IR (ATR): ν = 3340*br*, 2938*br*, 1728*s*, 1585*vs*, 1338*vs*, 1240*vs*, 1005*s*, 686*w* cm^{-1}; UV-Vis ($CHCl_3$): λ_{max} (log ε) = 258 (0.3), 306 (0.1), 354 (0.1), 561 (1.0) nm; ^{1}H NMR (500 MHz, $CDCl_3$): δ = 7.72–7.43 (*m*, 3H, 42–H + 43–H + 41–H), 7.38–7.29 (*m*, 1H, 44–H), 7.36–7.24 (*m*, 2H, 49–H + 49′–H), 7.04 (*d*, *J* = 37.5 Hz, 2H, 48–H + 48′–H), 6.83–6.63 (*m*, 2H, 51–H + 51′–H), 5.21 (*d*, *J* = 3.6 Hz, 1H, 12–H), 4.76 (*dd*, *J* = 11.5, 4.9 Hz, 1H, 3–H), 3.96–3.80 (*m*, 1H, 23–H_a), 3.69–3.57 (*m*, 3H, 23–H_b + 53–H + 53′–H), 3.41–3.32 (*m*, 2H, 36–H_a + 36–H_b + 37–H_a + 37–H_b), 3.27–3.22 (*m*, 2H, 35–H_a + 35–H_b + 38–H_a + 38–H_b), 3.02–2.83 (*m*, 1H, 18–H), 2.63–2.40 (*m*, 1H, 5–H), 2.05 (*d*, *J* = 2.6 Hz, 3H, 32–H), 2.02 (*s*, 3H, 34–H), 1.96–1.75 (*m*, 2H, 11–H_a + 11–H_b), 1.72–1.38 (*m*, 14H, 16–H_a + 16–H_b + 19–H_a + 7–H_a + 7–H_b + 2–H_a + 2–H_b + 1–H_a + 9–H + 6–H_a + 6–H_b + 15–H_a + 22–H_a + 21–H_a), 1.31 (*t*, *J* = 6.9 Hz, 2H, 54–H + 54′–H), 1.24–1.08 (*m*, 5H, 19–H_b + 15–H_b + 22–H_b + 1–H_b + 21–H_b), 1.07 (*s*, 3H, 27–H), 1.00 (*d*, *J* = 23.5 Hz, 3H, 29–H), 0.92 (*s*, 3H, 25–H), 0.86 (*d*, *J* = 1.9 Hz, 3H, 30–H), 0.81 (*s*, 3H, 24–H), 0.64 (*s*, 3H, 26–H) ppm; ^{13}C NMR (125 MHz, $CDCl_3$): δ = 175.7 (C–28), 171.0 (C–31), 170.6 (C–33), 167.7 (C–37), 157.7 (C–52), 157.7 (C–52′), 155.8 (C–46), 155.7 (C–50), 155.6 (C–50′), 144.6 (C–13), 135.1 (C–45), 132.3 (C–49), 132.3 (C–49′), 130.7 (C–40), 130.4 (C–44), 130.2 (C–42), 130.2 (C–43), 127.6 (C–41), 121.4 (C–12), 114.3 (C–48), 114.3 (C–48′), 113.8 (C–47), 113.8 (C–47′), 96.3 (C–51), 96.3 (C–51′), 74.5 (C–3), 65.4 (C–23), 55.8 (C–5), 47.9 (C–9), 47.7 (C–17), 47.5 (C–36), 47.5 (C–37), 46.2 (C–19), 46.1 (C–53), 46.1 (C–53′), 45.4 (C–4), 43.5 (C–18), 41.7 (C–35), 41.7 (C–38), 40.5 (C–14), 39.0 (C–8), 37.7 (C–1) 36.8 (C–10), 34.0 (C–21), 32.9 (C–30), 32.5 (C–7), 32.3 (C–20), 30.3 (C–15), 29.9 (C–2), 27.8 (C–27), 25.7 (C–29), 24.0 (C–11), 23.4 (C–16), 22.9 (C–22), 21.2 (C–32), 20.9 (C–34), 17.9 (C–6), 16.9 (C–26), 15.8 (C–25), 13.1 (C–24) 12.7 (C–54), 12.7 (C–54′) ppm; and MS (ESI): *m*/*z* (%) 1049.86 ($[M-Cl]^+$, 60); analysis calculated for $C_{66}H_{89}ClN_4O_7$ (1085.91): C 73.00, H 8.26, N 5.16; found: C 72.84, H 8.41, N 4.87.

*3.26. N-9-[2-({4-[(3β,4α)-3,23-Bis(acetyloxy)-28-oxours-12-en-28-yl]-1,4-diazepan-1-yl} carbonyl)phenyl]-6-diethylamino-3H-xanthen-3-ylidene]-N-ethylethanaminium Chloride (**22**)*

Following GPC from **14** (156 mg, 0.24 mmol) followed by chromatography (SiO_2, chloroform/methanol, 9:1), **22** (49 mg, 31%) was obtained as a purple solid; m.p.: 243–248 °C; R_F = 0.29 (SiO_2, $CHCl_3$/MeOH, 9:1); IR (ATR): ν = 3424*br*, 2941*br*, 1732*s*, 1640*w*,1588*s*, 1338*w*, 1244*s*, 690*w* cm^{-1}; UV-Vis ($CHCl_3$): λ_{max} (log ε) = 256 (0.2), 304 (0.1), 354 (0.1), 558 (0.5) nm; ^{1}H NMR (500 MHz, $CDCl_3$): δ = 7.84–7.68 (*m*, 1H, 42–H), 7.67–7.55 (*m*, 2H, 43–H + 44–H), 7.43 (*d*, *J* = 6.6 Hz, 1H, 45–H), 7.26 (*s*, 2H, 50–H + 50′–H), 7.05 (*t*, *J* = 11.1 Hz, 2H, 49–H + 49′–H), 6.89–6.70 (*m*, 2H, 52–H + 52′–H), 5.31–5.17 (*m*, 1H, 12–H), 4.80–4.69 (*m*, 1H, 3–H), 3.84 (*t*, *J* = 10.3 Hz, 1H, 23–H_a), 3.74–3.40 (*m*, 5H, 23–H_b + 54–H+ 54′–H + 39–H_a + 39–H_b), 3.13 (*d*, *J* = 75.5 Hz, 2H, 35–H_a + 35–H_b), 2.94–2.82 (*m*, 5H, 18–H + 36–H_a + 36–H_b + 37–H_a+ 37–H_b), 2.18–2.07 (*m*, 1H, 16–H_a + 22–H_a) 2.05 (*s*, 3H, 34–H), 2.00 (*s*, 3H, 32–H), 1.87 (*tq*, *J* = 18.0, 9.1, 8.6 Hz, 2H, 11–H_a + 11–H_b), 1.74–1.35 (*m*, 14H, 16–H_b + 19–H_a + 19–H_b + 15–H_a + 38–H_a + 38–H_b + 2–H_a + 2–H_b + 22–H_b + 1–H_a + 7–H_a + 6–H_a + 6–H_b +21–H_a), 1.26–1.13 (*m*, 5H, 7–H_b + 9–H + 1–H_b + 21–H_b + 15–H_b + 55–H + 55′–H), 1.12 (*s*, 3H, 27–H), 0.94 (*s*, 3H, 25–H), 0.93 (*s*, 3H, 29–H), 0.89 (*s*, 3H, 30–H), 0.81 (*s*, 3H, 24–H), 0.74 (*s*, 3H, 26–H) ppm; ^{13}C NMR (125 MHz, $CDCl_3$): δ = 174.5 (C–28), 171.0 (C–31), 170.7 (C–33), 166.8 (C–40), 157.7 (C–53), 157,7 (C–53′), 155.7 (C–47), 155.7 (C–51), 155,6 (C–51′), 144.7 (C–13), 135.0 (C–46), 132.2 (C–50), 132.2 (C–50′), 130.6 (C–41), 130.4 (C–45),130.3 (C–43), 130.2 (C–44), 127.8 (C–42), 121.4 (C–12), 114.3 (C–49), 114.3 (C–49′), 113.9 (C–48), 113.9 (C–48′), 96.2 (C–52), 96.2 (C–52′), 74.6 (C–3), 65.5 (C–23), 56.3 (C–39), 48.0 (C–5), 47.9 (C–9), 47.8 (C–36), 46.6 (C–17), 46.3 (C–37), 46.2 (C–54), 46.2 (C–54′), 45.5 (C–19), 43.7 (C–35), 41.9 (C–4), 40.6 (C–14), 40.5 (C–18), 39.1 (C–8), 37.7 (C–1), 36.8 (C–10), 34.1 (C–21), 33.0 (C–30), 32.4 (C–7), 32.3 (C–20), 30.3 (C–15), 30.0 (C–2), 27.9 (C–27), 25.8 (C–29), 23.9 (C–11), 23.4 (C–16), 22.9 (C–22), 21.2 (C–32), 20.9 (C–34), 18.0 (C–6), 16.8 (C–26), 15.8 (C–25), 13.1 (C–24), 12.9 (C–55), 12.9 (C–55′) ppm; and MS (ESI): *m/z* (%) = 1064.1 ($[M-Cl]^+$, 70); analysis calculated for $C_{67}H_{91}ClN_4O_7$ (1099.94): C 73.16, H 8.34, N 5.09; found: C 72.87, H 8.53, N 4.85.

*3.27. N-{6-Diethylamino-9-[2-({4[(2α,3β,4α,6β)-2,3,23-tris(acetyloxy)-6-hydroxy-28-oxours-12-en-28-yl)-1-piperazinyl]carbonyl]phenyl]-3H-xanthen-3-ylidene)-N-ethylethanaminium Chloride (**23**)*

Following GPC from **17** (156 mg, 0.22 mmol) followed by chromatography (SiO_2, chloroform/methanol, 9:1), **23** (88 mg, 56%) was obtained as a purple solid; m.p.: 228–233 °C; R_F = 0.20 (SiO_2, $CHCl_3$/MeOH, 95:5); IR (ATR): ν = 2915*w*, 2897*w*, 1735*s*, 1568*s*, 1466*s*, 1340*s*, 1232*s*, 1160*vs*, 1077*s* cm^{-1}; UV-Vis ($CHCl_3$): λ_{max} (log ε) = 256 (0.4), 305 (0.2), 354 (0.1), 560 (1.0) nm; ^1H NMR (500 MHz, $CDCl_3$): δ = 7.84–7.61 (*m*, 2H, 44–H, 45–H), 7.54–7.47 (*m*, 1H, 43–H), 7.35–7.27 (*m*, 3H, 46–H, 51–H, 51′–H), 7.18–6.93 (*m*, 2H, 50–H, 50′–H), 6.92–6.67 (*m*, 2H, 53–H, 53′–H), 5.32–5.24 (*m*, 1H, 12–H), 5.13 (*dd*, *J* = 10.4, 6.7 Hz, 2H, 3–H, 2–H), 4.23 (*dd*, *J* = 11.9, 7.7 Hz, 2H, 6–H, 23–H_a), 3.78–3.51 (*m*, 3H, 55–H, 55′–H, 23–H_b), 3.49–3.18 (*m*, 8H, 37–H_a, 37–H_b 40–H_a, 40–H_b, 38–H_a, 38–H_b, 39–H_a, 39–H_b), 2.23–2.11 (*m*, 1H, 22–H_a), 2.09 (*s*, 3H, 36–H), 2.16–2.07 (*m*, 2H, 18–H, 16–H_a), 2.02 (*s*, 3H, 32–H), 2.00 (*s*, 3H, 34–H), 1.98 (*s*, 3H, 1–H_a, 16–H), 1.92–1.77 (*m*, 2H, 11–H_a, 11–H_b), 1.80–1.54 (*m*, 1H, 9–H), 1.66–1.27 (*m*, 14H, 6–H_a, 6–H_b, 7–H_a, 7–H_b, 16–H_b, 22–H_b, 21–H_a, 1–H_b, 15–H_a, 21–H_b, 20–H, 19–H_a, 56–H, 56′–H), 1.25 (*s*, 3H, 26–H), 1.22–0.92 (*m*, 2H, 15–H_b, 19–H_b), 1.12 (*s*, 3H, 29–H), 0.99 (*s*, 3H, 25–H), 0.93 (*s*, 3H, 27–H), 0.86 (*s*, 3H, 30–H), 0.82–0.75 (*m*, 1H, 5–H), 0.83 (*s*, 3H, 24–H) ppm; ^{13}C NMR (125 MHz, $CDCl_3$): δ = 174.6 (C–28), 171.0 (C–35), 170.5 (C–31), 170.2 (C–33), 167.7 (C–41), 157.7 (C–54), 157.7 (C–54′), 155.9 (C–48), 155.6 (C–52), 155.6 (C–52′), 144.7 (C–13), 135.0 (C–47), 132.3 (C–51), 132.3 (C–51′), 130.7 (C–42), 130.3 (C–46), 130.2 (C–44), 130.1 (C–45), 127.7 (C–43), 126.0 (C–12), 114.3 (C–50), 114.3 (C–50′), 113.9 (C–49), 113.9 (C–49′), 96.2 (C–53), 96.2 (C–53′), 73.5 (C–3), 69.1 (C–2), 67.5 (C–6), 64.9 (C–23), 58.7 (C–18), 48.7 (C–37), 48.7 (C–39), 46.2 (C–17), 45.9 (C–55), 45.9 (C–55′), 45.9 (C–9), 45.7 (C–4), 45.5 (C–5), 45.3 (C–10), 45.0 (C–38), 45.0 (C–39), 42.3 (C–1), 40.6 (C–20), 39.3 (C–19), 38.6 (C–8), 38.3 (C–7), 38.2 (C–14), 32.3 (C–22), 30.4 (C–21), 30.3 (C–16), 27.4 (C–15), 25.4 (C–11), 23.4 (C–25), 23.3 (C–27), 22.4 (C–26), 22.3 (C–30), 21.9 (C–34), 21.1 (C–29), 20.9 (C–32), 20.7 (C–36) 17.4 (C–24), 12.7 (C–56), 12.7 (C–56′) ppm; and MS (ESI): *m/z* (%) = 1123.7 ($[M-Cl]^-$, 35); analysis calculated for $C_{68}H_{91}ClN_4O_{10}$ (1159.94): C 70.41, H 7.91, N 4.83; found: C 7021, H 8.13, N 4.74.

*3.28. N-{6-Diethylamino-9-[2-({4[(2α,3β,4α,6β)-2,3,23-tris(acetyloxy)-6-hydroxy-28-oxours-12-en-28-yl)-1,4-diazepan-1-yl}carbonyl]phenyl]-3H-xanthen-3-ylidene)-N-ethylethanaminium Chloride (**24**)*

Following GPC from **18** (250 mg, 0.35 mmol) followed by chromatography (SiO_2, chloroform/methanol, 9:1), **24** (197 mg, 48%) was obtained as a purple solid; m.p.: 269–273 °C; R_F = 0.34 (SiO_2, $CHCl_3$/MeOH 9:1); IR (ATR): ν = 2925*w*, 1739*m*, 1645*w*, 1626*m*, 1587*vs*, 1412*s*, 1395*m*, 1336*s*, 1244*s*, 1179*vs*, 1160*m*, 1073*m*, 1029*m*, 976*m*, 746*s*, 683*s*, 472*w*, 410*w* cm^{-1}; UV-Vis ($CHCl_3$): λ_{max} (log ε) = 260 (4.43), 307 (4.10), 355 (3.80), 562 (4.98) nm; ^1H NMR (500 MHz, $CDCl_3$): δ = 7.72–7.54 (*m*, 2H, 46–H + 45–H), 7.50–7.37 (*m*, 1H, 44–H), 7.33–7.07 (*m*, 3H, 47–H + 51–H + 51′–H), 6.96–6.62 (*m*, 2H, 54–H + 54′–H), 5.58–5.46 (*m*, 1H, 12–H), 5.38–5.20 (*m*, 1H, 2–H), 5.11 (*d*, *J* = 10.4 Hz, 1H, 3–H), 4.21 (*d*, *J* = 11.8 Hz, 1H, 23–H_a), 4.15–2.81 (*m*, 19H, 56–H + 56′–H + 23–H_b + 37–H + 38–H + 39–H + 40–H + 41–H), 2.52–2.22 (*m*, 4H, 18–H + 22–H_a + 16–H), 2.20–1.84 (*m*, 3H, 1–H_a + 11–H), 2.02 (*s*, 3H, 36–H), 1.97 (*s*, 3H, 34–H), 1.96 (*s*, 3H, 32–H), 1.83–1.66 (*m*, 1H, 9–H), 1.64–1.50 (*m*, 1H, 22–H_b), 1.31 (*s*, 12H, 57–H + 57′–H), 1.49–1.22 (*m*, 5H, 21–H_b + 1–H_b + 19–H + 6–H +20–H), 1.18 (*s*, 3H, 25–H), 1.10 (*s*, 3H, 24–H), 1.03–0.87 (*m*, 1H, 5–H), 0.93 (*s*, 3H, 27–H), 0.91 (*s*, 3H, 29–H), 0.83 (*s*, 3H, 26–H), 0.82 (*s*, 3H, 30–H) ppm; ^{13}C NMR (125 MHz, $CDCl_3$): δ = 176.8 (C–28), 171.1 (C–35), 170.5 (C–31), 170.4 (C–33), 168.1 (C–42), 157.9 (C–55), 157.9 (C–55′), 155.9 (C–53), 155.9 (C–53′), 155.8 (C–49), 143.1 (C–13), 134.1 (C–48), 132.5 (C–51), 132.5 (C–51′), 131.4 (C–52), 131.4 (C–52′), 130.2 (C–46), 130.1 (C–47), 129.7 (C–45), 126.9 (C–44), 122.7 (C–12), 114.2 (C–51), 114.2 (C–51′), 114.0 (C–50), 113.8 (C–50′), 96.4 (C–54), 96.4 (C–54′), 73.7 (C–3), 69.3 (C–2), 65.1 (C–23), 55.8 (C–18), 49.4 (C–37), 49.4 (C–41), 46.6 (C–40), 46.4 (C–39), 46.3

(C–56), 46.6 (C–56′), 46.2 (C–38), 46.2 (C-17), 46.0 (C-9), 45.1 (C-4), 43.9 (C-14),42.4 (C-1), 38.8 (C-19), 38.6 (C-5), 38.5 (C-20), 38.4 (C-6), 38.4 (C-8), 38.3 (C-10), 34.2 (C-7),32.4 (C-22), 30.4 (C-21), 27.4 (C-15), 25.4 (C-16), 23.5 (C-11), 23.1 (C-27), 22.4 (C-25), 22.0 (C-24), 21.3 (C-29), 21.2 (C-26), 21.0 (C-34), 21.0 (C-32), 20.8 (C-36), 17.7 (C-30), 12.8 (C-57 + C-57′) ppm; and MS (ESI): m/z (%) 1137.7 ($[M-Cl]^+$, 25); analysis calculated for $C_{69}H_{93}ClN_4O_{10}$ (1173.97): C 70.59, H 7.99, N 4.77; found: C 70.33, H 8.16, N 4.52.

4. Conclusions

Several amides and rhodamine B conjugates derived from parent triterpenoic acids gypsogenin, hederagenin, and madecassic acid were synthesized and their cytotoxicity was evaluated in SRB assay. While the parent acids exhibited very low cytotoxicity, their corresponding acetates proved better. Acetylated amides, however, gave significantly lower EC_{50} values than the acetates. A significant increase in cytotoxicity was observed for the corresponding rhodamine B conjugates obtained from the latter. While rhodamine B is not cytotoxic (cut-off 30 µM), triterpenoic conjugates of rhodamine B holding a piperazinyl or homopiperazinyl spacer were cytotoxic, even in nano-molar concentration, with compound **24** being the most cytotoxic one. In comparison, homopiperazinyl-spacered compounds were more tumor-cell selective than their piperazinyl-spacered analogs. The preparation of benzyl and phenylamides succeeded in generating compounds holding similar bioactivity as previously reported for some analogs derived from betulinic, ursolic, glycyrrhetinic, or oleanolic acid. Our present studies showed spacered conjugates derived from madecassic acid of excellent cytotoxicity in single-digit nanomolar concentration combined with a noteworthy tumor/non-tumor cell selectivity.

Supplementary Materials: The following are available online at https://www.mdpi.com/article/10.3390/ijms23084362/s1, Supplementary File S1: details of the SRB assay, and depicted NMR (^{1}H, ^{13}C).

Author Contributions: R.C. brought the idea, managed the research, and prepared the manuscript; O.K., A.-K.H., and I.S. prepared the compounds for screening, O.K. and R.C. undertook draft preparation, and S.H. conducted biological experiments. All authors have read and agreed to the published version of the manuscript.

Funding: We acknowledge the financial support within the funding program Open Access Publishing by the German Research Foundation (DFG).

Institutional Review Board Statement: Not applicable.

Informed Consent Statement: Not applicable.

Data Availability Statement: Not applicable.

Acknowledgments: We like to thank D. Ströhl and his team for the NMR spectra and T. Schmidt for numerous MS spectra; IR, UV/vis spectra and elemental analyses were measured by M. Schneider; the cell lines were kindly provided by Th. Müller (Dep. of Haematology/Oncology, Martin-Luther University Halle-Wittenberg).

Conflicts of Interest: The authors declare no conflict of interest.

References

1. Cancer. Available online: https://www.who.int/news-room/fact-sheets/detail/cancer (accessed on 20 September 2021).
2. Latest Global Cancer Data: Cancer Burden Rises to 19.3 Million New Cases and 10.0 Million Cancer Deaths in 2020. Available online: https://www.iarc.who.int/news-events/latest-global-cancer-data-cancer-burden-rises-to-19-3-million-new-cases-and-10-0-million-cancer-deaths-in-2020/ (accessed on 20 September 2021).
3. Siddiqui, B.S.; Begum, S.; Siddiqui, S.; Lichter, W. Two cytotoxic pentacyclic triterpenoids from Nerium oleander. *Phytochemistry* **1995**, *39*, 171–174. [CrossRef]
4. Chudzik, M.; Korzonek-Szlacheta, I.; Krol, W. Triterpenes as potentially cytotoxic compounds. *Molecules* **2015**, *20*, 1610–1625. [CrossRef] [PubMed]
5. Goncalves, B.M.F.; Salvador, J.A.R.; Marin, S.; Cascante, M. Synthesis and biological evaluation of novel asiatic acid derivatives with anticancer activity. *RSC Adv.* **2016**, *6*, 3967–3985. [CrossRef]

6. Kim, M.-R.; Lee, H.-H.; Hahm, K.-S.; Moon, Y.-H.; Woo, E.-R. Pentacyclic triterpenoids and their cytotoxicity from the stem bark of Styrax japonica S. et Z. *Arch. Pharmacal Res.* **2004**, *27*, 283–286. [CrossRef]
7. Baratto, L.C.; Porsani, M.V.; Pimentel, I.C.; Pereira Netto, A.B.; Paschke, R.; Oliveira, B.H. Preparation of betulinic acid derivatives by chemical and biotransformation methods and determination of cytotoxicity against selected cancer cell lines. *Eur. J. Med. Chem.* **2013**, *68*, 121–131. [CrossRef]
8. Drag, M.; Surowiak, P.; Drag-Zalesinska, M.; Dietel, M.; Lage, H.; Oleksyszyn, J. Comparison of the cytotoxic effects of birch bark extract, betulin and betulinic acid towards human gastric carcinoma and pancreatic carcinoma drug-sensitive and drug-resistant cell lines. *Molecules* **2009**, *14*, 1639–1651. [CrossRef]
9. Kommera, H.; Kaluderovic, G.N.; Dittrich, S.; Kalbitz, J.; Dräger, B.; Müller, T.; Paschke, R. Carbamate derivatives of betulinic acid and betulin with selective cytotoxic activity. *Bioorg. Med. Chem. Lett.* **2010**, *20*, 3409–3412. [CrossRef]
10. Wiemann, J.; Heller, L.; Perl, V.; Kluge, R.; Ströhl, D.; Csuk, R. Betulinic acid derived hydroxamates and betulin derived carbamates are interesting scaffolds for the synthesis of novel cytotoxic compounds. *Eur. J. Med. Chem.* **2015**, *106*, 194–210. [CrossRef]
11. Mazumder, K.; Tanaka, K.; Fukase, K. Cytotoxic activity of ursolic acid derivatives obtained by isolation and oxidative derivatization. *Molecules* **2013**, *18*, 8929–8944. [CrossRef]
12. Lewinska, A.; Adamczyk-Grochala, J.; Kwasniewicz, E.; Deregowska, A.; Wnuk, M. Ursolic acid-mediated changes in glycolytic pathway promote cytotoxic autophagy and apoptosis in phenotypically different breast cancer cells. *Apoptosis* **2017**, *22*, 800–815. [CrossRef]
13. Hao, J.; Liu, J.; Wen, X.; Sun, H. Synthesis and cytotoxicity evaluation of oleanolic acid derivatives. *Bioorg. Med. Chem. Lett.* **2013**, *23*, 2074–2077. [CrossRef]
14. Friedrich, S.; Serbian, I.; Hoenke, S.; Wolfram, R.K.; Csuk, R. Synthesis and cytotoxic evaluation of malachite green derived oleanolic and ursolic acid piperazineamides. *Med. Chem. Res.* **2020**, *29*, 926–933. [CrossRef]
15. Schwarz, S.; Csuk, R. Synthesis and antitumour activity of glycyrrhetinic acid derivatives. *Bioorg. Med. Chem.* **2010**, *18*, 7458–7474. [CrossRef]
16. Rodriguez-Hernandez, D.; Barbosa, L.C.A.; Demuner, A.J.; Ataide Martins, J.P.; Fischer, L.; Csuk, R. Hederagenin amide derivatives as potential antiproliferative agents. *Eur. J. Med. Chem.* **2019**, *168*, 436–446. [CrossRef]
17. Liu, X.-x.; Yang, Y.-t.; Wang, X.; Wang, K.-y.; Liu, J.-q.; Lei, L.; Luo, X.-m.; Zhai, R.; Fu, F.-h.; Wang, H.-B.; et al. Design, synthesis and biological evaluation of novel α-hederagenin derivatives with anticancer activity. *Eur. J. Med. Chem.* **2017**, *141*, 427–439. [CrossRef]
18. Emirdag-Ozturk, S.; Karayildirim, T.; Capci-Karagoz, A.; Alankus-Caliskan, O.; Ozmen, A.; Poyrazoglu-Coban, E. Synthesis, antimicrobial and cytotoxic activities, and structure-activity relationships of gypsogenin derivatives against human cancer cells. *Eur. J. Med. Chem.* **2014**, *82*, 565–573. [CrossRef]
19. Valdeira, A.S.C.; Darvishi, E.; Woldemichael, G.M.; Beutler, J.A.; Gustafson, K.R.; Salvador, J.A.R. Madecassic Acid Derivatives as Potential Anticancer Agents: Synthesis and Cytotoxic Evaluation. *J. Nat. Prod.* **2019**, *82*, 2094–2105. [CrossRef]
20. Pavlova, N.I.; Savinova, O.V.; Nikolaeva, S.N.; Boreko, E.I.; Flekhter, O.B. Antiviral activity of betulin, betulinic and betulonic acids against some enveloped and non-enveloped viruses. *Fitoterapia* **2003**, *74*, 489–492. [CrossRef]
21. Wang, H.M.; Soica, C.M.; Wenz, G. A comparison investigation on the solubilization of betulin and betulinic acid in cyclodextrin derivatives. *Nat. Prod. Commun.* **2012**, *7*, 289–291. [CrossRef]
22. Pisha, E.; Chai, H.; Lee, I.-S.; Chagwedera, T.E.; Farnsworth, N.R.; Cordell, G.A.; Beecher, C.W.W.; Fong, H.H.S.; Kinghorn, A.D.; Brown, D.M.; et al. Discovery of betulinic acid as a selective inhibitor of human melanoma that functions by induction of apoptosis. *Nat. Med.* **1995**, *1*, 1046–1051. [CrossRef]
23. Serbian, I.; Ströhl, D.; Csuk, R. Interconversion of hederagenin and gypsogenin and accessing 4-epi-hedragonic acid. *Phytochem. Lett.* **2020**, *39*, 35–38. [CrossRef]
24. Heller, L.; Schwarz, S.; Weber, B.A.; Csuk, R. Gypsogenin Derivatives: An Unexpected Class of Inhibitors of Cholinesterases. *Arch. Pharm.* **2014**, *347*, 707–716. [CrossRef] [PubMed]
25. Sommerwerk, S.; Heller, L.; Kuhfs, J.; Csuk, R. Selective killing of cancer cells with triterpenoic acid amides—The substantial role of an aromatic moiety alignment. *Eur. J. Med. Chem.* **2016**, *122*, 452–464. [CrossRef] [PubMed]
26. Wolfram, R.K.; Fischer, L.; Kluge, R.; Ströhl, D.; Al-Harrasi, A.; Csuk, R. Homopiperazine-rhodamine B adducts of triterpenoic acids are strong mitocans. *Eur. J. Med. Chem.* **2018**, *155*, 869–879. [CrossRef]
27. Kahnt, M.; Wiemann, J.; Fischer, L.; Sommerwerk, S.; Csuk, R. Transformation of asiatic acid into a mitocanic, bimodal-acting rhodamine B conjugate of nanomolar cytotoxicity. *Eur. J. Med. Chem.* **2018**, *159*, 143–148. [CrossRef]
28. Hoenke, S.; Serbian, I.; Deigner, H.-P.; Csuk, R. Mitocanic Di- and Triterpenoid Rhodamine B Conjugates. *Molecules* **2020**, *25*, 5443. [CrossRef]
29. Kozubek, M.; Serbian, I.; Hoenke, S.; Kraft, O.; Csuk, R. Synthesis and cytotoxic evaluation of hydroxycinnamic acid rhodamine B conjugates. *Results Chem.* **2020**, *2*, 100057. [CrossRef]
30. Siewert, B.; Pianowski, E.; Obernauer, A.; Csuk, R. Towards cytotoxic and selective derivatives of maslinic acid. *Bioorg. Med. Chem.* **2014**, *22*, 594–615. [CrossRef]
31. Christman, J.E.; Miller, D.S.; Coward, P.; Smith, L.H.; Teng, N.N.H. Study of the selective cytotoxic properties of cationic, lipophilic mitochondrial-specific compounds in gynecologic malignancies. *Gynecol. Oncol.* **1990**, *39*, 72–79. [CrossRef]
32. Sakamuru, S.; Attene-Ramos, M.S.; Xia, M. Mitochondrial Membrane Potential Assay. *Methods Mol. Biol.* **2016**, *1473*, 17–22.

33. Sommerwerk, S.; Heller, L.; Kerzig, C.; Kramell, A.E.; Csuk, R. Rhodamine B conjugates of triterpenoic acids are cytotoxic mitocans even at nanomolar concentrations. *Eur. J. Med. Chem.* **2017**, *127*, 1–9. [CrossRef]
34. Kaminskyy, D.; Bednarczyk-Cwynar, B.; Vasylenko, O.; Kazakova, O.; Zimenkovsky, B.; Zaprutko, L.; Lesyk, R. Synthesis of new potential anticancer agents based on 4-thiazolidinone and oleanane scaffolds. *Med. Chem. Res.* **2012**, *21*, 3568–3580. [CrossRef]
35. Amanmuradov, K.; Tanyurcheva, T.N. Triterpenic glycoside from Acanthophyllum adenophorum. *Khim. Prir. Soedin.* **1969**, *5*, 326.
36. Van der Haar, A.W. Saponin-like Substances from the Leaves of Polyscias nodosa and Hedera helix. *Arch. Pharm.* **1913**, *250*, 424–435.
37. Ruzicka, L.; Giacomello, G. Polyterpenes and polyterpenoids. CVII. Conversion of gypsogenin (albsapogenin) into oleanolic acid. *Helv. Chim. Acta* **1936**, *19*, 1136–1140. [CrossRef]
38. Mitra, A.K.; Karrer, P. Holboellia latifolia, a new source of hederagenin. *Helv. Chim. Acta* **1953**, *36*, 1401. [CrossRef]
39. Haynes, L.J.; Plimmer, J.R.; Sue-Ho, W.M. Isolation and identification of hederagenin from ackee, Blighia sapida. *J. Chem. Soc.* **1963**, 744–745.
40. Van Loc, T.; Nhu, V.T.Q.; Chien, T.V.; Ha, L.T.T.; Thao, T.T.P.; Sung, T.V. Synthesis of madecassic acid derivatives and their cytotoxic activity. *Z. Naturforsch. B J. Chem. Sci.* **2018**, *73*, 91–98. [CrossRef]
41. Rastogi, R.P.; Sarkar, B.; Dhar, M.L. Chemical examination of *Centella asiatica* L. Isolation of the chemical constituents. *J. Sci. Ind. Res.* **1960**, *19B*, 252–257.

P4

European Journal of Medicinal Chemistry 250 (2023) 115189

Contents lists available at ScienceDirect

European Journal of Medicinal Chemistry

journal homepage: www.elsevier.com/locate/ejmech

Research paper

Asiatic acid as a leading structure for derivatives combining sub-nanomolar cytotoxicity, high selectivity, and the ability to overcome drug resistance in human preclinical tumor models

Oliver Kraft [a], Anne-Kathrin Hartmann [a], Sarah Brandt [b], Sophie Hoenke [a], Niels V. Heise [a], René Csuk [a,*], Thomas Mueller [b]

[a] *Martin-Luther-University Halle-Wittenberg, Organic Chemistry, Kurt-Mothes-Str. 2, D-06120, Halle (Saale), Germany*
[b] *Martin-Luther-University Halle-Wittenberg, Medical Faculty, University Clinic for Internal Medicine IV, Hematology/Oncology, Ernst-Grube-Str. 40, D-06120, Halle (Saale), Germany*

ARTICLE INFO

Keywords:
Asiatic acid
Cytotoxicity
Drug resistance
Tumor model

ABSTRACT

Amides and rhodamine B conjugates of different pentacyclic triterpene acids have been shown outstanding cytotoxicity for human tumor cells. Starting from asiatic acid, a new rhodamine B hybrid has been synthesized, and its cytotoxic activity was investigated employing several human tumor cell lines (A375 (melanoma), HT29 (colorectal carcinoma), MCF7 (breast adenocarcinoma), A2780 (ovarian carcinoma), HeLa (cervical carcinoma), (NIH 3T3 (non-malignant murine fibroblasts). For these conjugates of this kind it has been established that the spacer attached to the carboxyl group at ring E governs the magnitude of the cytotoxicity. These asiatic acid - rhodamine B conjugates were highly cytotoxic for human tumor cell lines but also selective. For example, **7**, an acetylated homopiperazinyl spacered rhodamine B conjugate, held an $EC_{50} = 0.8$ nM for A2780 ovarian carcinoma cells. Additional staining experiments showed the rhodamine B conjugates to act as mitocans and to effect apoptosis. In further tests using 3D spheroid models of colorectal- and mamma carcinoma, **7** demonstrated activity in the lower nanomolar range and the ability to overcome resistance to clinically used standard chemotherapeutic drugs. Therefore **7** induces cytotoxic effects leading to an equal response in the chemotherapy of both sensitive and resistant tumor models. Analyses of mitochondrial function and glycolysis and respiration derived ATP production confirmed compound **7** to act as mitocan but also revealed a rapid perturbation of the cellular energy metabolism as the primary mechanism of action, which is completely different to conventional chemotherapeutic drugs and thereby explains the ability of compound **7** to overcome chemotherapeutic drug resistance.

1. Introduction

For millennia, people have utilized the beneficial effects of natural substances to alleviate and even to heal diseases [1–5]. Thereby, the health-promoting effects of predominantly herbal substances were used; the positive properties attributed to these compounds are demonstrably based on their content of secondary plant metabolites.[6–8] These substances, were also used to treat non-communicable diseases such as high blood pressure, inflammation or to act as immune-modulators [9–11]. Several of them also hold anti-carcinogenic, antioxidant and anti-inflammatory effects. Consequently, they are predestinated to develop derivatives of even higher bioactivity and increased selectivity.

Especially their cytotoxic activity towards malignant tumor cells is currently of great and unbroken interest. As early as 1924, O. Warburg [12] put forward a hypothesis on the connection between the impairment of mitochondrial function and the growth of tumor cells. Recently, his assumptions have entered the scientific focus again and triggered the development of theory-based methods to treat cancer. Compounds that act preferentially on the mitochondria are now referred as so-called mitocans [13,14], and their mode of action is primarily based on targeted apoptosis in the mitochondria [15,16]. One way to develop new mitocans was found in the synthesis of triterpenoic acid derived carboxamides, holding an extra rhodamine moiety. As in 2014 works by B. Siewert et al. and S. Sommerwerk et al. dealt with the cytotoxic activity of selected triterpene carboxylic acid derivatives [17–22]. Thereby, various compounds derived from betulinic, oleanolic, ursolic,

---

* Corresponding author.
E-mail address: rene.csuk@chemie.uni-halle.de (R. Csuk).

https://doi.org/10.1016/j.ejmech.2023.115189
Received 8 January 2023; Received in revised form 1 February 2023; Accepted 4 February 2023
Available online 9 February 2023
0223-5234/© 2023 Elsevier Masson SAS. All rights reserved.

glycyrrhetinic, boswellic and maslinic acid were investigated regarding their cytotoxic activity and tumor cell/non-tumor cell selectivity [17, 23–25].

While the unsubstituted triterpenoic acids held no or only low cytotoxic activity, their corresponding conjugates demonstrated activity even at single-digit nanomolar concentrations [17,26]. Recent studies from our group also revealed that the attachment of a benzylamine, phenylamine and especially of a rhodamine moiety to a triterpenoic acid dramatically improves cytotoxicity [15,27–31]. Thus, a madecassic acid derived conjugate, held EC_{50} (0.0029 ± 0.0005 μM) values even in extremely low nanomolar ranges [30]. Thereby, this conjugate was more than 2.4 times higher cytotoxic than an analog derived from maslinic acid conjugate and it was of almost the same cytotoxicity as an analog derived from corosolic acid [17,32]. In terms of structure, maslinic and corosolic acid differ only in the number hydroxyl groups when compared to madecassic or asiatic acid. Therefore, we assumed that the presence of an additional hydroxyl group is essential for obtaining compounds of increased cytotoxicity while retaining high selectivity [33,34]. Thus, it becomes evident, that the synthesis of novel asiatic acid derived derivatives offers a great possibility to access compounds of high anticarcinogenic activity. In this work, a variety of asiatic acid derivatives was synthesized and their cytotoxicity was examined by SRB assays.

2. Results and discussion

Asiatic acid (**1**) was selected as starting material. This triterpenoic acid is available in large quantities and very good purity from a local supplier (Carbolution GmbH). Acetylation of asiatic acid gave triacetylated **1** whose reaction with oxalyl chloride followed by the addition of piperazine or homopiperazine yielded the corresponding amides **3** and **4**. Compounds **3** and **4** were coupled with rhodamine B acid chloride (in situ prepared from **5**) to afford conjugates **6** and **7** (Scheme 1), respectively. Compounds **1**–**7** were subjected to SRB assays employing a selection of human tumor cell lines and non-malignant fibroblasts (NIH 3T3) to assess both their cytotoxicity and their tumor cell/non-tumor cell selectivity [18–20,31,35]. The results from these assays are compiled in Table 1.

In general, derivatives of asiatic acid are higher cytotoxic than their analogs derived from oleanolic, ursolic or maslinic acid [17,19,27]. Compounds **3**–**5** are similar in cytotoxicity but **6** and especially **7**, however, are significantly more cytotoxic (Fig. 1). This increase in cytotoxicity might be caused by a higher bioavailability, due to an increased solubility resulting from the presence of an extra acetyl group at position 23 in asiatic acid derived compounds paralleling the solubility behavior of the parent compounds inasmuch as asiatic acid is about 5 times better soluble than maslinic acid. Their tumor cell/non-tumor cell selectivity is also nearly the same, but significantly better for **7** than of the other conjugates.

Table 1
SRB assay: EC_{50} values [μM] after 72 h of treatment; averaged from three independent experiments performed each in triplicate; confidence interval CI = 95%. Human cancer cell lines: A375 (melanoma), HT29 (colorectal carcinoma), MCF7 (breast adenocarcinoma), A2780 (ovarian carcinoma), HeLa (cervical carcinoma), (NIH 3T3 (non-malignant murine fibroblasts); cut-off 30 μM, n.d. not determined. Doxorubicin (**Dox**) has been used as a positive standard.

#	A375	HT29	MCF7	A2780	HeLa	NIH 3T3
1	>30	>30	>30	28.2 ± 0.3	n.d.	26.2 ± 2.5
2	n.d.	8.9 ± 0.8	7.0 ± 1.4	5.8 ± 0.8	n.d.	6.2 ± 0.2
3	1.3 ± 0.2	1.3 ± 0.1	2.0 ± 0.1	0.8 ± 0.09	n.d.	1.8 ± 0.04
4	0.58 ± 0.1	1.35 ± 0.05	1.63 ± 0.5	1.12 ± 0.2	n.d.	1.44 ± 0.2
5	>30	>30	>30	>30	n.d.	>30
6	n.d.	0.017 ± 0.013	0.012 ± 0.002	0.008 ± 0.002	n.d.	0.178 ± 0.027
7	0.0028 ± 0.0005	0.0055 ± 0.0023	0.0071 ± 0.0021	0.0008 ± 0.0001	0.0177 ± 0.0049	0.0650 ± 0.0262
Dox	n.d	0.9 ± 0.2	1.1 ± 0.3	0.02 ± 0.01	n.d.	1.7 ± 0.3

The results of some extra staining experiments employing A375 cells and compound **7** are depicted in Fig. 2; they allow a quantification of the ratio apoptosis/necrosis. Thereby, cells found in R1 are found to be necrotic, late apoptotic cells show up in R2, while viable cells are measured in R3 and apoptotic cells are found in R4. Treatment of A375 cells with **7** for 24 h showed 81.4% of the cells being viable; after 2 days 44.1% of the cells were apoptotic, and only 3.9% of the cells were necrotic. This clearly indicates that A375 cells die rather by apoptosis than by necrosis.

However, the results revealed the asiatic acid conjugates to be more cytotoxic than the corresponding analogs obtained from oleanolic, ursolic, maslinic or madecassic acid and above all, better than those previously described derivatives from betulinic and glycyrrhetinic acid.

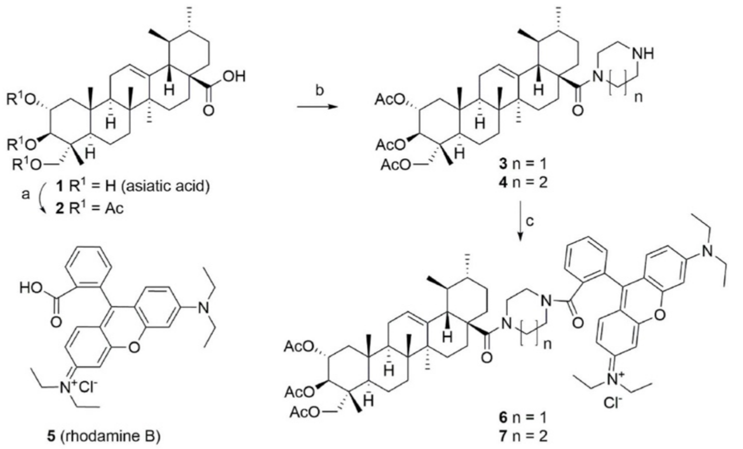

Scheme 1. Synthesis of compounds: (a) Ac_2O, NEt_3, DMAP (cat.), DCM, 23 °C, 1 h, **1** (98%); (b) $(COCl)_2$, DCM, DMF (cat.), then piperazine or homopiperazine, 23 °C, 1 h; **3** (90%), **4** (79%); rhodamine B (**5**), $(COCl)_2$, DCM, NEt_3 (cat.), DMF (cat.), 23 °C, 1 h, then **3** or **4**, 0 °C → 23 °C, 1 h; → **6** (73%) and **7** (56%).

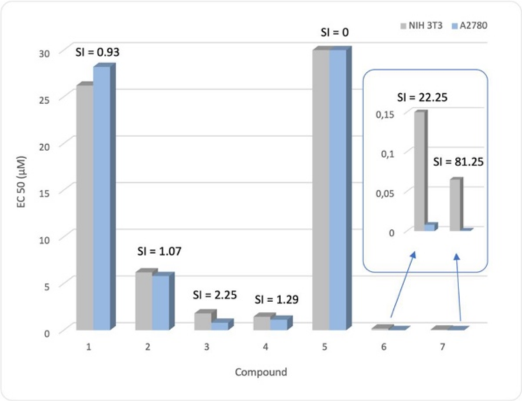

Fig. 1. Comparison of cytotoxicity and selectivity of compounds for A2780 (tumor cell line) and NIH 3T3 (non-malignant murine fibroblasts). Selectivity index (SI) is defined as: SI = EC_{50} (NIH 3T3)/EC_{50} (A2780).

This confirms our initial assumption that not only the triterpene skeleton and the type of amide, but also the number of acetoxy groups and the linking position of the rhodamine residue significantly influences the cytotoxic activity and tumor cell selectivity.

The most active compound **7** was further investigated in 3D spheroid models to prove potential antitumor activity and the ability to overcome resistance to conventional chemotherapeutic drugs. Tumor spheroids are useful *in vitro* models representing several important aspects of real tumor tissues, i.e., three-dimensional growth with structural organization and physiologically relevant cell-cell and cell-matrix interactions, establishment of tumor microenvironmental characteristics such as nutrient gradients, hypoxia, and acidosis, as well as in terms of drug resistance mechanisms [36,37]. Our model comprises two colorectal carcinoma- and two mamma carcinoma cell line derived spheroid types with one of each showing resistance to the clinically relevant drugs 5-FU, oxaliplatin and irinotecan or doxorubicin and paclitaxel, respectively. In addition, the tumor cells stably express luciferase enabling analysis of spheroid growth and response to therapy by measurement of bioluminescent signal intensity.

As exemplary depicted in Fig. 3 and summarized in Table 2, treatment with compound **7** resulted in a dose dependent inhibition of spheroid growth in all spheroid types with an overall activity in the lower nanomolar range. The dose-dependent drug accumulation could be visualized employing the intrinsic fluorescence of compound **7** (Fig. 3). Interestingly, there was no cross-resistance to the clinically used standard chemotherapeutic drugs, i.e., chemo-sensitive and -resistant spheroids of each model were comparably sensitive to compound **7** resulting in nearly equal IC_{50} values (Table 2). In addition, compound **7** showed an about 4-fold higher activity in models of mamma carcinoma compared to colorectal carcinoma. In contrast, spheroids formed from non-malignant fibroblasts were 15 to 58-fold less sensitive indicating a pronounced tumor selective activity of compound **7**, which further confirmed the observations from the 2D model.

To investigate the processes induced by compound **7** which eventually led to the inhibition of spheroid growth within spheroids, we analysed time-dependent drug accumulation, cell proliferation and the induction of cell death during treatment on tissue slides prepared from the spheroids. Identification and tracking of compound **7** were accomplished by multispectral fluorescence microscopy and using spectral unmixing. Markers of proliferation (Ki67) and apoptosis (cleaved PARP) were analysed immunohistochemically. Compound **7** completely penetrated the spheroid tissue within 24h and showed interstitial and cellular accumulation, but not nuclear accumulation, and became more concentrated in the periphery compared to the core of the spheroids in the following days (Fig. 4). The treatment led to a clear reduction of Ki67-positive proliferating cells within 48h and occurrence of numerous apoptotic cells after 96h, but without considerable occurrence of necrosis (Fig. 5). Thus, the main effect by which compound **7** affects spheroid growth comprises inhibition of tumor cell proliferation

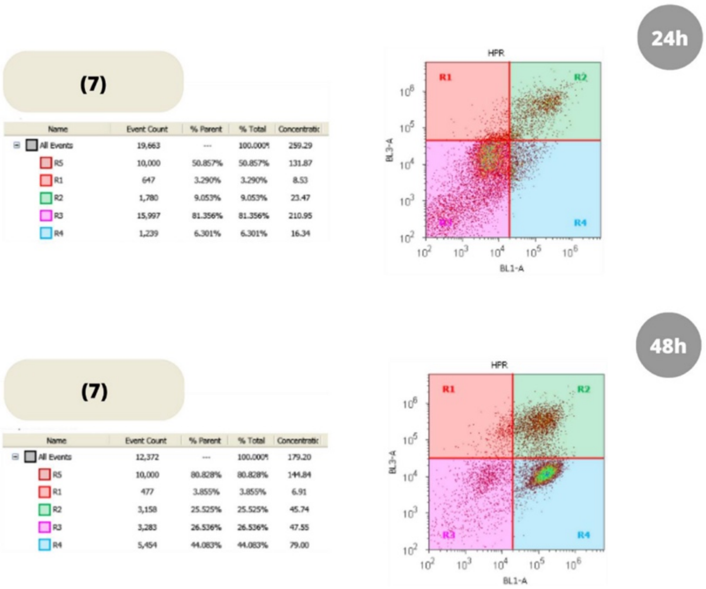

(7)

Name	Event Count	% Parent	% Total	Concentratic
⊟ ■ All Events	19,663	---	100.000%	259.29
□ R5	10,000	50.857%	50.857%	131.87
□ R1	647	3.290%	3.290%	8.53
□ R2	1,780	9.053%	9.053%	23.47
□ R3	15,997	81.356%	81.356%	210.95
□ R4	1,239	6.301%	6.301%	16.34

(7)

Name	Event Count	% Parent	% Total	Concentratic
⊟ ■ All Events	12,372	---	100.000%	179.20
□ R5	10,000	80.828%	80.828%	144.84
□ R1	477	3.855%	3.855%	6.91
□ R2	3,158	25.525%	25.525%	45.74
□ R3	3,283	26.536%	26.536%	47.55
□ R4	5,454	44.083%	44.083%	79.00

Fig. 2. FITC/Annexin V/Propidium iodide assay employing compound **7** (A375 cells, 24h and 48 h, 2 × IC_{50} concentration).

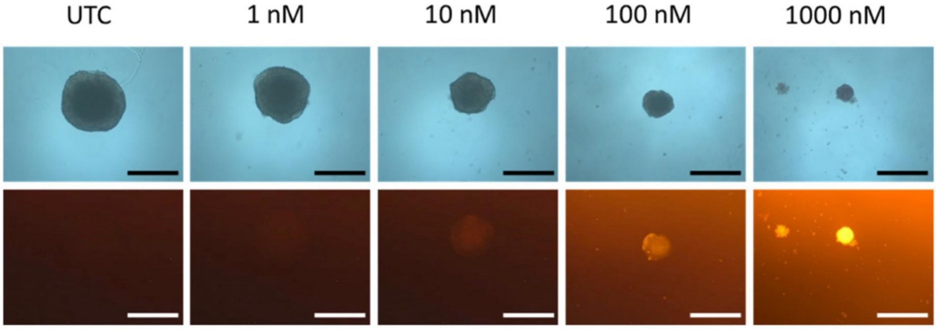

Fig. 3. Dose-dependent inhibition of spheroid growth and drug accumulation of compound **7** in DLD1 spheroids on day7. Scale bar: 0.5 mm.

Table 2
Spheroid cytotoxicity assay: IC_{50} values after 7 days of treatment; averaged from at least 3 independent experiments, comprising 8 spheroids per concentration; Drugs: 5-fluorouracil (5-FU), oxaliplatin (Oxa), irinotecan (Irino), doxorubicin (Dox), paclitaxel (Pac), compound 7 (C7); human cell line derived spheroids: LS1034 (colorectal carcinoma, multi-resistant), DLD1 (colorectal carcinoma), MDA-MB-231 (triple negative breast cancer), Hs578T (mamma carcinoma), CCD18Co (non-malignant fibroblasts); Resistance index (RI): IC_{50} ratio of DLD1/LS1034 and Hs578T/MDA-MB-231, Selectivity index (SI): IC_{50} ratio of DLD1/CCD18Co and Hs578T/CCD18Co; n.d. - not determined.

#	LS1034	DLD1	MDA-MB-231	Hs578T	CCD18Co	RI (fold) SI (fold)
5-FU (μM)	0.11 ± 0.02	4.16 ± 1.19	n.d.	n.d.	n.d.	37.8
Oxa (μM)	0.37 ± 0.14	4.10 ± 0.84	n.d.	n.d.	n.d.	11.1
Irino (μM)	4.09 ± 0.52	13.17 ± 2.50	n.d.	n.d.	n.d.	3.2
Dox (nM)	n.d.	n.d.	22.2 ± 9.5	1345.5 ± 240.0	n.d.	60.6
Pac (nM)	n.d.	n.d.	0.7 ± 0.3	14.8 ± 5.1	n.d.	21.1
7 (nM)	9.3 ± 4.9	11.1 ± 2.5	2.7 ± 1.0	2.8 ± 0.5	164.2 ± 82.3	1.19/ 1.02 14.8/ 58.6

accompanied by induction of apoptosis, which apparently do not differ from those effects induced by conventional chemotherapeutic drugs. Notably, all five chemotherapeutic drugs have distinct primary targets and mechanisms. Therefore, it is not unlikely that compound **7** might act by a completely different primary mechanism of action to induce cytotoxic effects leading to an equal response in chemotherapy sensitive and -resistant tumor models. This is supported by the postulated feature of compound **7** to act as a mitocan.

To further explore the underlying mode of action of compound **7** compared to chemotherapeutic drugs, we employed the Seahorse cell analysis technology platform from Agilent enabling real time automatic measurement of the energy metabolism in live cells. We performed the Seahorse XF Cell Mito Stress Test combined with the Seahorse XF Real-Time ATP Rate assay, which provide complementary and confirmative data. The assays are based on the measurement of oxygen consumption rate (OCR) and extracellular acidification rate (ECAR) of live cells during sequential manipulation with specific chemicals to obtain information about mitochondrial function and to quantify cellular bioenergy level (ATP), which are mainly fuelled by the processes of mitochondrial respiration and glycolysis. To this end, the tumor cells were treated with IC_{50} doses of drugs based on a 72h cytotoxicity assay, but were analysed after 24h, before apparent signs of cytotoxicity can be observed, to preferentially analyse early processes, which eventually lead to cytotoxic effects. The results are summarized in Fig. 6. All measured parameters associated with functional mitochondrial respiration were strongly or completely decreased after treatment with compound **7**, whereas those of chemotherapeutic drugs showed comparable levels with untreated control cells. This is confirmed by the ATP production rate assay revealing that mitochondrial respiration derived ATP production is almost lacking after treatment with compound **7** and glycolysis derived ATP compensates this to some extent. Interestingly, the intrinsic characteristic of analysed tumor cells to generate ATP by respiration and glycolysis in the relation of about one third and two

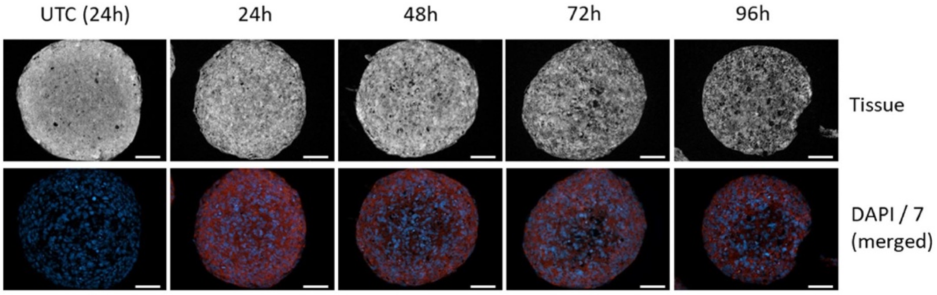

Fig. 4. Pattern of tissue accumulation of compound **7** in DLD1 spheroids at indicated time points. Depicted are images of the same spheroid (vertical), generated under violet and green fluorescent light and after spectral dependent isolation of signals of the tissue background (upper row), and of DAPI and compound **7**, shown as merged version of both (lower row). Scale bar: 50 μm.

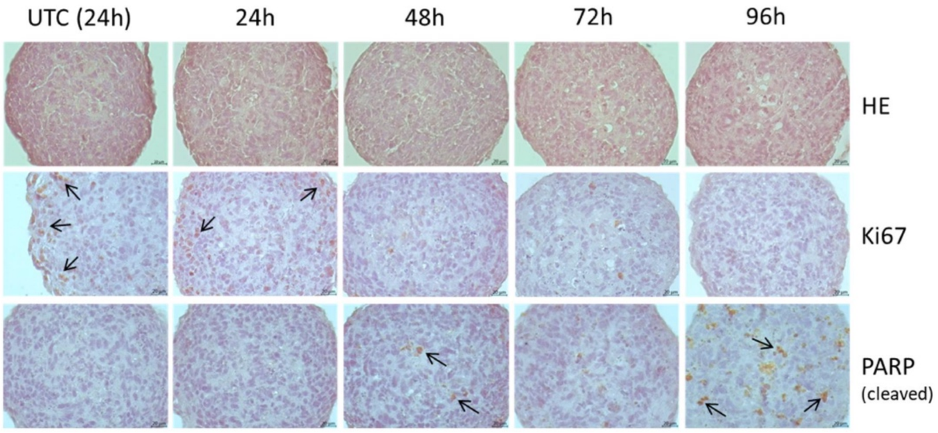

Fig. 5. Histological/immunohistochemical analyses of tissue slides prepared from DLD1 spheroids treated with compound **7** and harvested after indicated time points. Upper row: hematoxylin/eosin (HE) staining showing compact tissue with signs of damage after 72h and 96h but without occurrence of necrotic areas. Middle row: Ki67-positive, proliferating cells, which are typically found in the peripheral areas of spheroids (arrows), disappear within 48h. Lower row: Occurrence of numerous apoptotic cells (arrows) after 96h stained for cleaved PARP with first apoptotic cells occurring after 48h.

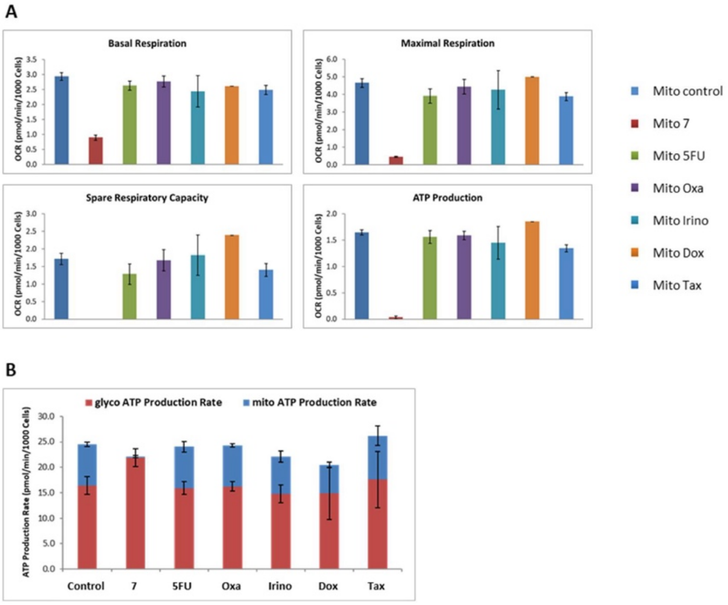

Fig. 6. Analyses of mitochondrial function and ATP production in DLD1 cells 24h after start of treatment with compound **7** and chemotherapeutic drugs. (A) Parameters obtained from the Seahorse XF Cell Mito Stress Test. Basal respiration: oxygen consumption used to meet cellular ATP demand resulting from mitochondrial respiration at baseline; Maximal respiration: oxygen consumption rate (OCR) attained by stimulating the respiratory chain to operate at maximum capacity, shows the maximum rate of respiration that the cell can achieve. Spare respiratory capacity: indicates the capability of the cell to respond to an energetic demand and how closely the cell is to respiring to its theoretical maximum. ATP production: oxygen consumption linked cellular ATP production rate. (B) Seahorse XF Real-Time ATP Rate assay. Shows the proportion of ATP production rate from glycolysis and mitochondrial respiration.

third, is not altered in cells treated with the chemotherapeutic drugs, although decreasing level of overall ATP could already be observed in doxorubicin treated cells. These data strongly confirm that compound **7** to act as a mitocan. Hence, the primary mechanism of action comprises a rapid perturbation of the cellular energy metabolism, which is completely different to conventional chemotherapeutic drugs and which explains the ability of compound **7** to overcome chemotherapeutic drug resistance.

3. Conclusion

Different triterpene conjugates derived from asiatic acid were synthesized and screened for their cytotoxicity and tumor cell/non-tumor cell selectivity. This work builds on previous results and knowledge of similar compounds derived from triterpenoic acid such as betulinic, glycyrrhetinic, boswellic, oleanolic, ursolic, maslinic or madecassic acid which are also mitocans of high cytotoxicity. As a result, the conjugates reported herein show, that the presence of an additional acetyl group led to an even better performance concerning their cytotoxic activity.

Thereby, the most active compound **7** – an asiatic acid homopiperazinyl rhodamine B conjugate**,** held an EC_{50} = 0.8 nM for A2780 ovarian carcinoma cells. Additional staining experiments showed that this rhodamine B conjugate of asiatic acid led to apoptosis. Furthermore, compound **7** demonstrated high activity in 3D spheroid models combined with the ability to overcome chemotherapeutic drug resistance. This is achieved by acting as a mitocan comprising a completely different primary mechanism compared to conventional chemotherapeutic drugs. Furthermore, this compound holds equal activity in the chemotherapy in sensitive as well as in resistant tumor models.

4. Experimental

4.1. General

NMR spectra were recorded using the Varian spectrometers (Darmstadt, Germany) DD2 and VNMRS (400 and 500 MHz, respectively). MS spectra were taken on a Advion expression^L CMS mass spectrometer (Ithaca, NY, USA; positive ion polarity mode, solvent: methanol, solvent flow: 0.2 mL/min, spray voltage: 5.17 kV, source voltage: 77 V, APCI corona discharge: 4.2 μA, capillary temperature: 250 °C, capillary voltage: 180 V, sheath gas: N_2). Thin-layer chromatography was performed on pre-coated silica gel plates supplied by Macherey-Nagel (Düren, Germany). IR spectra were recorded on a Spectrum 1000 FT-IR-spectrometer from Perkin Elmer (Rodgau, Germany). The UV/Vis-spectra were recorded on a Lambda 14 spectrometer from Perkin Elmer (Rodgau, Germany); optical rotations were measured at 20 °C using a JASCO-P2000 instrument (JASCO Germany GmbH, Pfungstadt, Germany) The melting points were determined using the Leica hot stage microscope Galen III (Leica Biosystems, Nussloch, Germany) and are uncorrected. The solvents were dried according to usual procedures. Microanalyses were performed with an Elementar Vario EL (CHNS) instrument (Elementar Analysensysteme GmbH, Elementar-Straße 1, D-63505, Langenselbold, Germany).

All dry solvents were distilled over respective drying agents except for DMF which was distilled and stored under argon and molecular sieve. Reactions using air- or moisture-sensitive reagents were carried out under argon atmosphere in dried glassware. Triethylamine was stored over potassium hydroxide. Biological assays were performed as previously reported employing cell lines obtained from the Department of Oncology [Martin-Luther-University Halle Wittenberg; they were bought from ATCC: malignant: A 375, HT29, MCF7, A2780 and HeLa; non-malignant: NIH 3T3]. Asiatic acid was obtained from local vendors.

For the SRB assay: cells were seeded into 96 well plates on day zero at appropriate cell densities to prevent confluence of the cells during the period of the experiment. After 24 h, the cells were treated with different concentrations (1, 3, 7, 12, 20 and 30 μM), but the final concentration of DMSO/DMF never exceeded 0.5%, which was non-toxic to the cells. After 72 h treatment, the supernatant media from the 96 well plates were discarded, then the cells were fixed with 10% trichloroacetic acid and allowed to rest at 4 °C. After 24 h of fixation, the cells were washed in a strip washer and then dyed with SRB solution (200 μL, 10 mM) for 20 min. Then the plates were washed four times with 1% acetic acid to remove the excess of the dye and allowed to air-dry overnight. Tris base solution (200 μL, 10 mM) was added to each well. The absorbance was measured with a 96 well plate reader from Tecan Spectra.

4.2. Syntheses

4.2.1. (2α,3β,4α,6β) 2,3,23-Tris(acetyloxy)-urs-12-en-28-oic acid (2) [57688-73-0]

Asiatic acid (**1**, 1120 mg, 2.30 mmol. 1 eq.) was dissolved in dry DCM (20 mL), treated with TEA (4.5 eq.), DMAP (cat.) and acetic anhydride (4.0 eq.). The mixture was stirred at room temperature for 24h; for work-up, aq. ammonium hydroxide (7 M, 0.5 mL) was added. After 30 min, the mixture was diluted with Et_2O (250 mL), washed with HCl (0.1 M, 1 × 250 mL), water (2 × 250 mL) and brine (1 × 125 mL), dried ($MgSO_4$), and the organic phase was concentrated under reduced pressure. The crude product was subjected to column chromatography (SiO_2, *n*-hexane/ethyl acetate, 8:2) to afford compound **2** (1380 mg, 98%) as a colourless solid; m.p.: 159–161 °C (lit.: [38]: 160–163 °C); $[\alpha]_D^{20}$ = +35.4° (*c* = 0.50, $CHCl_3$)] (lit.: [38]: $[\alpha]_D^{20}$ = +34.71° (*c* = 0.35 $CHCl_3$)]; MS (ESI): *m/z* (%) 615.0 ($[M+H]^+$ (90)).

4.2.2. General procedure for the synthesis of triterpenoic amides 3 and 4 (GPA)

To a solution of **2** (1 eq.) in dry DCM (10 mL), oxalyl chloride (4 eq.), DMF (0.24 eq.) and TEA (2.4 eq.) were added. After stirring for 2h at room temperature, the solvent was removed under reduced pressure, re-evaporated with DCM (3 × 10 mL), and the residue was dissolved in dry DCM (10 mL). A solution of the respective diamine (3 eq.) in dry DCM, TEA (1 eq.) and DMAP (cat.) was added, and stirring at room temperature was continued until completion of the reaction (as indicated by TLC). The solvent was removed under reduced pressure, and the crude product was subjected to column chromatography to yield compounds **3** and **4**.

4.2.3. (2α,3β,4α)-2,3,23-Tris(acetyloxy)-N-(piperazinyl)-urs-12-en-28-amide (3) [2247305-89-9]

Following GPA from **2** (200 mg, 0.30 mmol) and piperazine (77 mg, 0.90 mmol) followed by chromatography (SiO_2, chloroform/methanol, 9:1) **3** (184 mg, 90%) was obtained as a colourless solid; m.p.: 158–160 °C (lit.: [39]: 157–160 °C); $[\alpha]_D^{20}$ = +16.3° (*c* = 0.18, $CHCl_3$) [lit.: [39]: $[\alpha]_D^{20}$ = +17.48° (*c* = 0.27, $CHCl_3$); MS (ESI): *m/z* (%) 683.1 ($[M+H]^+$ (95)).

4.2.4. (2α,3β,4α)-2,3,23-Tris(acetyloxy)-N-(homopiperazinyl)-urs-12-en-28-amide (4)

Following GPA from **2** (500 mg, 0.81 mmol) and homopiperazine (210 mg, 2.43 mmol) followed by chromatography (SiO_2, chloroform/methanol, 9:1) **4** (446 mg, 79%) was obtained as a colourless solid; m.p.: 185.3–186.3 °C; R_F = 0.41 (SiO_2, chloroform/methanol, 9:1); $[\alpha]_D^{20}$ = 14.38° (*c* = 0.145 $CHCl_3$); IR (ATR): ν = 2923*w*, 1741*s*, 1621*w*, 1455*w*, 1368 *m*, 1230*vs*, 1156*w*, 1087*w*, 1043 *m*, 1029 *m*, 964*w*, 920*w*, 751 *m*, 665*w*, 460*w*, 422*w* cm^{-1}; ^1H NMR (500 MHz, $CDCl_3$): δ = 5.21–5.07 (m, 2H, 12–H + 2–H), 5.02 (d, *J* = 10.3 Hz, 1H, 3–H), 4.20–2.80 (m, 11H, 37–H + 38–H + 39–H + 40–H + 41–H + 23–H_a), 3.79 (d, *J* = 11.8 Hz, 1H, 23–H_b), 2.49–2.31 (m, 1H, 18–H), 2.21–2.06 (m, 2H, 16–H), 2.09–1.81 (m, 3H, 1–H_a + 11–H), 2.03 (s, 3H, 36–H),1.97 (s, 3H, 32–H), 1.93 (s, 3H, 34–H),1.79–1.47 (m, 1H, 9–H), 1.42–1.17 (m, 10H, 21–H + 7–H + 6–H + 22–H + 19–H + 5–H), 1.13–0.95 (m, 4H, 1–H_b + 15–H + 20–H), 1.03 (s, 3H, 25–H), 1.00 (s, 3H, 27–H), 0.94–0.86 (m, 3H, 30–H), 0.83 (s, 3H, 24–H), 0.82 (s, 3H, 29–H), 0.82 (s, 3H, 29–H), 0.67 (s, 3H, 26–H) ppm;^{13}C NMR (125 MHz, $CDCl_3$): δ = 204.5 (C-23), 176.2 (C-28), 170.3 (C-31), 144.7 (C-13), 121.3 (C-12), 73.4 (C-3), 65.4 (C-23), 54.3 (C-4), 49.2 (C-35), 47.9 (C-5), 47.8 (C-17), 47.7 (C-9), 47.2 (C-34), 46.5 (C-33 + C-37), 46.3 (C-19), 46.2 (C-38), 46.2 (C-39), 46.1 (C-40), 46.1 (C-41), 43.6 (C-18), 42.0 (C-14), 39.4 (C-8), 37.7 (C-1), 35.9 (C-10), 33.9 (C-21), 33.0 (C-29), 32.1 (C-7), 30.4 (C-20), 30.0 (C-22), 27.8 (C-15), 26.6 (C-36), 25.9 (C-27), 24.0 (C-30), 23.3 (C-11), 22.5 (C-16), 22.5 (C-2), 21.0 (C-32), 20.4 (C-6), 16.9 (C-25), 15.6 (C-26), 9.5 (C-24) ppm; MS (ESI): *m/z* (%) 697.5 ($[M+H]^+$, 100); analysis calcd for $C_{41}H_{64}N_2O_7$ (696.97): C 70.66, H 9.26, H 4.02; found: C 70.42, H 9.41, N 3.85.

4.2.5. General procedure for synthesis of rhodamine B derivates 6 and 7 (GPB)

A solution of rhodamine B (1.5 eq.), oxalyl chloride (6 eq.), DMF (0.2 eq.) and TEA (0.2 eq.) in dry DCM (30 mL) was stirred at ambient temperature for 3h. The solvent was removed under reduced pressure, re-evaporated with dry DCM (3 × 30 mL), and the residue was dissolved in dry DCM (30 mL). To this solution compounds **3** and **4** (1 eq.), TEA

(1.5 eq.) and DMAP (cat.) were added. After stirring for 1h, the solvent was removed under reduced pressure, and the resulting solid was subjected to column chromatography (SiO_2, chloroform/methanol, 9:1 or *n*-hexane/ethyl acetate, 7:3) to yield compounds **6** and **7** each as a purple solid.

4.2.6. N-{6-diethylamino-9-[2-({4[(2α,3β,4α)-2,3,23-tris(acetyloxy)-28-oxours-12-en-28-yl)-1-piperazinyl}carbonyl]phenyl]-3H-xanthen-3-ylidene)-N-ethylethanaminium chloride (6)

Following GPB from **3** (250 mg, 0.36 mmol) followed by chromatography (SiO_2, chloroform/methanol, 9:1) **6** (304 mg, 73%) was obtained as a purple solid; m.p.: 244–246 °C (lit.: [27]: 244–246 °C); MS (ESI): *m/z* (%) 1107.7 ($[M - Cl]^-$ (45)).

4.2.7. N-{6-diethylamino-9-[2-({4[(2α,3β,4α)-2,3,23-tris(acetyloxy)-28-oxours-12-en-28-yl)-1,4-diazepan-1-yl}carbonyl]phenyl]-3H-xanthen-3-ylidene)-N-ethylethanaminium chloride (7)

Following GPB from **4** (181 mg, 0.26 mmol) followed by chromatography (SiO_2, chloroform/methanol, 9:1) **7** (169 mg, 56%) was obtained as a purple solid; m.p.: 254–258 °C; $R_F = 0.31$ (SiO_2, chloroform/methanol, 9:1); IR (ATR): ν = 2935*w*, 1731*w*, 1624 *m*, 1586*vs*, 1529*w*, 1481 *m*, 1466 *m*, 1412*s*, 1335*s*, 1244*s*, 1179*vs*, 1160 *m*, 1132 *m*, 1045*w*, 746 *m*, 683*s*, 628*w*, 427*w* cm^{-1}; UV–Vis ($CHCl_3$): λ_{max} (log ε) = 260 (4.36), 307 (4.04), 356 (4.74), 562 (4.91) nm; ^1H NMR (500 MHz, $CDCl_3$): δ = 7.69–7.51 (m, 2H, 46–H + 45–H), 7.47–7.35 (m, 1H, 44–H), 7.28–7.02 (m, 5H, 47–H + 51–H + 51′–H + 52–H + 52′–H), 6.98–6.66 (m, 2H, 54–H + 54′–H), 5.21–5.07 (m, 2H, 12–H + 2–H), 5.02 (d, *J* = 10.3 Hz, 1H, 3–H), 4.20–2.80 (m, 18H, 37–H + 38–H + 39–H + 40–H + 41–H + 56–H + 56′–H + 23–H_b), 3.79 (d, *J* = 11.8 Hz, 1H, 23–H_a), 2.49–2.31 (m, 1H, 18–H), 2.21–2.06 (m, 2H, 16–H), 2.09–1.81 (m, 3H, 1–H_a + 11–H), 2.03 (s, 3H, 36–H), 1.97 (s, 3H, 32–H), 1.93 (s, 3H, 34–H), 1.79–1.47 (m, 1H, 9–H), 1.28 (t, *J* = 4.9 Hz, 12H, 57–H + 57‘–H), 1.42–1.17 (m, 10H, 21–H + 7–H + 6–H + 22–H + 19–H + 5–H), 1.13–0.95 (m, 4H, 1–H_b + 15–H + 20–H), 1.03 (s, 3H, 25–H), 1.00 (s, 3H, 27–H), 0.94–0.86 (m, 3H, 30–H), 0.83 (s, 3H, 24–H), 0.82 (s, 3H, 29–H), 0.67 (s, 3H, 26–H) ppm; ^{13}C NMR (125 MHz, $CDCl_3$): δ = 176.0 (C-28), 170.9 (C-35), 170.5 (C-31), 170.4 (C-33), 167.7 (C-42), 157.8 (C-55), 157.8 (C-55’), 155.9 (C-53), 155.7 (C-53′), 138.8 (C-13), 136.1 (C-50), 135.9 (C-50′), 132.3 (C-51), 132.2 (C-51′), 131.9 (C-52), 131.8 (C-52′), 130.3 (C-43), 130.2 (C-47), 130.1 (C-46), 129.7 (C-45), 126.9 (C-44), 124.7 (C-12), 114.0 (C-49′), 113.9 (C-49), 113.8 (C-48′), 113.7 (C-48), 96.1 (C-54), 96.0 (C-54′), 75.0 (C-3), 70.0 (C-2), 65.4 (C-23), 55.3 (C-18), 47.7 (C-5), 47.6 (C-9), 46.9 (C-17), 46.3 (C-37), 46.3 (C-56), 46.3 (C-56′), 46.2 (C-38), 46.2 (C-39), 46.2 (C-54), 46.2 (C-54′), 46.1 (C-40), 46.1 (C-41), 43.8 (C-1), 42.4 (C-14), 42.0 (C-4), 39.4 (C-8), 39.4 (C-19), 38.7 (C-20), 37.9 (C-10), 32.4 (C-7), 30.4 (C-21), 30.1 (C-22), 28.0 (C-15), 23.4 (C-11), 23.4 (C-27), 21.3 (C-30), 21.1 (C-34), 20.9 (C-36), 20.9 (C-16), 20.8 (C-32), 17.9 (C-6), 17.5 (C-29), 17.1 (C-25), 17.1 (C-26), 14.0 (C-24), 12.8 (C-57), 12.8 (C-57′) ppm; MS (ESI) *m/z* (%) = 1121.1 ($[M - Cl]^+$, 100); analysis calcd for $C_{69}H_{93}ClN_4O_9$ (1156.66): C 71.57, H 8.10, N 4.84; found: C 71.36, H 8.31, N 3.65.

4.2.8. Cell culture/spheroid assays and analyses

Cell lines and derived spheroids were cultivated in RPMI medium (Sigma-Adrich, Taufkirchen, Germany) containing 10% fetal bovine serum (BioWest, Nuaillé, France) and 10% penicillin/streptomycin (Sigma-Adrich) at 37 °C/5% CO_2 in a humid atmosphere. Luciferase expressing variants of the cell lines LS1034, DLD1 (colorectal carcinoma) and MDA-MB-231, Hs578T (mamma carcinoma) were used. For generation of single tumor spheroids, tumor cells re-suspended in culture medium were seeded into 96-well plates, which were coated before with 0.7% agarose (SeaKem® GTG™ Agarose, Lonza, Basel, Switzerland). After formation of spheroids (48h) they were treated with serial dilutions of the following drugs: 5-fluoruracil (5-FU medac, 50 mg/mL), irinotecan (Irinotecan-Actavis, 20 mg/mL), and oxaliplatin (Eloxatin, 5 mg/mL), Doxorubicin (Adrimedac, 2 mg/mL), Taxol/Paclitaxel (NeoTaxan, 6 mg/mL) all provided from our own hospital pharmacy, and compound **7**. Measurements of luciferase activity were performed on day 7. Generation of dose-response curves and calculation of IC_{50} values including standard deviations were accomplished using GraphPad Prism8.

To analysed time-dependent drug accumulation, cell proliferation and induction of cell death, spheroids were treated with 1 μM compound **7** and harvested after 24h, 48h, 72h and 96h. An untreated control was harvested after 24h. Spheroids were rinsed and formalin-fixed, embedded in paraffin and sliced to perform histological analysis. Hematoxylin/eosin (HE) staining and immunohistochemistry for detection of Ki67 and cleaved PARP was performed according to standard protocols and as previously performed [40]. Following primary antibodies were used: Ki67 (rabbit monoclonal, ab 16667, 1:100, Abcam, Cambridge, UK), cleaved PARP (rabbit monoclonal, Cat. 1051-1, 1:100, Epitomics Inc, Burlingame, CA, USA). For fluorescence analyses, slides were stained with DAPI to visualize cell nuclei. Tracking of compound **7** was accomplished by multispectral fluorescence microscopy using the Nuance® Ex multispectral imaging system from PerkinElmer (Hopkinton, MA, 01748, USA) as previously described [41]. For cube acquisition to get spectral information of compound **7**, the green filter set was used. DAPI was detected using the violet filter set. The obtained single spectral species were separated from spectra of background and tissue autofluorescence using the Nuance™ software (version: 3.0.2.). Composite images of compound **7** and DAPI were created using GIMP.

To investigate the drug induced alteration in cellular energy metabolism, the Seahorse cell analysis technology platform from Agilent was utilized, applying the Seahorse XF Cell Mito Stress Test Kit combined with the Seahorse XF Real-Time ATP Rate Assay Kit (Agilent Technologies, Inc., Santa Clara, CA, USA). The analyses were performed in the Core Facility “Analyse” in the Center for Basic Medical Research (ZMG) of the Medical Faculty on a Seahorse XF 96 - Extracellular Flux Analyzer. DLD1 cells were seeded in specific 96 well plates on day 0 at a density of 12000 cells per well, were treated with IC50 concentrations of drugs on day 1, and were measured on day 3. The complete procedure was performed according to instructions of the manufacturer without modifications. For detailed description see: https://www.agilent.com/en/product/cell-analysis/real-time-cell-metabolic-analysis/xf-assay-kits-reagents-cell-assay-media/seahorse-xf-cell-mito-stress-test-kit-740885.

Declaration of competing interest

The authors declare that they have no known competing financial interests or personal relationships that could have appeared to influence the work reported in this paper.

Data availability

Data will be made available on request.

Acknowledgments

We would like to thank Dr. D. Ströhl, Y. Schiller and S. Ludwig for the NMR spectra and T. Schmidt for the MS measurements. IR, UV/Vis spectra and optical rotation were recorded by M. Schneider and S. Ludwig; microanalyses were performed by M. Schneider. The analyses of cellular energy metabolism were accomplished in the Center for Basic Medical Research (ZMG) of the Medical Faculty. We thank Dr. Samiya Al-Robaiy for helpful cooperation.

Appendix A. Supplementary data

Supplementary data to this article can be found online at https://doi.org/10.1016/j.ejmech.2023.115189.

References

[1] B. Patwardhan, A.D.B. Vaidya, M. Chorghade, Ayurveda and natural products drug discovery, Curr. Sci. 86 (2004) 789–799.

[2] Y. Xiang, Z. Guo, P. Zhu, J. Chen, Y. Huang, Traditional Chinese medicine as a cancer treatment: modern perspectives of ancient but advanced science, Cancer Med. 8 (2019) 1958–1975.

[3] P. Hao, F. Jiang, J. Cheng, L. Ma, Y. Zhang, Y. Zhao, Traditional Chinese medicine for cardiovascular disease: evidence and potential mechanisms, J. Am. Coll. Cardiol. 69 (2017) 2952–2966.

[4] B.B. Aggarwal, H. Ichikawa, P. Garodia, P. Weerasinghe, G. Sethi, I.D. Bhatt, M. K. Pandey, S. Shishodia, M.G. Nair, From traditional Ayurvedic medicine to modern medicine: identification of therapeutic targets for suppression of inflammation and cancer, Expert Opin. Ther. Targets 10 (2006) 87–118.

[5] J. Roopesh, K. Susmit, T. Archana, Ayurveda and cancer, Pharmacogn. Res. 2 (2010) 393–394.

[6] B. Patwardhan, R.A. Mashelkar, Traditional medicine-inspired approaches to drug discovery: can Ayurveda show the way forward? Drug Discov. Today 14 (2009) 804–811.

[7] D. Kuntal, S. Gezici, Review article Plant secondary metabolites, their separation, identification and role in human disease prevention, Ann. Phytomed. 7 (2018) 13–24.

[8] S. Fulda, T. Efferth, Selected secondary plant metabolites for cancer therapy, World J. Tradl. Chin. Med. 1 (2015) 24–28.

[9] C.D.R. Nunes, M. Barreto Arantes, S. Menezes de Faria Pereira, L. Leandro da Cruz, M. de Souza Passos, L. Pereira de Moraes, I.J.C. Vieira, D. Barros de Oliveira, Plants as sources of anti-inflammatory agents, Molecules 25 (2020) 3726.

[10] C. Attardo, F. Sartori, Pharmacologically active plant metabolites as survival strategy products, Boll. Chim. Farm. 142 (2003) 54–65.

[11] J.M. Barbosa-Filho, M.R. Piuvezam, M.D. Moura, M.S. Silva, K.V.B. Lima, E.V.L. da-Cunha, I.M. Fechine, O.S. Takemura, Anti-inflammatory activity of alkaloids: a twenty-century review, Revista Brasileira de Farmacognosia 16 (2006) 109–139.

[12] K.P.E.N.O. Warburg, Metabolism of carcinoma cells, Biochem. Z. 154 (1924) 309–344.

[13] V. Panda, P. Khambat, S. Patil, Mitocans as novel agents for anticancer therapy: an overview, Int. J. Clin. Med. 2 (2011) 515–529.

[14] V. Gogvadze, B. Zhivotovsky, S. Orrenius, The Warburg effect and mitochondrial stability in cancer cells, Mol. Aspect. Med. 31 (2010) 60–74.

[15] R.K. Wolfram, L. Heller, R. Csuk, Targeting mitochondria: esters of rhodamine B with triterpenoids are mitocanic triggers of apoptosis, Eur. J. Med. Chem. 152 (2018) 21–30.

[16] J. Neuzil, L.F. Dong, J. Rohlena, J. Truksa, S.J. Ralph, Classification of mitocans, anti-cancer drugs acting on mitochondria, Mitochondrion 13 (2013) 199–208.

[17] S. Sommerwerk, L. Heller, C. Kerzig, A.E. Kramell, R. Csuk, Rhodamine B conjugates of triterpenoic acids are cytotoxic mitocans even at nanomolar concentrations, Eur. J. Med. Chem. 127 (2017) 1–9.

[18] B. Siewert, E. Pianowski, R. Csuk, Esters and amides of maslinic acid trigger apoptosis in human tumor cells and alter their mode of action with respect to the substitution pattern at C-28, Eur. J. Med. Chem. 70 (2013) 259–272.

[19] B. Siewert, E. Pianowski, A. Obernauer, R. Csuk, Towards cytotoxic and selective derivatives of maslinic acid, Bioorg. Med. Chem. 22 (2014) 594–615.

[20] B. Siewert, J. Wiemann, A. Kowitsch, R. Csuk, The chemical and biological potential of C ring modified triterpenoids, Eur. J. Med. Chem. 72 (2014) 84–101.

[21] S. Sommerwerk, L. Heller, J. Kuhfs, R. Csuk, Urea derivates of ursolic, oleanolic and maslinic acid induce apoptosis and are selective cytotoxic for several human tumor cell lines, Eur. J. Med. Chem. 119 (2016) 1–16.

[22] I. Serbian, B. Siewert, A. Al-Harrasi, R. Csuk, 2-O-(2-chlorobenzoyl) maslinic acid triggers apoptosis in A2780 human ovarian carcinoma cells, Eur. J. Med. Chem. 180 (2019) 457–464.

[23] S. Sommerwerk, L. Heller, R. Csuk, Synthesis and cytotoxic activity of pentacyclic triterpenoid sulfamates, Arch. Pharm. (Weinheim) 348 (2015) 46–54.

[24] D. Rodriguez-Hernandez, A.J. Demuner, L.C. Barbosa, R. Csuk, L. Heller, Hederagenin as a triterpene template for the development of new antitumor compounds, Eur. J. Med. Chem. 105 (2015) 57–62.

[25] B. Brandes, L. Koch, S. Hoenke, H.P. Deigner, R. Csuk, The presence of a cationic center is not alone decisive for the cytotoxicity of triterpene carboxylic acid amides, Steroids 163 (2020), 108713.

[26] O. Kraft, S. Hoenke, R. Csuk, A tormentic acid-homopiperazine-rhodamine B conjugate of single-digit nanomolar cytotoxicity and high selectivity for several human tumor cell lines, Eur. J. Med. Chem. Rep. 5 (2022), 100043.

[27] M. Kahnt, J. Wiemann, L. Fischer, S. Sommerwerk, R. Csuk, Transformation of asiatic acid into a mitocanic, bimodal-acting rhodamine B conjugate of nanomolar cytotoxicity, Eur. J. Med. Chem. 159 (2018) 143–148.

[28] M. Kozubek, S. Hoenke, H.P. Deigner, R. Csuk, Betulinic acid and glycyrrhetinic acid derived piperazinyl spacered rhodamine B conjugates are highly cytotoxic and necrotic, Results Chem. 4 (2022), 100429.

[29] L. Heller, A. Knorrscheidt, F. Flemming, J. Wiemann, S. Sommerwerk, I.Z. Pavel, A. Al-Harrasi, R. Csuk, Synthesis and proapoptotic activity of oleanolic acid derived amides, Bioorg. Chem. 68 (2016) 137–151.

[30] O. Kraft, A.K. Hartmann, S. Hoenke, I. Serbian, R. Csuk, Madecassic acid-A new scaffold for highly cytotoxic agents, Int. J. Mol. Sci. 23 (2022) 4362.

[31] S. Hoenke, N.V. Heise, M. Kahnt, H.P. Deigner, R. Csuk, Betulinic acid derived amides are highly cytotoxic, apoptotic and selective, Eur. J. Med. Chem. 207 (2020), 112815.

[32] N.V. Heise, S. Hoenke, I. Serbian, R. Csuk, An improved partial synthesis of corosolic acid and its conversion to highly cytotoxic mitocans, Eur. J. Med. Chem. Rep. 6 (2022), 100073.

[33] R. Csuk, H.P. Deigner, The potential of click reactions for the synthesis of bioactive triterpenes, Bioorg. Med. Chem. Lett 29 (2019) 949–958.

[34] J. Wiemann, A. Al-Harrasi, R. Csuk, Cytotoxic dehydroabietylamine derived compounds, Anti Cancer Agents Med. Chem. 20 (2020) 1756–1767.

[35] R. Csuk, B. Siewert, C. Dressel, R. Schafer, Tormentic acid derivatives: synthesis and apoptotic activity, Eur. J. Med. Chem. 56 (2012) 237–245.

[36] E.C. Costa, A.F. Moreira, D. de Melo-Diogo, V.M. Gaspar, M.P. Carvalho, I. J. Correia, 3D tumor spheroids: an overview on the tools and techniques used for their analysis, Biotechnol. Adv. 34 (2016) 1427–1441.

[37] A.S. Nunes, E.C. Costa, A.S. Barros, D. de Melo-Diogo, I.J. Correia, Establishment of 2D cell cultures derived from 3D MCF-7 spheroids displaying a doxorubicin resistant profile, Biotechnol. J. 14 (2019), e1800268.

[38] T.V. Loc, Q.N.V. Thi, T.V. Chien, P.T.T. Thi, N.P. Thi, T.T. Nguyen, T.H.L. Lthi, N. T. Nguyen, T.D. Thi, T.V. Sung, Synthesis of asiatic acid derivatives and their cytotoxic activity, Med. Chem. Res. 27 (2018) 1609–1623.

[39] M. Kahnt, J. Wiemann, L. Fischer, S. Sommerwerk, R. Csuk, Transformation of asiatic acid into a mitocanic, bimodal-acting rhodamine B conjugate of nanomolar cytotoxicity, Eur. J. Med. Chem. 159 (2018) 143–148.

[40] T. Mueller, L.P. Mueller, H.-J. Holzhausen, R. Witthuhn, P. Albers, H.-J. Schmoll, Histological evidence for the existence of germ cell tumor cells showing embryonal carcinoma morphology but lacking OCT4 expression and cisplatin sensitivity, Histochem. Cell Biol. 134 (2010) 197–204.

[41] A.K. Noack, H. Lucas, P. Chytil, T. Etrych, K. Mäder, T. Mueller, Intratumoral distribution and pH-dependent drug release of high molecular weight HPMA copolymer drug conjugates strongly depend on specific tumor substructure and microenvironment, Int. J. Mol. Sci. 21 (2020) 6029.